UNIVERSIDAD AUTONOMA DE MADRID

FACULTAD DE CIENCIAS

Departamento de Biología Molecular

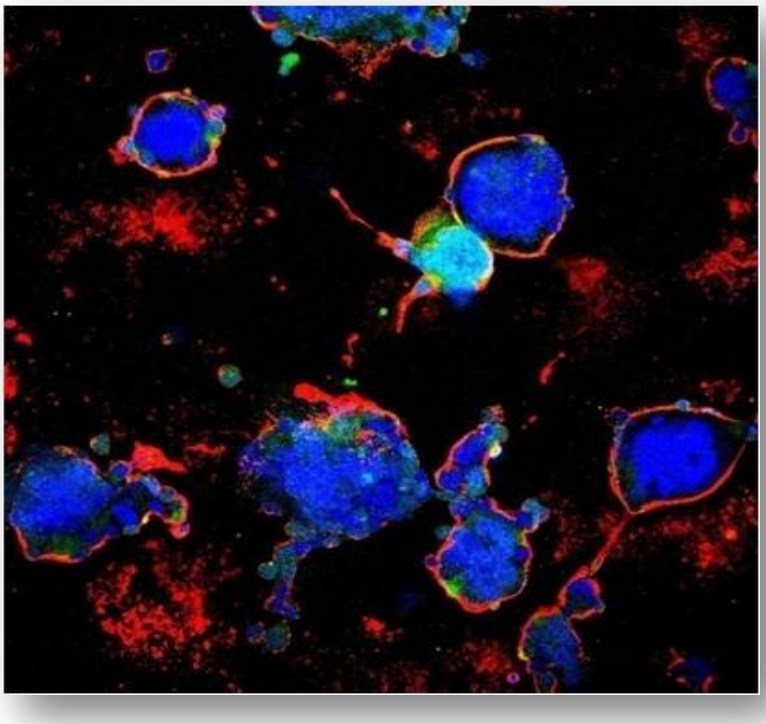

DOCTORAL THESIS

POLYANIONIC CARBOSILANE DENDRIMERS AGAINST VIRAL INFECTIONS: HUMAN IMMUNODEFICIENCY VIRUS TYPE 1, HERPES SIMPLEX TYPE 2 AND RESPIRATORY SYNCYTIAL VIRUS

RAFAEL CEÑA DIEZ

Madrid, 2017

Departamento de Biología Molecular

Facultad de Ciencias

Universidad Autónoma de Madrid

TESIS DOCTORAL

POLYANIONIC CARBOSILANE DENDRIMERS AGAINST VIRAL INFECTIONS: HUMAN IMMUNODEFICIENCY VIRUS TYPE 1, HERPES SIMPLEX TYPE 2 AND RESPIRATORY SYNCYTIAL VIRUS

Memoria presentada por el licenciado en Biología y Bioquímica

Rafael Ceña Diez

Directora de Tesis

Dra. Mª Ángeles Muñoz Fernández

Lugar de realización

Laboratorio de Inmuno-Biología Molecular

Hospital General Universitario Gregorio Marañón

Madrid, 2017

This thesis has been conducted at Laboratorio de Inmuno-Biología Molecular, Sección de Inmunología and Spanish HIV HGM Biobank at Hospital General Universitario Gregorio Marañón under the direction of Mª Ángeles Muñoz Fernández. This thesis has been (partially) funded by the RD12/0017/0037 and RD16/0025/0019, projects as part of Acción Estratégica en Salud, Plan Nacional de Investigación Científica, Desarrollo e Innovación Tecnológica (2008-2011; 2013-2016) and cofinanced by Instituto de Salud Carlos III (Subdirección General de Evaluación) and Fondo Europeo de Desarrollo Regional (FEDER), RETIC PT13/0010/0028, Fondo de Investigación Sanitaria (FIS) (grant number PI16/01863), CYTED 214RT0482 and EPIICAL project. CIBER-BBN is an initiative funded by the VI National R&D&i Plan 2008-2011, Iniciativa Ingenio 2010, the Consolider Program, and CIBER Actions and financed by the Instituto de Salud Carlos III with assistance from the European Regional Development Fund.

La Dra. Mª Ángeles Muñoz Fernández, Jefe de Sección del Servicio de Inmunología y Directora del Biobanco VIH del Hospital General Universitario Gregorio Marañón,

CERTIFICA QUE,

El trabajo de investigación y la redacción de la Tesis Doctoral titulada: “Polyanionic carbosilane dendrimers against viral infections: Human Immunodeficiency Virus Type 1, Herpes Simplex Virus Type 2 and Respiratory Syncytial Virus” ha sido realizado por Rafael Ceña Diez, bajo mi dirección. Revisado el trabajo, considero éste como satisfactorio y autorizo su presentación y defensa para optar al grado de Doctor con Mención Internacional por la Universidad Autónoma de Madrid.

Y para dar constancia de ello, firmo el presente documento.

Madrid, 18 de octubre de 2017

Fdo. Dra. Mª Ángeles Muñoz Fernández

ACKNOWLEDGEMENTS

Hace más de tres años comencé una andadura sin saber muy bien donde me llevaría, parece que hoy ha llegado el momento de poner punto y final a la que ha sido mi primera etapa en la ciencia y una de las más bonitas de mi vida. He crecido como persona y como profesional. Ha habido grandes momentos, tanto malos como buenos, y todos ellos han sido mejores y más llevaderos gracias a todas las personas que han estado a mi lado. Sin vuestro apoyo, confianza, comprensión y empuje no lo habría logrado, sin todos vosotros no sería la persona que soy hoy, GRACIAS.

En primer lugar me gustaría agradecer a mi directora de tesis, Mª Angeles. Sin ti esto no habría sido posible. Gracias por haberme dado esta oportunidad, por tu confianza, experiencia, dedicación y paciencia. Gracias por animarme y motivarme tras cada error, por la dedicación y pasión que pones a cada cosa que haces y por el esfuerzo que haces por los demás. Agradezco poder hablar contigo en confianza, la calma que me transmites cuando yo no tengo, y que sabes frenarme cuando me acelero.

A las 4 personas que han conseguido que ir al laboratorio no fuese solo ir a trabajar si no un gotero de grandes momentos! Soy realmente afortunado de haberos tenido en mi vida. A Quique, por enseñarme con dedicación y pasión, eres el mejor maestro que alguien pudiera desear. Por tu paciencia, entré a mil revoluciones y supiste ponerme freno e ir guiándome y dando correa poco a poco hasta que pude volar solo. Gracias por haber forjado los cimientos de mi "yo investigador". A Pili, porque nos hemos gritado como energúmenos y nos hemos hecho rabiar y llorar. Durante gran parte de mi tesis has sido mi motor, mi guía, compañera y amiga. Has estado ahí siempre que lo he necesitado, me has aconsejado y evitado muchos disgustos. A Silvia, gracias por haberme permitido que te redescubriera. Si antes me encantabas, ahora te adoro. Convertiste mi estancia en Dresde en algo inolvidable. Me encantan nuestras conversaciones. Eres autentica al 100%, vas a llegar muy lejos! Todavía estoy esperando una tarta y un café. A Alba, por estar, si no estas nada es igual. Por como eres capaz de arrancarme una sonrisa en los días grises, por la complicidad y la telepatía, por hacerme ver el lado bueno del mundo, por ser mi psicóloga personal y porque estos agradecimientos jamás se hubieran escrito sin ti. Gracias por ser como eres, incombustible, no me imagino haber acabado esta tesis sin ti a mi lado,

invadiendo mi espacio!! Porque a veces te digo que me pones nervioso o que te distraes y me ignoras… pero en el fondo, es lo mejor de ti.

A Jose, gracias por saber estar ahí sin decir nada, porque a veces lo dices todo sin abrir la boca. Siempre estás de buen humor y tomándonos el pelo, pero sabes estar serio cuando hay que estarlo. Gracias por mantenerme en el camino cuando perdía el rumbo. A Chusa, gracias porque aunque te niegues a leerlo, aún así quiero darte las gracias. Gracias por enseñarme tanto, por tu guía y orientación. Gracias por defender siempre lo justo, y porque aunque siempre acabemos chillándonos, nunca nos enfadamos. Dentro de muchos años te mandaré a mis predocs para que les des con la cachaba.

A los chicos de Inmuno2, sois los mejores!! A Nacho, gracias por ser mi alumno predilecto. Gracias porque irradias buen rollo y eres el buffer perfecto para todas las personalidades del laboratorio. A Laura, Selene e Irene, gracias por haberme hecho creer que no soy tan mal profe. Carlos, gracias por nuestras grandes conversaciones, aunque a veces las retrasamos demasiado. Gracias por hacer esos días en el animalario mucho más entretenidos. Dani, gracias por todos tus consejos y por esos tintos de verano que suavizan los días más pesados.

A Laura y Jacobo, porque empezamos prácticamente juntos y acabamos de la mano. Gracias por vuestra companya y apoyo moral estos últimos meses.

Al resto de integrantes del laboratorio: Susana, Raquel, Marta, Judith, Santi, Nacho, Marjorie, Adrián, Rafa Correa, Esther, Verónica, Raul, Miguel, Lola, Maribel y Laura; gracias por haber sido una gran familia durante estos tres años. Gracias por el buen ambiente y los grandes momentos que he vivido a vuestro lado.

A los chicos del Biobanco, Isa, Irene, Coral y Jorge, por tener siempre una palabra amable y haberme ayudado siempre en todo lo que habéis podido. Y gracias en especial a Paula por tu alegría y por ayudarme a ver las cosas desde otra perspectiva.

También gracias a Carmen, del CBM; porque sin ti faltarían la mitad de los experimentos de esta tesis. Gracias por arreglar todos los papeleos y conseguir todos los permisos que yo solo no habría sido capaz de conseguir.

Gracias a todas las personas del IPF por haberme recibido con los brazos abiertos durante mi estancia, y haberme hecho sentir como en casa. Especialmente a Robin, por esas tardes en el rocódromo.

Gracias a mis amigos: Óscar, Álvaro, Alfonso, Amanda, Laura, los Casposillos… por vuestro apoyo todos estos años. Gracias por ser el ancla que me ha mantenido estable en la tempestad.

Y por supuesto, gracias a toda mi familia. En especial, a mi tio Valentin, porque creo que tú fuiste el germen de este gusanillo por la ciencia. Tu apoyo ha sido fundamental para mí. A mi abuela, por dejar que me desahogue contigo sobre todo en el mundo, sé que son nuestras pequeñas confidencias y secretos. Gracias por no decir una palabra de más, pero tampoco una de menos, y porque cuando consigo sacarte tu opinión, siempre sueles tener razón. Y finalmente, a las dos personas más importantes de mi vida, porque todo lo que soy en esta vida, lo soy gracias a vosotros. Mamá, por tu cariño, amor y apoyo incondicional, por empujarme siempre hacia adelante y no dejar nunca que me rinda. Por hacerme creer que puedo hacer todo lo que me proponga, y que tengo “estrella”. Papá, porque tu coletilla “aunque en todo se puede mejorar” es un gran estímulo para superarme. Eres la persona a la que tengo en mayor estima, el modelo en que aspiro a convertirme, y por ello, que pienses que puedo mejorar siempre me impulsa a hacerlo. Gracias porque pase lo que pase, sé que puedo contar contigo. Gracias por ser la persona que más ha definido mi vida y me ha marcado como persona.

SUMMARY

The most common way to become infected by HIV-1 is by sexual intercourse. In the absence of an effective vaccine, topical microbicides provide a new approach to avoid the infection. However, during the recent years countless compounds have been evaluated in clinical trials to prevent HIV-1 infection, but all have failed due to “semen-derived enhanced virus infection” (SEVI) or induction of vaginal irritation and inflammation. Dendrimers have shown the ability to abrogate semen-enhanced viral infection *in vitro* when combined with antiretrovirals such us Tenofovir Disopropil Fumarate (TDF) or Maraviroc (MVC). When the biocompatibility of the polyanionic carbosilane dendrimer G2-S16 was evaluated *in vivo,* it was observed that 3% (w/v) vaginal application of G2-S16, in BALB/c mice, limits its distribution to the female vaginal tract, specifically to the non-sterile part, and that its vaginal application during 7 consecutive days did not produce vaginal irritation.

Importantly, many sexual transmitted infections (STIs), such as HSV-2, may increase vulnerability to HIV-1 infection. A screening was performed to evaluate the ability of polyanionic carbosilane dendrimers with anti-HIV-1 activity against HSV-2. These polyanionic carbosilane dendrimers inhibit the viral infection during the first steps of the HSV-2 life-cycle: binding/entry-mediated events. Molecular modeling of G1-S4 and G2-S16 with HSV-2 glycoprotein B (gB) showed that, in general, G1-S4 binds better than G2-S16 to selected binding sites on HSV-2 gB surface. Moreover, G1-S4, G2-16 and G3-S16 showed synergistic or additive effect in combination with TDF or Acyclovir (ACV).

In addition to STIs, there are about 200 million pregnancies every year, being 40% unintended. To also address this problem, studies based on the combination of the spermicide Platycodin D (PD) with different polyanionic carbosilane dendrimers (G1-S4 or G2-S16) showed that not only HIV-1 and HSV-2 infections were decreased, but also the combination acted as a spermicide which can also reduce the rate of unintended pregnancies.

Respiratory syncytial virus (RSV) is the most common cause of respiratory infection and bronchiolitis requiring hospitalization for infants under one year of age. RSV entry into the host cell is highly associated to heparin sulfate (HS). By using a cell-based screening, we have identified G1-S4, G2-S16 and G3-S16 as RSV inhibitors *in vitro*. These dendrimers inhibit early aspects of RSV infection: G1-S4 and G3-S16 bind directly to the virus, inactivating it, whereas G2-S16 adheres to the host cell surface proteins preventing further virus binding. Furthermore, when evaluated *in vivo*, G2-S16 inhibited RSV replication by 80%. In conclusion, G2-S16 is effective against RSV, supporting additional clinical research on the development of an effective therapy against RSV infection.

SUMMARY

La forma más habitual de la transmisión del VIH-1 son las relaciones sexuales. En ausencia de una vacuna preventiva eficaz frente al VIH-1, los microbicidas se consideran una posible alternativa para evitar nuevas infecciones. Sin embargo, en los últimos años se han evaluado un número importante de posibles compuestos que actuarían como microbicidas que han fracasado en ensayos clínicos, probablemente debido al aumento de la infección viral por el semen (SEVI) y a la inducción de irritación e inflamación a nivel vaginal y rectal. Los dendrímeros polianiónicos carbosilanos anulan la capacidad del semen de incrementar la infección por el VIH-1 *in vitro* en combinación con Tenofovir Disopropil Fumarato (TDF) o Maraviroc (MVC). Cuando se evaluó *in vivo* la biocompatibilidad del dendrimero G2-S16, se observó que la aplicación a nivel vaginal al 3% (p/v) de G2-S16, en ratones BALB/c, limita su biodistribución al tracto vaginal femenino. Además, la aplicación del G2-S16 a nivel vaginal durante 7 días consecutivos no produjo inflamación e irritación en la vagina.

Es importante destacar que muchas enfermedades de transmisión sexual (ETS) pueden incrementar la infección por el VIH-1, como el VHS-2. Se realizó un estudio para evaluar la capacidad de los dendrímeros G1-S4 y G2-S16 con actividad anti-VIH-1 contra el VHS-2. Estos dendrímeros inhiben la infección por el VHS-2 en los primeros pasos del ciclo viral: a nivel de la unión del VHS-2 con la célula huésped. El modelaje molecular con la glicoproteína B (gB) del VHS-2 demostró que el G1-S4 se unía mejor a los sitios de unión sobre la superficie de la gB en comparación con el G2-S16. También, G1-S4, G2-16 y G3-S16 mostraron efecto sinérgico o aditivo en combinación con TDF o Acyclovir (ACV).

Además del número de ETS, anualmente hay alrededor de 200 millones de embarazos, de los cuales el 40% no son programados. Las combinaciones realizadas con el espermicida Platycodin D (PD) y los dendrímeros G1-S4 o G2-S16 mantuvieron su perfil dual de inhibición frente a infecciones virales, tales como el VIH-1 y VHS-2, manteniendo en paralelo su función como espermicida.

El virus respiratorio sincitial (VRS) es la causa más común de infección respiratoria y bronquiolitis que requiere hospitalización en lactantes menores de un año de edad. Actualmente, no existe una cura eficaz frente a la infección por el VSR y el tratamiento existente se reduce a aliviar los síntomas de la infección. La entrada del VRS en la célula está asociada al heparan sulfato (HS). Tras realizar un cribado *in vitro* de diferentes dendrimeros se seleccionaron G1-S4, G2-S16 y G3-S16 como inhibidores del VRS. Estos tres dendrímeros inhiben los primeros pasos de la infección por el VRS, uniéndose G1-S4 y G3-S16 directamente al VRS y G2-S16 a las proteínas de la superficie de la célula. En los estudios realizados *in vivo*, G2-S16 inhibió un 80% la infección por el VRS.

TABLE OF CONTENTS

TABLE OF CONTENTS

ABBREVIATIONS

INTRODUCTION

HYPOTHESIS & OBJECTIVES

MATERIALS & METHODS

RESULTS

LIST OF ABBREVIATIONS

LIST OF ABBREVIATIONS

3,4-DCA	3,4-Dichloroaniline
3-OS-HS	3-O-Sulfated Heparan Sulfate
Ab	Antibody
ABTS	2,2≪-azinobis(3-ethylbenzthiazolinesulfonic acid)
ACV	Acyclovir
AEC	3-amino-9-ethylcarbazole
AIDS	Acquired Immune Deficiency Syndrome
ARTc	Antiretroviral Therapy Combination
ARV	Antiretroviral
ATCC	American Type Culture Collection
BrdU	Bromodeoxyuridine
BSA	Bovine Serum Albumin
CBMSO	Centro de Biología Molecular Severo Ochoa
CCR	Chemokine (C-C motif) Receptor. It can be extended to the rest of abbreviations: CCR2, CCR3 and CCR5
CD	Cluster of Differentiation. It can be extended to the rest of abbreviations: CD3, CD4, CD8…
CEEA-CBMSO	Institutional Animal Care and Use Committee-CBMSO
CI	Combination Index
CX3C	A human transmembrane protein. Chemokine Receptor 1, also known as the fractalkine receptor or G-protein coupled receptor 13 (GPR13)
CXCR4	Chemokine (C-X-C motif) Receptor 4
dH	Total enthalpic contribution to free binding energy

DMEM	Dulbecco's Modified Eagle's Medium
DMSO	Dimethyl Sulfoxide
DNA	Deoxyribonucleic Acid
DPX	Distyrene Platiciser Xilene
dS	Solute entropy change due to binding
E. Coli	*Escherichia coli*
EC_{50}	Effective concentration 50%. It can be extended to the rest of abbreviations: EC_{75} andEC_{90}
EEL	Electrostatic contribution in vacuum
EGF	Epithelial Growth Factor
ENP	Estimate non-polar contribution
Env	Gene encoding the structural Env polyprotein of HIV-1
EPB	Energetic contribution, electrostatic solvent-solute interaction (desolvation penalty)
FBS	Fetal Bovine Serum
FET	Fish Embryo Toxicity Test
FITC	Fluorescein Isothiocyanate.
G0, G1, G2,G3, G4	Generations 0, 1, 2, 3, 4 of dendrimers according to the number of layers with branching units forming the dendrimer
G1-C8	A first generation carboxylate dendrimer fully capped with 8 carboxylate groups
G1-S4	A first generation sulfate dendrimer fully capped with 4 sulfate groups
G2-CTE16	A thiol-<ene second generation carboxylate dendrimer fully capped with 16 carboxylate groups
G2-NF16	A second generation naphthylsulfonated dendrimer fully capped

	with 16 naphthylsulfonate groups
G2-S16	A second generation sulfonated dendrimer fully capped with 16 sulfonate groups
G2-S24P	A second generation polyphenolic-core sulfonate dendrimer fully capped with 24 sulfonate groups
G2-STE16	A thiol-ene second generation sulfonate dendrimer fully capped with 16 sulfonate groups
G3-S16	A third generation sulfate dendrimer fully capped with 16 sulfate groups
gag	Group-specific antigen. Gene encoding the structural gag polyprotein of HIV-1
GAG	Glycosaminoglycan
gB	Glycoprotein exposed in the surface of HSV-2 membrane. It can be extended to the rest of abbreviations: gB, gC, gD, gE, gG, gH, gI, gJ, gK, gL and gM
gF	Fusion protein of RSV. F1 and F2
gG	Host cell binding protein of RSV
gp120	Surface glycoprotein exposed on the surface of HIV-1 envelope
gp41	Transmembrane envelope glycoprotein of the HIV-1
HBD	Heparin Binding Domains
h-BLT	Mice implanted with human fetal thymus/liver cells followed by bone marrow transplantation with human CD34+ cells
HE	Hematoxylin-Eosin
HEC	Hydroxyethyl Cellulose
HIV-1	Human Immunodeficiency Virus Type 1
HN	Hemagglutinin-Neuraminidase
Hpf	Hours post fertilization

HS	Heparan Sulfate
HSPGs	Heparansulfate Proteoglycans
HSV-2	Herpes Simplex Virus Type 2
HVEM	Herpes Virus Entry Mediator
IC_{50}	The half maximal inhibitory concentration
ip.	Intraperitoneal
IgG	Immunoglobulin G
IL-2	Interleukin 2. It can be extended to the rest of interleukins
IN	Integrase of HIV-1
IRL	Inverted Repeat Long
IRS	Inverted Repeat Short
Isoflurane	2-chloro-2-(difluoromethoxy)-1,1,1-trifluoro-ethane
LC_{50}	Lethal Concentration 50
LMP	Low Melting Point
LOEC	Lethal concentration 50 and minimal observed effect concentration
LRTI	Lower Respiratory Tract Infection
LTR	Long Terminal Repeat
MDT	Maximum Dose Tolerated
MOI	Multiplicity of Infection
MTT	3-(4,5-dimethylthiazol-2-yl)-2,5-diphenyl tetrazolium bromide
MVC	Maraviroc
N9	Nonoxynol-9
NIH	National Institutes of Health

NOEC	Maximum Concentration without Observed Effect
NP	Nanoparticle
NS	Non-structural proteins of RSV: NS1 and NS2
NT	Non Treated
OECD	Organization of Economic Cooperation and Development
ORF	Open Reading Frame
PAMAM	Polyamidoamine Dendrimer
PAMANOS	Polyamidoamine-Organosilicon Dendrimer
PBMC	Peripheral Blood Mononuclear Cell
PBS	Phosphate Buffered Saline
PD	Platycodin D
PDB	Protein Data Base
PFU	Plaque Forming Unit
pi	Post-infection
PIC	Pre-Integration Complex
PLL	Polylysine Dendrimer
PPI	Polypropylene-imine Dendrimer
PR	Protease of HIV-1
QM	Quantum Mechanics
Rev	Regulator of expression of virion proteins. Gene encoding the Rev protein of HIV-1
RNA	Ribonucleic Acid
rpm	revolutions per minute
RPMI	Roswell Park Memorial Institute

RSV	Respiratory Syncytial Virus
RT	Reverse Transcriptase of HIV-1
RT*	Room Temperature
SD	Standard Deviation
SDS	Sodium Dodecylsulfate
S.E.M.	Standard Error of the Mean
SEVI	Semen-derived enhanced viral infection
SH	Small Hydrophobic protein of RSV.
SP	Seminal Plasma
STI	SexuallyTransmitted Infection
T/F	Transmitted/Founder viruses
$TCID_{50}$	50% Tissue Culture Infective Dose
TDF	Tenofovir Disopropil Fumarate
TRL	Terminal Repeat Long
TRS	Terminal Repeat Short
UL	Long Unique Región
UL20	Virion membrane protein of HSV-2
UNAIDS	United Nations Programme on HIV and AIDS
VDW	Van der Waals contribution to binding enthalpy
vif	Viral infectivity factor. Gene encoding the accessory Vif protein of HIV-1
VL	Viral Load
Vpr	Viral Protein R. Gene encoding the accessory Vpr protein of HIV-1
Vpu	Viral Protein Unique. Gene encoding the accessory Vpu protein of

	HIV-1
w/v	weight/volume
WHO	World Human Organization

INTRODUCTION

1. Human Immunodeficiency Virus Type 1

1.1. Epidemiology

In spite of the significant efforts made in the last years, the latest data available at WHO report that in 2016 about 1.8 million new diagnoses for HIV-1 occurred per year and there were a total of 36.7 million people infected worldwide, of which about half were unaware of the diagnosis (UNAIDS, 2016). Of all HIV-1 patients, 28.3 million are currently candidates for antiretroviral therapy combination (ARTc), although only 19.7 (54%) million people are being treated. Most infected patients come from developing countries, with significant differences between countries, and even between regions.

Despite this, there has been a global trend of improvement in the situation of the pandemic, especially in sub-Saharan Africa (UNAIDS, 2016) and, more modestly, in Latin America, Oceania, Western and Central Europe and North America, where it was observed a decrease in the numbers of new infections and mortality. This has been possible due to the policies implemented by each country and the increase of resources aimed at improving access to ARTc, health care and preventive measures. Regrettably, in some regions, such as the Middle East, North Africa, Central Asia and Eastern Europe, the HIV-1 situation has worsened, with an increase in the number of new infections and mortality. Africa is the most affected region, with 25.6 million people living with HIV-1 in 2016. The African region also accounts for almost two thirds of the global total of new HIV-1 infections.

1.2. Morphology and structure

The HIV-1 is the infectious agent that causes acquired immunodeficiency syndrome (AIDS). It is an RNA virus of the human retrovirus family (*Retroviridae*) and the genus Lentivirus (Barre-Sinoussi et al., 1983). The virion is spherical in shape and consists of an outer envelope or lipid bilayer taken from the membrane of the HIV-1 infected human cell where the glycoprotein (gp)-120 bound to the transmembrane gp41 in the form of trimers is inserted. Underneath the envelope is the protein matrix and within it is the icosahedral capsid with the viral enzymes and the genetic material of the virus formed by two single strands of RNA of positive polarity of approximately 9.8 kb associated with proteins of the nucleocapsid (Muesing et al., 1985). The HIV-1 genome contains three major genes: gag, pol and env (**Table 1**). The gag gene encodes primarily the structural proteins that make up the matrix, the capsid and the nucleocapsid, whereas the pol gene encodes the viral proteins protease (PR), reverse transcriptase (RT) and integrase (IN) involved in viral maturation, in the synthesis of DNA from the virus RNA and its integration into the cellular genome, respectively. The env gene

encodes the envelope glycoprotein precursor. The HIV-1 has other genes: tat, vif, vpr, vpu, and nef, with regulatory capacity (**Table 1**) (Emerman and Malim, 1998, Gallo et al., 1988), essential for the viral cycle. At the 5' and 3' ends of the genome are long terminal repeats (LTRs), which enable to their circularisation and integration, into the cellular genome.

Table 1. Summary of the HIV-1 genome function

Gene	Protein	MW (Kd)	Function
Env	gp160	160	Pre-protein precursor
	gp120	120	Viral envelope protein Interaction with CD4 receptor
	gp41	41	Membrane fusion
Gag	p55	55	Pre-protein precursor
	p24	24/25	Nucleocapsid protein
	p17	17	Matrix Protein
	p9	9	Ribonucleoprotein
	p6	6	Ribonucleoprotein, essential for viral encapsidation
Pol	Reverse transcriptase	63	Retrotranscription. Activity RNAse H
	Integrate	11	Integration
	Protease	15	Post-transductional processing of viral proteins
Tat	Tat	14	Transactivator
Rev	Rev	19	Regulator of transport and mRNA processing
Nef	Nef	27	Negative regulation of CD4 and HLA I. Increase viral infectivity. Increase of the retrotranscription
Vif	Vif	23	Increase viral infectivity
Vpr	Vpr	18	Viral transactivator. Induction of apoptosis. Transportation of the pre-integration complex (PIC)
Vpu	Vpu	15	Increases virion release
Tev	Tev	16	Activate tat and rev

1.3. Viral Cycle

The life cycle of HIV-1 begins with its entry into the target cells through interaction between the viral gp120 and the CD4 receptor expressed in the helper T lymphocytes and in mononuclear-phagocytic cells, which determines the viral tropism by these cell types (Klatzmann et al., 1984, Dalgleish et al., 1984). In addition, HIV-1 interactions with chemokine receptors are required. These receptors can act as HIV-1 co-receptors. The most well-known co-receptors are CCR5 and CXCR4 (Feng et al., 1996, Dragic et al., 1996). Several HIV-1 variants able to bind to CCR2 or CCR3 receptors and enter the cell through multiple co-receptors have been also described (Choe et al., 1996).

The infective and replication of HIV-1 life cycle has 7 stages (**Fig. 1**).

i) **Binding and fusion:** Binding CD4 to gp120 causes conformational changes in the structure of the viral envelope proteins that allow the interaction domain of gp120 to the chemokine receptors CCR5 or CXCR4. The interaction with these co-receptors leads to new conformational changes that expose the N-terminal domain of gp41, leading to membrane fusion and internalization of the viral nucleocapsid.

ii) **Retrotranscription:** Once the nucleocapsid penetrates into the cell, retrotranscription of one of the strands of viral RNA by the RT enzyme transported by the virion itself occurs. Since RT has intrinsic the DNA polymerase and RNAse, it generates a double DNA strand by duplicating the LTRs, which are located at both ends of the viral genome.

iii) **Integration:** This DNA is transported to the nucleus and is integrated into the cellular genome by the action of the IN, constituting what is called an integrated provirus. In the DNA transport process involved viral proteins such as Vpr, Vpu and p17 matrix protein (Bukrinsky and Haffar, 1998, Gonzalez, 2017, Soper et al., 2017). However, the process of retrotranscription and integration does not depend solely on viral factors, but also on induced cellular factors in the course of cellular activation processes. Thus, in resting $CD4^+$ T lymphocytes the viral genome is incompletely retrotranscribed, and the completion of retrotranscription and integration is not achieved unless the cell is activated (Zack et al., 1990), constituting a non-integrated proviral DNA reservoir susceptible to integration and replication when the cells are activated.

iv) **Transcription:** The provirus integrated into the target cell genome may remain latent for a length of time, it can be replicated in a controlled manner, or it can experience a massive replication with the consequent cytopathic effect on the HIV-1 infected cell. HIV-1 replication begins with the synthesis of mRNA from the integrated proviral DNA. This transcriptional activation depends on cellular factors that interact with the regulatory sequences located in the viral LTR (Gaynor, 1992).

v) **Translation:** The mRNA is synthesized as a single transcript that is transported to the cytosol and processed into transcripts of different sizes, generating the viral proteins by using the infected cell machinery through the action of the viral protein Rev (Chang and Sharp, 1990).

vi) **Assembling:** The viral proteins once synthesized are processed with the participation of Vif, Vpu and the viral PR, to finally be assembled constituting (Soper et al., 2017).

vii) **Virion release:** The new viral particles leave the target cell.

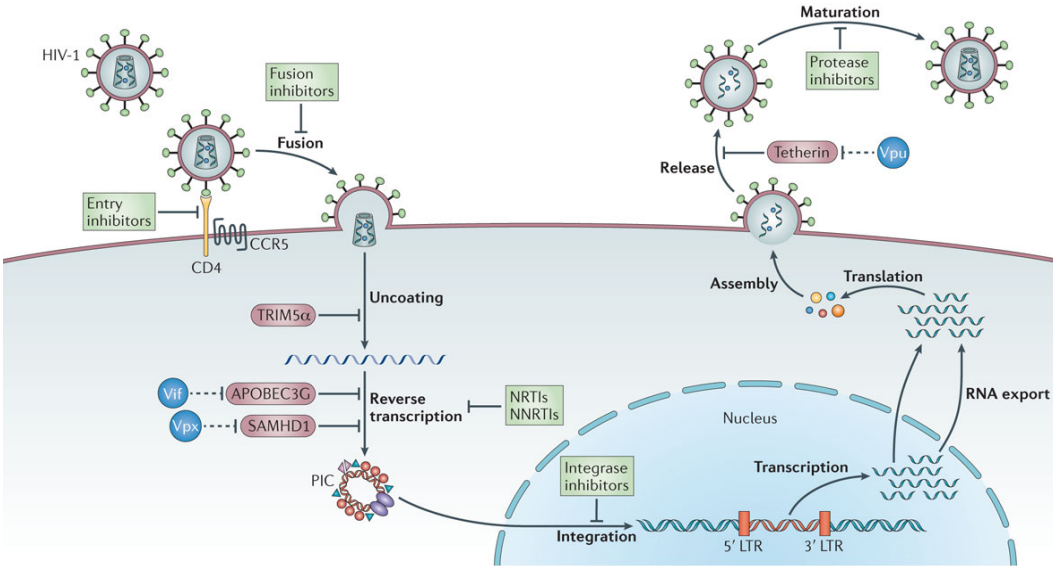

Figure 1. HIV-1 replication cycle: binding to the CD4 receptor and co-receptors, fusion with the host cell membrane, uncoating of the viral capsid, release of the HIV RNA and proteins into the cytoplasm, RT of HIV RNA to DNA, formation of the pre-integration complex (PIC), and translocation into the nucleus. Once in the nucleus, the viral DNA is integrated into the host DNA and subsequently transcribed and translated to form new viral RNA and viral proteins that translocate to the cell surface to assemble into new immature virus forms. The new viruses bud off and are released. Finally, during maturation, the protease enzyme cleaves the structural polyprotein to form mature Gag proteins, resulting in the production of new infectious virions. The principal families of antiretroviral drugs (green) and the step of the life cycle that they blockare indicated (Barre-Sinoussi et al., 2013).

By analyzing the viral load (VL), it has been shown that in an infected individual they occur daily of the order of 10^9 to 10^{10} viral particles (Perelson et al., 1996). This assumes that the half-life of a virion is between 7-8h and the half-life of an HIV-1 infected lymphocyte in which HIV-1 actively replicates is between 24-27 h. Globally, it has been estimated that each infected cell produces between 10^4 and 10^5 viral particles, mostly defectives. These numbers indicate that HIV-1 has a very aggressive replication kinetic, and higher than other lentiviruses.

1.4. Clinical course

During the first years of the HIV-1 infection, the clinical course on individuals without treatment includes three phases: i) primary infection, ii) clinical latency phase, and iii) AIDS disease (Buchbinder et al., 1994, Clark et al., 1991, Daar et al., 1991, Le et al., 2013, Lifson et al., 1991, Tindall and Cooper, 1991).

However, the majority of the population in the developed countries (> 90%) and 54% of the HIV-1 infected world population are under ARTc. In conclusion, HIV-1 infected individuals are beginning to die from non-AIDS events, which are associated to causes beyond the AIDS progression.

The impact of HIV-1 infection *per se* on the risk for developing non-AIDS-related diseases has become increasingly important as a result of the improved survival of HIV-1-infected patients on ARTc. As the HIV-1-infected population in the Western world is ageing, it is expected that the incidence of non-AIDS-related diseases will increase in the coming years exceeding that expected for age- and gender-matched general population.

1.5. Transmission mechanism

The HIV-1 is transmitted primarily in three ways: i) sexual; ii) parenteral; and iii) mother-to-child transmission. The later can occur in three different moments: a) prenatal, intrauterine, or transplacental; b) intrapartum or perinatal transmission; and c) postnatal transmission or postpartum.

80% of new HIV-1 infections are due to sexual transmission. Therefore, we focus on curbing new infections through prophylactic treatment with topical microbicides based on nanotechnology.

2. Herpes Virus Simplex Type 2

2.1. Epidemiology

Genital herpes can be caused by herpes simplex virus type 1 (HSV-1) or type 2 (HSV-2). However, globally, the vast majority of cases are due to HSV-2 infection, being the most prevalent STI in developing and industrialized countries (Marchi et al., 2017, Pickering et al., 2005).

HSV-2 infection has not been evaluated since 2012 and in 2015 was reported that the estimated number of people aged between 15-49 years who were living with HSV-2 were 417 million worldwide and approximately 19 million new infections occur each year (Gupta et al., 2007). However, any estimation based on the number of reported cases of HSV-2 infection will underestimate the prevalence of infection, since most HSV-2 infected people are unaware of their infection, as it occurs with other STIs (Fleming et al., 1997, Stanberry et al., 2000, Wald and Ashley-Morrow, 2002). HSV-2 causes genital herpes lesions, which, when symptomatic, is characterized by periodic recurrences of painful genital ulcers. The large majority of HSV-2 infected individuals, about 80-90% of the adult population worldwide, do not know they are infected due to the fact that asymptomatic viral reactivation and shedding are common. Thus, although individuals with HSV-2 are most infectious when they are symptomatic, most transmissions are thought to occur when the source partner is asymptomatic (Schiffer and Corey, 2013). Genital HSV-2 infection can considerably affect relationships through feelings of shame and stigma and concerns about risk of transmission.

Summing up, despite the asymptomatic nature of genital herpes, which eases its spread, HSV-2 is associated with considerable morbidity and even mortality (Pinninti and Kimberlin, 2013).

The prevalence of HSV-2 is generally higher in developing regions than in developed countries. Factors that contribute to differences in prevalence by region for HSV-2 are likely to be similar to those for HIV-1 (Drain et al., 2004, Paz-Bailey et al., 2007). The associations remain significant but are slightly lower among higher-risk populations than among general populations, perhaps because these people have an increased risk of HIV-1 independent of HSV-2 or because higher-risk individuals infected with HSV-2 might be more likely to use condoms or abstain from sex when symptomatic (Looker et al., 2017).

These may include regional differences in the frequency and pattern of sexual risk behaviour including rates of oral versus vaginal sex, differences in age at first sex (Pettifor et al., 2004, Kaestle et al., 2005), differences in the prevalence of sexually transmitted infection cofactors for HSV-2 transmission such as HIV-1 (Looker et al., 2017) and differences in the structure of sexual networks (Omori and Abu-Raddad, 2017). It could be that HSV-2 prevalence is a product of slowly spreading pandemics with regions experiencing different epidemic stages. In some parts of the world, immune suppression associated with HIV-1 could have increased the transmission of HSV-2. HSV-2 infection is associated with a three-fold increased risk of HIV-1 acquisition among both women and men globally, suggesting that, in areas of high HSV-2 prevalence, a high proportion of HIV-1 is attributable to HSV-2 (Freeman et al., 2006). Different rates of HSV-1 infection may also contribute to differences in the pattern of HSV-2 infection across regions as a consequence of cross-immunity (Looker and Garnett, 2005).

Currently, there is neither cure for HSV-2 persistent infection nor effective vaccines. HSV-2 pathology can be mitigated or modulated through current antiviral treatment, but latent infection cannot be eliminated (Gupta et al., 2007, Johnston et al., 2014, Johnston et al., 2012, Looker et al., 2015).

2.2. Morphology and structure

Herpes viruses have a unique four-layered structure: i) a core containing the large, double-stranded DNA genome is enclosed by ii) an icosapentahedral capsid which is composed of capsomers. The capsid is surrounded by iii) anamorphous protein coat called the tegument which is encased in a iv) glycoprotein-bearing lipid bilayer envelope.

i) **Core**: The core consists of a single linear molecule of double strand DNA in form of a torus.

ii) **Capsid**: Surrounding the core is an icosahedral capsid with 100nm diameter capsomeres.

iii) Tegument: Between the capsid and envelope is an amorphous, sometimes asymmetrical, feature named the tegument. It consists of viral enzymes, some of which are needed to take control of the cell's chemical processes and subvert them to virion production, some of which defend against the host cell's immediate responses, and others for which the function is not yet understood.

iv) Envelope: The envelope is the outer layer of the virion and is composed of altered host membrane and a dozen unique viral glycoproteins.

The virions are spherical particles 150-200 nm in diameter with glycoprotein spikes protruded from each virion, making their full diameter about 225 nm. The nucleocapsid occupies an eccentric position: on one virion side, it is close to the envelope; on the other side, it is 30-35 nm apart from it. The tegument is an amorphous layer with some structured regions containing 7 nm with filaments opposed to the membrane. The virion consists of 40 proteins of viral and cellular origin, 10 of which are glycosylated. The outer envelope consists of lipid bilayer and 11 glycoproteins (gB, gC, gD, gE, gG, gH, gI, gJ, gK), membrane gL, and gM, and at least two unglycosylated membrane proteins (UL20 and US9). The lipid bilayer is formed by cell membrane during virus egress by exocytosis.

Three types of capsids can be isolated from infected cells: i) capsids (pro-capsids) lack both scaffold proteins and viral DNA; ii) capsids do not contain viral DNA but contain the protein scaffold for it; iii) capsids contain the viral genome.

The linear DNA circularizes in the absence of protein biosynthesis after entering from the nucleus of infected cells. The genes are characterized as either essential or dispensable for growth in cell culture. Essential genes regulate transcription and are needed to construct the virion. Dispensable genes for the most part function to enhance the cellular environment for virus production, to defend the virus from the host immune system and to promote cell to cell spread. The large numbers of dispensable genes are in reality required for a productive *in vivo* infection.

The HSV-2 genome is large (155 kbp) and structurally complex, consisting of two unique regions (UL and US) flanked by inverted repeat elements (TRL-IRL and IRS-TRS), arranged as ab-UL-b′a′c′-US-ca (Cortini and Wilkie, 1978, Roizman, 1979) (**Fig. 2**). The *a* sequence is a directly repeated sequence of some 254 bp at the genome termini, with one or more copies in the opposing orientation (the *a′* sequence) at the internal joint between IRL and IRS (Davison and Wilkie, 1981). Of the 74 known ORFs, UL contains 56 viral genes, whereas US contains only 12. Transcription of HSV genes is catalyzed by RNA polymerase II of the infected host (McGeoch et al., 2006). Due to the presence of

inverted repeats, the U_L and U_S units of the genome can be inverted relative to one another to yield four linear isomers. However, it was shown that neither the presence of internal repeats nor the orientation of the genome components affect viral viability in Vero cell line (Baldwin et al., 2013).

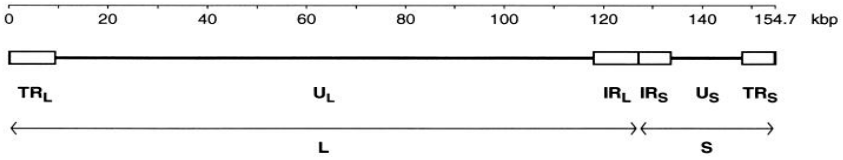

Figure 2. Organization of the genome of HSV-2. The linear double-stranded DNA is represented at the top. The unique portions of the genome (U_L and U_S) are shown as heavy solid lines, and the principal repeat elements (TR_L, IR_L, IR_S, and TR_S) are shown as open boxes. As indicated, TR_L, U_L, and IR_L are regarded as comprising the L region, and IR_S, U_S, and TR_S are considered as comprising the S region.

2.3. Viral cycle

The entry mechanism is due to the fusion of the viral envelope with the plasma membrane and further transport of the viral capsid to the nucleus. The initial and essential step is the interaction of surface viral glycoproteins with cell surface receptors. The interaction between four glycoproteins, gD, gB, and the heterodimer gH/gL, is required for viral entry into the host cell by fusion of the viral outer envelope with the plasma membrane (Avitabile et al., 2009, Cooper and Heldwein, 2015, Heldwein, 2016).

First interaction of the virion with the cell surface is mediated by gC and gB of HSV-2, which interact with cell surface glycosaminoglycans, in particular requires viral gB binding to unmodified heparin sulfate (HS) (Akhtar and Shukla, 2009, Spear, 2004, Tiwari et al., 2015), starting a phenomenon for the transport of extracellular virus particles, termed “viral surfing”. In the next step, the process is triggered by conformational changes in viral gD, which can bind to the receptors of three types: nectin-1 and nectin- 2, herpes virus entry mediator (HVEM), and 3-O-sulfated heparan sulfate (3-O-S-HS), this interaction causes an hemifusion state (Hu et al., 2017, Petermann et al., 2015, Fujimoto et al., 2017). Alteration in gD conformation then mobilizes the heterodimer gH and gL and gB to initiate the fusion process at the cell surface. In addition to binding of gD to cellular receptors, it triggers membrane fusion by interaction with the gB and gH/gL complex (**Fig. 3**).

In the last decade, an additional pathway by which the HSV-2 enters the cell through endocytosis of the enveloped virion followed by fusion of the envelope with intracellular vesicles and/or a phagocytosis-like uptake have also been proposed. Independently of the mechanism of uptake (endocytosis or phagocytosis-like), the virion envelope eventually fuses with the vesicular membrane. It is suggested that interactions similar to the one described above for the plasma membrane facilitate

fusion with the vesicular membrane and result in the release of viral capsid into the cytoplasm (Arii et al., 2009, Clement et al., 2006, Nicola and Straus, 2004). A gD receptor has been colocalized with endosomal markers and electron micrographs show the fusion and exit of nucleocapsids from the intracellular vesicles. The choice between endocytosis and fusion at the cellular membrane appears to be cell type-dependent. It is speculated that one or more envelope glycoproteins and the availability of a unique set of corresponding host receptors dictate the mode of entry.

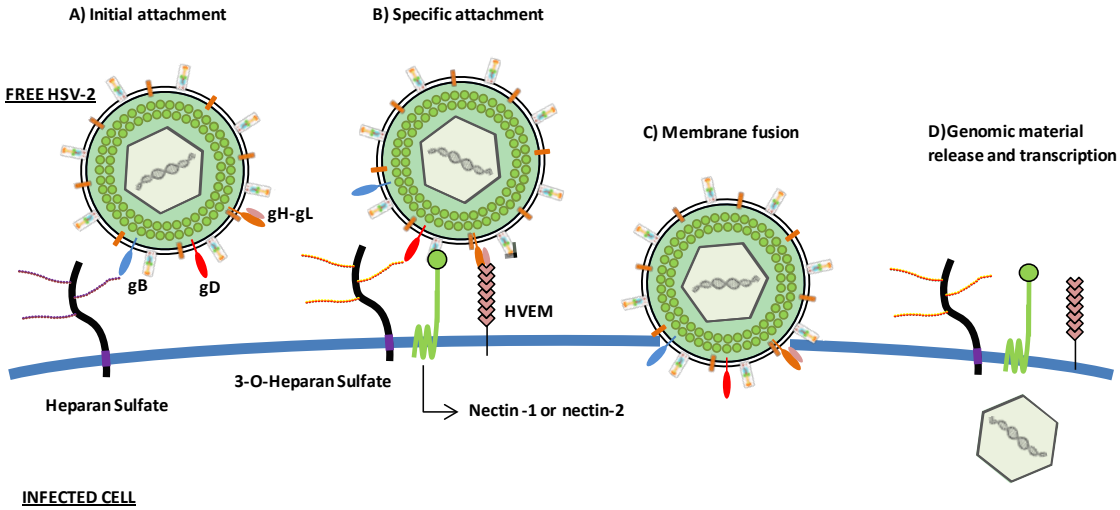

Figure 3. Schematic representation of heparan sulfate and 3-O sulfated heparan sulfate during HSV-2 entry to the host cell. A) Initial virus attachment to unmodified HS, which is mediated by HSV-2 gB, followed by a process of surfing which increases viral attachment strength. **B)** This interaction leads to HSV-2 gD to interact with at least one of the following co-receptors: the modified form of HS (3-OS HS), Herpes virus entry mediator (HVEM) or Nectin-1 or 2, which promotes virus-cell membrane hemifusion state. **C)** Alteration in gD conformation then mobilizes the heterodimer gH and gL and gB to initiate the fusion process at the cell surface and **D)** release of viral genomic material.

After entering of the viral particle into the host cell, which is the capsid coated with the tegument, it is transported to the nuclear pores with subsequent transfer into the nucleus. The transport is mediated by the cytoplasmic protein dynein (Sodeik et al., 1997). Very large tegument, UL36 and UL37 proteins play a role in a linking chain between the motor proteins and the capsid. However, if the capsids are not coated with the tegument or are coated with tegument that contains other proteins; do not bind the motor proteins. When the outer envelope of the virion is fused with the cell membrane, the outer tegument proteins remain bound to the membrane. Therefore, the proteins of the inner tegument are exposed to the capsid surface and bind to dynein (Radtke et al., 2010). The capsid binds to the nuclear pore complex in such a way that its unique “portal”-containing vertex sits just above the nuclear pore. Presumably, all these interactions are needed for transport of the viral DNA by the nuclear import pathway mediated by importin β (Copeland et al., 2009). Transcription and replication

of the viral genome, as well as the assembly of progeny capsids, take place within the nucleus. However, the infection comes with the reorganization of the nucleus causing an increase of its size, disruption of the nucleolus (Calle et al., 2008) and chromatin condensation and subsequent destruction of the latter and the nuclear lamina (Simpson-Holley et al., 2005) in the late steps of the HSV-2 infection.

2.4. Clinical course

Genital HSV-2 infection occurs by inoculating the virus on mucosal surfaces or through small skin wounds. Primary infection with HSV-2 is characterized by viral replication at the site of infection, followed by retrograde axonal transport of the virus to the corresponding sensory ganglia where infection can follow two very different pathways (Valyi-Nagy et al., 1991, Kosz-Vnenchak et al., 1993, Farrell et al., 1994).

Latent Infection: In some neurons, the virus expresses productive cycle genes, replicates, and causes host cell death, whereas, in other neurons, the virus establishes a latent infection.

Reactivation: Occasionally, the virus is reactivated and when this occurs, it travels back to epithelial cells to form herpetic lesions. Reactivation can be caused by numerous factors, including stress, heat, fever, hormonal changes, menstruation, immune depression, and physical trauma to the neuron. The episodes of HSV-2 disease, especially primary infections are characterized by fever, headache, malaise, and myalgia. The predominant local symptoms are pain, dysuria, urethral and vaginal discharge and painful inguinal lymphadenopathy. Skin and mucosal lesions may be in different stages of evolution: vesicles, pustules and painful erythematous ulcers (Thellman and Triezenberg, 2017).

Despite the efforts, no antiviral agent has been shown to be useful in the prophylaxis of primary infection, although acyclovir, valacyclovir and famciclovir may be used as suppressive therapy to reduce the frequency of recurrences or as episodic therapy to shorten the duration of injury. All of them are analogous of guanine and lifelong treatments. However, prolonged therapy with the available anti-HSV-2 drugs has induced the emergence of drug-resistant virus (Hassan et al., 2017, Mitterreiter et al., 2016).

3. Respiratory Syncytial Virus

3.1. Epidemiology

Respiratory syncytial virus (RSV) is a mRNA virus belonging to the family *Paramyxoviridae*, within which most of the common respiratory viruses are included. The family *Paramyxoviridae* consists of four general groups, three of which form the subfamily *Paramyxovirinae* composed of Paramyxoviruses, containing human parainfluenza virus types 1 and 3; Rubulaviruses, which include the mumps and parainfluenza virus types 2 and 4, and Morbilliviruses, represented by the measles virus. The species RSV belongs to the fourth genus, Pneumovirus, of the subfamily *Pneumovirinae*.

There are two subtypes of RSV, A and B, which can circulate simultaneously in the community during the winter. Antigenic and molecular analyses of the relationships between strains circulating simultaneously on the same mean and in several regions of the world showed that the strains within each group have genetic diversity. These strains appear to be distributed worldwide, and in each epidemic was detected the simultaneous presence of several of them, both group A and B, in varying proportions according to the season, geographical area and year. It is unclear which of the two subgroups is most virulent. Some studies point to a greater severity in group A, RSV-associated infections, at least in infants, although the epidemiological and clinical implications of the different nucleotide sequences have not yet been adequately elucidated (Nair et al., 2010).

Infections generated in the respiratory tract represent one of the main causes of diseases during childhood, mainly during the lactation (Reis and Shaman, 2016). RSV is the main pathogen associated with lower respiratory tract infection (LRTI) worldwide (Berkley et al., 2010, Hall et al., 2009), highly associated with infections of the lower respiratory tract in neonates up to two years (Hall et al., 2009). RSV infects almost all children within the first two years of life and is the most common cause of respiratory infection and bronchiolitis requiring hospitalization for infants under the age of one (Hall et al., 2009). Acute lower respiratory infection is the leading cause of global child mortality. In 2005 there were about 34 million new LTRI and episodes of RSV-associated ALRI in children up to 5 years of age and at least 4 million hospitalizations caused by RSV. Among them, 0.15-0.2% of children infected with RSV died, most of which were from developed countries (Nair et al., 2010). One study in children younger than 3 years old revealed that at least 86% of children were infected with RSV although only about 35% showed pathology (Reis and Shaman, 2016).

In addition, the burden of RSV on the elderly is also high. Sometimes in developed countries, RSV hospitalization rates are higher in individuals 75 years old and older than in children one to 4 years

old. Especially on people with heart or chronic lower respiratory disease, which makes them potential priority groups for a RSV prophylaxis and treatment (Samaras et al., 2010, Goldstein et al., 2015).

Prompt treatment of RSV is indispensable to avoid damage to lung tissue, complications from sustained oxygen deprivation, and the potential development of reactive airway disorders. Currently, there is no effective cure for RSV infection and the treatment is reduced to alleviate the symptoms (Ralston et al., 2014, Poets, 1998, Walsh and Rothenberg, 2015). Antiviral treatment against RSV is limited to the use of Ribavirin. However, Ribavirin presents controversies due to its side effects as well as its efficiency (Burrows et al., 2015, Roberts et al., 2010). In addition, a humanized monoclonal antibody, Palivizumab, has been used as immunoprophylactic therapy against RSV infection, but only in high-risk patients, such as preterm infants or immunosuppressed patients (Chow et al., 2017, Meissner et al., 1999). Palivizumab is an epitope of the antigenic site A of the fusion protein F of RSV. This monoclonal antibody prevents the cell from being infected by RSV avoiding the fusion process. Treatment with Palivizumab consists of monthly intramuscular injections, prior to RSV exposure (Wu et al., 2008). The main problems associated to Palivizumab are its high cost and the scheduling of immunoprophylaxis, which presents considerable restrictions on its use (Sanchez-Luna et al., 2017).

However, while there is currently no licensed vaccine for RSV, a vaccine candidate for pregnant women is undergoing clinical trial phase 3 (Hogan et al., 2017, Smith et al., 2017).

3.2. Morphology and structure

The RSV genome consists of a single, non-segmented, negative-sense RNA chain associated with viral proteins along its entire length, forming the helical nucleocapsid. The viral capsid consists of a lipid bilayer from the plasma membrane of the host cell, with surface glycoprotein spikes of 10-12 nm, separated from each other by 6-8 nm.

To date, 10 essential viral proteins have been characterized (**Fig. 4**), and viral RNA, consisting of 15,222 nucleotides transcribed in 10 polyadenylated monocistronic messengers, each of which codes for an essential polypeptide chain: the host cell binding protein G, the protein F responsible for the fusion of membranes and the formation of syncytia, phosphoprotein P, the polymerase L that make up the nucleotide (N), and the non-glycosylated proteins that are a small hydrophobic protein (-SH-) the virus capsule is associated with genomic RNA, and two non-structural proteins (NS1 and NS2), capable of inhibiting the action of interferon, present in very small amounts in the virions, but accumulated in the RSV infected cells (Dickens et al., 1984, Hirsh et al., 2014).

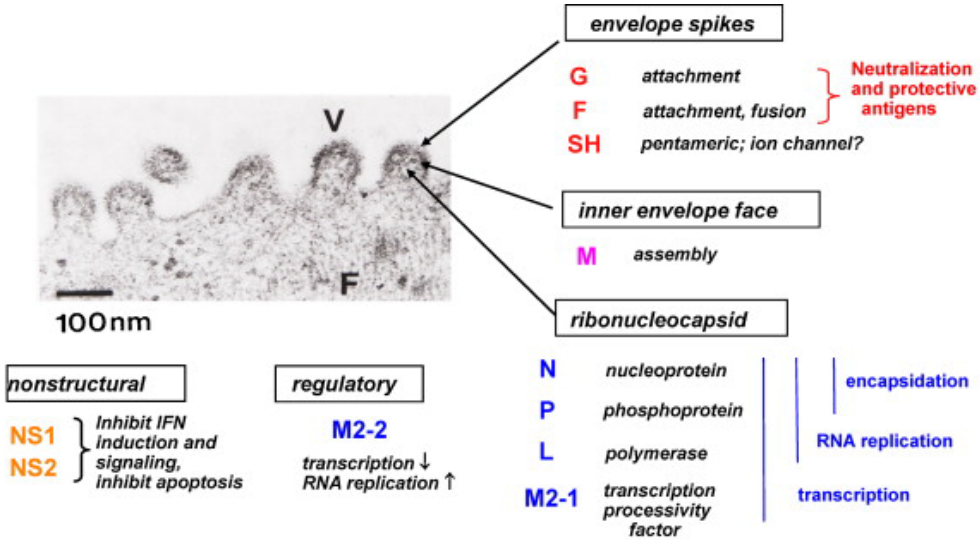

Figure 4. RSV proteins. Negatively-stained electron micrograph of budding RSV virions: V indicates a budding virion and F indicates filamentous cytoplasmic structures thought to be nucleocapsids. The locations of viral proteins in the virion, and their functions when known, are indicated. The viral proteins are as follows: G, attachment glycoprotein; F, fusion glycoprotein; SH, small hydrophobic glycoprotein; M, matrix protein; N, nucleoprotein; P, phosphoprotein; L, large polymerase protein; M2-1, product of the first ORF in the M2 mRNA; M2-2, product of the second ORF in the M2 RNA; NS1, nonstructural protein 1; NS2, nonstructural protein 2 (Collins and Melero, 2011).

The G and F envelope-associated proteins are the major antigenic determinants of RSV. G protein is related to virus adhesion to the cell and is predominantly related to a Th2 immune response, while protein F is related to virus entry and viral RNA insertion into the host cell, as well as syncytium formation (Brandenburg et al., 2000, Devincenzo, 2004, Dickens et al., 1984).

Protein F is structurally very similar to other F proteins of other *Paramyxoviridae*, concerning the localization of the hydrophobic domains and cysteine residues, as well as the proteolytic activation that results in the exposure of the hydrophobic fusion peptide. The F protein of RSV is accessible on the surface of the virus, is one of the most active proteins of this virus and plays a very important role in the formation of syncytia and has always been the preferred target for drug development antivirals. Protein F combines fusion and adhesion activities in the membrane and this is enough to produce respiratory epithelial infection (Collins and Melero, 2011).

Like other class I fusion proteins, the F protein is a trimer and is composed of an N-terminal F2 protein bound by one or probably two disulphide bridges to the transmembrane F1 protein. This form of the F protein is fully active and capable of causing cell fusion. Thus, initially, the F protein of RSV is a meta-

stable "pre-trigger" form, once it is activated a series of important and irreversible changes occur that especially affect the helical region "HRA", where it inserts the fusion peptide in the target cell (**Fig. 5**).

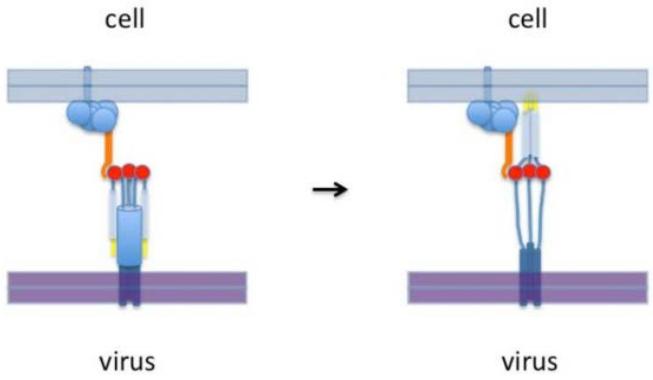

Figure 5. Model of RSV F-protein binding to nucleolin. On the left, the F-protein is shown in its trimeric pre-fusion conformation. The red circles are putative nucleolin binding sites. Nucleolin is shown in orange as part of a protein complex that includes proteins anchored to the membrane by either a transmembrane domain or a GPI anchor. Only one nucleolin molecule is shown binding the F-protein trimer for clarity but in this model as many as three could bind at once. To the right the F-protein is shown in the “extended” conformation with fusion peptides (yellow) inserted into the cell membrane. After this step virus-cell membrane fusion would proceed without nucleolin.

G protein is not structurally similar to hemagglutinin and hemaglutinin-neuraminidase proteins. The specific receptors for RSV are not well understood. Cell surface glycosaminoglycans (GAGs), in particular HS, are very important for RSV infection. Both proteins F and G are capable of binding GAGs thus contributing to cell binding. Although there are numerous mechanisms by which the immune response can be altered against the RSV, the role of protein G in these immunological changes is becoming increasingly important. The focus has been on the CX3C region which has very low immunogenicity. Studies target protein G as a target for therapeutic interventions to reduce RSV morbidity in short to medium term. Protein G has become a very promising target for RSV therapy, since it is involved in the innate immune response. In experimental models in mice, a monoclonal Ab against the protein G of RSV proved to be effective against the infection and decreased VL. Recently, a high affinity of the monoclonal antibody against the K epitope of the protein G of RSV has been described and it is assumed that these data may have clinical applications in the next years. In fact, it is considered that a vaccine strategy could be the neutralization of protein G (Kauvar et al., 2010).

The F2 subunit of protein F is responsible for species-specific infection while protein G is not involved in the specificity of RSV infection. Thus, only the F2 subunit is responsible for the specificity of RSV infection. This makes the protein F very similar to the spiked proteins of other viruses that require specific receptors for adhesion and fusion, such as HIV-1 or influenza virus and hemagglutinin. The

identification of F2 as the necessary companion of the RSV specific entry should facilitate the identification of other receptors and provide the basis for the development of specific tools that interfere with the infection of this virus and that are effective in the treatment of this disease (August et al., 2017, Wang et al., 2017, Boyoglu-Barnum et al., 2017).

3.3. Viral cycle

Interactions between RSV envelope glycoproteins gG and gF and cell surface heparan sulfate proteoglycans (HSPGs) are required for binding and entry of RSV into host cells (Escribano-Romero et al., 2004, Feldman et al., 1999, Harris and Werling, 2003, Krusat and Streckert, 1997, Martinez and Melero, 2000, Taylor et al., 2014). At the molecular level, sulfate groups with negative charges of HSPG interact with the positive charges of the amino acids present in the heparin binding domains (HBD), belonging to the gG of RSV (Feldman et al., 2000). The first stage of infection consists of an interaction between the RSV binding gG and the cell surface proteoglycans, mainly with HSPG, which initiates infection. Once this first interaction is performed, the fusion gF undergoes a series of conformational changes, mainly the formation of a homotrimer, and the insertion of the fusion peptide into the target cell membrane (Weisshaar et al., 2015). In addition, a HBD has been identified in gF, suggesting that the interaction between HSPG-HBD is a common interaction between RSV-mediated proteins (Donalisio et al., 2012). This binding promotes fusion of the outer sheets of the bilayers (hemifusion stage). Therefore, a strong interaction occurs, and completes fusion of the RSV and cell membranes, allowing the release of the genetic material into the host cell.

Transcription of the genome and replication occur simultaneously in the cytoplasm and 4-6 h after inoculation of the virus already detects mRNA and RSV proteins at the intracellular level. The infected cells develop cytoplasmic inclusion bodies that become visible as early as 12 h after infection (Lindquist et al., 2011, Lifland et al., 2012).

Inclusion bodies are believed to be the places where mRNA is synthesized, although more recently it has been shown that inclusion bodies are capable of inhibiting the cellular response to infection (Rincheval et al., 2017).

4. Nanotechnology

The prefix *nano* derives from the Greek word for dwarf. One nanometer (nm) equals 10^{-9} m, or approximatly the width of 6 carbon atoms or 10 water molecules. A human hair is approximately

80,000 nm wide, and a red blood cell is around 7,000 nm wide. Atoms are smaller than 1 nm, whereas many molecules including some proteins have sizes of about 1 nm and are even larger (Whitesides, 2003).

Nanotechnology is the science and engineering that comprises the design, synthesis, characterization and application of materials and devices whose functional organization in at least one dimension is on the nanometer scale. This new technology has allowed the development of different tools and materials such as nanocrystals, nanocapsules, nanoparticles (NPs), etc. with exceptional properties and multiple applications in various areas of research, ranging from catalysis to biomedicine.

4.1. Nanomedicine

The first nanosystems applied in medicine were introduced to improve the efficacy of the already used drugs (Schutz et al., 2013). Nanoparticles present specific properties such as:

i) Small particle size, which can facilitate drug delivery into anatomically privileged sites (Parboosing et al., 2012, Kumar et al., 2012).

ii) Large surface area to volume ratios, which together with their multifunctionality or the chemical characteristics of their surface, can have significant implications to increase the solubility of compounds or acting as effective vectors for transport and release of molecules (McNeil, 2011).

iii) Modified surface charges, to facilitate cellular entry across the negatively charged cellular membrane (Caron et al., 2010, Petros and DeSimone, 2010), make NPs ideal tools for viral treatment.

It has been shown that some NPs present **biomimetic properties** (Gagliardi, 2017, Sanvicens and Marco, 2008, Bowman et al., 2008), which results in intrinsic antiviral activity. One clear example of these are dendrimers (Sepulveda-Crespo et al., 2017, Mallipeddi and Rohan, 2010).

The posibility of **drug encapsulation** (Chiappetta et al., 2011, Kumar et al., 2012), functionalization by the formation of stable structures (Goldberg et al., 2007), or modifications with polymers such as poly(ethylene glycol)(McNeil, 2011) can lead to optimized drug dosing and improved delivery by increasing stability and drug retention times (Gabizon et al., 1994, Santos-Martinez et al., 2014).

It is generally assumed that **drug delivery** can be vastly improved by decorating NPs with targeting moieties to increase specificity towards desired sub-cellular compartments, cell types or target tissues (McNeil, 2011, Muthu and Singh, 2009).

NPs can have various chemical compositions and shapes and can be classified according to the way drugs are delivered or by the characteristics of the matrix of which it is composed. The most common

types of nanocompounds used in nanomedicine, based on their composition are: **i)** nanocapsules (Mora-Huertas et al., 2010); **ii)** nanosphere (Baram-Pinto et al., 2012); **iii)** liposome (Zhong et al., 2012); **iv)** micelle; **v)** dendrimers (Dutta et al., 2007); and **vi)** gold NPs (Giljohann et al., 2010) (**Fig.6**). Among all the NPs types, this work is focussed on the use of dendrimers as antiviral agents.

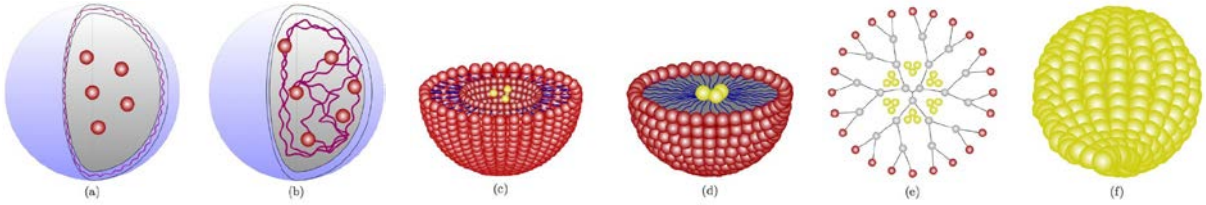

Figure 6. Most common types of nanocompounds used in nanomedicine, based on their composition are: **(a)** nanocapsules, **(b)** nanosphere, **(c)** liposome, **(d)** micelle, **(e)** dendrimers, and **(f)** gold NPs.

4.2. Dendritic structures: Dendrimers

There are different subsets of dendritic systems. They are characterized by a high degree of branching, but differ in the degree of arrangement of their skeleton: **i)** polydispersed skeletons, such as hyper branched polymers, dendrigrafts and dendronized polymers; and **ii)** monodisperse skeletons such as dendrimers and dendrons (**Fig.7**).

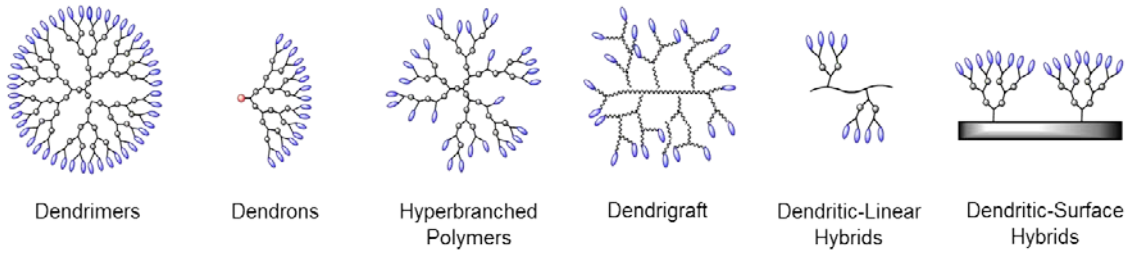

Figure 7. Schematic overview of the different macromolecules belonging to the dendritic family.

Dendrimers (dendri = tree; mer = branching) are nanometric macromolecules characterized by high branching, defined size and three-dimensional structure. Dendrimers are monodisperse particles, which are highly packed spherical structures. The structure of these materials has a high impact on their physical and chemical properties (**Fig. 8**).

In the field of biomedicine, biocompatible, water-soluble systems that do not cause toxicity in the organism are required. The stability and synthecic flexibility of dendritic systems, together with their high local concentration of functional groups, make them ideal candidates for a possible use in various biomedical applications.

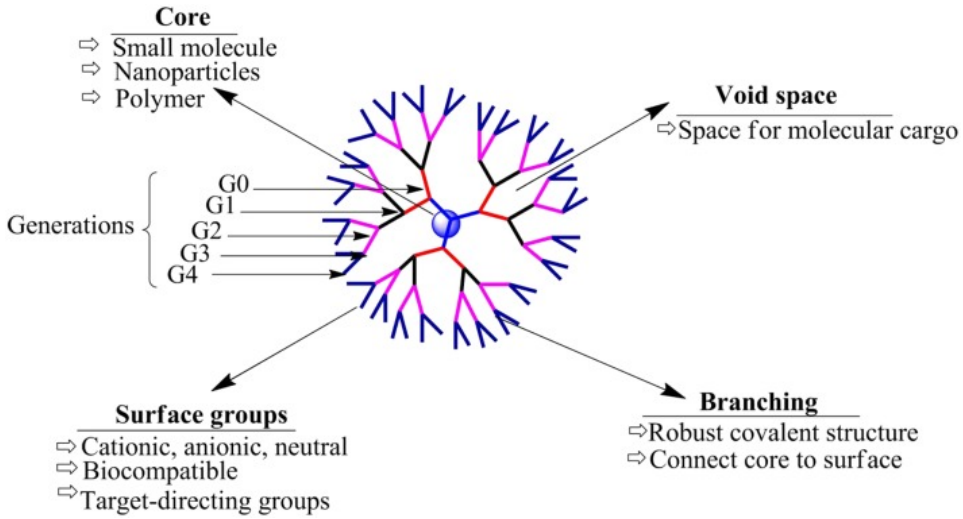

Figure 8. Schematic of the typical structure of a dendrimer: The different generations of a dendrimer are determined by its progressive higher level of branching.

4.2.1. Properties

The controlled synthesis of dendrimers enables the assembly of simple structures as branching from a central initiator core, and can result in different generations of dendrimers based on their "layers". The layers of the dendrimer may define its nomenclature as well as their generation. The dendrimers generation can be defined by the number of repeated layers forming the dendrimer where generation 0 (G0) describes the dendrimer after the first reaction cycle and the successive addition of repeated layers leads to higher generations.

Most dendrimers have a diameter ranging from 1-20 nm. However, since the size of dendrimers is obtained by a controlled synthesis in a stepwise growth for each generation, the diameter of dendrimers increases linearly at a rate of around 1nm/generation, while the surface groups raises exponentially for each generation.

The type of core and branches can be designed to generate a huge variety of dendrimers with different shape and size. Furthermore, the branches of the dendrimer may be functionalized with various chemical groups that determine its biological and pharmacological properties. As a result of their unique behaviour, dendrimers have been used in a wide variety of industrial and biomedical applications and have become a unique tool for the synthesis of new antiviral agents (Klajnert and Bryszewska, 2001, Svenson and Tomalia, 2005, Lazniewska et al., 2012, Parboosing et al., 2012, Tomalia and Khanna, 2016). In addition, unlike other smaller molecules, due to their hyperbranched structure they can interact with their targets in a multivalent manner.

4.2.2. Synthesis

Dendrimers are generally prepared using either divergent method or convergent one (**Fig. 9**). There is a fundamental difference between these two construction concepts (Svenson and Tomalia, 2005).

The **divergent method** is the dendrimers self-assembly from initiator core to outward by Michael addition. Each step of Michael addition must be a complete reaction and should not give rise to mistakes in the synthetic procedure, avoiding trailing generations. Although, the divergent method could synthesize higher generations and dendrimers with large molecular weight, it still has many shortcomings such as rigorous reactive conditions and rough separation products from reactants.

The **convergent method** was developed as a response to the weaknesses of the divergent synthesis. The convergent method performed initial reaction based on small molecules from outside to inner and eventually attached to the focal point. When the growing branched polymeric arms, called dendrons, are large enough, they are attached to a multifunctional core molecule. This method basically involves attachment of the outermost functional groups to an inner generation and the attachment of the inner generations to the core. The structural units before the final attachment to the core are called “wedge”. Each wedge can have different functional groups at the periphery. Each generation of dendrimers involves less active sites, so their properties are quite different between the reactant and final product. The convergent method makes it much easier to remove impurities and shorter branches during the synthetic procedure, so that the final dendrimer is more monodisperse. However, the size of dendrimers is gradually limited around crowed centre core.

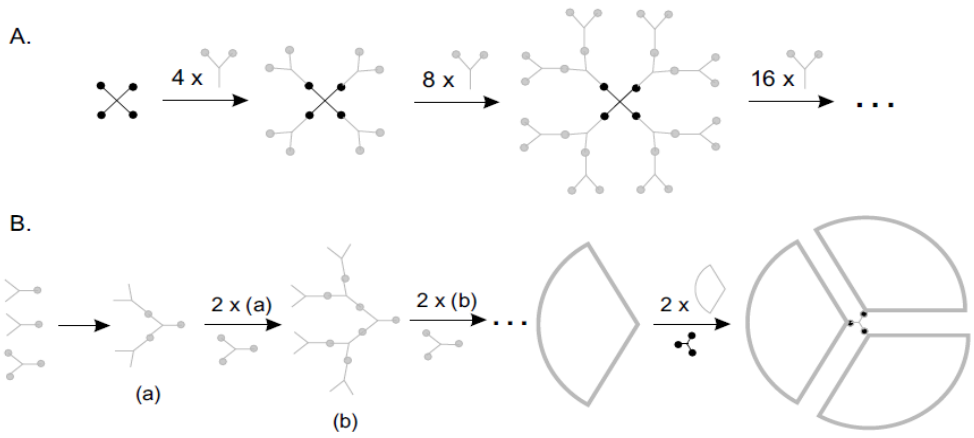

Figure 9. (A) The divergent growth method. **(B)** The convergent growth method.

A series of accelerated growing methods for dendritic compounds are gradually brought up, such as supernuclecus, superbranched monomer, double index growth and two-step methods. These methods

summarized the former typical methods and prepared new dendrimers with higher generations and regular structures. In addition, click chemistry including Diels-Alder reactions and Thiolyne reactions have been employed to synthesize polyphenylene dendrimers (Rejinold et al., 2011, Ma et al., 2013).

4.2.3. Polyanionic carbosilane dendrimers

According to their chemical nature there are different types of dendrimers. Among them, the most common are carbon/oxygen-based dendrimers (polyether, polyester, glycodendrimers), chiral dendrimers, metallodendrimers, derivatives of polyamidoamines dendrimers (PAMAM), derivatives of poly (propylene imines) (PPI), peptide dendrimers, polylysine dendrimers (PLL), polyamidoamineorganosilicon dendrimers (PAMAMOS), hybrid dendrimers, silicon-based dendrimers, triazine dendrimers or those of carbosilane structure (Klajnert and Bryszewska, 2001) (**Fig. 10**).

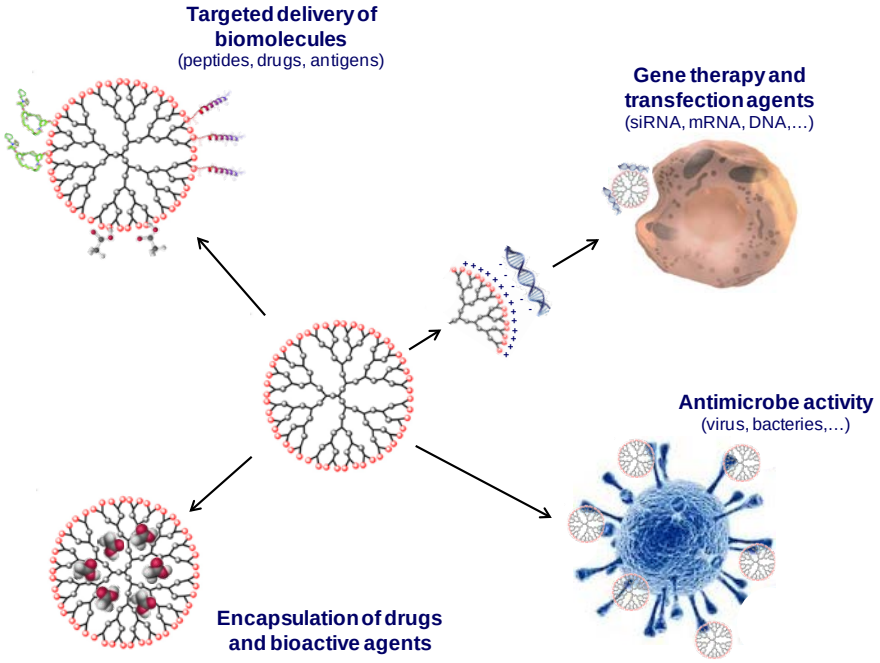

Figure 10. Schematic representain of the different applications of dendrimers on biomedicine.

Polyanionic carbosilane dendrimers have a skeleton based on carbon and silicon and differ from the other dendrimer groups in the great apolarity of their central nucleus and in the high mobility of the dendritic branches, which makes them excellent candidates for biomedical application. These dendrimers have been widely used in nanomedicine: i) for the synthesis of agents with antiviral activity against sexually transmitted pathogens; ii) as carriers for chemical drugs; iii) for peptides delivery; iv) for gene silencing; v) as antibacterial agents; vi) in cancer therapy; and vi) for prionic diseases and Alzheimer disease. Anionic dendrimers are mostly compatible for clinical applications, such as their use as microbicides.

HYPOTHESIS & OBJECTIVES

Sexually transmitted infections are a major global cause of acute diseases, infertility, mobility and death with serious medical and psychological consequences for millions of men, women and infants. HIV-1 infection is one of the mayor health issues of the last decades. Despite a steady decline in new HIV-1 infections from the late 1990s to the present, yet 1.8 million people became HIV-1 infected in 2016. Sexual transmission is responsible for more than 80% of these new HIV-1 infections. The development of prophylactic strategies based on microbicides emerged as a promising option in the last years. However, after numerous unsuccessful research and clinical trials on topical microbicides, it has been found that *in vivo* ineffectiveness of these topical microbicides was not only due to the lack of adherence but also due to the induction of inflammation and cytotoxic effect. In addition, the semen-derived enhanced viral infection (SEVI) showed to capture HIV-1 virions promoting their adhesion to the target cells, increasing the ability of HIV-1 to infect human cells, regardless of the cell type. Two main objectives appear in this section:

- **Objective 1:** to evaluate the ability of several polyanionic carbosilane dendrimers with anti-HIV-1 activity to halt SEVI in combination with TDF or MVC *in vitro*.
- **Objective 2:** to perform a tough pre-screening to assess the biocompatibility of the sulfated second generation dendrimer G2-S16 formulated as topical microbicides in BALB/c mice, Zebrafish and human EpiVaginal tissue, prior to human clinical trials.

Although the emphasis has been on preventing HIV-1 infection, protection from other STIs is desirable in terms of avoiding diseases and associated consequences. Importantly, many STIs may increase vulnerability to HIV-1 infection (e.g., genital herpes infection facilitates the transmission of HIV-1). HSV-2 is the STIs with the highest global prevalence and appears frequently associated with other sexual infections. Consistent with this, the specific objective of this section was:

- **Objective 3:** to evaluate the *in vitro* and *in vivo* ability of several polyanionic carbosilane dendrimers with anti-HIV-1 activity against HSV-2 infection and exactly elucidate their mechanism of action and their possible combination with antivirals.

Although the transmission of STIs stands out as the greatest problem of unprotected sex, it is also needed to take into account the possibility of unintended pregnancies. Annually there are about 200 million pregnancies, of which 40% are unintended. The specific objective of this section was:

- **Objective 4:** the evaluate the potential of the combination of the dendrimer G1-S4 or G2-S16 with the spermicide PD, in order to know if it is possible to develop microbicidal gels of topical use for the prevention of STIs and unintended pregnancies.

The RSV is the leading viral cause of respiratory morbidity and mortality in infants and young children worldwide. The RSV is the major causal agent of bronchiolitis and diseases related to of the low respiratory track and it is estimated that 90% of children under 2 years of age have suffered some type of infection caused by this type of virus and 2% of the annual hospitalizations of children under 5 years of age are related to RSV. Despite the existence of drugs used in severe cases of RSV infection or as prophylaxis in high-risk patients, such as Palivizumab, the fact that there is no effective drug to deal with RSV shows the need for the development of a new treatment effective against this virus. Specifically:

- **Objective 5:** to develop a novel anti-RSV nanocompound by *in vitro* and *in vivo* based screening of polyanionic carbosilane dendrimers, to evaluate the anti-RSV activity and to characterize them by determining the time/site of antiviral activity in the RSV life cycle.

MATERIALS & METHODS

5. Materials

5.1. Dendrimers

Stable and water soluble polyanionic carbosilane dendrimers were synthesized according to methods reported by the Dendrimers for Biomedical Applications Group (BioInDen) of the University of Alcalá (UAH, Alcalá de Henares, Madrid, Spain). In this work, the eight polyanionic carbosilane dendrimers used were (**Fig. 11**): first-generation carboxylate-functionalized G1-C8 ($C_{72}H_{124}N_{16}Na_8O_{16}Si_5$, MW: 1794.20 g/mol); first-generation G1-S4, with 4 sulfated end groups ($C_{52}H_{101}N_{12}Na_4O_{16}S_4Si_5$, MW: 1509 g/mol); third generation G3-S16, with 16 sulfated end groups ($C_{256}H_{508}N_{48}Na_{16}O_{64}S_{16}Si_{29}$, MW: 6978.41 g/mol); second-generation G2-NF16, with 16 naphthylsulfonated end groups ($C_{184}H_{244}N_{24}Na_{16}O_{56}S_{16}Si_{13}$, MW: 4934.02 g/mol); second-generation sulfonate-functionalized G2-S16 ($C_{112}H_{244}N_8Na_{16}O_{48}S_{16}Si_{13}$, MW: 3717.15 g/mol); second-generation via-thiol-ene-synthetized G2-STE16 with 16 sulfonated end groups ($C_{144}H_{300}Na_{16}O_{48}S_{32}Si_{13}$, MW: 4558.92 g/mol); second-generation via-thiol-ene-synthetized G2-CTE16 with 16 carboxylated end groups ($C_{128}H_{236}Na_{16}O_{32}S_{16}Si_{13}$, MW: 3533.21 g/mol); and second-generation polyphenolic core-sulfonated G2-S24P ($C_{189}H_{402}N_{24}Na_{24}O_{75}S_{24}Si_{21}$, MW: 5954.36 g/mol). The batches of these dendrimers were dissolved in distilled water, and stock was generated to a final concentration of 1 mM. Working dilutions (μM) were obtained from the stock of dendrimers by diluting them in phosphate buffered saline (PBS; Lonza, Walkersville, USA) or nuclease-free water (Promega, Madison, WI; USA).

Table 2. Chemical and structural characteristics of polyanionic carbosilane dendrimers.

Dendrimer	Molecular Formula	Mw (g/mol)	Groups	Charges	Core
G1-C8	$C_{72}H_{124}N_{16}Na_8O_{16}Si_5$	1794.20	Carboxilate	8	Silicon
G1-S4	$C_{52}H_{101}N_{12}Na_4O_{16}S_4Si_5$	1509	Sulphate	4	Silicon
G3-S16	$C_{256}H_{508}N_{48}Na_{16}O_{64}S_{16}Si_{29}$	6978.41	Sulphate	16	Silicon
G2-NF16	$C_{184}H_{244}N_{24}Na_{16}O_{56}S_{16}Si_{13}$	4934.02	Naphthylsulfonate	16	Silicon
G2-S16	$C_{112}H_{244}N_8Na_{16}O_{48}S_{16}Si_{13}$	3717.15	Sulfonate	16	Silicon
G2-STE16	$C_{144}H_{300}Na_{16}O_{48}S_{32}Si_{13}$	4558.92	Sulfonate	16	Silicon
G2-S24P	$C_{189}H_{402}N_{24}Na_{24}O_{75}S_{24}Si_{21}$	5954.36	Sulfonate	24	Polyphenolic
G2-CTE16	$C_{128}H_{236}Na_{16}O_{32}S_{16}Si_{13}$	3533.21	carboxilate	16	Silicon

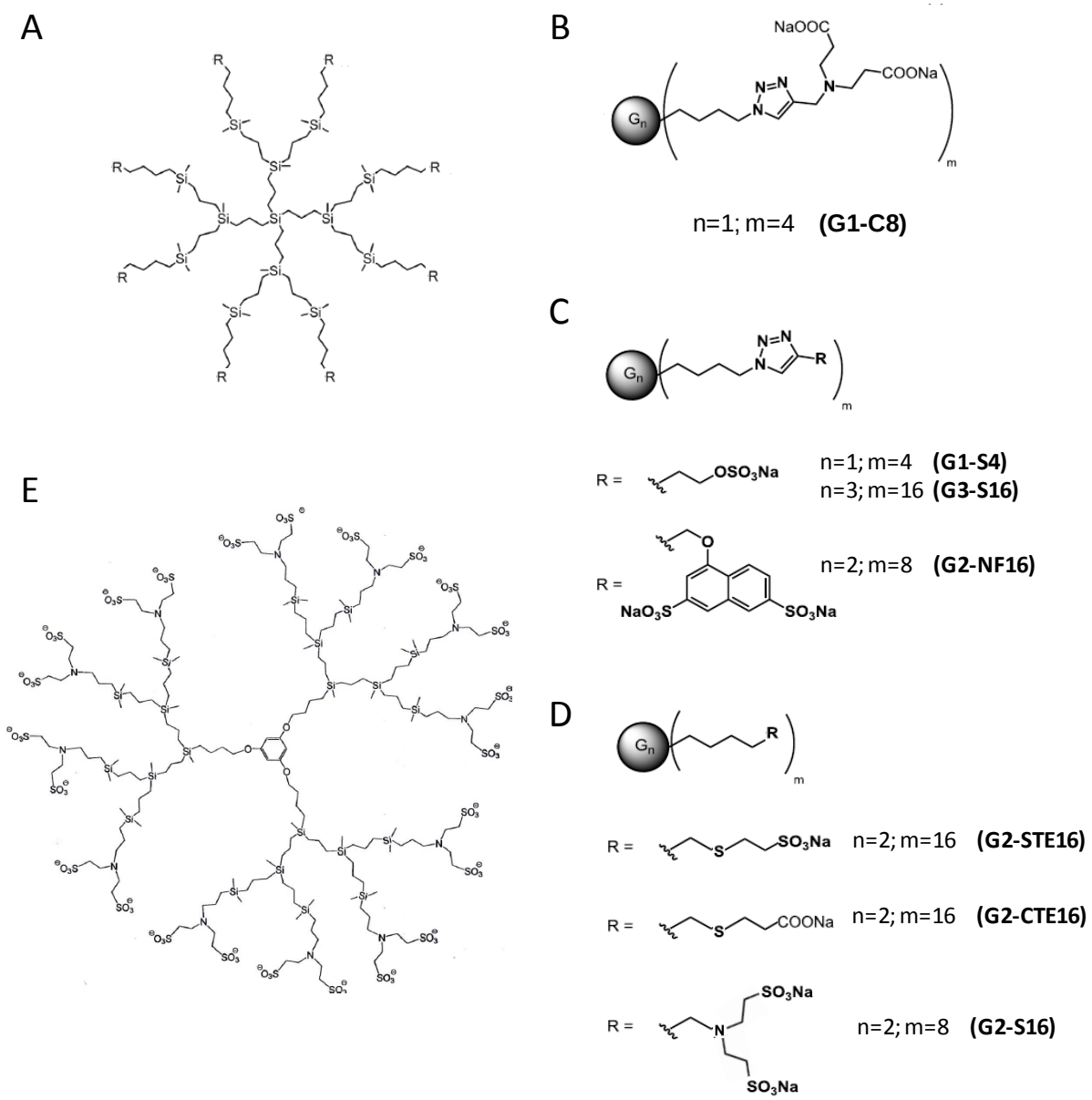

Figure 11. Structure of polyanionic carbosilane dendrimers. A) Representative scheme of a second-generation carbosilane dendrimer. **(B)** Structure of carboxylate-terminated dendrimers. **(C)** Scheme of sulfated and naphthylsulphonated decorated dendrimers. **(D)** Schematic structure of carbosilane dendrimers bearing sulfonate or carboxylate groups at their periphery synthetized by thiol-eneor Michael addition chemistry. **(E)** Polyphenolic core-sulfonated carbosilane dendrimer of second-generation.

Polyanionic carbosilane dendrimer G2-STE16 was labelled with FITC for *in vivo* assays. G2-STE16 acts as an analogous of G2-S16 dendrimer. Labelling of anionic carbosilane dendrimers with fluorescein was achieved only in the case of the dendrimer whose functionalization was carried out by thiol-ene addition reactions (**Fig. 12**).

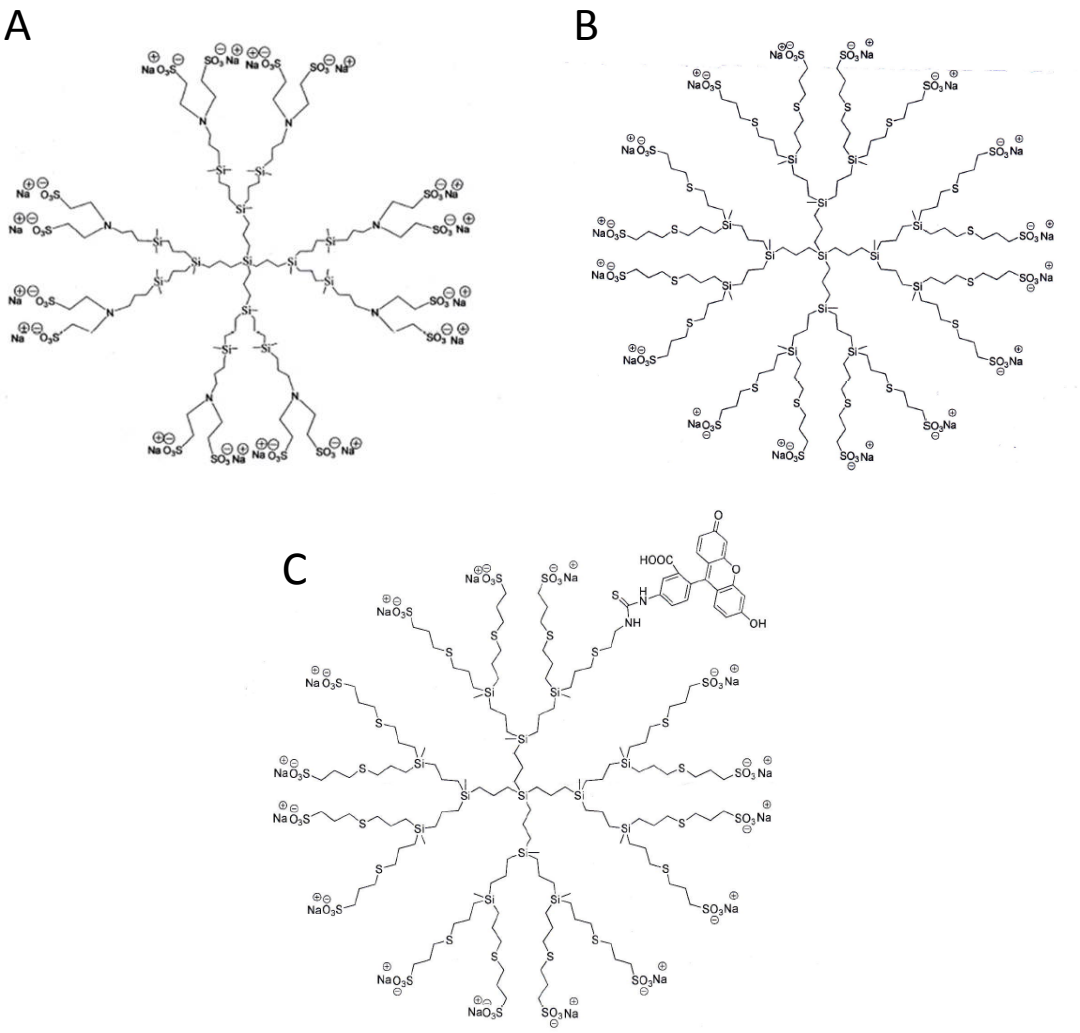

Figure 12. Chemical structure of second-generation of polyanionic carbosilane dendrimers. (A) The molecular formula of G2-S16 is $C_{112}H_{244}N_8Na_{16}O_{48}S_{16}Si_{13}$, and the molecular weightis MW: 3717.15 g/mol; (**B)** the molecular formula of G2-STE16 is $C1_{44}H_{300}Na_{16}O_{48}S_{32}Si_{13}$, and the molecular weight is MW: 4558.92g/mol. **(C)** G2-STE16–FITC dendrimer labelled with FITC.

The soft reaction conditions used during the functionalization enables the introduction of terminal sulphonate units and one amino group (-NH2) in the periphery of carbosilane dendrimers simultaneously, by the sequential addition of two different thiols over allyl terminated carbosilane dendrimers (**Fig. 13A**).

The terminal –NH2 groups present in this derivative can be bonded to fluorescein isotiocianate through the formation of a thiourea bond (**Fig. 13B**).

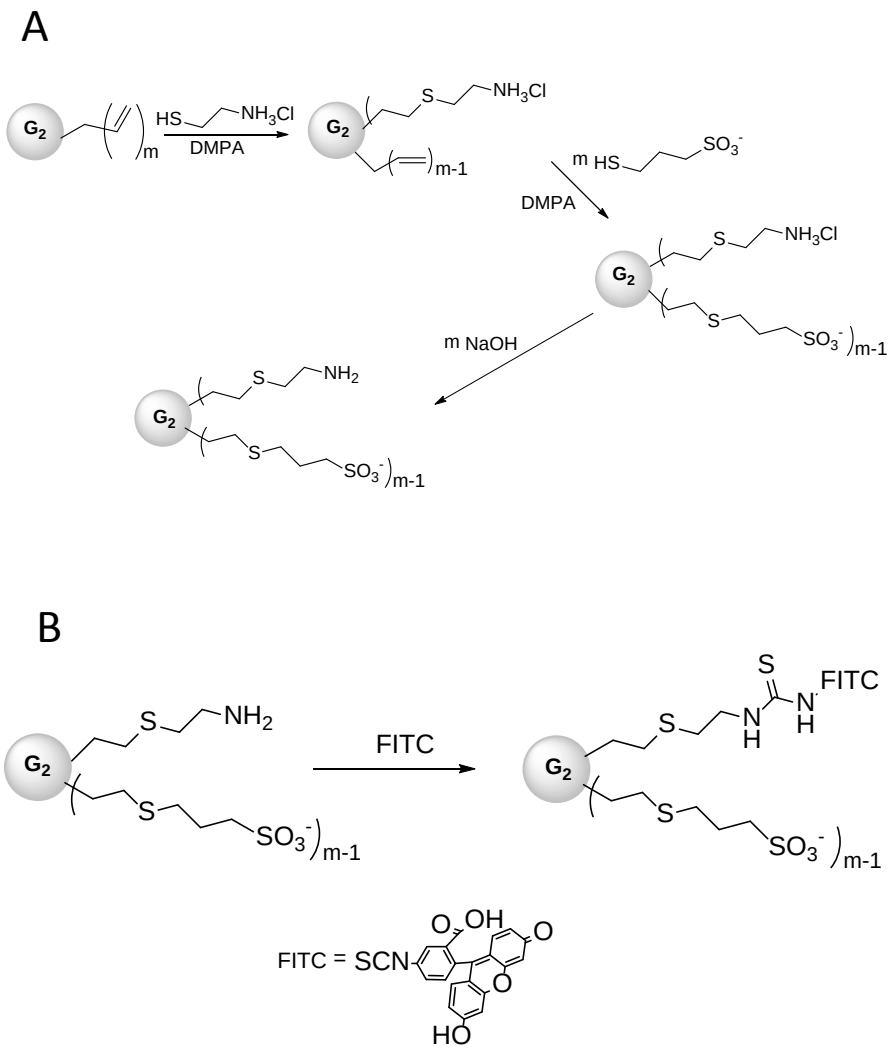

Figure 13. Scheme of the soft reaction conditions used during the functionalization of the dendrimers. A) Sequential addition of two different thiols over allyl terminated carbosilane dendrimers **B**) –NH2 groups present in this derivative can be bonded to fluorescein isotiocianate through the formation of a tiourea bond

5.2. Reagents and Antivirals

Throughout this report, different substances and ARVs have been used as controls for inhibition of viral replication. Among them are: ACV ($C_8H_{11}N_5O_3$, MW: 225,21g/mol; GlaxoSmithKline, Middlesex, UK), a guanosine analogue antiviral drug which works as RT inhibitor against HIV-1 and as polymerase inhibitor against HSV-2; TDF ($C_9H_{14}N_5O_4P$; MW: 287,2 g/mol;Selleckchem, Munich, Germany) a guanosine analogous RT inhibitor; and Maraviroc (MVC; $C_{29}H_{41}N_5F_2P$; MW: 513,7 g/mol; Selleckchem, Munich, Germany) a CCR5-receptor inhibitor. All compounds were freshly dissolved in dimethyl sulfoxide assays (DMSO,Sigma-Aldrich, St-Louis, MO, USA) or destillated water and filter sterilized.

Platycodin D (PD; $C_{57}H_{92}O_{28}$. MW: 1225.335 g/mol; Biomol, Hamburg, Germany) is a triterpenic saponin-like compound extracted from the root of the Platycodon grandiflorum plant, widely used in traditional Eastern medicine. PD has been studied primarily as a chemotherapeutic, anti-inflammatory and spermicidal agent (Wu et al., 2016, Zhu and Zhang, 2017, Zhang et al., 2017, Zare-Zardini et al., 2016, Lu et al., 2013).

Other chemicals also used in experiments throughout this report were: Dextran (Pm: $4.84x10^5$g/mol, Sigma-Aldrich, St-Louis, MO, USA), an inert molecule that is used as a negative control in cell toxicity or DMSO, used as death control in toxicity assays; 3,4-Dichloroaniline (3,4-DCA; $C_6H_5Cl_2N$, MW: 162g/mol; Merck, Darmstadt, Germany) used as a toxicity reference substance in the zebrafish test; Phytohaemagglutinin (PHA; Remel, Santa Fe, USA) used as a positive control of cell proliferation and used to induce activation of peripheral blood mononuclear cells (PBMC); Medroxyprogesterone acetate (Depo-Provera®, New York, NY, USA) hormone to synchronize the estrous cycle of female mice; Hydroxyethylcellulose (HEC) (NIH-ARRRP) gel (Sulky, Lab. Bohm, Fuenlabrada, Spain) as the vehicle of the dendrimers in the *in vivo* assays; Nonoxynol-9 (N9, $C_{33}H_{60}O_{10}$; Mw: 616.83g/mol) as a positive control of vaginal irritation in the *in vivo* experiments; Isoflurane ($C_3H_2ClF_5O$, MW: 184.5 g/mol, Forane®, Abbott, Peru) as an inhalation anesthetic; Ketamine ($C_{13}H_{16}NCLO$; MW: 237.72g/mol) and Xylazine ($C_{12}H_{16}N_2S$; MW: 220.33g/mol) in combination as a potent anesthetic.

5.3. Cell cultures

i. Primary cells

Blood samples were obtained from buffy coats from healthy anonymous donors from the Madrid transfusion centre following the recommendations of the current legislation (Royal Decree 1088/2005).

PBMC were isolated by a Ficoll gradient (Rafer, Spain) following the Spanish HIV HGM BioBank Standards operating procedure (SOP) (Garcia-Merino et al., 2009) (Madrid, Spain). The blood was diluted 1:1 with PBS and density gradient centrifugation was performed. After centrifugation, the area containing the PBMC was recovered, and several wash centrifugation cycles were carried out with PBS (10 min to 1500 r.p.m.) for the cleaning and purification. The resulting PBMC were resuspended in RPMI 1640 (Life technology, Spain) culture medium supplemented with 10% heat-inactivated fetal bovine serum (FBS), 1% L-glutamine and a cocktail of antibiotics (125 mg/mL ampicillin, 125 mg/mL cloxaciclin and 40 mg/mL gentamicin; Sigma-Aldrich, St-Louis, MO, USA). PBMC were cultured with

60 IU/mL interleukin 2 (IL-2, Bachem, Switzerland) and stimulated with 2 µg/mL PHA (Remel, Santa Fe, USA) for 72 h under culture conditions (37 °C in an atmosphere of 5% CO_2 and 95% relative humidity).

ii. Cell lines

Vero cell line from the American Type Culture Collection (ATCC, Teddington, UK), kidney epithelial cells derived from the monkey Cercopithecus aethiops were grown in complete DMEM medium (Lonza, Switzerland) supplemented with 5% FBS, 2 mM L-glutamine and a cocktail of antibiotics and (125 mg/mL ampicillin, 125 mg/mL cloxaciclin and 40 mg/mL gentamicin; Sigma-Aldrich, St-Louis, MO, USA).

HEC-1A, human endometrial carcinoma cells, a human epithelial cell line derived from an endometrial adenocarcinoma, was cultured in McCoy's 5A modified medium (Biochrom AG, Germany) supplemented with 10% FBS, 2 mM L-glutamine and antibiotic cocktail.

VK2/E6E7 (ATCC, Teddington, UK), a human epithelial cell line derived from the vaginal mucosa, was cultured in keratinocyte-serum free medium (Gibco, Loughborough, Leicestershire, UK), medium supplemented with recombinant human epithelial growth factor 0.1 ng/mL, (Invitrogen, Merelbeke, Belgium), 0.05 mg/ml bovine pituitary extract (Sigma-Aldrich, St-Louis, MO, USA) and 44.1 mg/L calcium chloride final concentration 0.4 mM.

HEK 293T (ATCC,Teddington, UK), a renal cell epithelial derived packaging line, was cultured in DMEM medium supplemented with 5% FBS, 2 mM L-glutamine and a cocktail of antibiotics.

TZM.bl cell line (National Institutes of Health [NIH] AIDS Research and Reference Reagent Program, Germantown, MD, USA), HeLa (ATCC, Teddington, UK) a human cervical epithelial carcinoma cell line, generated from the JC53-bl line, which expresses the CD4 and CCR5 markers, and contains the luciferase and ß galactosidase genes under the control of the LTR regions of the HIV-1 promoter, was cultured in DMEM medium with 5% FBS, 1% L-glutamine and a cocktail of antibiotics.

HEp-2 cell line (ATCC CCL-23), a human epithelial cell line derived from an epithelial carcinoma, was grown and maintained as monolayers in modified Dulbecco's Eagle's medium (DMEM) supplemented with heat-inactivated 10% FBS, 2 mM L-glutamine and a cocktail of antibiotics, in an environment at 5% CO_2 and 37 ºC.

A549 cell line (ATCC CCL-185), a human epithelial cell line derived from alveolar adenocarcinoma, was cultured in DMEM medium supplemented with 10% FBS, 2 mM L-glutamine and a cocktail of antibiotics.

Primary cells and cell lines were cultured in 96, 24, 12 or 6-well culture plates at different concentrations, depending on the type of experiment to be performed.

5.4. Viral isolates: growth and titers

The CCR5-tropic HIV-$1_{NL(AD8)}$ and CXCR4-tropic HIV-$1_{NL4.3}$ viral isolates, and HIV-$1_{89.6}$ CCR5/CXCR4 dual-tropic isolate (NIH AIDS Research and Reference Reagent Program, Division of AIDS, NIAID, USA) are laboratory tropic-isolates produced by transfection of plasmids pNL(AD8), pNL4.3 and p89.6, respectively, in the HEK293T cell line. Moreover, HIV-1 CH058 and THRO transmitted/founder viruses (T/F) were obtained and titrated using the same method pCH058.c/2960 and pTHRO.c/2626 plasmids. For this, plasmids containing the viral genome grown in *E. coli* (Plasmid MaxiPrep, QIAGEN®, Hilden, Germany) were isolated and purified. HEK293T cell culture dishes were transfected with 15 µg plasmid/plate using a calcium chloride transfection method (Sigma-Aldrich, St Louis, MO; USA). After 24 h the medium was removed, and the cultures were washed twice to remove the non-integrated plasmid in the cellular genome. Fresh medium was added to the culture, collecting the viral production present in the culture supernatant at 24 h and 48 h. Viral stocks were clarified by filtration (0.45 µm filter), and centrifugation and their viral titration were carried out. Stocks were titrated to determine infectivity expressed as the 50% tissue culture infective dose ($TCID_{50}$)/ml. Briefly, PHA-activated PBMC were infected with 4-fold serial dilutions of viral stock ranging from 4^{-4} to 4^{-10}. On day 4 of infection, 100 µl of medium were removed and refreshed. On day 7 post-infection, supernatants were scored for infection by $TCID_{50}$/ml using Spearman-Karber method and Reed and Muench methods. These viruses contain the luciferase gene in their genome, an enzyme that will be expressed in those infected cells in which the viral genome is integrated.

The HSV-2 strain 333 isolate was provided by Dr A. Alcamí (Severo Ochoa Centre for Molecular Biology (CBMSO), Spain). Stock of HSV-2 was prepared and titrated by plaque assay and stored at -80 °C. Briefly, Vero cells were seeded at a density of $2x10^5$ cells/well in 12 well plates, when the cells were in a confluent monolayer, the culture medium was removed and infected with different dilutions of the viral stock in a volume of 0.5 mL of DMEM 2% FBS and incubated under culture conditions at

37 °C and 5% CO_2 for 1 h, moving the plate every 10 min to prevent the monolayer from drying out. After that time, virus surplus was removed and 2 mL of fresh DMEM 5% FBS added with 0.4% IgG. After 48 h of incubation, the cells were stained with methylene blue, the viral plaques were counted, and the viral stock was titrated in plaque forming units (PFU).

The RSV (long Strain, ATCC VR-26) obtained from the American Type Culture Collection (ATCC, Rockville, MD) was provided by Dr. Isidoro Martinez (Unidad de Interacción Virus-Célula, Centro Nacional de Microbiología, Instituto de Salud Carlos II, Madrid, Spain). The RSV was propagated in HEp-2 cells in DMEM, as previously described (Martinez et al., 1997). Viruses were purified from culture supernatants by polyethylene glycol precipitation and centrifugation in a 30–45–60% discontinuous sucrose gradient in TNE buffer (Mbiguino and Menezes, 1991). Virus titters were determined by plaque assay in HEp-2 cells layered with 0.5% low melting- point agarose (Conda Laboratories, Madrid, Spain). After 5 days, cells were fixed with 4% formaldehyde (Panreac Quimica, Barcelona, Spain) in PBS, followed by methanol, and incubated with a mixture of monoclonal antibodies against the two major glycoproteins of the virus (2F, 47F, 56F, 021/1G, 021/2G; Sigma-Aldrich, St-Louis, MO, USA); plaques were visualized using an anti-mouse IgG horseradish peroxidise-linked whole antibody (Amersham Pharmacia Biotech Europe GmbH, Freiburg, Germany) and 3-amino-9-ethylcarbazole (AEC; Sigma-Aldrich, St-Louis, MO, USA). Virus inactivation was achieved by irradiation with ultraviolet light for 90 min and confirmed by plaque assay.

5.5. Human spermatozoa

Semen samples were collected after masturbation in a sterile vial from 10 healthy, young and fertile donors, after a period of abstinence of at least 3 days. In collaboration with the Human Reproduction Unit of the Hospital General Universitario Gregorio Marañón, a basic initial seminal assessment of the collected samples was carried out. The manual of laboratory for the examination and processing of the human semen published by the WHO in 2010 was used. Only those samples that surpassed the criteria of inclusion: i) the volume of the sample should be at least 2 ml; ii) the total number of spermatozoa should be > $65x10^6$ sperm/ml; and iii) the nature of these (vitality and > 70% motility) were accepted for later use in spermicidal trials.

For other experiments, the semen was maintained at room temperature (RT) between 30 and 120 min for liquefaction, due to the semen to be presented in a condensed state after ejaculation. Semen pools

were kept in various aliquots of 500 µl at -20 °C. Samples were quickly used after thawing and surplus were discarded (**Fig. 14**).

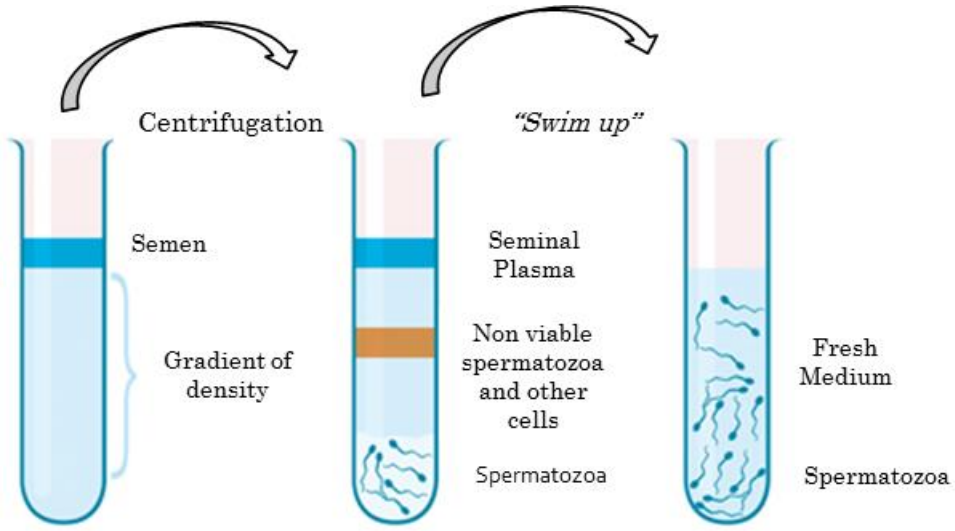

Figure 14. Density gradient centrifugation process to obtain high motile spermatozoa. The density gradient centrifugation comprised continuous or discontinuous gradients. The ejaculate is placed on top of the density media with higher density and is then centrifuged for 15–30 min. During this procedure, all cells reach the semen sediment. However, highly motile spermatozoa move actively in the direction of the sedimentation gradient and can therefore penetrate the boundary quicker than poorly motile or immotile cells, thus, highly motile sperm cells are enriched in the soft pellet at the bottom.

6. Methods

6.1. Cell viability assays: MTT assay

MTT assay is a colourimetric assay based on the selective ability of living cells to reduce 3-(4,5-dimethylthiazol-2-yl)-2,5-diphenyl tetrazolium bromide in soluble formazan crystals. This allows determining the cytotoxic effect of the compounds under study, in this case the dendrimers, on the cellular metabolism. This assay was carried out according to the manufacturer's instructions (MTT, Sigma-Aldrich, St. Louis, USA). Briefly, after the incubation at 24, 48 or 72 h of various cell populations with different concentrations of dendrimers in 96-well plates (10^5 cells/well), the supernatant containing the dendrimer was removed and replaced with 200 µL of Opti-MEM® without serum or phenol red, adding 20 µL well of MTT substrate (Thiazolyl Blue, 5 mg/mL, final concentration in well of 0.5 mg MTT/mL). After 2h of incubation under culture conditions, the plate was centrifuged at 2000 r.p.m for 10 min, and the supernatant with an excess of MTT that did not react was removed. Formazan crystals were dissolved in 200 µl DMSO. The plate was shaken at 700 r.p.m to ensure correct dissolution of the crystals and the formazan concentration was determined by

spectrophotometry by using a plate reader (Synergy 4 Plate Multileaver, Biotek Instrument, USA) at a wavelength of 570/690 nm. The spectrophotometer was calibrated at 0 using only Opti-MEM®. Relative cell viability (%) to the control (untreated cells) was calculated based on the formula: [A] test/ [A] control x 100. Dextran was used as a negative control of cell death because of its harmless effect, whereas 10% DMSO was used as a positive control of cell death. Each experiment was performed in triplicate.

6.2. Experiments related to HSV-2

6.2.1. HSV-2 *in vitro* assays

6.2.1.1. *HSV-2 infection inhibition assay*

To screen the potential anti-HSV-2 activities of selected dendrimers, 175×10^3 Vero or HEC-1A cells were seeded in 24-well plates. After 24 h, cells were treated with dendrimers for 1 h at 37 °C before HSV-2 333 infection at a multiplicity of infection (MOI) of 0.1. After 6 h, cells were washed to remove unabsorbed virus. At 30–40 h pi, HSV-2 culture supernatants were collected and their infectivity was assessed by plaque reduction assay. Briefly, Vero cells, seeded in six-well plates, were treated with 100 µL of various supernatant dilutions for 1 h at 37 °C. Then, Vero cells were covered with DMEM containing 2% FBS and 0.4% of IgG (Beriglobin; Behring, King of Prussia, PA, USA) and incubated for 48 h. Subsequently, Vero cells were stained with 0.03% methylene blue (Sigma-Aldrich, St. Louis, Mo, USA) in distilled water and viral plaques were counted. VK2/E6/E7 cells seeded in 24-well plates were exposed to maximum non-toxic concentration of dendrimers for 1 h before HSV-2 exposure at an inoculum to 150 PFU/well. VK2/E6/E7 cells were incubated for 2 h at 37 °C and then washed and overlaid with complete keratinocyte-serum free medium containing 0.4% human IgG. Viral plaques were counted after 48 h and the percentages of plaques relative to plaques on control wells were calculated. Each experiment was performed in triplicate.

6.2.1.2. *Effect of pH in anti-HSV-2 activity of dendrimers*

Selected dendrimers were incubated at acidic pHs (3, 4, 5.5), PBS or physiologic pH (7.4) at 37 °C for 1 h. Afterward, Vero cells at a cell density of $175x10^3$ cells/well were pretreated for 1 h with the mixtures and infected with HSV-2 333, 150 PFU/well, for 2 h. Subsequently, cells were washed to remove unbound virus and compounds and covered with 2% FBS DMEM containing 0.4% human IgG. HSV-2 infection, measured as number of viral plaques, was determined at 48 h pi. Each experiment

was performed in triplicate. Anonymous samples of healthy donors were provided by the Spanish HIV HGM BioBank (Garcia-Merino et al., 2009).

6.2.1.3. *Time of addition assay*

Vero cells were seeded in p24 plates at a cell density of $175x10^3$ cells/well and infected with 0,1 MOI of HSV-2 333. Antiviral compounds and dendrimers were added at 0, 1, 2, 4, 6, 8, and 24 h post-infection. After 2 h post-infection, cells were washed with DMEM 2% FBS and covered with fresh medium containing 0.4% human IgG. ACV 10 µM was used as control. The viral plaques were counted after 48 h to determine the HSV-2 infection.

6.2.1.4. *HSV-2 attachment assay*

Prechilled Vero cell monolayers in 24-well plates ($175×10^3$ cells/well) were treated with dendrimers for 1 h at 4°C and infected with 150 PFU/well HSV-2 for 2 h at 4°C. Cells were washed with cold 2% FBS/DMEM to remove unattached dendrimers and unabsorbed HSV-2 and overlaid with medium containing 0.4% human IgG. After 48 h at 37 °C, cells were stained with methylene blue and viral plaques were counted.

6.2.1.5. *HSV-2 inactivation assay*

To assess the ability of polyanionic carbosilane dendrimers to bind to viral surface proteins and decrease viral infectivity, dendrimers were added to aliquots of HSV-2 333 (10^4 PFU), and the HSV-2-dendrimers samples were incubated at 4 ºC at various times: 30 min, 1 h or 2 h. After incubation, 150 PFU of dendrimer-treated HSV-2 were added on cultured Vero cells for titration. After 48 h, cells were washed with cold 2% FBS/DMEM to remove unattached dendrimers, unabsorbed HSV-2, and overlaid with medium containing 0,4% human IgG. The viral plates were stained and counted at 48 h post-infection. When HSV-2 was added to cultured cells, dendrimer concentration was diluted to one that was not active in an antiviral assay (0.08 µM).

6.2.1.6. *Binding of dendrimers to cell surface molecules*

The ability of carbosilane dendrimers to bind cellular surface proteins and block the viral attachment and entry were analyzed. Vero cells monolayers seeded at a density of $175x10^3$ were pretreated with dendrimers for 1 h. After incubation, Vero cells were extensively washed with PBS to remove unbound dendrimers. Cells were infected with 150 PFU of HSV-2 333. After 48 h post-infection, Vero cells were stained and HSV-2 plaques were counted.

6.2.1.7. *Molecular modelling of G2-16 and G1-S4 with HSV-2 surface protein gB*

3D computer models of dendrimer structures were created using dendrimer builder, as implemented in the Materials Studio software package from BIOVIA (formerly Accelrys) as well as in several software (GAMESS, GAFF and R.E.D.-IV tools) as previously described (Bayly et al., 1993, Dupradeau et al., 2010, Perri and Weber, 2014, Schmidt et al., 1993, Wang et al., 2005). Missing force field parameters were fitted by minimizing the differences between Quantum mechanics (QM) and force field based relative energies of properly chosen molecular fragments. QM energies were calculated at MP2/HF/6-31G** level of theory using GAMESS and fitting was accomplished using paramfit routine from AMBER14 software (D.A. Case et al., 2014, Perri and Weber, 2014, Schmidt et al., 1993). Slightly adjusted van der Waals parameters for Si atoms from MM3 force field were used in this work (Lii and Allinger, 1991). The protein components were parametrized using force field ff14SB. As the template for the main part of the simulated structure of protein HSV-2 gB (strain 333, residues 98-720) the available experimental structure of the HSV-1 gB protein (PDB: 4BOM) was used (Maurer et al., 2013). First the short protein part “RKPRNATPAPLREAPSANASVER”, which is the short loop missing sequence 471-489 extended at each end with 2 amino acids, was created and simulated in explicit solvent for 28 ns. Then was attached to all 3 monomers of 4BOM structure and necessary mutations were performed to match primary sequence of the HSV-2 gB (strain 333, residues 98-720). After this step, the edited 4BOM structure was shortly simulated in explicit solvent (5 ns) mainly to adjust properly configurations of newly added residues. Then just one monomer was chosen for consequent processing. The initial configuration of the missing C-terminal (residues 721-904) was generated and attached to the previously prepared monomer of HSV-2 gB (strain 333, residues 98-720). This extended HSV-2 gB monomer fragment (residues 98-904) was first simulated in implicit solvent for 153 ns with restrained part (residues 98-720, restraint 80 kcal/(mol Å2)) to obtain sufficiently stable configuration of the newly added C-terminal. Preparation of this HSV-2 gB part was finished by simulation in explicit water (66 ns) with restrained part (residues 98-720, restraint 20 kcal/(mol Å2)) during the first 30 ns and the rest (36 ns) without any restraints. Let just notice that the added C-terminal was incorporated into the simulated structure just to “naturally” close this uncomplete gB end and stabilize structure of simulated monomer. In reality is the most of this gB part anchored in viral membrane where it has indeed tertiary structure different from that obtained by our simulations. Preparation of N-terminal of the HSV-2 333 gB comprising residues 1-100 was as follows: first the

initial configuration of this protein part was generated based on known primary sequence and consequently the tertiary structure was estimated using simulation in implicit solvent for 862 ns. Protein tertiary structure was consequently finalized using simulation in explicit water (41 ns). Models of dendrimer molecules were simulated in explicit solvent (G1-S4 for 10 ns, G2-S16 for 36 ns) and then the most representative conformations were chosen using cluster analysis of the resulting MD trajectories. The dendrimer/HSV-2 gB monomer fragment (residues 98-904) systems (cases A, B, C, D, E and F) were simulated in explicit water for 70 ns dendrimer/ HSV-2 gB N-terminal (residues 1-100) for 50 ns. Initial configurations of the missing protein parts were generated using Leap routine from Amber14. Mutations and attachments of the missing parts to the main fragment as well as creation of the initial configurations of dendrimer/protein complexes and all visualizations were done using UCSF Chimera software (Pettersen et al., 2004). Cluster analysis and post-processing of MD trajectories were done using cpptraj module from Amber14. Simulation details: In case of simulations in explicit solvent the molecules were solvated in explicit water (TIP3P model) with the proper number of Na+ and Cl- ions to preserve neutrality of the system and to ensure the correct ionic strength (0.15 M) (Jorgensen et al., 1983). First the solvated molecular systems were minimized (5000 steps with 2 kcal/(mol Å2) restraint + 5000 without restraint), heated (200 ps NVT) to 310K and then equilibrated using molecular dynamics simulation in NPT ensemble (T=310 K, P= 105 Pa - lengths of simulations are mentioned in each case above). The first 0.5 ns with restrained solute (2 kcal/(mol Å2) restraint). Hydrogens were constrained with the SHAKE algorithm to allow 2 fs time step (Ryckaert et al., 1977) and langevin thermostat with collision frequency 2 ps-1 was used for all MD runs (Wu and Brooks, 2003, Wu et al., 2014). The pressure relaxation time for weak-coupling barostat was 2 ps. Particle mesh Ewald method was used to treat long range electrostatic interactions under periodic conditions with a direct space cut-off of 10 Angstroms. The same cut-off was used for van der Waals interactions. In case of simulations in an implicit solvent, the optimized GBn implicit solvent model (ibg=8) was used together with recommended Born radii set mbondi3 (Nguyen et al., 2013). Infinite cut-off (cut=9999.0) for non bond interactions was used and the temperature was controlled with Langevin thermostat. The pmemd.cuda module from Amber14 package was used for all the above described simulation steps (Gotz et al., 2012). The last 10 ns of the whole simulation were used for energetic analyses (enthalpic contribution (dH) calculated with 0.1 ns sampling step (i.e. 100 frames used), entropic contribution (TdS) calculated using 3 ns sampling step (i.e. 4 frames used) by using the molecular

mechanics/poisson–boltzmann surface area (MM/PBSA) methodology + normal mode analysis as implemented in Amber14 routine MMPBSA.py to obtain estimates of free energies of binding (Miller et al., 2012). PBSA calculations were done using adaptive poisson-boltzmann solver sander. APBS from Amber14 (Baker et al., 2001, D.A. Case et al., 2014). The probe radius used for calculation of solvent accessible surface area (SASA) was 1.4 A. Default APBS value a = 0.02508 kcal*mol-1*A-2 of cavity surften parameter for calculation of the non-polar solvent contribution ENPOLAR= a*SASA was used. The dielectric constant of the solute was set to one and in the case of solvent to 80. Normal mode analysis was done taking in account solvation using HCT generalized born implicit solvation model (Hawkins et al., 1996).

6.2.2. HSV-2 inhibition assays *in vivo*

6.2.2.1. *In vivo vaginal challenge assay*

The G2-S16 and G1-S4 carbosilane dendrimers and their combinations with PD or TDF were selected for analyzing their ability to inhibit the HSV-2 infection in BALB/c mice. Female BALB/c mice (20 ± 2 g) that were 6 to 8 weeks old were purchased from Charles River Labs, and housed at the CBMSO. Animal studies were conducted and approved by the CBMSO Institutional Animal Care and Use Committee (CEEA-CBM, Madrid, Spain). A HEC placebo gel was formulated mixing HEC gel with sterile PBS to obtain a final concentration of 1% w/v. G2-S16 or G1-S4 was added to previously prepared 1% HEC placebo gel to a final concentration of 3% w/v to obtain a homogeneous and transparent solution. TDF was added to the gel on a final concentration of 1% and PD was added at final concentration of 0.25 mM. Prior to vaginal HSV-2 challenge, BALB/c mice received a single 2 mg subcutaneous injection of medroxyprogesterone acetate to increase susceptibility to HSV-2 infection (Parr et al., 1994). Five days later, BALB/c mice were anesthetized with isoflurane (2-chloro-2-(difluoromethoxy)-1,1,1-trifluoro-ethane) for the gel applications and for the HSV-2 infection. Then BALB/c mice were randomized into four groups of 10 mice per group; placebo group only received 50 µl 1% HEC gel vaginally, G2-S16 group received 1% HEC gel with 3% G2-S16, G1-S4 group was treated with 1% HEC with 3% G1-S4 and control group did not received treatment at all. One hour later the 40 BALB/c mice were inoculated intravaginally with 10^5 PFU/20 µl of HSV-2 333 strain and maintained in a supine position with slight elevation of the pelvis for 15 min post-application.

BALB/c mice were examined daily for body weight and genital pathology over 16 days. Disease score was graded according to a 4-point scale: 0, no apparent infection; 1, genital erythema; 2, moderate

genital infection; 3, purulent genital ulceration and hair loss, generally poor condition; 4, severe ulceration of genital and surrounding tissue, and hind limb paralysis (leading to euthanasia).

6.2.2.2. *In vivo rectal challenge assay*

As in the case of vaginal infection experiment, the G2-S16 and G1-S4 dendrimers were chosen for evaluation of rectal infection. Due to the viscosity of the gels, rectal assays were performed by dissolving G2-S16 and G1-S4 in PBS. The experiment was conducted in BALB/c mice of both genders, 10 mice per group (NT, G1-S4, G2-S16 and G2-S16/TDF) for each sex. Mice are fasted for 24 h prior to the rectal HSV-2 challenge assay, but water complemented with 1% glucose was available ad libitum. Following initial infection food and water were available ad libitum. Mice were anesthetized intraperitoneally with Ketamine-Xylacine (100 mg-10 mg/kg) and randomized into three groups of 5 mice per group. Mice were allowed to defecate prior to rectal inoculation so as to prevent immediate expulsion of treatment and viruses. Anesthetized BALB/c mice were treated with 40 µl of PBS vehicle, 3% G2-S16, 3% G1-S4 or 3% G2-S16/1%TDF applied rectally with a gavage needle and maintained in a supine position with slight elevation of the pelvis for 30 min post-application. Subsequently, 10^5 PFU of HSV-2 333 strain diluted in PBS to a final volume 10 µl was applied atraumatically to the rectum mucosa of anesthetized BALB/c mice maintained in a supine position with slight elevation of the pelvis until they woke up. In addition, the same experiment was held at 15 male mice but increasing the HSV-2 333 dose to 10^6 PFU for inoculation.

BALB/c mice were examined daily for body weight and genital pathology over 18 days. Disease score was graded according to a 4-point scale: 0, no apparent infection; 1, genital erythema; 2, moderate genital infection; 3, purulent genital ulceration and hair loss, generally poor condition; 4, severe ulceration of genital and surrounding tissue, and hind limb paralysis (leading to euthanasia).

6.3. *In vivo* bioluminescent imaging

To assay if dendrimers cross-vaginal epithelium or not, *in vivo* bioluminescent imaging were performed. BALB/c mice studies were approved by the CBMSO Institutional Animal Care and Ethical Committee (CEEA, CBMSO, Madrid, Spain). Prior to vaginal administration, mice were injected subcutaneously with 2 mg of medroxyprogesterone acetate. HEC placebo gel was formulated by mixing HEC gel with sterile PBS to obtain a final concentration of 1% w/v. G2-STE16-FITC was added to 1% HEC placebo gel to a final concentration of 3% w/v. To acquire the bioluminescent images,

some parameters were based on the level of bioluminescent emission such as the time of exposure, which ranged from a few seconds to 5 min, the number of pixels, and the field of view with automatic focus. The living image software automatically coregistered the luminescent images, which were taken in darkness and displayed in pseudocolours that represent the intensity of the signal and the photographic image, generating an overlay image.

6.4. Confocal microcopy

Tissues collected from mice treated vaginally with G2-STE16-FITC dendrimer (vagina) were flash frozen in Tissue-Tek O.C.T. (Sakura Finetex, USA) using dry ice. Following cryogenic sectioning, slides were fixed in 3,7-4% formaldehyde w/v (Panreac AppliChem, Darmstadt, Germany) for 15 min followed by two PBS washes. Slides were then incubated in 0.1% Triton X-100 for 5 min followed by a PBS wash. To avoid non-specific binding, slides were blocked for 30 min with 5% BSA and incubated with Alexa Fluor® 647 anti-mouse CD192 (Life Technologies-Molecular Probes, NY, USA) at a 1:100 dilution in 2.5% BSA for 1 h and washed three times with PBS. ProLong Gold anti-fade reagent with DAPI (Thermo Fisher Scientific, Waltham, MA, USA) was used to adhere a coverslip. Slides were observed and imageswere obtained with a Zeiss LSM710 confocal microscope by using Zen 2011 software (Carl Zeiss Microimaging Inc., Thornwood, NY, USA).

6.5. BALB/c vaginal irritation assay

We studied whether G2-STE16 and G2-STE16-FITC dendriners were toxic in vagina or not after 20 h with a single dose. 12 female BALB/c mice 8 weeks old, 20±3 g (Charles River Laboratories, Wilmington, MA, USA) were purchased and housed in the animal facility at the CBMSO. An HEC (NIH-ARRRP) placebo gel was formulated by mixing HEC gel with sterile PBS to obtain a final concentration of 1% w/v. G2-STE16 or G2-STE16+FITC was added to 1% HEC placebo gel to a final concentration of 3% w/v. Mice were injected subcutaneously with 2 mg of medroxyprogesterone acetate (Depo-Provera [depo]), (Pfizer, New York, USA). Five days later, BALB/c mice were randomized into four groups of three mice/group. Control group was treated with 30 µL 1% HEC gel vaginally, G2-STE16 group was treated with 1% HEC gel with 3% G2-STE16, G2-STE16-FITC group was treated with 1% HEC gel with 3% G2-STE16-FITC, and irritation control group was treated with 6% N9 in PBS. Treatment was applied with a vaginal gavage needle in BALB/c mice previously anesthetized with isoflurane (Forane, Abott, Madrid, Spain). The following day, mice were sacrificed

and vaginas were extracted and conserved in 3.7-4% formaldehyde w/v (Panreac AppliChem, Darmstadt, Germany). The same experiment was repeated with G2-STE16 and G2-S16, despite G2-S16 having already proved not to induce vaginal irritation or inflammation in BALB/c mice and they were well tolerated for topical application (Chonco et al., 2012, Sepulveda-Crespo et al., 2015b, Vacas Cordoba et al., 2013). This experiment was conducted applying the treatment intravaginally daily for seven consecutive days. Controls included mice that received PBS (control group) and 4.5% N9 in PBS (irritation control group).

6.6. Histological studies in BALB/c mice

The presence of histological lesions in the mice vaginas was evaluated with hematoxylin-eosin staining. Samples were embedded in paraffin by passage in increasing degree of alcohols [Rectapur (VWR)], two baths of xylene [Analar (VWR)] and other of paraffin, before being placed in paraffin mold. Subsequently, they were cut by using a microtome semimotorized RM2145 Leica and processed for staining. For dewaxing, samples were submitted to two baths of xylene (10 min) and three baths in descending order of alcohols (100%, 90% and 70%) (5 min), before being stained with hematoxylin (Merck, Madrid, Spain) for 5 min and eosin (Merck, Madrid, Spain) for another 5 min. Post-eosin staining dehydration was performed with passage in increasing degree of alcohols (70%, 90% and 100%) and bath of xylene solution. Finally, they were mounted with DPX (Prolabo, Obregón, Mexico). The existence of injury in vaginal epithelium, inflammatory infiltrate, vascular congestion and/oredema in the submucosa was evaluated in each histological sample. The score assigned for each of these lesions were: 0 (no change) when no injury or the observed changes were within normal range; 1 (minimum) when changes were sparse but exceeded those considered normal; 2 (light) when injuries were identifiable but with no severity; 3 (moderate) for significant injury that could increase in severity; 4 (very serious) for injuries that occupy most of the analyzed tissue. These values were added up and determined the level of vaginal irritation as minimum 1-3, average 4-6, moderate 7-9 and severe 9+ (Chonco et al., 2012).

6.7. Full-thickness EpiVaginal tissue toxicity

Three dimensional, full thickness VEC-100 FT Epivaginal tissues were purchased from Mattek Corporation (Ashland, MA, USA). The tissues were doused with 100 µL of each test sample, including various concentrations of G2-S16, Triton as death control, and water as negative control. After 24 h

incubation at 37 ºC, 5% CO_2, an MTT assay was performed to determine the cell viability, following the instructions provided by the manufacturer (Mattek Corporation, USA). The tissues were washed with PBS and treated with 300 µL of MTT at a concentration of 1 mg/mL, and incubated at 37 ºC, 5% CO_2 for 3 h. After the incubation, the tissues were submerged in 2 mL of extractant solution and incubated overnight in the darkness at RT. The optical density was measured spectrophotometrically at 570/650 nm, and the viability of the treated tissues was calculated by normalizing the absorbance of the treated tissue to the absorbance of the negative control, expressed as percent viability.

6.8. Zebra fish toxicity test

We used zebrafish embryos to carry out fish embryo toxicity test (FET), a standard test recommended by Organization of Economic Cooperation and Development (OECD) and has an excellent correlation with acute adult fish toxicity tests (Lammer et al., 2009, Lawrence, 2011). We analyze biosecurity and determine the maximum tolerated dose (MDT), the lethal concentration 50 (LC_{50}) and minimal observed effect concentration (LOEC) of G2-S16. The results show a strong correlation with those obtained in the acute toxicity tests in adult fish (Knobel et al., 2012). The determination of acute toxicity of substances on zebrafish eggs (Danio rerio) by static method was carried out. Briefly, five concentrations of the test solutions of G2-S16 at 100 mg/L, 46 mg/L, 22 mg/L, 10 mg/L and 4.6 mg/L in vehicle, dilution water, were evaluated with a vehicle control group (with vehicle: AD with 0.1% DMSO) in order to ensure that the medium used in the assay is biosafety for the embryos, and with a reference substance group, 3, 4 dichloroaniline (3,4-DCA) at 3.7 mg/L, to ensure that the test conditions are reliable. To perform the FET, only those fertilized eggs that had no external abnormality were used. Subsequently, through the use of a Pasteur pipette, only the fertilized eggs were separately transferred into each well of a 24-well microplate, so that the eggs did not come into contact with the air and so that each well contained a single egg in a volume of 2 mL of the test concentrations, the controls or the vehicle. Twenty replicates of all tested doses of G2-S16 vehicle group, positive control and 24 replicates of the control group were performed. The microplates were incubated at 26±1 °C for 24, 48, 72 and 96 h. After each incubation period, the eggs/embryos were examined and the results obtained were recorded according to the criteria specified. **Lethal parameters**: i) number of coagulated eggs; ii) detachment of the tail; iii) absence of heart rate; or iv) formation of somite's and eyes, after treatment, an embryo is determined to be dead if any of the lethal parameters described above are detected. **Sublethal parameters**: i) spontaneous movements; ii)

pigmentation; and iii) formation of edema or clots. **Teratogenic parameters**: i) malformations in organs and structures; ii) Scoliosis; iii) ricketsand; or iv) generalized delay of development. The conservation of breeding fish is carried out according to the specifications defined in technical instruction IT-DD-17 maintenance and care of adult zebrafish. The production of eggs for the test is carried out according to the specifications defined in technical protocol PT-DD-12 obtaining and growing of zebrafish fertilized eggs.

6.9. Experiments related to SEVI

6.9.1. Inhibition of HIV-1 infection in the presence semen in TZM.bl cells

To evaluate the activity of dendrimers or their combination with ARV in the presence of semen, TZM.bl cells were seeded into 96-well plates at a density of $15x10^3$ cells/200 µl. After 24 h, the cells were treated with various concentrations of test compounds or their combinations for 1 h at 37ºC 5% CO_2 prior to the infection. R5-HIV-$1_{NL(AD8)}$ or T/F HIV-1 isolates were incubated with semen for 5 min to obtain semen concentrations of 10% during virion treatment. After the semen/virus incubation, the cells were infected with 14 µl of semen-virus (20 ng virus/10^6 cells) or PBS-virus (20 ng virus/10^6 cells); the final concentrations of semen were 0.67% and 0%, respectively. TZM.bl cells were incubated for 2 h, then they were washed twice, and 200 µl fresh medium was added. Two days later, HIV-1 replication was determined after quantification of luciferase expression (Promega, Madrid, Spain). Fifty percent of effective concentrations (IC_{50}) were determined using CalcuSyn software (Biosoft, Cambridge, UK), based on the median effect principle.

6.9.2. Inhibition of HIV-1 infection in the presence of semen in primary PBMC

The PBMC were isolated and cultured as described (Garcia-Merino et al., 2009). Activated PBMC were seeded in 96-well plates at a density of $200x10^3$ cells/200 µl and pre-incubated with different concentrations of test compounds or their combinations for 1 h at 37 ºC, 5% CO_2 prior to the infection. R5-tropic HIV-$1_{NL(AD8)}$ or T/F HIV-1 isolates were incubated with semen for 5 min to obtain semen concentrations of 10% during virion treatment. After the semen/virus incubation, cells were infected with 14 µl of semen-virus (20 ng virus/$1x10^6$ cells) or PBS-virus (20 ng virus/$1x10^6$ cells); the final well concentrations of semen were 0.67% and 0%, respectively. TZM.bl cells were incubated for 3 h and pelleted at 1200 r.p.m. for 5 min. The cells were washed twice and resuspended in 200 µl of fresh medium. Three days later, the supernatants were collected and 100 µl were used to treat TZM.bl cells

that had been seeded in 96-well plates at a density of $15x10^3$ cells/100 µl per well the previous day. Two days later, HIV-1replication was determined after the quantification of luciferase expression (Promega, Madrid, Spain). IC_{50} concentrations were determined using CalcuSyn software.

6.10. Cell proliferation assays

The PBMC treated with IL-2 60 IU/mL were passed to a 96-well round bottom plate ($2x10^5$ cells/well), and thereafter the corresponding stimuli were added. After 72 h incubation period, the experiment was developed using a Millipore® proliferation kit, based on the incorporation of bromodeoxyuridine (BdrU), a thymidine analog, into the DNA of proliferating cells. Briefly, PBMC were washed and fresh medium was added with 1x BrdU solution. After 6 to 8 h at 37 °C, PBMC were centrifuged at 300 g for 10 min and medium was removed. BrdU assay began with addition of 100 µl/well of the fixing/denaturing solution for 30 min at RT. Thereafter, solution was removed and 100 µl/well of 1x detection antibody solution was added. After 1 h at RT, three extensive washes were performed and samples incubated with 100 µl/well of HRP-conjugate secondary ab solution for 1 h at RT. Subsequently, PBMC were washed and 100 µl/well of TMB (3,3',5,5''-tetramethylbenzidine) substrate was added for 30 min at RT followed by 100 µl/well of STOP solution (if color change was too drastic it may be necessary to stop the reaction prior to the standard 30 min). Absorbance was measured at 450 nm.

6.11. Sperm training: Evaluation of the sperm cell count

This experiment determines the mobile sperm count after the treatment of semen samples with the combinations of dendrimers G1-S4 or G2-S16, with the spermicide PD. After collection and processing of the seminal samples, they were incubated for 20 min at RT to allow their liquefaction. After this period, a seminal training was performed by density gradient selection on SpermGradTM medium in two 45% and 90% solutions. Subsequently, the protocol was followed according to the kit 1069 Sperm Preparation Medium (ORIGIO MediCut, Spain) to process and wash the sediment of displaced spermatozoa to the bottom of the tube, in order to collect the final sample of trained spermatozoids to be used in the experiment. An initial evaluation of relative mobile spermatozoa was performed to select aliquots with a final concentration of progressive mobile spermatozoa of $5x10^6$/ml. Spermatozoa were treated with combinations of the compounds for which their spermicidal capacity was tested: G1-S4 or G2-S16 at 10 µM in combination with PD at 0.25 mM. Previously, Lu et al. have demonstrated

that the effect on sperm motility and viability depend on the administered dose of PD, observing the maximum spermicidal effect for PD at the concentration of 0.25 mM (Lu et al., 2013). The calculation of sperm survival and the percentage of progressive spermatozoa were performed at 0, 20, 30, 40, 50, 60, 70, 80, 90, 100 s and 3 h post-treatment.

6.12. Experiments related to RSV

6.12.1. RSV *in vitro* assays

6.12.1.1. *RSV Infection inhibition assay*

Once the maximum non-toxic concentrations were selected for each dendrimer, the inhibitory capacity against RSV of each dendrimer was evaluated. Briefly, 5×10^5 A549 cells/well were seeded in 6-well plates. After 24 h, the monolayer was infected with 3 MOI of RSV and then treated with maximum non-toxic concentrations of each dendrimer. After 1 h, the supernatant was removed, and the infection was left in 2 mL in fresh medium at 2% FBS for 24 h at 37°C.

One day post infection, supernatants were collected and viral titters were determined by plaque assay in HEp-2 cell line. 1.2×10^6 HEp-2 cells/well were seeded in 6-well plates. HEp-2 cells monolayers were incubated with serial dilutions of the cell supernatants. After 90 min, cell were overlaid with DMEM 2% FBS with 0.7% low melting point (LMP) agarose (Conda Laboratories, Madrid, Spain) and maintained at 4 °C for 30-45 min for the agarose to solidify. Five days later, infection was determined by inmunostain. HEp-2 cell monolayers were fixed with 4% formaldehyde in PBS, followed by methanol permeabilization. The cells were incubated with a mixture of monoclonal antibodies against RSV (Martinez et al., 2007, Gonzalez-Sanz et al., 2016), and plaques were visualized using an anti-mouse IgG horseradish peroxidase-linked whole antibody (Abcam) and AEC. Immunostained plaques were counted, and viral infectivity was determined by comparing the number of plaques in treated wells with the number of untreated control wells.

6.12.1.2. *RSV attachment assay*

The mechanism of action of G2-S16, G1-S4 and G3-S16 was evaluated, starting to analyze the RSV inhibition by the ability of the dendrimer to halt RSV to bind to the host cell.

A549 cell plate was pre-cooled to 4 °C for 30 min. Then, A549 cells were infected with 3 MOI of the RSV, and simultaneously, they were treated with different dendrimers at the previously selected concentrations for 1 h at 4 °C to ensure viral attachment but not entry. Subsequently, the A549 cells

were washed with fresh DMEM medium at 2% FBS, and incubated for 24 h at 37 ºC. The following day, HEp-2 cells monolayer was infected with A549 cells supernatant as described above. After 2h, cells were overlaid with DMEM 2% FBS with 0.7% LMP agarose, shifted to 37 °C for 5 days. Subsequently, cells were fixed and immunostained as described above. Immunostained plaques were counted and viral infectivity was determined.

6.12.1.3. *RSV dendrimer-cell interaction assay*

To analyze the effectiveness of dendrimers to prevent the A549 cells from being infected with RSV by interaction with proteins on the host cell surface, A549 cells were seeded in 6 well plates and treated at 10 µM, the maximum non-toxic concentration of G2-S16 for 2 h. Subsequently, the A549 cells were washed to remove any dendrimer that did not bind to the cell surface, and the RSV infection was performed at 3 MOI. The supernatant was removed to remove the virus that had not infected the A549 cells, and 2 mL of fresh medium at 2% FBS was added. The following day, the viral titration was performed in the HEp-2 cells, after 5 days of infection, immunostain was performed and plaques were counted, according to the procedure used in the previous sections.

6.12.1.4. *RSV inactivation assay*

To test the ability of dendrimers to interact with RSV particles, 3 MOI of RSV were preincubated with G2-S16 10 µM, G1-S4 10 µM and G3-S16 0.5 µM for 1 h at 4 ºC. HEp-2 cells were seeded (30,000 cells/well) in a flat bottom 96-well plate in DMEM medium 2% with FBS, and further incubated for 2 h at 4 °C. Cells were washed twice to remove unbound virus. Subsequently, cells were fixed with 3.7% formaldehyde, air dried, and blocked with 5% BSA in PBS–Tween. Bound virus was detected using the RSV monoclonal antibody (diluted 1:50) incubated for 2 h at RT. After removing the primary ab and washing the plates three times with PBS-Tween, goat anti-mouse IgG conjugated to horseradish peroxidase (1:500) was added. At the end of incubation, plates were washed three times with PBS-Tween, ABTS [2,2≪-azinobis(3-ethylbenzthiazolinesulfonic acid)] substrate was added (Thermo Scientific, Rockford, IL), and incubated for 20 min at RT. The reaction was stopped with 100 µl of a 1% SDS, and the absorbance at 405-410 nm was read.

6.12.1.5. *Syncytium formation assay*

The ability of polyanionic carbosilane dendrimers to block cell-to-cell RSV spread was evaluated. Cell viability was determined by MTT assay (Sigma-Aldrich, St-Louis, MO, USA) at 48 and 72 h post-exposure according to manufacturer's instructions. Cytotoxicity of dendrimers was evaluated in HEK-293T cell line, a range of concentrations between 0,1 µM and 10 µM. Subsequently, $6x10^4$ HEK-293T cells/well were seeded on a 24 well plate which have a crystal with poly-L-Lysine so cells could attach to the crystal, inside. The following day, cells were infected with RSV 1 MOI. Subsequently, increasing concentrations of the dendrimers were added to cells immediately after RSV adsorption and, 72 h later, monolayers were immunostained and examined for syncytium formation. Briefly, cover slips were fixed in 3.7-4% formaldehyde w/v (Panreac AppliChem, Darmstadt, Germany) for 10 min followed by two PBS washes. Cover slips were then incubated in 0.1% Triton X-100 for 5 min followed by a PBS wash. To avoid non-specific binding, they were blocked for 30 min in PBS-BSA 5% and incubated with anti-human RSV fusion protein and anti-human heparan sulfate proteogycan 2 (Sino Biological Inc, Beijing, China) at a 1:500 and 1:100 dilution, respectably, in PBS-BSA 2.5% for 1 h and washed three times with PBS-BSA 0,1%. Subsequently, samples were incubated with secondary ab, FITC anti-mouse IgG (Jackson InmunoResearch, Suffolk, UK) and Alexa Fluor® 633 anti-rabbit IgG (Thermo Fisher Scientific, Waltham, MA, USA) at a 1:100 dilution in 2.5% BSA for 1 h and washed three times with PBS. ProLong Gold anti-fade reagent with DAPI (Thermo Fisher Scientific, Waltham, MA, USA) was used to adhere a coverslip. Samples were observed and imagines were obtained with a Zeiss LSM710 confocal microscope by using Zen 2015 software (Carl Zeiss Microimaging Inc., Thornwood, NY, USA). Syncytium inhibition was determined counting number of syncytium in 10 random imagenes of each sample and percentage of inhibitionwas determined against control.

6.12.2. RSV *in vivo* assays

6.12.2.1. *In vivo pulmonary histopathological assay*

Once the mechanism of action by which G2-S16 inhibits RSV infection was determined. We evaluated the ability of this dendrimer to induce irritation and damage on the lung when G2-S16 was administrated intranasally. Once again, G2-S16 was selected as the compound to perform *in vivo* assays due to show high inhibitory profile as well as a controlled synthesis. In addition, G2-S16 has showed great biocompatibility in zebra fish toxicity assays, even at concentration over 100 mg/L.

Twelve male BALB/c mice (Charles River Laboratories, Wilmington, MA) (22±2 g) that were 8 weeks old were purchased and housed at the CBMSO. Animal studies were approved by the CEEA-CBMSO. Several concentrations of G2-S16 were prepared by dissolving G2-S16 in PBS. BALB/c mice were randomized into four groups of three mice; control group received 50 µL of PBS intranasally and G2-S16 was administrated intranasally in three different doses (100 µm, 500 µM and 1 mM), which corresponded to the remaining groups. Treatment was applied intranasally with a p10 pipette in mice previously anesthetized with isoflurane (Forane, Abott, Madrid, Spain). Five days later, mice were sacrificed and lungs were extracted and conserved in 3.7-4% formaldehyde w/v.

The presence of histological lesions in the mouse lungs was evaluated with hematoxylin-eosin staining. Samples were embedded in paraffin by passage in increasing degree of alcohols, two baths of xylene (Analar (VWR)) and other of paraffin, before being placed in paraffin mold. Subsequently, they were cut using a microtome semimotorized RM2145 Leica and processed for staining. For dewaxing, samples were submitted to two baths of xylene (10 min) and three baths in descending order of alcohols (100%, 90% and 70%) (5 min), before being stained with hematoxylin for 5 min and eosin for another 5 min. Post-eosin staining dehydration was performed with passage in increasing degree of alcohols (70%, 90% and 100%) and bath of xylene solution. Finally, they were mounted with DPX.

The existence of injury in pulmonary parenchyma (inflammation, edema, alveolar congestion, bleeding and vascular thrombosis and congestion) and pleura (inflammatory infiltrate, edema, bleeding, fibrosis and neovasculation) was evaluated in each biological sample. The values (score) assigned for each of these lesions were: 0 (no change) when no injury or the observed changes were within normal range; 1 (minimum) when changes were sparse but exceeded those considered normal; 2 (light) when injuries were identifiable but with no severity; 3 (moderate) for significant injury that could increase in severity; 4 (very serious) for very serious injuries that occupy most of the analyzed tissue. These values were added up and determined the level of vaginal irritation as minimum 1-6, average 7-10, moderate 10-14 and severe 14+.

6.12.2.2. *In vivo RSV challenge assay*

Eighteen male BALB/c mice (Charles River Laboratories, Wilmington, MA) (22±2 g) that were 8 weeks old were purchased and housed at the CBMSO. Animal studies were approved by the CEEA-CBMSO.

Several concentrations of G2-S16 were prepared by dissolving G2-S16 in PBS. BALB/c mice were randomized into three, PBS, G2-S16 250 µM and G2-S16 500 µM. Briefly, all mice were infected with $2x10^6$ pfu of RSV long intranasallly while anesthetized with isoflurane (Forane, Abott, Madrid). Two days later, treatment was applied intranasally with a p10 pipette in animals previously anesthetized. Five days later, mice were sacrificed and lungs were extracted.

Lungs were grinded in 5 ml of medium and filtered in order to extract the virus. Viral load of each lung was determined performing serial dilutions of the virus and HEp-2 cells were infected as previously described above.

6.13. IC_{50} and EC_{50} calculation

The drugs interactions, the half maximal effective concentration (EC_{50}) and the half maximal inhibitory concentration (IC_{50}) were determined using Calcusyn software (Biosoft, Cambridge, UK). All statistical analyses were performed using GraphPad software Prism v.6 (San Diego, CA, USA).

6.14. Statistical analysis

Statistical analysis, including the calculation of the mean, standard deviation (SD), standard error of the mean (SEM) and *p*-values was performed using Mann–Whitney U non-parametric test. The significance level was set as p=0.05. GraphPad Prism V5.0 software (San Diego, CA, USA) was used. All data were generated from duplicate or triplicate wells in at least three independent experiments.

RESULTS

7. HIV-1 antiviral efficacy of polyanionic carbosilane dendrimers in presence of semen

After numerous unsuccessful research and clinical trials on topical microbicides (Grant et al., 2008, Vanpouille et al., 2012, Fichorova et al., 2001, McCormack et al., 2010), it has been found that *in vivo* ineffectiveness of these topical microbicides was not only due to the lack of adherence, but also due to the induction of inflammation and cytotoxic effect. Even more important, Zirafi et al. have shown that semen reduces the sensitive of HIV-1 of PLL dendrimer SPL7013 based on anionic naphthalene sulfonate 32 groups in the periphery (VivaGel®) (Bernstein et al., 2003, Price et al., 2011) and other anionic polymers acting on target HIV-1 and in nucleotide or non-nucleoside RT inhibitors or IN inhibitor acting on intracellular targets (Abdool Karim et al., 2011, Grant et al., 2008, Huskens et al., 2009, McCormack et al., 2010, Mohan et al., 1992, Rusconi et al., 1996, Scordi-Bello et al., 2005, Van Damme et al., 2008) that were considered for microbicides development due to their potent *in vitro* activity but failed to prevent HIV-1 transmission in individuals (Zirafi et al., 2014). Amyloid fibrils of the semen were called SEVI. These SEVI showed that capture HIV-1 virions promoting their adhesion to target cells, increasing the ability of HIV-1 to infect human cells, regardless of cell type (Kim et al., 2010, Roan et al., 2011).

G2-STE16, G3-S16 and G2-S16 polyanionic carbosilane dendrimers have low toxicity and high inhibitory capacity *in vitro* and *in vivo* experiments, as well as synergic effects with ARV that strengthen their inhibitory activity against HIV-1 infection (Briz et al., 2015, Chonco et al., 2012, Sanchez-Rodriguez et al., 2015, Sepulveda-Crespo et al., 2015a, Sepulveda-Crespo et al., 2014, Sepulveda-Crespo et al., 2015c, Vacas Cordoba et al., 2013). In this section the capacity of G2-STE16, G2-S16 and G3-S16 as potential microbicides candidates to stop the spread of HIV-1 infection in the presence of amyloid fibrils in semen in combination with ARV was analyzed. First, we study the effect of SEVI on the antiviral activity of G2-STE16 and G3-S16 dendrimers against HIV-1 infection on TZM.bl cell line and PBMC. Moreover, G2-S16 dendrimer was selected because it was shown to be safe as a topical vaginal microbicide, not only *in vitro* (Vacas Cordoba et al., 2013, Sanchez-Rodriguez et al., 2015, Chonco et al., 2012), but also *in vivo* (Sepulveda-Crespo et al., 2015c). G2-S16 is an ideal retrovirucidal agent because this dendrimer plays a major role in a multifunctional manner (Cena-Diez et al., 2017, Sepulveda-Crespo et al., 2017, Vacas-Cordoba et al., 2016).

7.1. G2-STE16 and G3-S16 dendrimers

G2-STE16 and G3-S16 were tested and displayed a less efficient inhibitory profile against R5-HIV-$1_{NL(AD8)}$ isolate, pTHRO.c and pCH058.c T/F viruses in the presence of semen. However, both dendrimers retained their inhibitory ability against R5-HIV-$1_{NL(AD8)}$ at non-toxic concentrations. G2-STE16, a second-generation carbosilane dendrimer with sulphonate groups on its surface (Galan et al., 2014), inhibited infection of pTHRO.c and pCH058.c T/F viruses and R5-HIV-$1_{NL(AD8)}$ in the TZM.bl cells in the presence of semen over 98% at concentrations of 10 and 20 µM, the highest non-toxic concentrations (**Fig. 15**).

G3-S16, a third-generation polyanionic carbosilane dendrimer with sulfate terminal groups (**Fig. 16**) (Arnaiz, 2014) was also studied. This G3-S16 dendrimer had the best potential HIV-1 inhibitory capacity in the presence of amyloid fibrils in semen against pTHRO.c and pCH058.c T/F viruses and R5-HIV-$1_{NL(AD8)}$ isolate, obtaining higher inhibitory effect at lower concentration than G2- STE16. Inhibition of T/F viruses and R5-HIV-$1_{NL(AD8)}$ isolate at 93%, 96% and 82%, respectively, was achieved at concentration of 5 µM.

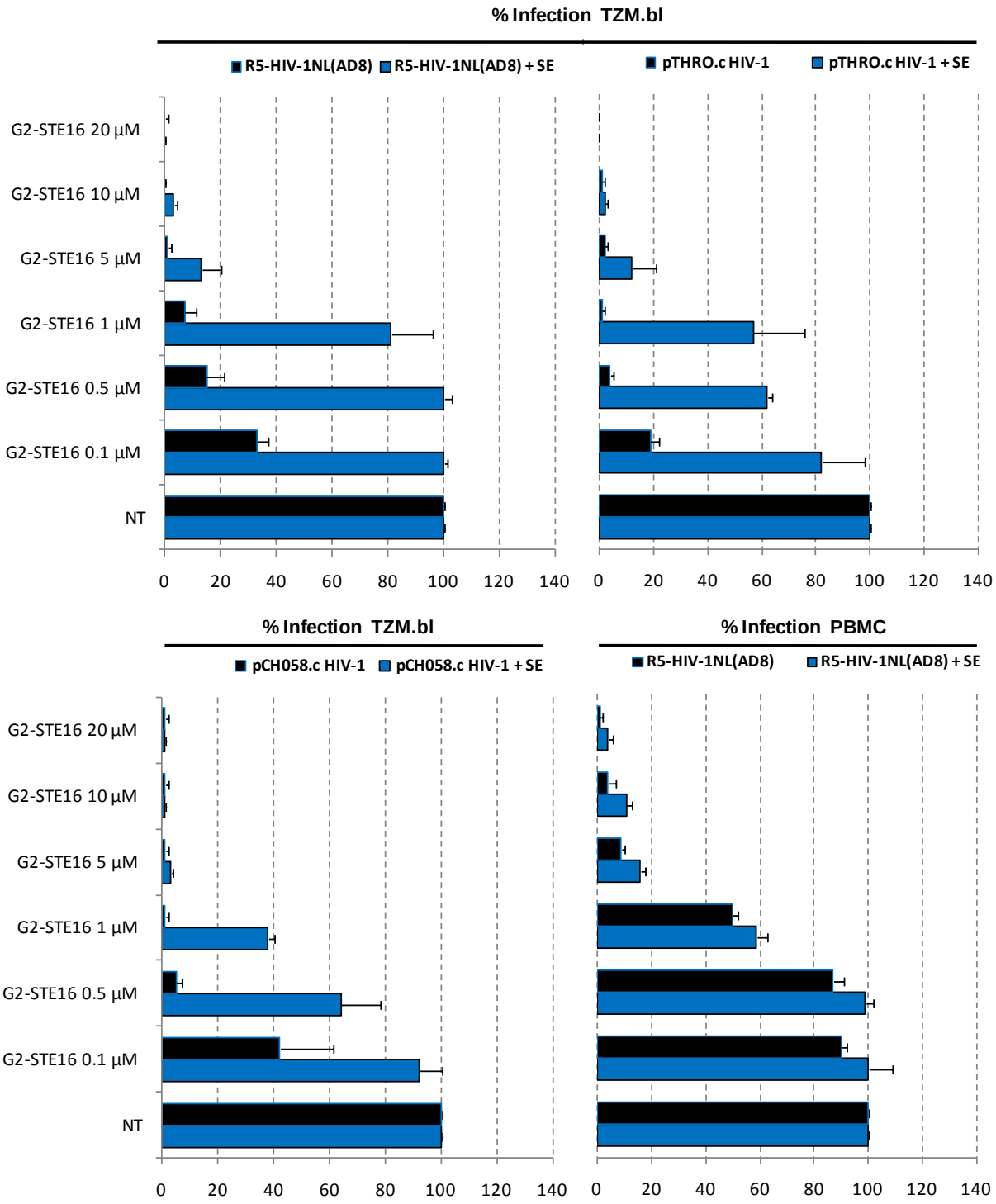

Figure 15. Effect of SEVI on antiviral activity of G2-STE16 as microbicides to block HIV-1 infection of TZM.bl cells and PBMC. Cells were pre-treated with a range of concentrations of 0.1 µM to 20 µM of G2-STE16. After 1 h, cells were infected with R5-$HIV_{1NL(AD8)}$ isolates, pTHRO.c and pCH058.c T/F viruses in the absence and presence of semen (SE) at a concentration of 20 ng/10^6 cells. Infection rates were measured 48 h after HIV-1 infection by quantification of luciferase expression. Data represent the mean ± S.E.M. (n = 3).

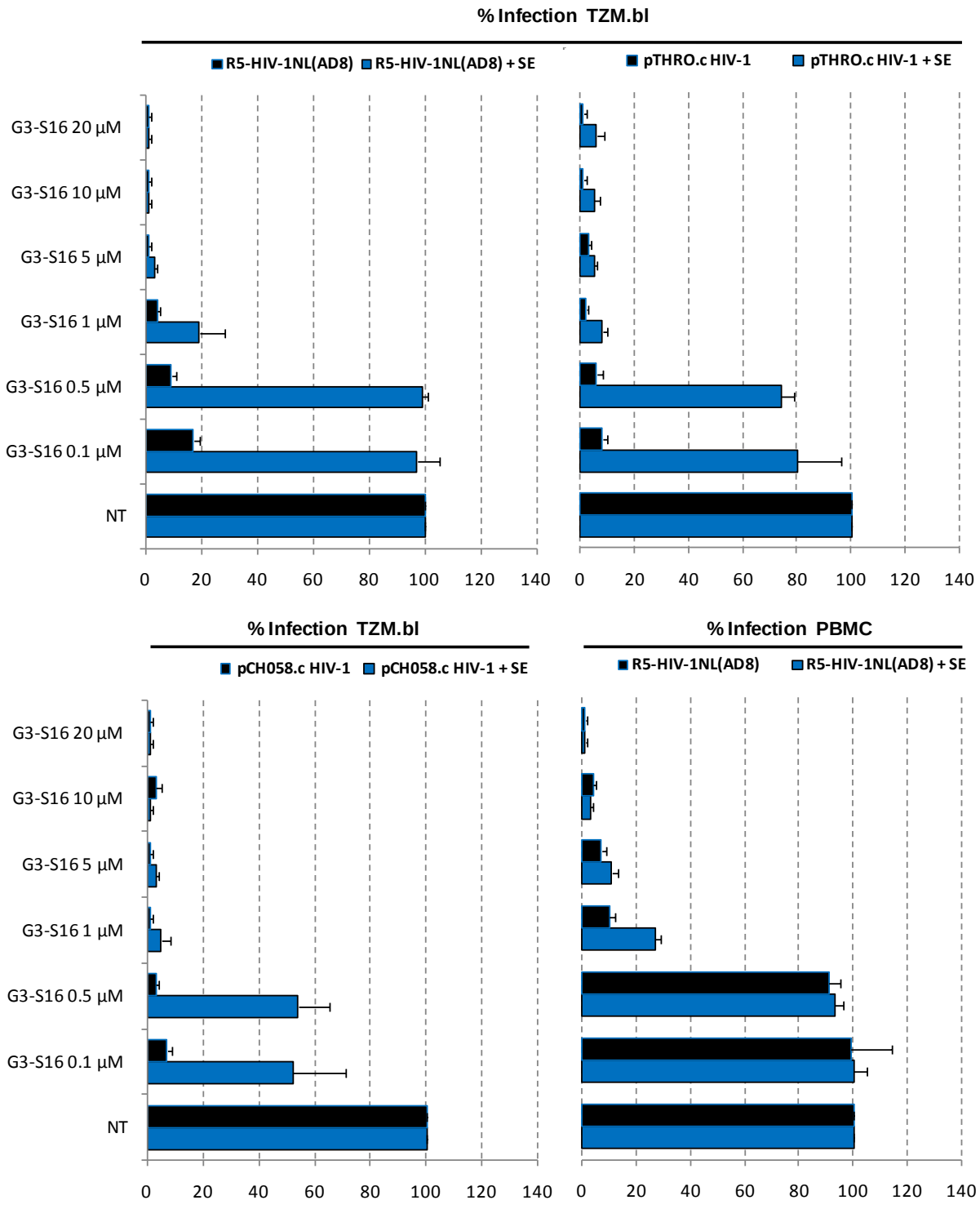

Figure 16. Effect of SEVI on antiviral activity of G3-S16 as microbicides to block HIV-1 infection of TZM.bl cells and PBMC. Cells were pre-treated with a range of concentrations of 0.1 µM to 20 µM of G3-S16. After 1 h, cells were infected with R5-HIV-$_{1NL(AD8)}$ isolates, pTHRO.c and pCH058.c T/F viruses in the absence and presence of semen (SE) at a concentration of 20 ng/10^6 cells. Infection rates were measured 48 h after HIV-1 infection by quantification of luciferase expression. Data represent the mean ± S.E.M. (n = 3).

Table 3. Antiviral activity of microbicides against HIV-1 and semen-exposed HIV-1 in TZM.bl cells or PBMC.

Compound	Cell line	IC_{50}		Fold	IC_{50}		Fold	IC_{50}		Fold
		$R5_{NL(AD8)}$	$R5_{NL(AD8)}$ + SE		pTHRO	pTHRO + SE		pCH058	pCH058 + SE	
G2-S16	TZM.bl	0.04 ± 0.025 µM	8.169 ± 4.155 µM	**204**	0.089 ± 0.013 µM	11.079 ± 0.78 µM	**125**	0.886 ± 0.606 µM	1.87 ± 1.009 µM	**2**
	PBMC	3.345 ± 0.413 µM	4.938 ± 1.641 µM	**1**						
G2-S16+TDF	TZM.bl	0.004 ± 0.001 µM	0.003 ± 0.002 µM	**1**	0.002 ± 0.002 µM	0.009 ± 0.008 µM	**5**	0.000 ± 0.000 µM	0.003 ± 0.000 µM	**3**
	PBMC	0.003 ± 0.002 µM	0.006 ± 0.000 µM	**2**						
G2-S16+MVC	TZM.bl	0.006 ± 0.001 µM	0.015 ± 0.017 µM	**2**	0.004 ± 0.001 µM	0.011 ± 0.003 µM	**3**	0.015 ± 0.006 µM	0.015 ± 0.001 µM	**1**
	PBMC	0.004 ± 0.001 µM	0.008 ± 0.001 µM	**2**						
G2-STE16	TZM.bl	0.121 ± 0.014 µM	3.718 ± 2.095 µM	**31**	0.017 ± 0.010 µM	1.486 ± 1.234 µM	**88**	0.033 ± 0.015 µM	0.810 ± 0.445 µM	**25**
	PBMC	1.642 ± 1.311 µM	7.082 ± 1248 µM	**4**						
G2-STE16+TDF	TZM.bl	0.005 ± 0.002 µM	0.022 ± 0.005 µM	**4**	0.005 ± 0.004 µM	0.012 ± 0.007 µM	**3**	0.008 ± 0.005 µM	0.013 ± 0.001 µM	**2**
	PBMC	0.009 ± 0.002 µM	0.049 ± 0.006 µM	**5**						
G2-STE16+MVC	TZM.bl	0.019 ± 0.007 µM	0.154 ± 0.016 µM	**8**	0.012 ± 0.000 µM	0.087 ± 0.099 µM	**7**	0.037 ± 0.001 µM	0.158 ± 0.020 µM	**4**
	PBMC	0.108 ± 0.011 µM	0.250 ± 0.012 µM	**2**						
G3-S16	TZM.bl	0.009 ± 0.219 µM	6.027 ± 4.192 µM	**688**	0.005 ± 0.005 µM	1.614 ± 0.865 µM	**324**	0.001 ± 0.000 µM	0.635 ± 0.182 µM	**869**
	PBMC	5.678 ± 0.315 µM	6.415 ± 0.097 µM	**1**						
G3-S16+TDF	TZM.bl	0.035 ± 0.005 µM	0.036 ± 0.024 µM	**1**	0.010 ± 0.003 µM	0.068 ± 0.011 µM	**7**	0.011 ± 0.003 µM	0.056 ± 0.009 µM	**5**
	PBMC	0.024 ± 0.007 µM	0.053 ± 0.008 µM	**2**						
G3-S16+MVC	TZM.bl	0.085 ± 0.048 µM	0.466 ± 0.009 µM	**6**	0.030 µM	0.051 µM	**2**	0.034 ± 0.012 µM	0.212 ± 0.015 µM	**5**
	PBMC	0.057 ± 0.000 µM	0.180 ± 0.004 µM	**3**						
TDF	TZM.bl	0.007 ± 0.001 µM	0.016 ± 0.003 µM	**2**	0.008 µM	0.012 µM	**2**	0.005 ± 0.001 µM	0.010 ± 0.008 µM	**2**
	PBMC	0.005 ± 0.005 µM	0.010 ± 0.010 µM	**2**						
MVC	TZM.bl	0.208 ± 0.011 µM	0.458 ± 0.051 µM	**2**	0.084 µM	0.206 µM	**2**	0.037 ± 0.012 µM	0.287 ± 0.170 µM	**8**
	PBMC	0.245 ± 0.000 µM	0.380 ± 0.453 µM	**1.5**						

Fold increase in IC_{50} of semen-exposed relative to non-exposed HIV-1 antiviral activity of G2-S16, G2-STE16, G3-S16, TDF, MVC and their combinations against control and semen-exposed R5-HIV-$1_{NL(AD8)}$, pTHRO and pCH058 in TZM.bl cells and PBMC.

G2-STE16 dendrimer showed that the lowest fold increases in IC_{50} against the three viral isolates were 31, 88 and 25, respectively as the inhibitory effect of G2-STE16 was less affected by the presence of semen, yielding lower IC_{50} values against semen-exposed virus than the other two dendrimers. The greater activity of G2-STE16 in both the absence and the presence of semen was confirmed according to their IC_{50} values for the pTHRO.c and pCH058.c T/F viruses (0.017 µM vs. 1.486 µM; 0.033 µM vs. 0.810 µM), respectively, in comparison to 0.121 µM vs. 3.718 µM in case of R5-HIV-$1_{NL(AD8)}$ isolate (**Table 3**). G2-STE16 showed a similar inhibitory profile to G3-S16, although the fold increase in IC_{50} was much higher; it was 688, 324 and 869 for R5-HIV-$1_{NL(AD8)}$ isolate, pTHRO.c

and pCH058.cT/F viruses, respectively. G3-S16 was the dendrimer that had the highest efficacy against HIV-1 infection with IC_{50} values of 0.009 µM, 0.005 µM and 0.001 µM in the absence of semen compared with 6.027 µM, 1.614 µM and 0.635 µM in the presence of semen (**Table 3**).

7.2. G2-STE16 and G3-S16 dendrimers in combination with ARV

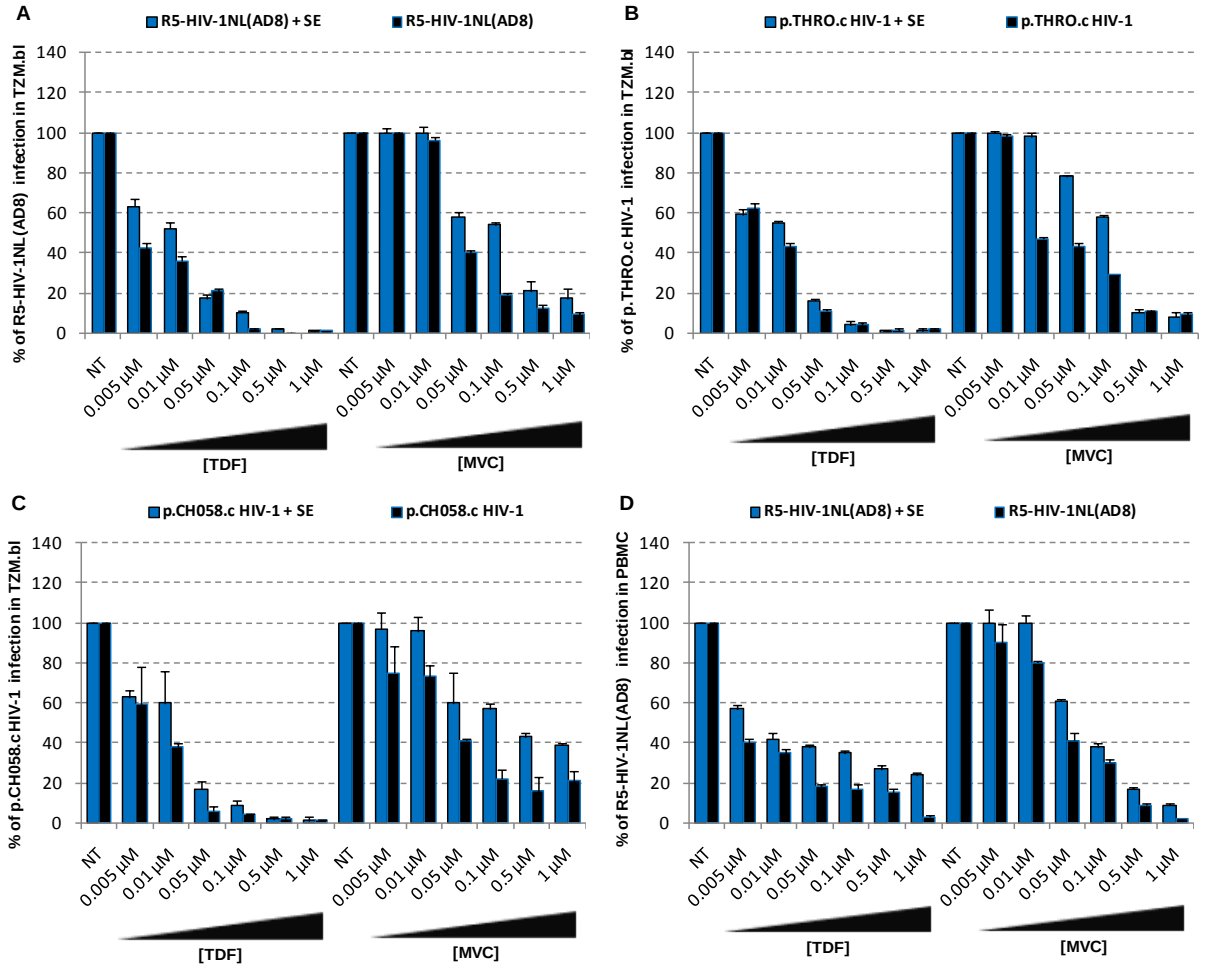

Figure 17. Effect of SEVI on antiviral activity of TDF and MVC to block HIV-1 infection of TZM-bl cells (A to C) and PBMC (D). Cells were pre-treated with range concentrations of TDF and MVC, 0.005 µM to 1 µM. After 1 h, cells were infected with R5-HIV-$1_{NL(AD8)}$ isolate **(A and D)**, pTHRO.c **(B)** and pCH058.c **(C)** T/F viruses in absence and presence of semen (SE) at a concentration 20 ng/10^6cells. Infection rates were measured 48 h after HIV-1infection by quantification of luciferase expression. Data represent the mean ± S.E.M. (n = 3).

The synergistic concentrations of dendrimers and ARV were previously determined by Sepulveda et al (Sepulveda-Crespo et al., 2014, Sepulveda-Crespo et al., 2015b). Thus, we used these concentrations to evaluated their efficiency against semen enhanced HIV-1. First, ARV were tested in a concentration range of 0.005 to 1 µM against R5-HIV-$1_{NL(AD8)}$ isolate and T/F viruses pTHRO.c and pCH058.c in TZM.bl cell line. In the case of TDF, its antiviral effect almost was not modified by

exposure to semen, with values greater than 90% of inhibition from 0.1 µM against all HIV-1 isolates tested, whereas the inhibitory capacity of MCV, depending on the viral isolate was altered by semen-exposed HIV-1, avoiding the HIV-1 infection in 84% at 1 µM against R5-HIV-$1_{NL(AD8)}$, 90% at 0.5 µM againstp THRO.c and only 60% at 1 µM (maximum dose tested) against pCH058.c (**Fig. 17**).

It was observed that TDF inhibitory profile was altered by the exposure to amyloid fibrils in PBMC; only an inhibition of 74% at 1 µM (maximum concentration tested) was observed (**Fig. 17D**), unlike in TZM.bl cells, which showed 90% efficacy at 0.1 µM regardless of the viral isolate (**Fig. 17A-C**). Moreover, MVC showed the same pattern observed in the TZM.bl cells with a value of 90% at 1 µM (**Fig. 17**).

When combined dendrimers with ARV, the best inhibition values for R5-HIV-$1_{NL(AD8)}$ isolate, pTHRO.c and pCH058.c T/F viruses were achieved when mixed with TDF, 0.1 µM G2-STE16 dendrimer + 0.05 µM TDF. However, when G2-STE16 combined with MVC, the inhibitory effect for the three HIV-1 isolates at the maximum concentration tested (0.5 µM G2- STE16 + 0.5 µM MVC) was 90%, 93% and 87%, respectively (**Fig. 18**).

The best results were obtained with G3-S16-TDF combination than with G3-S16-MVC combination. Inhibition percentages against HIV-1 infection with the G3-S16 isolate, pTHRO.c and pCH058.c T/F viruses were 97%, 92% and 78%, respectively, at 1 µM G3-S16 + 0.5 µM MVC in the presence of semen. Despite the slight decrease of the inhibitory capacity of the dendrimers due to amyloid fibrils in semen, the dendrimers remained highly active against HIV-1 infection at non-toxic concentrations (**Fig. 19**).

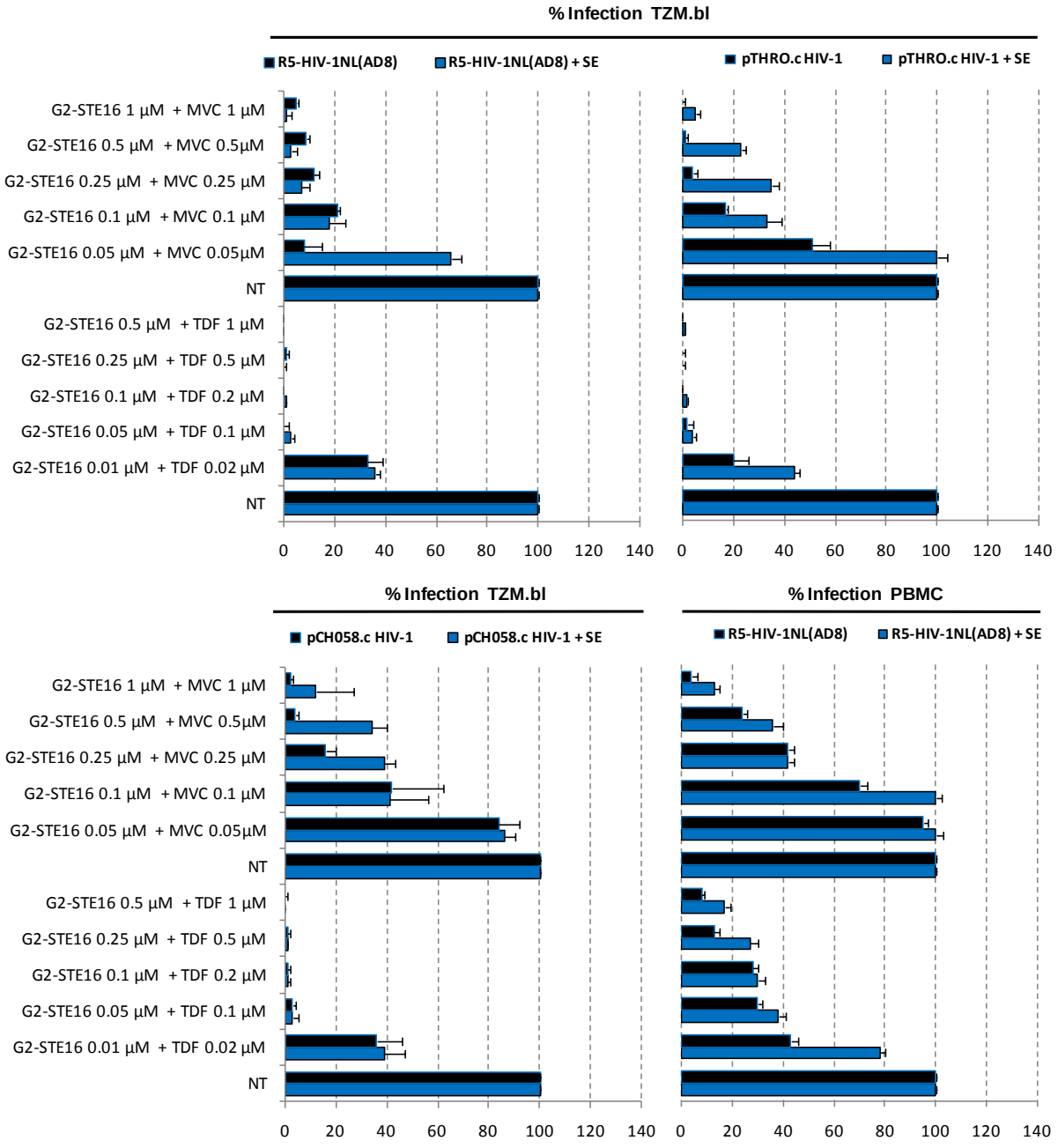

Fig.18. Effect of SEVI on antiviral activity of G2-STE16 in combination with TDF and MVC as microbicides to block HIV-1 infection in TZM.bl cells and PBMC. Cells were pre-treated with a range of concentrations of 0.01 µM to 1 µM of G2-STE16 in combinations with TDF and MVC, 0.02 µM to 1 µM of TDF and 0.05 µM to 1 µM MVC. After 1 h, cells were infected with R5-HIV-$1_{NL(AD8)}$ isolates, pTHRO.c and pCH058.c T/F viruses in the absence and presence of semen (SE) at the concentration of 20 ng/10^6 cells. Infection rates were measured 48 h after HIV-1 infection by quantification of luciferase expression. Data represent the mean ± S.E.M. (n = 3).

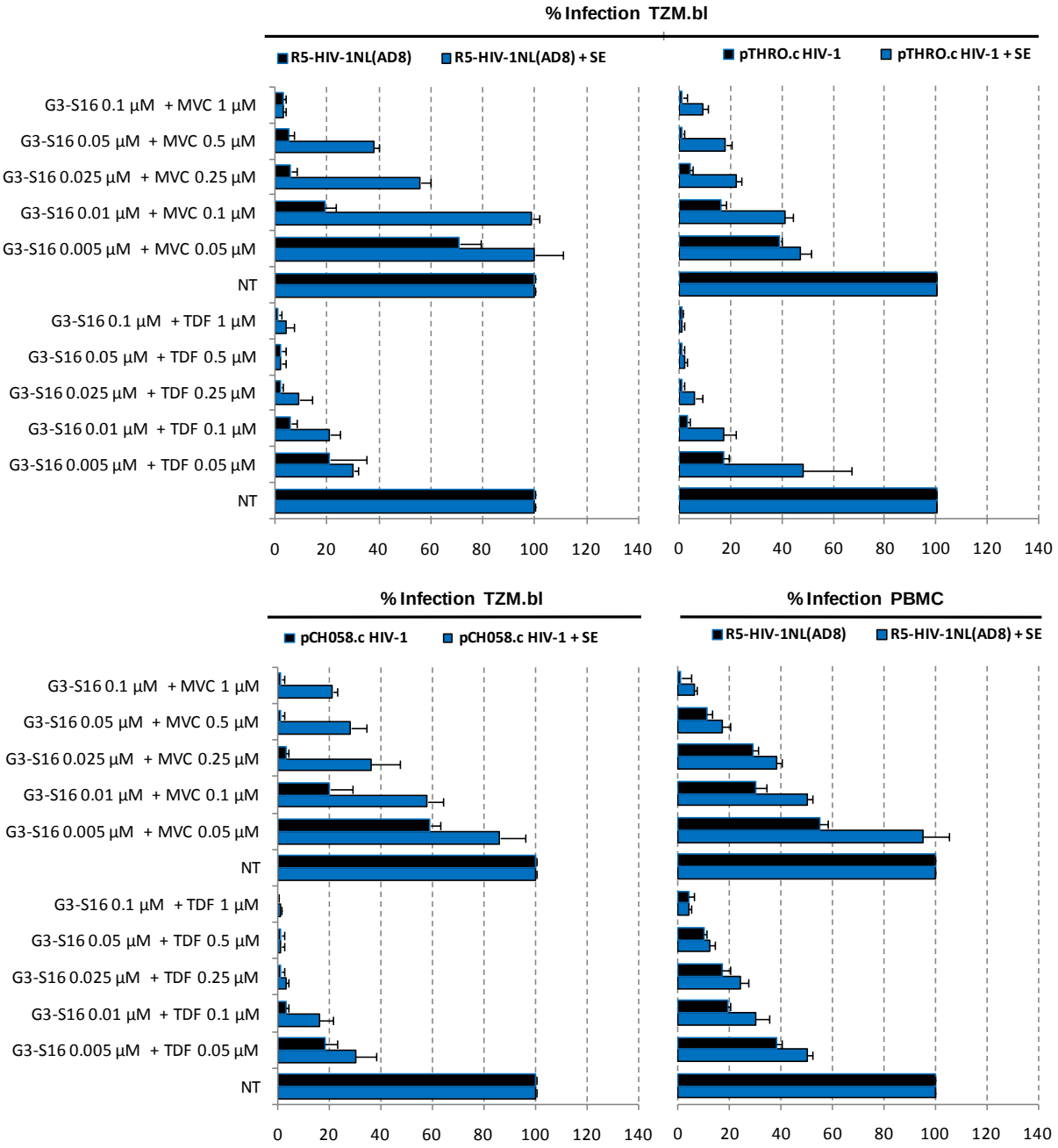

Fig.19. Effect of SEVI on antiviral activity of G3-S16 in combination with TDF and MVC as microbicides to block HIV-1 infection in TZM.bl cells and PBMC. Cells were pre-treated with a range of concentrations of 0.005 µM to 0,1 µM of G3-S16 in combinations with TDF and MVC, 0.005 µM to 1 µM of TDF and 0.05 µM to 1 µM MVC. After 1 h, cells were infected with R5-HIV-$1_{NL(AD8)}$ isolates, pTHRO.c and pCH058.c T/F viruses in the absence and presence of semen (SE) at a concentration of 20 ng/10^6 cells. Infection rates were measured 48 h after HIV-1 infection by quantification of luciferase expression. Data represent the mean ± S.E.M. (n = 3).

Moreover, dendrimers, ARV alone, and their combinations were assessed for efficacy, and antiviral potency against control or semen-exposed R5-HIV-$1_{NL(AD8)}$ isolate, pTHRO.c and pCH058.c T/F viruses in the TZM.bl cells according to their half maximal inhibitory concentration (IC_{50}) values (**Table 3**). The ARV had the best efficacy with 2-fold in increase of IC_{50} in the presence of semen in the

inhibition assay, except that for MVC against the T/F virus pCH058.c yielded an 8-fold difference. However, the IC_{50} values for TDF were 0.007 µM vs. 0.016 µM; 0.008 µM vs. 0.012 µM and 0.005 µM vs. 0.010 µM, which were lower than those for MVC; the values were 0.208 µM vs. 0.458 µM; 0.084 µM vs. 0.206 µM; and 0.037 µM vs. 0.287 µM against mock- and exposed-semen R5-HIV-$1_{NL(AD8)}$, pTHRO.c and pCH058.c isolates, respectively (**Table 3**).

Regardless of the TDF and MVR, the IC_{50} ratios were increased from 1- to 7-fold according to the potency of the combination of each dendrimer, G2-ST16 or G3-S16 with ARV. Nevertheless, the inhibition ability of TDF was higher than that of MVC. Its IC_{50} values were lower for all R5-tropic eleven HIV-1 tested in the presence of SEVI. In combination with TDF against the R5-HIV-$1_{NL(AD8)}$ isolate, G2-STE16 showed a 4-fold increase in IC_{50} (IC_{50} = 0.005 µM in the absence of semen and IC_{50} = 0.022 µM in the presence of semen), whereas G3-S16 maintained its IC_{50} values (0.004 µM and 0.034 µM, respectively) under both conditions. No increase in the IC_{50} was noted. G2-STE16, for the pTHRO.chad T/F virus, had IC_{50} values of 0.005 µM in the absence of semen and 0.009 µM in the presence of semen, indicating a 3-fold increase. G3-S16 had IC_{50} values of 0.01 µM in the absence of semen and 0.068 µM in the presence of semen, indicating a 7-fold increase. G2-STE16 had an IC_{50} of 0.008 µM in the absence of semen and 0.013 µM in the presence of semen, indicating a 2-fold increase. G3-S16 had an IC_{50} of 0.011 µM in the absence of semen and 0.056 µM in the presence of semen, indicating a 5-fold of difference (**Table 3**). G2-STE16 and G3-S16 dendrimers in combination with MVC, in the presence of semen, showed that the IC_{50} values went down, indicating recovery of the antiviral capacity compared with the dendrimers alone. For R5-HIV-$1_{NL(AD8)}$, the IC_{50} values were 0.154 µM and 0.466 µM. For pTHRO.c, the IC_{50} values were 0.087 µM and 0.051 µM. For pCH058.c, the IC_{50} values were 0.158 µM and 0.212 µM. However, in the absence of semen, the antiviral effect of G2-STE16 was scarcely improved when combined with MVC, and the IC_{50} values were practically the same against the T/F viruses. A value of 0.012 µM was indicated for pTHRO.c and 0.037 µM for pCH058.c. However, the IC_{50} with R5-HIV-$1_{NL(AD8)}$ was higher (0.019 µM), and the protective capacity of G3-S16 was reduced by the combination, which was indicated by higher IC_{50} values against the three viral isolates. For R5-HIV-$1_{NL(AD8)}$, the IC_{50} was 0.085 µM. For pTHRO.c, the IC_{50} was 0.030 µM, and for pCH058.c, the IC_{50} was 0.037 µM. Despite the reduced efficacy of the dendrimers combinations with MVC, the IC_{50} ratios in the presence or absence of semen were low for R5-HIV-$1_{NL(AD8)}$. The ratio for G2-STE16 was 8-fold, and 6-fold for G3-S16. For T/F isolate pTHRO.c the ratio

was 7-fold for G2-STE16 and 2-fold for G3-S16, and for pCH058.c, the ratio was 4-fold for G2-STE16 and 5-fold for G3-S16 (**Table 3**).

7.3. G2-S16 dendrimer

G2-S16 is a second-generation polianionic carbosilane dendrimer consisting of a silicon nucleus and sulfonate groups in its periphery with 16 negative charges. To assess if semen increases the infectious capacity of HIV-1 by affecting the inhibitory potential of the G2-S16 polyanionic carbosilane dendrimer, we performed an inhibition assay on TZM.bl cells with three R5-HIV-1 strains in the presence of semen. HIV-1 infection was enhanced by the presence of semen by 1 log when compared to mock-exposed HIV-1 infection in the absence of treatment (**Fig. 20**). Out of the R5-HIV-$1_{NL(AD8),}$ T/F pCH058.c and pTHRO.c strains studied in the absence of semen, G2-S16 was slightly more effective against R5-HIV-$1_{NL(AD8)}$, showing inhibitory values over 95% from 1 µM onward (IC_{50} =0.04 µM). Interestingly enough, T/F pCH058.c and pTHRO.c were also inhibited at non-toxic concentrations of G2-S16 (1 and 5 µM onward, respectively). The highest IC_{50} of 0.886 µM was obtained against pCH058.c T/F R5-HIV-1 (**Fig. 20 and Table 3**).

When the infectivity of HIV-1 was enhanced by the presence of semen, we observed an increase in IC_{50}. However, G2-S16 maintained high values of protection against HIV-1 infection at higher non-toxic concentrations (15–20 µM) (**Fig.20**), in comparison with the concentrations obtained in the absence of semen (1–5 µM). In the presence of semen, G2-S16 showed no inhibitory activity against any of the three R5-HIV-1 strains at concentrations <1 µM. However, G2-S16 completely halted HIV-1 infection in all cases when it was used at concentrations over 15 µM. G2-S16 showed IC_{50} values of 8.17, 1.87, and 11.08 µM against R5-HIV-$1_{NL(AD8)}$, T/F pCH058.c, and pTHRO.c, respectively, in the presence of semen (**Table 3**).

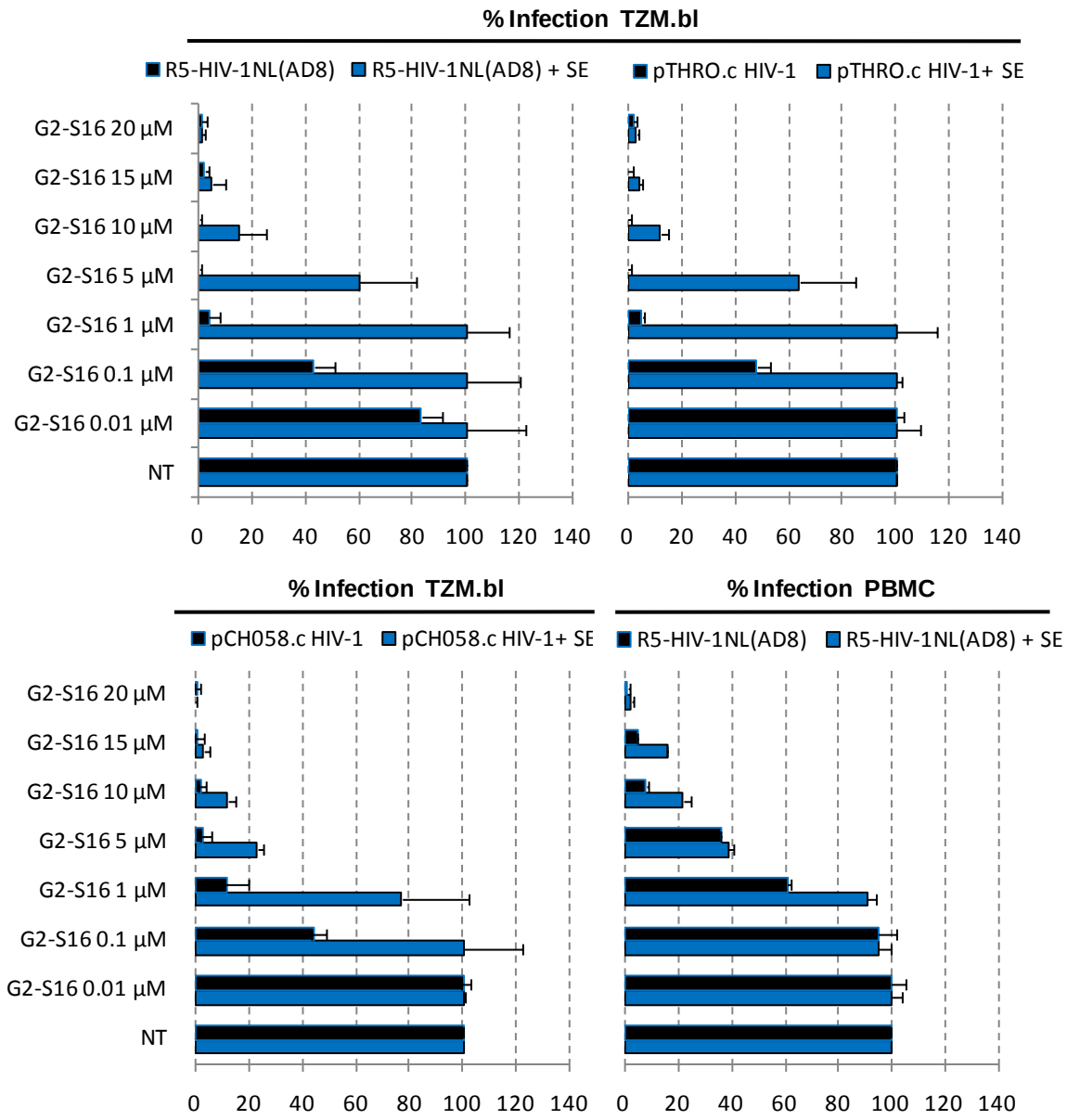

Figure 20. Effect of SEVI on antiviral activity of G2-S16 polyanionic carbosilane dendrimer to block the HIV-1 infection of TZM.bl cells and PBMC. Cells were pretreated with range concentration of 0.01 µM to 20 µM of G2-S16. After 1 h, cells were infected with R5-HIV-$1_{NL(AD8)}$, pCH058.c or pTHRO.c in absence and presence of semen (SE) at a concentration of 20 ng/10^6 cells. Infection rates were measured 72 h after infection by quantification of luciferase expression. Data represent the mean ± SEM (n = 3).

Interestingly enough, G2-S16 had an IC_{50} lower than 0.01 µM against pTHRO.c and R5-HIV-$1_{NL(AD8)}$ strains in the absence of semen. G2-S16 was found to be 204 fold, 125 fold, and 2 fold less effective against semen-exposed R5-HIV-$1_{NL(AD8)}$, pCH058.c, and pTHRO.c virus, respectively (**Table 3**). However, inhibition values of 100% were obtained in the non-toxic concentration range of G2-S16 (**Fig. 20**).

To confirm these results in a more physiological model, we studied the inhibitory ability of G2-S16 in PBMC against a single R5-HIV-1 strain. We found that the inhibitory values of R5-HIV-$1_{NL(AD8)}$ in PBMC were slightly lower than those obtained in TZM.bl cells, although the tendency shown by the results was similar. Interestingly, G2-S16 inhibited 90% of R5-HIV-$1_{NL(AD8)}$ at 10 µM in the absence of semen and 98% at 20 µM in the presence of semen (**Fig. 20**). The inhibition values of HIV-1 infection were practically not affected by the presence of semen when the cells were pre-treated with G2-S16, resulting in minimal changes in IC_{50} values in the absence (IC_{50} = 3.345 µM) or presence (IC_{50} = 4.938 µM) of semen. In other words, the difference was only 1.47-fold higher in the presence of semen in comparison to that in absence (**Table 3**).

7.4. G2-S16 dendrimer in combination with ARV

In combination with TDF and MVC, G2-S16 ability to halt HIV-1 infection in presence of semen was assessed by inhibition assays at several concentrations, maintaining a constant ratio of 1:10 (dendrimer/ARV).

High inhibitory profiles were achieved against R5-HIV-$1_{NL(AD8)}$ isolate, pTHRO.c and pCH058.c T/F viral isolates in TZM.bl cells with the combination of 0.01 µM G2-S16 + 0.1 µM TDF, 94%, 98% and 95%, respectively. However, a similar outcome was not obtained with MVC, which yielded inhibition values of only 87%, 90% and 68%, respectively, at a concentration 10-fold higher than that of TDF (0.1 µM G2-S16 + 1 µM MVC) (**Fig. 21**).

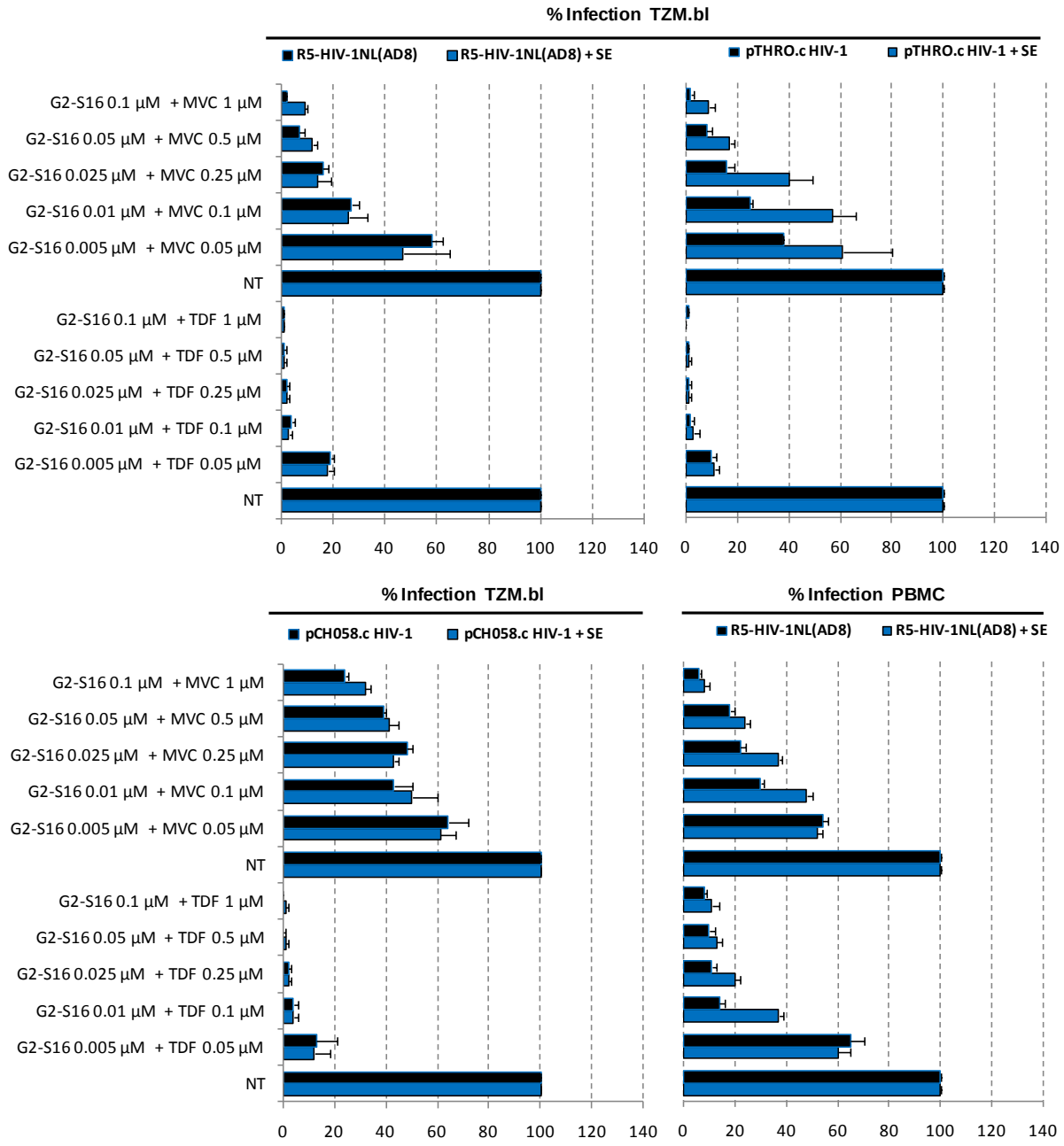

Figure 21. Effect of SEVI on antiviral activity of G2-S16 in combination with TDF and MVC as microbicides to block HIV-1 infection in TZM.bl cells and PBMC. Cells were pre-treated with a range of concentrations of 0.005 µM to 0,1 µM of G2-S16 in combinations with TDF and MVC, 0.005 µM to 1 µM of TDF and 0.05 µM to 1 µM MVC. After 1 h, cells were infected with R5-HIV-$1_{NL(AD8)}$ isolates, pTHRO.c and pCH058.c F viruses in the absence and presence of semen (SE) at a concentration of 20 ng/10^6 cells. Infection rates were measured 48 h after HIV-1 infection by quantification of luciferase expression. Data represent the mean ± S.E.M. (n = 3).

The effectiveness of G2-S16 was affected by presence of amyloid fibrils semen in the culture. It was needed increase its concentration to maintain the inhibition of HIV-1 infection of the three viral isolates. This dendrimer also showed less inhibitory capacity against mock-exposed T/F viruses, pTHRO.c and pCH058.c, than the other dendrimers, with higher IC_{50} values for mock- or semen-

exposed HIV-1. The values were 0.080 µM vs. 11.079 µM and 0.886 µM vs. 1.870 µM, corresponding to 125- and 2-fold increases, respectively. Against the R5-HIV-$1_{NL(AD8)}$ isolate $IC_{50,}$ values of 0.04 µM in the absence of semen and 8.169 µM (a fold increase of 204) in the presence of semen were obtained (**Table 3**).

In combination with TDF against the R5-HIV-$1_{NL(AD8)}$ isolate, G2-S16 maintained the IC_{50} value (0.004 µM) in presence and absence of semen and no increase in the IC_{50} was noted. For the T/F virus pTHRO.c, G2-S16 had a lower IC_{50} of 0.002 µM in the absence and 0.009 µM in the presence of semen, indicating a 5-fold increase. G2-S16 showed better results for pCH058.c in combination with TDF, showing low IC_{50} in the absence of semen that produced a 3-fold increase in IC_{50} in the presence of amyloid fibrils (IC_{50} = 0.003 µM).

Despite the need of higher concentrations, G2-S16 in combination with MVC showed high inhibitory values at maximum concentrations against R5-tropism viral isolates. In the absence of SEVI in cell cultures of R5-HIV-$1_{NL(AD8)}$ and pTHRO.c virus, the IC_{50} values were 0.006 µM and 0.004 µM and 0.015 µM and 0.011 µM in the presence of semen, indicating 2- and 3-fold increases, respectively. No IC_{50} increase was observed with pCH058.c of a value of 0.015 µM. Despite the slight decrease of the inhibitory capacity, G2-S16 remained highly active against HIV-1 infection at non-toxic concentrations (**Fig. 21**).

Regardless of the reduced efficacy of the combinations with MVC, the IC_{50} ratios in the presence or absence of semen were low for R5-HIV-$1_{NL(AD8)}$. The ratio for G2-S16 against R5 HIV-$1_{NL(AD8)}$ was 2-fold; for pTHRO.c, the ratio was 3-fold; and for pCH058.c, the ratio was 1-fold (**Table 3**).

To confirm the results in a model more reflective of the present physiology, we evaluated G2-S16 dendrimer against R5-HIV-$1_{NL(AD8)}$ in PBMC, the principal target cells of HIV-1 infection. In PBMC, combinations with ARV achieved the best inhibition values with TDF against semen exposed-R5-HIV-$1_{NL(AD8)}$, G2-S16 inhibited the infection at 87% at a concentration of 0.05 µM + 0.5 µM TDF onward.

The inhibitory efficiency in combination with MVC was lower in PBMC than in TZM.bl cells against R5-HIV-$1_{NL(AD8)}$ in mock- and semen exposed-HIV-1. However,a 1:10 ratio of G2-S16/MVC of 0.1 µM G2-S16 + 1 µM MVC obtained a value of 92% of HIV-1 inhibition.

The best results against R5-HIV-$1_{NL(AD8)}$ in PBMC were found with G2-S16; without ARVs in the absence of semen, the IC_{50} was 3.345 µM, whereas it was 4.038 µM in the presence of semen (a 1.5-

fold increase). In both combinations TDF and MVC the increase was of 2-fold; the values for TDF increased from 0.003 µM to 0.006 µM and from 0.004 µM to 0.008 µM for MVC.

8. *In vivo* biocompatibility of G2-S16 polyanionic carbosilane dendrimer

G2-S16 polyanionic carbosilane dendrimer has shown to be capable of retaining its inhibitory effect at nontoxic concentrations against HIV-1 which infectivity has been enhanced by the presence of amyloid fibrils of semen (Cena-Diez et al., 2016a).

However, several promising microbicides based on nanotechnology, such as PLL dendrimer SPL7013 with 32 anionic naphthalene sulfonate groups in the periphery (VivaGel®), were not successful due to the lack of broad anti-HIV-1 activity against R5-HIV-1 strains (Telwatte et al., 2011) and its increased risk of HIV-1 acquisition associated with epithelial injury after 7–14 days of twice-daily administration (Moscicki et al., 2012). To decrease HIV-1 transmission the role of the local inflammation should be taken into account. These data highlight the fact that the genital environmenthas a substantial influence on HIV-1 transmission (Blish et al., 2012). The above fact suggests the need for a tough pre-screening to assess the biocompatibility of compounds formulated as topical microbicides prior to human clinical trials.

8.1. *In vivo* bioluminescent imaging of G2-S16 dendrimer in BALB/c mice

G2-S16 dendrimer's ability to penetrate vaginal epithelium was assessed in BALB/c mice detecting the bioluminescence in the vagina and in the whole animal by using the IVIS Lumina Image System. G2-S16 could not be labelled with FITC due to its Michael type addition synthesis. Therefore, G2-STE16-FITC dendrimer functionalized by thiol-ene additional reactions, an analogous of G2-S16, was used. The vaginal administration of G2-STE16-FITC dendrimer formulated as HEC gel to BALB/c mice was evaluated at 30 min and 20 h (Xenogen,Madrid, Spain). In this sense, 12 female BALB/c mice of 7 weeks old and of weight 20±3 g were randomized into three groups of 4 mice. Group A (control) was treated vaginally only with 30 µL of 1% HEC gel (sacrificed after 30 min), group B was treated vaginally with 1% HEC gel and 3% G2-STE16-FITC (sacrificed after 30 min), and group C was treated vaginally with 1% HEC gel and 3% G2-STE16-FITC (sacrificed after 20 h) post-treatments. Mice were euthanized and their skin removed to avoid auto-flowering before imaging. Imagines of the vagina of whole BALB/c mice (**Fig. 22A**), extracted vagina (**Fig. 22B**), opened vagina along the axial exe (**Fig. 22C**) and opened vagina after being washed twice using PBS (**Fig. 22D**) with the objective to remove

possible excesses of the G2-STE16-FITC for each mice group were obtained. The Living Image Software automatically co-registered the luminescent images, which were taken in darkness and displayed in pseudo-colours that represent the intensity of the signal and the photographic image, producing an overlay image. Bioluminiscent BALB/c mice images were obtained in dorsal, ventral, and lateral positions. As expected, no signal was found when PBS was vaginally administrated (**Fig. 22A-D**). In contrast, a bright and intense signal was observed when the G2-ST16-FITC was administrated for 30 min and 20 h in the vagina (**Fig. 22E**). The vagina was extracted, and an increase of its fluorescence was observed, confirming the presence of the G2-ST16-FITC dendrimer over time (**Fig. 22F** and **22I**). Then, the vaginas were opened on its longitudinal axis exe to evaluate the presence of the G2-ST16-FITC dendrimer on the inner side of the tissue (**Fig. 22G** and **22J**) and washed twice, using PBS to remove possible excess of the G2-ST16-FITC (**Fig. 22H** and **22K**).

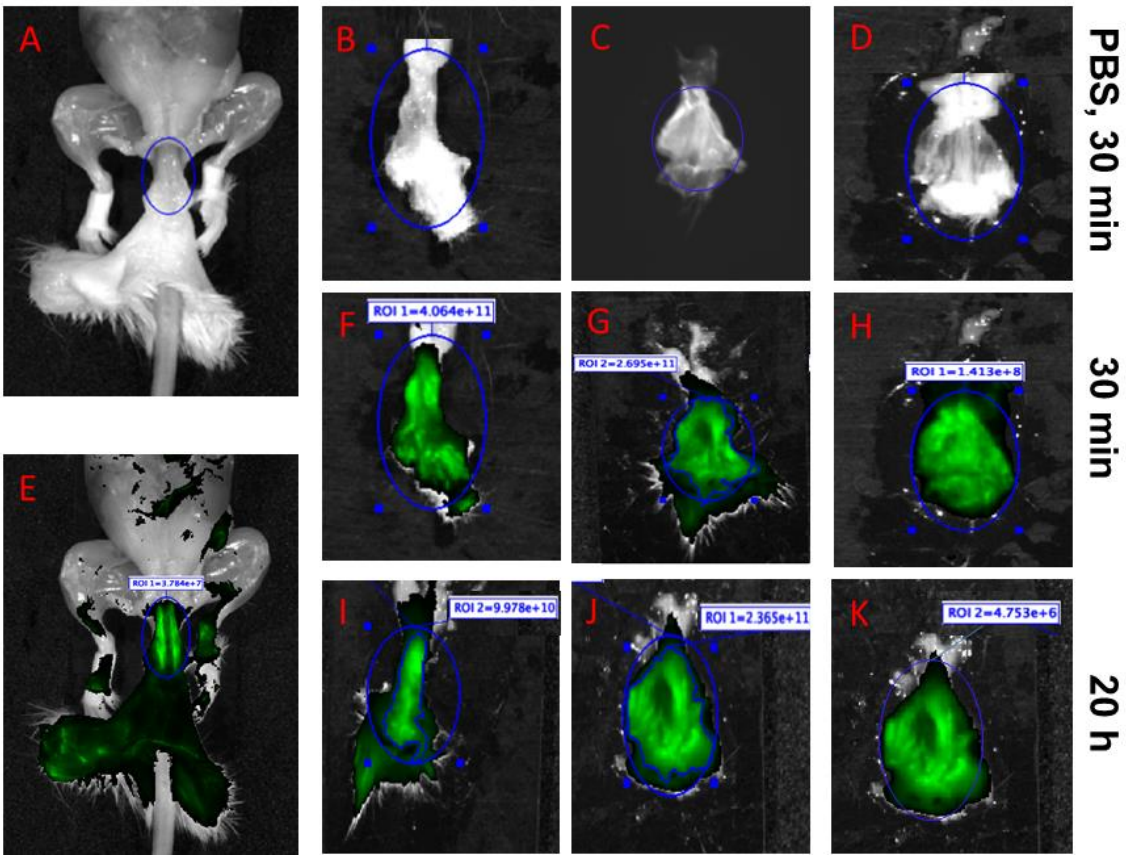

Figure 22. *In vivo* evaluation of G2-STE16-FITC ability to cross vaginal epithelium. Mice were treated with PBS (**A-D**) or G2-STE16-FITC (**E-K**). Bioluminescent images were obtained 30 min or 20 h post-treatment. Imagines of the whole animal (**A and E**), the vagina (**B, F** and **I**), open vagina though the axial exe (**C, G** and **J**) and open vagina though the axial exe washed with PBS (**D, H** and **K**) were obtained for each treatment and time.

8.2. Confocal microcopy of G2-S16 dendrimer in BALB/c mice

To determine whether the G2-ST16-FITC dendrimer was able to cross the epithelial barrier or not (**Fig. 23**), the same randomized three BALB/c mice groups as in *in vivo* bioluminescent imaging assay were used. First, we showed mice only treated with PBS as control todemonstrate that PBS does not cause fluorescence (**Fig. 23A-23B**). After having studied the vaginas of the mice group B treated with G2-STE16-FITC for 30 min, it was observed that in the non-sterile areas of the female reproductive tract, vagina (**Fig. 23C**), ectocervix (**Fig. 23D**) and fornix (**Fig. 23E**) the dendrimerwas not able to go through the vaginal epithelium, although there was an accumulation of the G2-ST16-FITC dendrimer. However, when the G2-ST16-FITC was applied to non-sterile area of the group C vagina for 20 h, G2-ST16-FITC dendrimer was observed to cross from the lumen of the vagina towards the matrix (**Fig. 23G-23I**). Nevertheless, the vaginal epithelium appeared to be slightly damaged and inflamed, which could help the dendrimer to pass through (**Fig. 23G-23H**). The use of a FITC-labelled dendrimer could be the cause of the above side effects and it is believed not to be the ideal candidate to be used as a microbicide. As it can be seen in **Figure 23**, in no case the G2-ST16-FITC dendrimer reaches the sterile part of the vagina, endocervix and uterus (**Fig. 23F and 23J**). Both the ectocervix and vagina of the female genital tract consist of stratified squamous epithelium; the endocervix is characterized by a simple columnar epithelium.

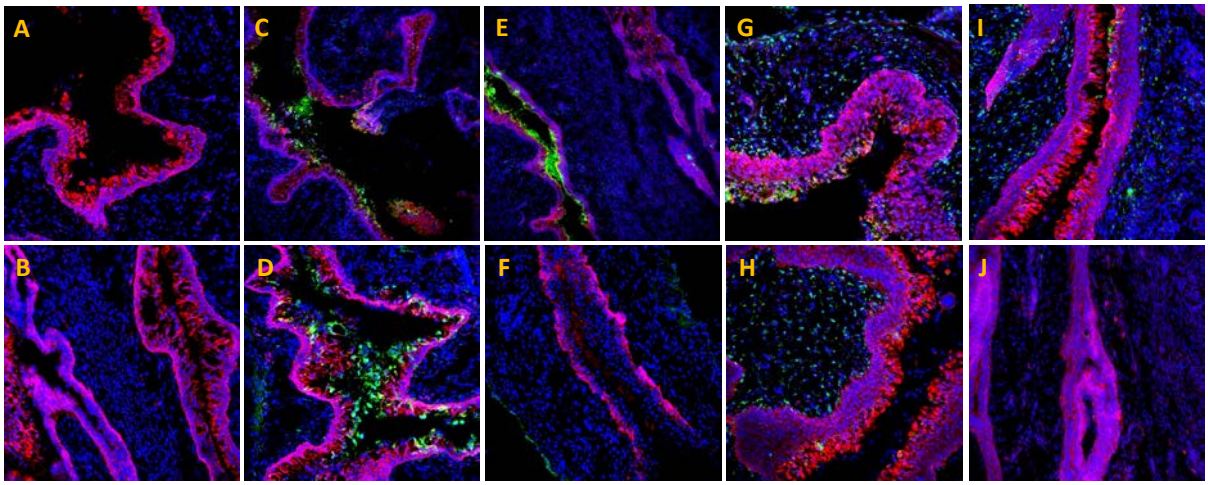

Figure 23. Confocal microscopy imagines of G2-STE16-FITC ability to cross vaginal epithelium. Mice were treated with PBS (**A-B**) or G2-STE16-FITC for 30 min (**C-F**) and for 20 h (**G-J**). Bioluminescent images were obtained 30 min or 20 h post-treatment. Imagines of the vagina (**A, C** and **G**), ectocervix (**D** and **F**), fornix (**E** and **I**) and endocervix (**B, F** and **J**) in each treatment and time were represented.

8.3. BALB/c vaginal irritation assay and histological studies

With the objective of knowing if the cause of the above side effects was due to the G2-STE16-FITC dendrimer, a vaginal irritation assay was performed in BALB/c mice for 20 h with a single dose of G2-STE16 or G2-STE16-FITC dendrimers, creating the same conditions of exposure as in the previous experiments. Twelve female BALB/c mice of 7 weeks old with the weight of 20±3 g were purchased. G2-STE16 or G2-STE16-FITC was added to 1% HEC placebo gel to a final concentration of 3% w/v. BALB/c mice were randomized into four groups of three mice per group. Group A (control) was treated vaginally only with 30 µL of 1% HEC gel, group B was treated vaginally with 1% HEC gel with 3% G2-STE16, group C was treated with 1% HEC gel with 3% G2-STE16+FITC and group D (irritation group) was treated with 4.5% N9 in PBS. The four conditions were applied intravaginally in female BALB/c mice previously anaesthetized with isoflurane. After 20 h, BALB/c mice were sacrificed and vaginas were extracted and conserved in 4% formaldehyde w/v. This histological study in BALB/c vaginal tissue showed that when mice were treated with G2-STE16 or with G2-STE16-FITC, after 20 h of exposure all mice had the same level of irritation and inflammation of their vaginal epithelium (total score = 7) (**Table 4**). This proved our hypothesis that the damage on the epithelium observed on the *in vivo* bioluminescent imaging and confocal microscopy assays were due to the irritation caused by the G2-STE16 or G2-STE16-FITC dendrimer.

Table 4. Vaginal toxicity assay of G2-ST16 or G2-ST16-FITC after a single dose

	PBS		Control N9 (4.5%)		G2-STE16 (3%)			G2-STE16-FITC (3%)		
Epithelial lesion	0	0	3	4	2	2	2	3	2	3
Inflammatory infiltrate	0	0	3	3	2	2	3	2	2	1
Vascular congestion	1	1	4	3	2	1	1	1	2	3
Edema/Fibrosis	0	0	2	2	1	1	1	1	1	1
TOTAL SCORE	**1**	**1**	**12**	**12**	**7**	**6**	**7**	**7**	**7**	**8**
Estrous cycle moment	**P**	**P**	**P-E**	**P-E**	**P**	**P**	**P**	**P**	**P**	**P**

The existence of injury in the vaginal epithelium was evaluated in each biological sample. 0 (no change) when no injury or the observed changes were within normal range; 1 (minimum) when changes were sparse but exceeded those considered normal; 2 (light) when injuries were identifiable but with no severity; 3 (moderate) for significant injury that could increase in severity; 4 (very serious) for very serious injuries that occupy most of the analyzed tissue. These values were added up and determined the level of vaginal irritation as minimum 1-3, average 4-6, moderate 7-9 and severe >9+.

Moreover, it was demonstrated that when BALB/c mice were treated with G2-S16 for 7 consecutive days, no damage or alteration onto the vaginal epithelium was caused, showing that G2-S16 dendrimer is safe for the development of a topical microbicide against HIV-1 infection (**Table 5**).

Table 5. Vaginal toxicity assay after 7 consecutive days

	PBS		Control N9 (4.5%)		G2-S16 (3%)		
Epithelial lesion	0	0	2	3	0	0	0
Inflammatory infiltrate	1	2	4	2	2	1	2
Vascular congestion	1	1	3	3	1	0	1
Edema/Fibrosis	0	0	2	1	1	1	1
TOTAL SCORE	**2**	**3**	**11**	**9**	**4**	**2**	**4**
Estrous cycle moment	**P**	**P-E**	**P**	**P-E**	**P**	**P-E**	**P**

G2-S16 or control was administrated daily for 7 consecutive days. The existence of injury in the vaginal epithelium was evaluated in each biological sample. 0 (no change) when no injury or the observed changes were within normal range; 1 (minimum) when changes were sparse but exceeded those considered normal; 2 (light) when injuries were identifiable but with no severity; 3 (moderate) for significant injury that could increase in severity; 4 (very serious) for very serious injuries that occupy most of the analyzed tissue. These values were added up and determined the level of vaginal irritation as minimum 1-3, average 4-6, moderate 7-9 and severe >9+.

8.4. Full-thickness EpiVaginal™ tissue toxicity

The EpiVaginal™ (VEC-100) ectocervical tissue model (Carl-Bertelsmann-Strasse, Gütersloh, Germany) was used to evaluate the safety of G2-S16 dendrimer for vaginal application. The EpiVaginal™ *in vitro* test is gradually replacing the traditional *in vivo* models to study vaginal irritation due to the fact that its high reliability and reproducibility. Three-dimensional full thickness VEC-100 FT EpiVaginal™ tissue is a highly differentiated structure, which parallels *in vivo* tissue and ideal for toxicity studies of feminine hygiene, vaginal care, and microbicide products. Full-thickness EpiVaginal™ tissues were dosed with 100 µL of each test sample, including G2-S16 dendrimer concentrations, triton as a death control, and water as negative control. After 24 h incubation at 37 ºC, 5% CO_2, a MTT assay was performed to determine the cell viability. Dendrimer concentrations with viability >80% in comparison with control were regarded as non-toxic. G2-S16 dendrimer was non-

toxic at concentration of 500 µM (**Fig. 24**). Our data revealed that G2-S16 is a safe nanocompound for vaginal application to control viral transmission.

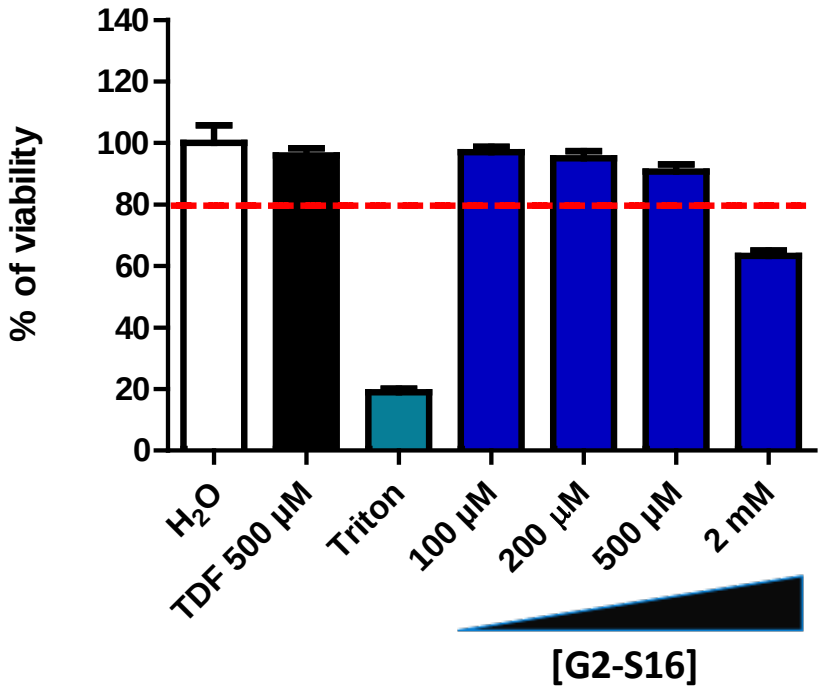

Figure 24. Biocompatibility of polyanionic carbosilane dendrimer G2-S16 in EpiVaginal™ tissue (VEC-100-FT). Viability of fullthickness EpiVaginal™ tissue was evaluated by MTT assay after 24 h of exposure to a range of dendrimer concentrations; 80% of viability was set as the limit of toxicity for all G2-S16 dendrimer concentrations. H_2O and Triton were used as negative and positive control of cellular death, respectively. Data were represented as mean ± standard deviation of three independent experiments.

8.5. Zebrafish toxicity test

Zebrafish embryo (*Daniorerio*) is emerging as an important tool for FET for the opportunity to carry out fast reproducible tests (Olivares et al., 2016, Strahle et al., 2012), a standard test recommended by Organization of Economic Cooperation and Development (Busquet et al., 2008) and has an excellent correlation with acute adult fish toxicity tests (Belanger et al., 2013, Lammer et al., 2009).

According to the quality criteria established for this study, the test is considered valid when:

- Survival of fertilized eggs in the control group is greater than 90% at 96 h POST fertilization (hpf).
- Survival of fertilized eggs in the vehicle group is greater than 90% at 96 hpf.
- The induction of death is greater than 30% for the reference compound (3,4-DCA) at 96 hpf.

In this study, the quality criteria were met.

Three aspects of toxicity, namely mortality, morphological developmental defects and teratogenicity effects, were evaluated and scored in zebra fish embryos at 24, 48 and 72 hpf. The evaluation of the cumulative mortality in the embryos at the various concentrations of G2-S16 at 24, 48, 72 and 96 h, showed no significant mortality in any dose of the G2-S16 dendrimer, being the survival greater than 90% in all cases. The test met the quality criteria, obtaining 95.8% survival in the control group and 100% in the vehicle group and 45% mortality of the eggs in the reference compound (3.7 mg/L 3,4-DCA) at 96 hpf (**Table 6A**). The sub-lethal effects (absence of spontaneous movement, depigmentation, the formation of edemaand/or formation of clots) induced by G2-S16 at each concentration at various times were evaluated. One case was recorded at 96 hpf in at 4.6 mg/L, 10 mg/L and 22 mg/L, in all cases a pericardial edema. In the remaining doses and in the negative and vehicle controls, no sub-lethal effects were recorded. On the other hand, positive control (3.4 DCA) at 3.7 mg/L induced the occurrence of sub-lethal effects from 24 hpf onwards (**Table 6B**). When evaluating the teratogenicity effects of G2-S16, it was observed that at 96 hpf at the concentrations of 22 mg/L, 10 mg/L and 4.6 mg/L, 5% of tail malformation occurred (**Table 6C**). In the remaining doses and in the negative and vehicle controls, no teratogenicity effect was recorded. The positive control (3.4 DCA) at 3.7 mg/L induced the appearance of teratogenicity effects from 24 hpf, affecting 96 hpf to 20% of total embryos (36.4% of viable embryos).

Table 6. G2-S16 toxicity evaluation on zebra fish.

	A % Embryonic mortality				B % Sublethal effects				C % Teratogenic effects			
	CONTROL				CONTROL				CONTROL			
hpf	24	48	72	96	24	48	72	96	24	48	72	96
Control	0.0	0.0	0.0	4.2	0.0	0.0	0.0	0.0	0.0	0.0	0.0	0.0
Vehicle	0.0	0.0	0.0	0.0	0.0	0.0	0.0	0.0	0.0	0.0	0.0	0.0
Positive control	25.0	25.0	40.0	45.0	40.0	40.0	25.0	35.0	40.0	40.0	25.0	20.0
	G2-S16				G2-S16				G2-S16			
hpf	24	48	72	96	24	48	72	96	24	48	72	96
100 mg/L	0.0	0.0	0.0	0.0	0.0	0.0	00	0.0	0.0	0.0	0.0	0.0
46 mg/L	5.0	5.0	5.0	5.0	0.0	0.0	0.0	0.0	0.0	0.0	0.0	0.0
22 mg/L	0.0	0.0	5.0	10.0	0.0	0.0	0.0	5.0	0.0	0.0	0.0	5.0
10 mg/L	0.0	0.0	0.0	0.0	0.0	0.0	0.0	5.0	0.0	0.0	0.0	5.0
4.6 mg/L	5.0	5.0	5.0	5.0	0.0	0.0	0.0	5.0	0.0	0.0	5.0	5.0

Determination of acute toxicity of substances on zebrafish eggs was performed. Eggs were treated with various concentrations of G2-S16 (100 mg L, 46 mg/L, 22 mg/L, 10 mg/L and 4.6 mg/L), 3,4 dichloroaniline (3,4-DCA) at 3.7 mg/L (positive control) or dilution water (vehicle) for different hpf (24, 48, 72 and 96). Embryonic mortality (**A**), sublethal effects (**B**) and teratogenic effects (**C**) were evaluated.

The parameters of lethal concentration 50 (LC_{50}), minimum LOEC and maximum concentration without observed effect, also denominated as maximum dose tolerated (MDT) at 48 and 96 hpf were all >100 mg/L. As no significant anomaly and mortality were recorded in the embryos, the toxicological parameters were above the maximum dose tested. It was shown that no significant differences were found in mortality, sublethal or teratogenic effects when the embryos were treated with G2-S16 100 mg/L in comparison with the negative control (**Table 6**).

9. Effect of polyanionic carbosilane dendrimers against HSV-2 infection

Several dendrimers showed a great anti-HIV-1 and anti-HIV-2 activity against clinical viral strains. However, their ability to inhibit other sexually transmitted infections is unknown. In this work, antiviral activity against HSV-2 333 of eight dendrimers, which previously showed high anti-HIV-1 activity were researched (Briz et al., 2015, Chonco et al., 2012, Sanchez-Rodriguez et al., 2015, Sepulveda-Crespo et al., 2015a, Sepulveda-Crespo et al., 2014, Sepulveda-Crespo et al., 2015c, Vacas Cordoba et al., 2013).

9.1. Cell viability assays

The cell viability was studied using a MTT assay 48 h post-treatment with eight dendrimers in Vero cell line (**Fig. 25**). Dendrimers concentrations with viability >80% in comparison with control were regarded as non-toxic. G2-CTE16 was the most toxic dendrimer, with a limit of viability of 0.1 μM. G3-S16 and G2-NF16 were nontoxic at 0.5 μM and G2-S24P and G2-STE16 at 1 μM. When Vero cells were treated with G2-S16 dendrimer, it was shown that G2-S16 was nontoxic up to 10 μM as previously reported in other cells (Vacas Cordoba et al., 2013). G1-C8 and G1-S4 were non-toxic at 5 and 10 μM, respectively. In each infection experiment, MTT assay was also performed to avoid false positives due to cell death by apoptosis or superinfection.

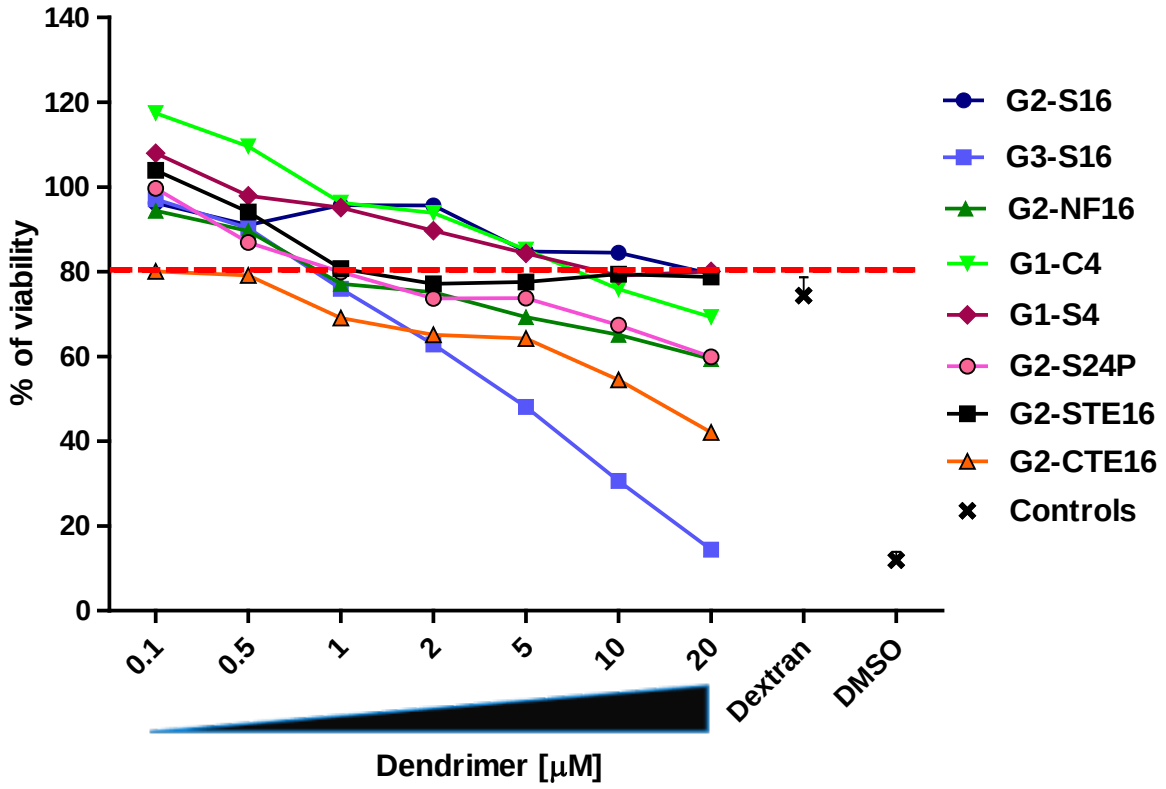

Figure 25. Biocompatibility of polyanionic carbosilane dendrimers in Vero cells. Viability of epithelial Vero cells was evaluated by MTT assay after 24 h of exposure to a range of dendrimer concentrations. 80% of viability was set as limit of toxicity for all dendrimers. Dextran 20 μM and DMSO 10% were used as negative and positive control of cellular death, respectively. Data are represented as mean ± SD of three independent experiments.

9.2. Identification of polyanionic carbosilane dendrimers as anti-HSV-2 agents

MTT assay provided nontoxic working concentrations for each dendrimer, a primary screening to test the ability of these dendrimers inhibiting HSV-2 333 strain infection in Vero cells, VK-2 and HEC-1A were performed. Four of the studied dendrimers, G2-S16, G1-S4, G3-S16, and G2-STE16 inhibited significantly the HSV-2 333 (**Fig. 26**). We achieved 100% anti-HSV-2 inhibitory activity when Vero cells were pre-treated with 10 μM of G2-S16. G1-S4, G3-S16, and G2-STE16 dendrimers achieved a reduction of anti-HSV-2 activity of 77%, 68%, and 28%, respectively. G2-S16, G1-S4, and G3-S16 were chosen for more detailed *in vitro* studies.

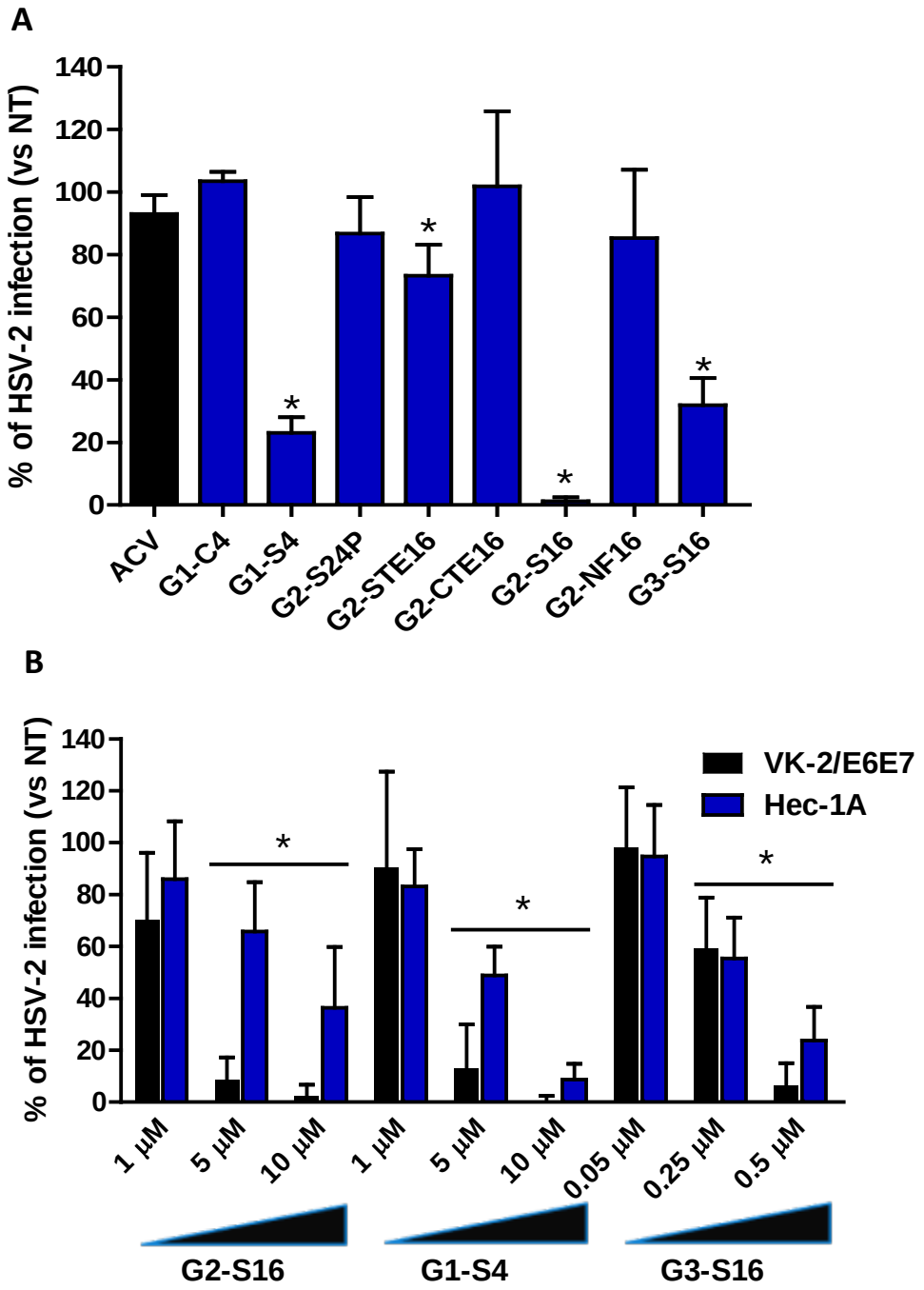

Figure 26. Dendrimers anti-HSV-2 activity. (A) Primary screening of candidates for inhibitory activity against HSV-2 333. Vero cells were pretreated with nontoxic concentrations of the compounds for 1 h and then infected with HSV-2 333. Percentage of infection was determined after 48 h. **(B)** Inhibition of HSV-2 by dendrimers in VK2/E6E7 and HEC-1A human epithelial cell lines. VK2/E6E7 or HEC-1A cells were treated with polyanionic dendrimers for 1 h before infection with HSV-2 333. At 30–40 h post-infection, supernatants were collected and their infectivity was assessed in a plaque reduction assay. Data were represented as mean ± standard deviation of three independent experiments (*p< 0.05 vs control).

When HEC-1A and VK2/E6E7 were pretreated with 10 μM of G2-S16, the HSV-2 333 strain inhibition was 68% and 98%, respectively and when pretreated with G1-S4 at 10 μM, the HSV-2 333 inhibition was 92% and 99%, respectively. Finally, a decrease of 72% and 94% of HSV-2 333 infection was achieved in HEC-1A and VK2/E6E7 cells when pretreated with G3-S16 at 0.5 μM (**Fig. 26B**). In conclusion, dendrimers were highly effective in inhibiting the infection of HSV-2 in HEC-1A and VK2/E6E7 cells.

9.3. Effect of pH in anti-HSV-2 activity of dendrimers

One critical point in the development of new microbicidal compounds is to evaluate their stability and biological activity during the critical vaginal pH change from around 4.5 to 7.0 which occurs at the time of ejaculation (Cutler and Justman, 2008). In order to study the effect of vaginal pH and semen in dendrimers anti-HSV-2 activity, G2-S16, G1-S4, or G3-S16 were incubated in different pH solutions from 3.0 to 7.0 and human seminal plasma to mimic the effects of the introduction of semen to the vagina. Afterwards, Vero cells were pretreated with dendrimers and then infected with HSV-2 333 strain. Viral infection was determined at 48 h post-infection.

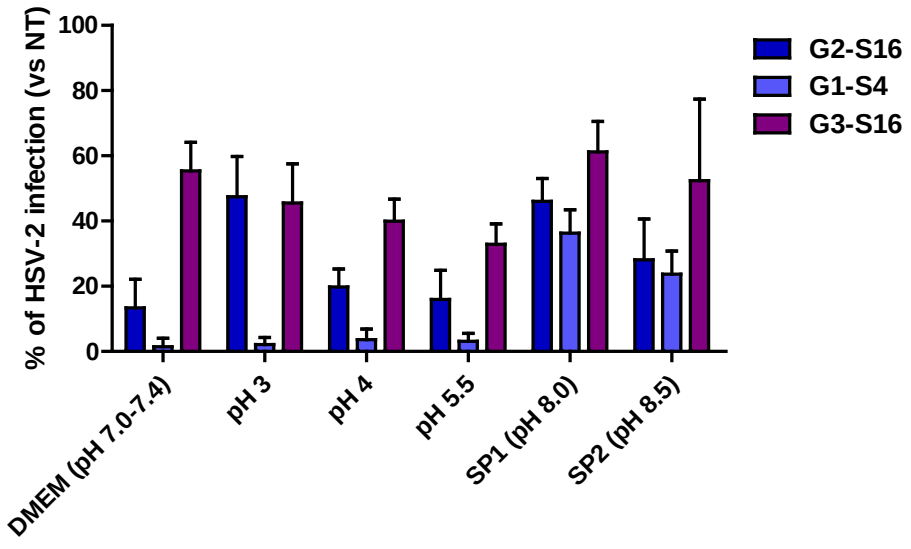

Figure 27. Effect of pH in dendrimer anti-HSV-2 activity. Tested dendrimers were incubated in different pH solutions of PBS (pH 3, 4, 5.5, and 7) for 1 h. Afterward, Vero cells were pretreated for 1 h with compounds and then infected with 150 FPU/well of HSV-2 333 strain for 2 h. Viral infection, measured as number of viral plaques, was determined at 48 h post-infection. Data were represented as mean ± standard deviation of three independent experiments (*p< 0.05 vs control).

As showed in **Fig. 27**, dendrimers mostly retained their activity against HSV-2 333 strain after incubation at pH in the range from 3 to 7 for 1 h. The three dendrimers retained their activity against HSV-2 333 after incubation at pH from 3 to 7 for 1 h. However, a non-significant drop in G2-S16 antiviral activity was found when this dendrimer was preincubated at pH 3.0. Furthermore, in all cases, a trend towards a reduction in the HSV-2 333 inhibitory ability of dendrimers was found when they were incubated with seminal plasma. This reduction was almost significant ($p = 0.07$) in case of G1-S4 dendrimer. Even so, this compound retained a great antiviral activity when incubated with seminal plasma, reducing the HSV-2 infection by around 70%.

9.4. Time of addition assays suggest an antiviral role of dendrimers at early stages of HSV-2 infection

To determine the stage of the HSV-2 333 strain lifecycle where G2-S16, G1-S4, or G3-S16 dendrimer act, a time-of-addition assay was performed (**Fig. 28A**). ACV was used as control. Very strong inhibition of HSV-2 333 infection was only found when G2-S16, G1-S4, or G3-S16 was added as a pre-treatment or 1 h post-infection (pi). It is important to note that the dendrimers G1-S4 and G3-S16 lost their inhibitory action when added at 1 h or 1 h pi. However, in case of G2-S16, approximately 50% of anti-HSV-2 activity was retained when added at 8 h pi. In conclusion, the role of these dendrimers is in the very first steps of the HSV-2 lifecycle, except for G2-S16 that, in addition, presents other secondary targeting levels.

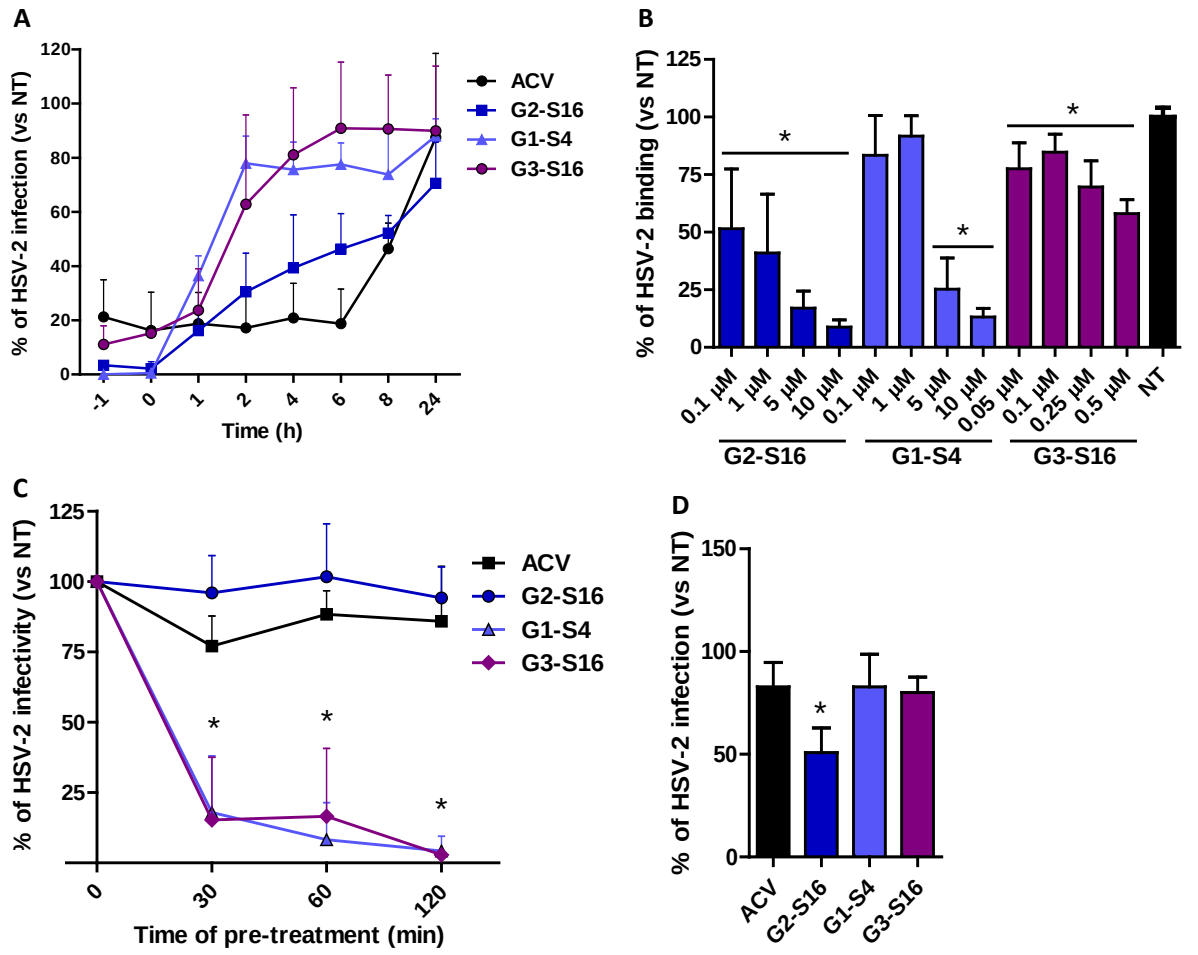

Figure 28. Mode of action of polyanionic carbosilane dendrimers against HSV-2 infection. (A) Time of addition assay. To stablish the stage of viral cycle where dendrimers are working, Vero cells were infected with HSV-2 333 and tested compounds were added at different times pre- and post-infection (-1, 0, 1, 2, 4, 6, 8 and 24 h). Percentage of infection (measured as the number of viral plaques) was determined after 48 h. **(B)** Effect of anionic carbosilane dendrimers on HSV-2 333 binding. Vero cells were pre-chilled at 4 ºC for 20 min and then treated with the dendrimers for 1 h before infection with HSV-2 333 for 2 h at 4 ºC. **(C)** HSV-2 333 inactivation by carbosilane dendrimers. To test the ability of dendrimers to bind to the viral surface, 10^4 PFU of HSV-2 333 were incubated with the dendrimers at their maximum non-toxic concentration for 1 h. Vero cells were then infected with 150 FPU/well of dendrimer-treated HSV-2. Viral infectivity, measured as number of viral plaques, was determined at 48 h post-infection. **(D)** Binding of dendrimers to cellular surface proteins. Vero cells were pretreated with dendrimers for 1 h. After incubation, cells were extensively washed to eliminate unbound dendrimer and then infected with HSV-2 333. After 48 h, cells were stained and viral plaques were counted. Data are represented as mean ± SD of three independent experiments. (*p< 0.05 vs control).

9.5. Polyanionic carbosilane dendrimers disrupt HSV-2 binding to the cell host: attachment assays

The antiviral activity of polyanionic dendrimers is associated with the establishment of electrostatic interactions between the viral envelope proteins and the anionic functional peripheral groups of

dendrimers (Chonco et al., 2012, Sepulveda-Crespo et al., 2015a, Vacas Cordoba et al., 2013, Vacas-Cordoba et al., 2014). The effect of polyanionic dendrimers in HSV-2 333 strain binding was studied (**Fig. 28B)**. The attachment of HSV-2 333 to Vero cells was inhibited in a dose–response effect by the three dendrimers (**Fig. 28B**). G2-S16, G1-S4, and G3-S16 achieved 91%, 87%, and 42% of reduction of HSV-2 333 binding in Vero cells, respectively, in comparison with HSV-2-infected non-treated Vero cells **(Fig. 28B)**.

9.6. G1-S4 and G3-S16 inactivate HSV-2

We studied how dendrimers performed their antiviral activity using a virus inactivation assay **(Fig. 28C**). G1-S4 and G3-S16 inhibited HSV-2 333 strain infection in Vero cells approximately 85% after 30 min of coincubation with HSV-2 333, and viral inactivation was completed after 2 h of co-incubation. These results suggest that G1-S4 and G3-S16 bind directly on viral proteins at the surface of HSV-2 333 and block and inactivate HSV-2 333, and G2-S16 is ineffective in reducing HSV-2 333 infectivity **(Fig. 28C).**

9.7. G2-S16 provide cell protection against HSV-2

One assay was performed to evaluate the binding ability of G2-S16, G1-S4, or G3-S16 onto cellular surface proteins. Therefore, block the HSV-2 333 strain attachment and entry (**Fig. 28D**). After incubation of G2-S16, G1-S4, or G3-S16 with Vero cells, only the G2-S16 reduced 50% the HSV-2 333 infection. G2-S16, unlike G1-S4 and G3-S16, was performing its inhibitory effect by binding to molecules on the surface of host cell.

9.8. Molecular modeling of dendrimers with HSV-2 surface protein gB

We focused on G2-S16 and G1-S4 for molecular modeling studies due to the fact that they achieved the maximum reduction of HSV-2 333 strain binding in Vero cells. The fusion protein gB is one of the most conserved in HSV-2 333 surface which together with help of fusion regulator gH-gL and receptor binding gD mediates HSV-2/cell fusion. We used computer simulations to study if G1-S4 and G2-S16 bind the gB from HSV-2 333 and which are the differences in binding modes of both dendrimers (Maurer et al., 2013) (**Fig. 29A** and **29B**).

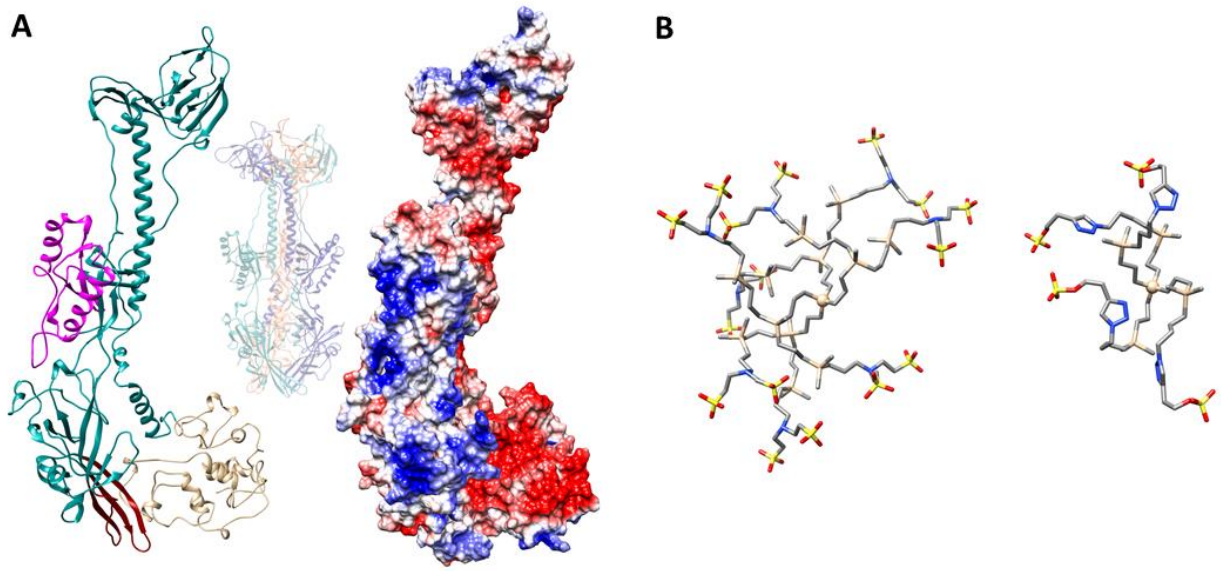

Figure 29. A) Left: **Equilibrated structure of the gB protein from HSV-2 333 strain** (residues 98-904). Right: **the same (including the view/orientation)** just with visualized electrostatic potential on the molecular surface (blue color denotes high values of positively charged domains with potential +3 kT/e and higher and low values of el. potential -3 kT/e and lower in rather anionic areas are in red). Middle - original gB trimer from HSV-1 (PDB: 4BOM) **B) Representative conformations of the computer models of dendrimers G2-S16 (left), G1-S4 (right),** simulated in salt water. Hydrogen atoms are omitted for the better clarity. The color coding is: C – grey, O – red, Si – beige, S – yellow, N – blue.

The simulation test of dendrimer/gB complexation at 6 binding sites on gB surface, which can have some inhibition effect, showed the creation of the stable complexes in all cases (**Fig. 30** and **Fig. 31**). The binding energies dG and their components are summarised in **Table 7**. Domains A and B are the binding areas for the interaction with heterodimer gH-gL (**Fig. 31A** and **31B)** (Basha et al., 2013), it is a rather cationic area suitable for binding of anionic molecules as it is the very favourable binding energies for both dendrimers showed (**Table 7**). Although the binding energies of both dendrimers are comparable, the G1-S4 binding affinity is clearly better than the G2-S16. Case C represents the binding area to the putative fusion loops or their proximity. Against, both dendrimers bound although binding energies were smaller than in cases A and B, G1-S4 was slightly better than G2-S16. However, G2-S16 interacted directly with fusion loops while G1-S4 interacted partly with fusion loop and partly with simulated C-terminal (**Fig. 31C**). Above Case C there is allocated the simulation case D **(Fig. 31D)**. For G2-S16 it was the worst result among all tested binding positions.

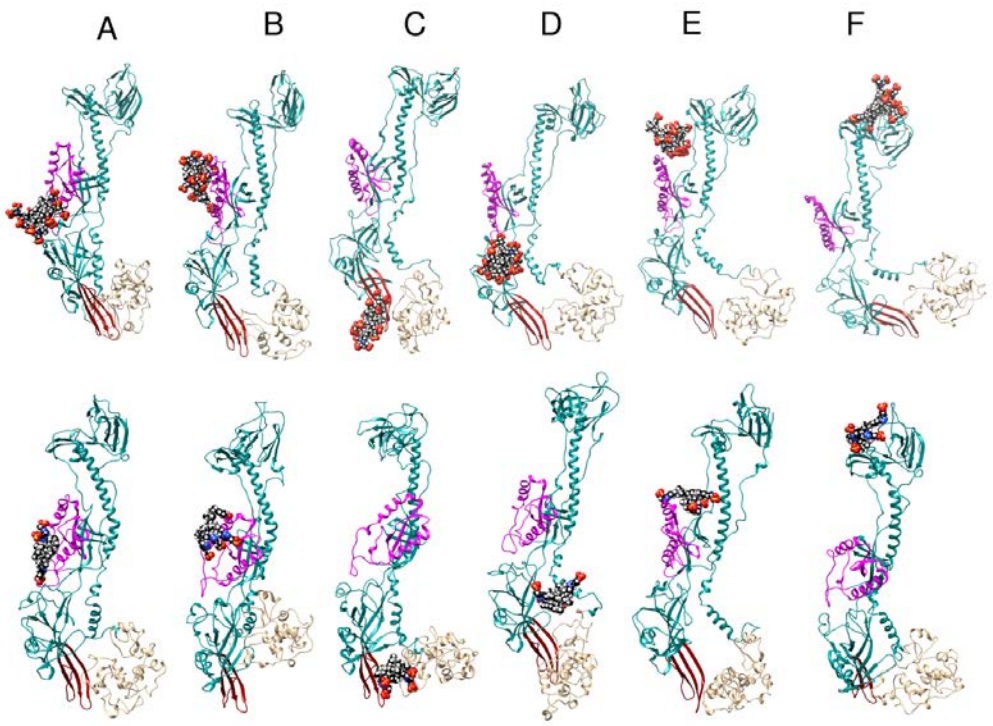

Figure 30. Final G2-S16/gB (top) and G1-S4/gB (bottom) complexes obtained from the initial configurations (A, B, C, D, E, and F). The main part of the supposed binding interface for the gH-gL is highlighted in magenta. The putative fusion loops are in red and the C-terminal part comprising residues 722-904 is in tan. This terminal part of the gB was not included in our template structure (4BOM). Thus, we simulated it from the primary amino acid sequence just to "naturally" close this uncomplete part. In reality is the most of this gB part anchored in viral membrane where it has also different tertial structure. Atoms of dendrimer are colored as follows: C–black, O–red, Si–gray, S– yellow, N–blue, H–white.

Table 7. MM-PBSA estimates of free energies of binding (dG) together with all important energetic components and numbers of dendrimer/protein H-bonds detected in final configurations.

	dH	TdS	dG	VDW	EEL	EPB	ENP	H-bonds
G2-S16 (A)	-106.78	-46.70	**-60.08**	-59.03	-526.49	516.57	-37.83	21
	(26.15)	(9.30)	(27.76)	(14.15)	(130.25)	(129.77)	(7.82)	
G2-S16 (B)	-109.21	-50.57	**-58.64**	-71.34	-343.05	345.61	-40.43	11
	(19.36)	(11.17)	(22.35)	(7.13)	(70.77)	(69.53)	(2.02)	
G2-S16 (C)	-101.43	-47.45	**-53.97**	-62.41	117.49	-119.16	-37.34	7
	(20.43)	(8.99)	(22.32)	(6.91)	(137.20)	(137.33)	(3.62)	
G2-S16 (D)	-70.98	-50.09	**-20.89**	-41.51	-341.54	340.26	-28.19	15
	(17.53)	(7.08)	(18.90)	(7.58)	(66.61)	(68.62)	(3.99)	
G2-S16 (E)	-66.65	-42.12	**-24.54**	-36.58	297.45	-299.85	-27.67	11
	(22.11)	(10.18)	(24.34)	(5.73)	(92.03)	(95.06)	(2.42)	
G2-S16 (F)	-151.57	-60.13	**-91.44**	-89.16	-413.22	402.39	-51.58	19
	(21.33)	(12.62)	(24.79)	(7.83)	(67.98)	(69.24)	(2.11)	
G2-S16	-140.61	-64.97	**-75.65**	-74.32	-3682.17	3663.67	-47.80	22
(N-term)	(10.98)	(5.60)	(12.33)	(5.77)	(170.52)	(169.95)	(2.65)	
G1-S4 (A)	-120.80	-45.54	**-75.26**	-74.92	-269.87	265.27	-41.28	7
	(8.49)	(4.34)	(9.54)	(6.55)	(44.99)	(44.09)	(2.19)	
G1-S4 (B)	-113.17	-43.17	**-70.01**	-73.51	-188.86	186.81	-37.61	6
	(12.74)	(11.74)	(17.32)	(9.51)	(40.40)	(39.35)	(2.97)	
G1-S4 (C)	-100.13	-41.24	**-58.88**	-63.51	-197.97	196.96	-35.61	5
	(12.99)	(5.45)	(14.08)	(9.33)	(63.33)	(62.63)	(3.58)	
G1-S4 (D)	-88.92	-34.52	**-54.40**	-55.02	-246.20	242.40	-30.10	6
	(8.28)	(9.66)	(12.73)	(6.01)	(46.48)	(45.52)	(2.76)	
G1-S4 (E)	-104.28	-45.43	**-58.85**	-65.73	20.09	-21.39	-37.25	6
	(10.37)	(7.08)	(12.56)	(7.48)	(30.60)	(30.10)	(3.23)	
G1-S4 (F)	-126.48	-44.02	**-82.46**	-81.21	-190.90	188.06	-42.43	5
	(8.64)	(4.16)	(9.59)	(5.78)	(35.65)	(36.18)	(1.71)	
G1-S4	-99.86	-38.60	**-61.27**	-58.89	-1321.18	1311.29	-31.09	9
(N-term)	(8.50)	(2.08)	**(**12.33**)**	(5.21)	(54.82)	(54.22)	(1.58)	

The units are [kcal/mol]. VDW is van der Waals contribution to binding enthalpy; EEL is electrostatic contribution in vacuum (i.e. without considering solvent); ENP is an estimate for non-polar contribution; EPB is the energetic contribution which arises from electrostatic solvent–solute interaction (desolvation penalty); dH is total enthalpic contribution to free binding energy; dS is solute entropy change due to binding and T is absolute temperature. dH=VDWAALS+EEL+EPB+ENPOLAR, dG=dH-TdS. Values of dH and TdS were not calculated from the identical MD frames so the standard deviation for dG obtained from the population of dH-TdS values are not available. Instead the square root of the sum of squares of the standard deviations for dH and TdS is provided as the upper bound estimate for dG deviation.

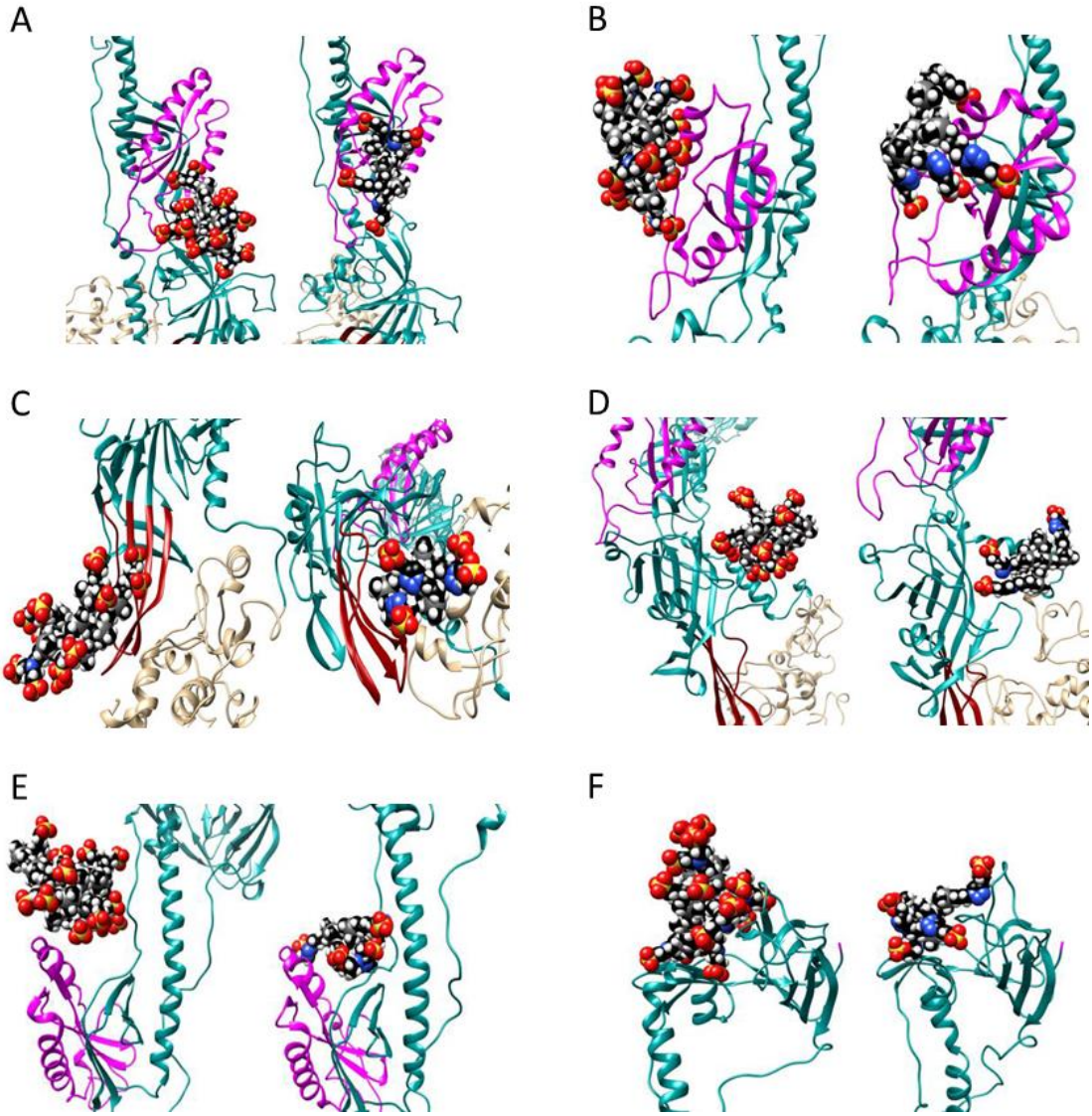

Figure 31. Detail view of the final G2-S16/gB (left) and G1-S4/gB (right) systems. (A) case A (interaction at gH-gL binding area). **(B)** Case B (interaction at gH-gL bindingarea). **(C)** Case C (interaction with putative fusion loops). **(D)** Case D (cationic area above the fusion loops). **(E)** Case E (interaction at "pocket" near the top edge of the gH-gL binding site). **(F)** Case F (the top part of the gB protein or N-terminal area). Atoms of dendrimer are colored as follows: C – black, O – red, Si – gray, S – yellow, N – blue, H – white.

Dendrimer bound in position D may have the best possibility to disturb suggested transition of the gB trimeric state from the more open pre-fusion to the final closed post-fusion (Basha et al., 2013). Both dendrimers partly interact with C-terminal of the given gB which could not be possible in gB trimeric state (C-terminal of the given gB monomer is too far from its D position) but they can interact very similarly with C-terminal of the opposite gB monomer. Simulation case E is a rather anionic area with

"pocket" shape character composed of the top-inner edge of gH-gL binding interface (**Fig. 29A, 29B** and **31E**). The electrostatic interaction of dendrimers just with protein in vacuum conditions is unfavourable for both, but in water this is compensated by the energy contribution from the electrostatic interactions of solvated molecules with water. In spite of the unfavourable values of electrostatic potential in this area, stable complexes were obtained in both cases although in case of G2-S16 the estimated binding energy was its second worst. On the other hand, G1-S4 bind here with significantly higher affinity dG=-58.85 kcal/mol **(Table 7)**, mainly due to the significantly more favourable WDV component -65.73 kcal/mol comparing to -36.58 kcal/mol in case of G2-S16. This is due to the small and flexible G1-S4 with better accessible "uncharged" C-Si inner part and also with smaller anionic charge is better accommodate in that pocket site and do more "WDV contacts" with protein. G1-S4 has also more favourable ENP part, which means that complexation here better reduced the total (dendrimer+gB) solvent accessible molecular surface than in case of bigger dendrimer.

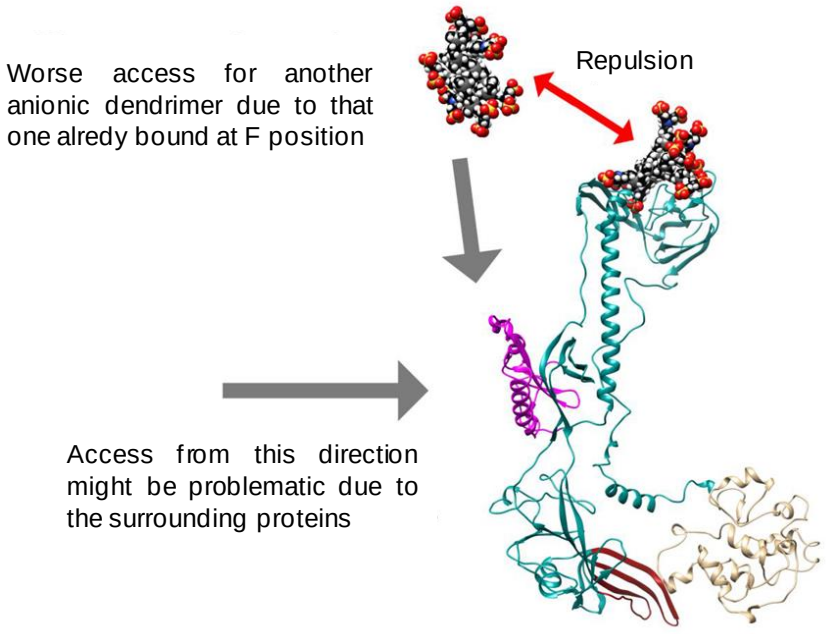

Figure 32. Illustration of disturbing role of already bound dendrimer at position F for access of the another dendrimer which would like to reach e.g. gH-gL binding domain. In case of already visualized dendrimer G2-S16 this "auto-blocking effect" will be stronger than in case of G1-S4 dendrimer.

Surprisingly, strong binding affinity was found in simulation case F where dendrimers interacted with the top part of the protein (**Fig. 31F**). Both dendrimers achieved their best results regarding binding energy. It was the only case where G2-S16 (dG= -91.44 kcal/mol) over-performed G1-S4 (dG= -82.46 kcal/mol) **(Fig. 32)**. Unfortunately, the N-terminal end of the gB structure is incomplete having the first

97 amino acid missing. As far as we know the experimental structure of this gB N-terminus part from HSV-2 333 strain is not in disposal so additionally we simulated N-terminus fragment comprising aa 1-100 to obtain its approximate tertiary structure to check if this part could be targeted with dendrimers or if position F is the only suitable dendrimer-binding site in N-terminus area. This small terminal part has quite cationic character (the total net charge+12) so it might partly “screen”/“mask” eventual anionic dendrimer bound in F position but also it can serve as attractive target for any anionic molecules so probably right here HSV-2 333 gB interacts also with anionic cell glycosaminoglycan like HS. This N-terminal part is indeed attractive also for the anionic dendrimers (**Fig. 33** and **Table 7)**. We notice that G2-S16 binds with higher affinity (dG= -75.65) to this target than G1-S4 (dG= -61.27) similarly as in position F.

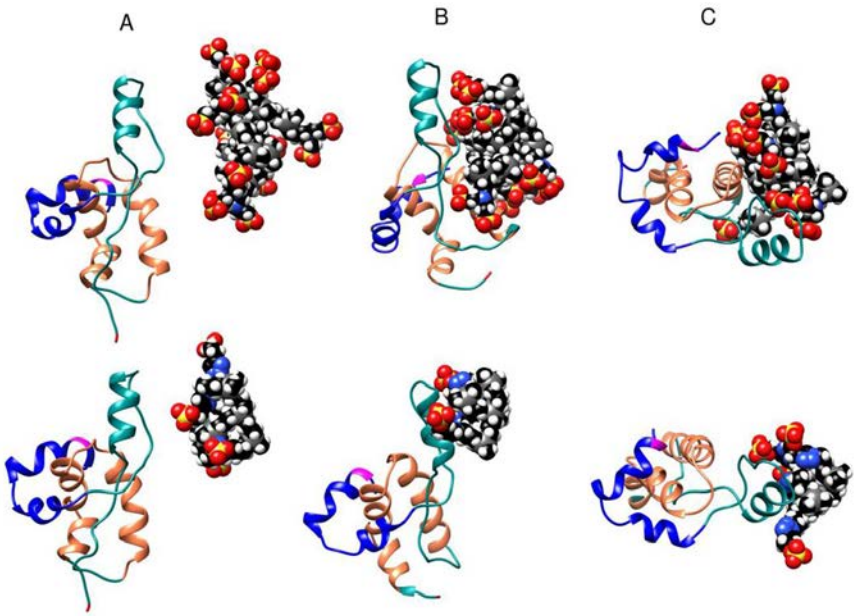

Figure 33. Simulated complexes N-terminal (residues 1-100) and dendrimers G2-S16 (top), G1-S4 (bottom). A - the initial state, B – final complex (side view), C – final complex (top view).

9.9. Increased efficiencies of polyanionic carbosilane dendrimers–antivirals combination analysis against HSV-2 infection

Since polyanionic carbosilane dendrimers seem to target different steps in viral life cycle in comparison with other antivirals such as ACV and TDF, the potential combinatorial profile of dendrimer and ACV or dendrimer and TDF was tested against HSV-2 333 strain. Interestingly, the nucleoside reverse-transcriptase inhibitor TDF is the only microbicide candidate, which shows high

efficacy to date. Neither the combinations nor the individual drug concentrations were toxic for Vero cells after 24 h of exposure. The combinations of G2-S16, G1-S4, and G3-S16 dendrimers with ACV or TDF resulted in a more efficient inhibitory profile against HSV-2 333 for most of the concentrations tested, measured as viral plaque formation (**Fig. 34**).

Table 8. Combination index (CI ± SD) and combinatorial profiles for different ARV (ACV and TDF) and G2-S16, G1-S4 and G3-S16 dendrimer combinations at equipotent ratio against HSV-2 333 strainin Vero cells.

Dendrimer	ARV	Combination Ratio	CI		
			EC_{50}	EC_{75}	EC_{90}
G2-S16	**ACV**	1:1	1.055 ± 0.122 (±)	0.705 ± 0.053 (++)	0.528 ± 0.041 (+++)
	TDF	1:1	1.305 ± 1.147 (-)	1.013 ± 0.702 (±)	0.843 ± 0.455 (++)
G1-S4	**ACV**	1:1	0.912 ± 0.103 (±)	0.616 ± 0.139 (+++)	0.442 ± 0.146 (+++)
	TDF	1:1	0.976 ± 0.244 (±)	0.826 ± 0.282 (++)	0.754 ± 0.315 (++)
G3-S16	**ACV**	1:10	0.852 ± 0.160 (+)	0.767 ± 0.231 (+)	0.911 ± 0.596 (±)
	TDF	1:20	1.108 ± 0.415 (-)	0.792 ± 0.369 (++)	0.597 ± 0.286 (+++)

Combination index (CI) calculated at the EC_{50}, EC_{75} and EC_{90} level. CI< 0.9 indicates synergism; 0.9< CI< 1.1 indicates additive effects and CI> 1.1 indicates antagonism (-). Synergy level: 0.85<CI< 0.9 + (slight synergism); 0.7< CI< 0.85 ++ (moderate synergism); 0.3<CI< 0.7 +++ (synergism); 0.1<CI< 0.3 ++++ (potent synergism); 0.1>CI +++++ (very strong synergism). Data are represented as mean ± SD of three independent experiments.

In addition, the CI were calculated to evaluate the type of dendrimer–ACV or dendrimer–TDF interactions (**Table 8**). CalcuSyn software (Biosoft, Cambridge, UK) based on the median effect principle was used. The CI values between 0.1 and 0.9 indicate a synergistic effect, whereas values between 0.9 and 1.1 represent an additive effect and those >1.1 represents antagonism. Synergistic profiles (CI values between 0.442 and 0.705) were found at the calculated EC_{75} and EC_{90} for G2-S16 and G1-S4 when combined with ACV against HSV-2 333 strain. G3-S16/ACV combination at 1:10 ratio showed slight and moderate synergism at the EC_{50} and EC_{75}, respectively, although only an additive effect was found at high concentrations (EC_{90}). All dendrimers showed a synergistic profile with TDF at EC_{90}. However, non-positive interactions or only an additive profile for G1-S4 dendrimer were found at the calculated EC_{50}. These results support that the combinations of nanoplatforms like dendrimers and other inhibitory drugs targeting different stages in virus life cycle are essential to develop more powerful and effective microbicides and to improve the existing ones.

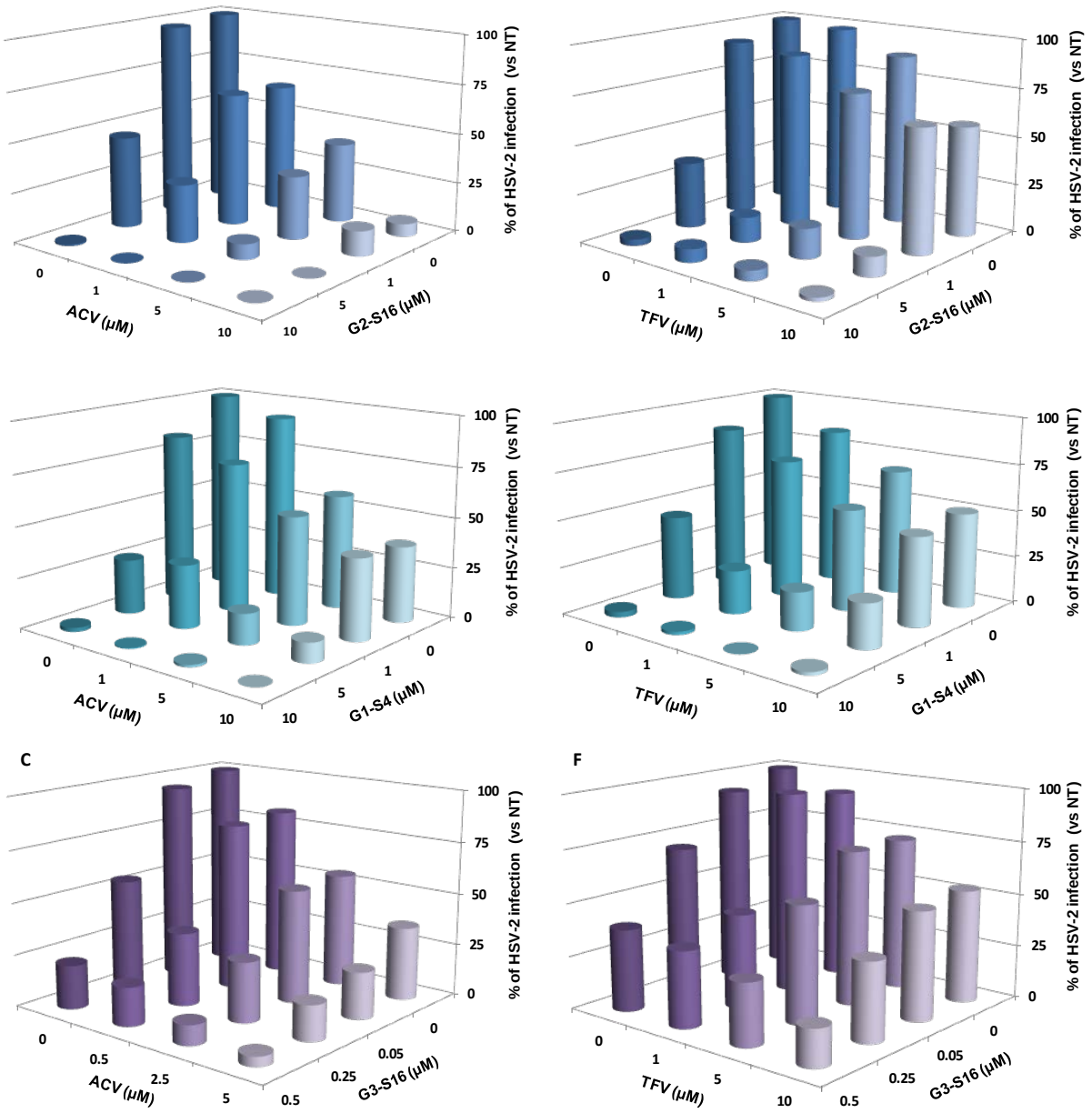

Figure 34. Activity profile of G2-S16 **(A-D),** G1-S4 **(B-E)** and G3-S16 **(C-F)** alone or combined with ACV **(A,B,C)** or TDF **(C,D,E)** against HSV-2 333 infection (% of infection was calculated as % of viral plaques vs non-treated cells) in Vero cell line. Vero cells were treated with different combinations of carbosilane dendrimers and ARV compounds 1 h before HSV-2 infection. Each experiment was performed by triplicate. Data are represented as mean of three independent experiments.

9.10. *In vivo* vaginal HSV-2 challenge assay

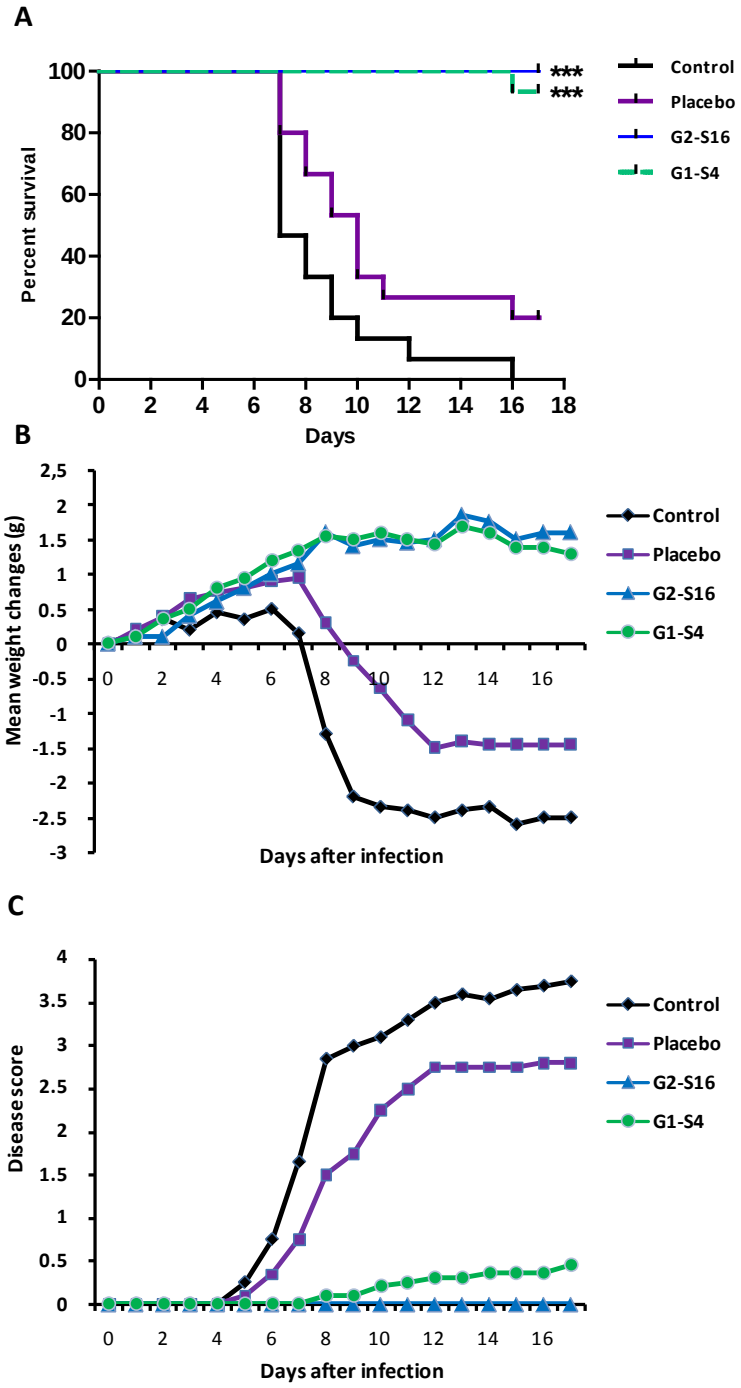

Figure 35. Polyanionic carbosilane dendrimers prevent vaginal high-dose HSV-2 infection. Medroxyprogesterone acetate treated BALB/c mice were vaginally challenged with 10^5 PFU HSV-2 1 h after applying the indicated gel (10 mice/group). Mice were examined daily for body weight and genital pathology over 17 days. **(A)** Percentages of infection over time are shown for each treatment group. Dendrimer based gels containing 3% dendrimer were significantly more protective than vehicle alone (***: p<0.001 vs Placebo) **(B)** Body weight changes were expressed as the mean values of ten animals in the same group. Each mean value was calculated by subtracting the weight at day 0 from the weight at day N after infection. **(C)** Clinical pathology

was scored as described in the text for 17 days. Lesion scores were expressed as the mean values of 10 mice in the same group.

This study was carried out to demonstrate the *in vivo* efficacy of topical G2-S16 and G1-S4 to prevent vaginal HSV-2 333 transmission. G2-S16 and G1-S4 proved capable to halt the infection in 100% and 90% of female mice, respectively, upon exposure to a lethal dose of HSV-2 333, showing significant differences compared with control and placebo groups (G2-S16, p = 0.0003 vs placebo) (G1-S4, p = 0.001 vs placebo) (**Fig. 35A**). The weight of female mice in control and placebo groups decreased steadily from day 6 pi. BALB/c groups treated with G2-S16 or G1-S4 body weight maintained its normal growth ratio (**Fig. 35B**). No female mice treated with G2-S16 showed signs of HSV-2 333 infection and only one female mouse treated with G1-S4 showed signs of HSV-2 infection. Accordingly, untreated BALB/c female mice and those just treated with placebo started showing the first signs of redness and inflammation on day 3 pi, increasing the symptomatology until the moment of sacrifice between days 8 and 16 pi. (**Fig. 35C**).

9.11. *In vivo* rectal HSV-2 challenge assay

This work was performed to show the *in vivo* efficacy of topical G2-S16 and G1-S4 to prevent rectal HSV-2 transmission. The experiments were conducted in the rectum of male and female BALB/c mice separately, using 15 BALB/c mice for each sex. Five females and 10 males were pretreated only with PBS, five females and 10 males were pre-treated with PBS 3% G2-S16, and five females and 10 males were pre-treated with PBS 3% G1-S4 rectally. As expected, when we compare the antiherpetic activity obtained in both sexes, no significant differences were found. Thus, we put together the rectal results of both experiments, with 45 BALB/c mice (15 control received topical PBS, 15 PBS with 3% G2-S16, and 15 PBS with 3% G1-S4) that were exposed to HSV-2 333 strain. Four out of 15 mice of the PBS control group were not HSV-2 333 infected. However, 7 out of 15 of G2-S16-treated group and 14 out of 15 of G1-S4-treated group were protected. G2-S16 was unable to stop the rectal infection in a significant way, but G1-S4 reached inhibition rectal values over 90%, showing significant differences (P< 0.0001 vs control) (**Fig. 36A**).

The antiherpetic activity of G1-S4 and G2-S16 was smaller in the case of rectal HSV-2 333 exposure than for vaginal exposure, leading to a faster appearance of the symptoms and death of the animals. Despite this, we observed a significant decrease in body weight in the control group and the G2-S16 treated group, while mice rectal pretreated with G1-S4 maintained their normal body growth ratio (**Fig.**

36B). Only one mouse pretreated with G1-S4 rectally showed signs of HSV-2 333 infection. Untreated BALB/c mice started showing first signs of redness and inflammation on day 5 pi, increasing the symptomatology until the moment of sacrifice between days 6 and 18 pi. (**Fig. 36C**).

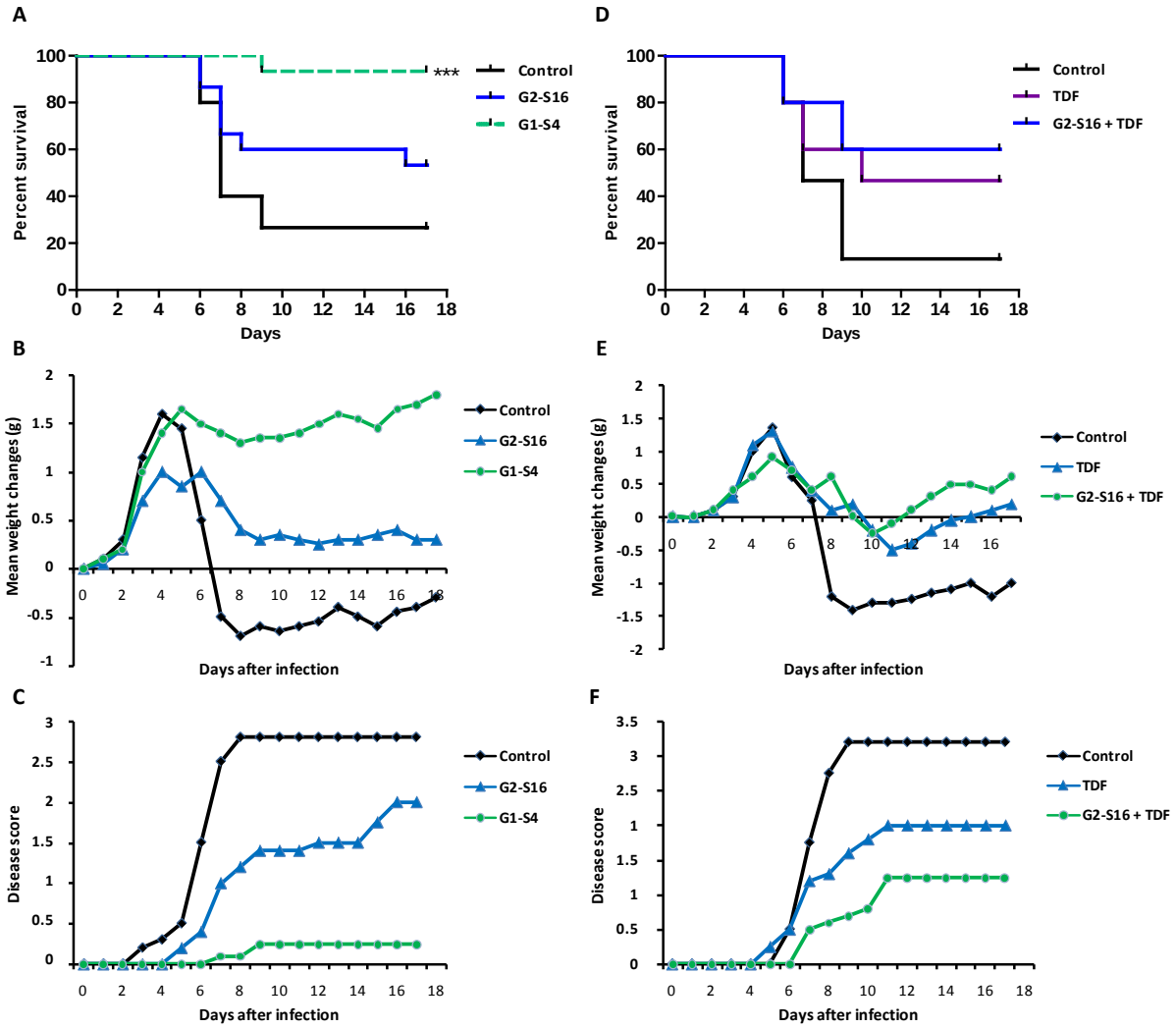

Figure 36. Polyanionic carbosilane dendrimers prevent rectal high-dose HSV-2 infection. BALB/c mice were rectally challenged with 10^5 PFU HSV-2 30 min after applying the indicated gel (15 mice/group).Mice were examined daily for body weight and genital pathology over 18 days. **(A and D)** The percentages of infection over time, based on symptoms, are shown for each treatment group. G1-S4 was significantly protective (**: p< 0.005 vs Control). **(B and E)** Body weight changes were expressed as the mean values of 10 mice in the same group. Each mean value was calculated by subtracting the weight at day 0 from the weight at day N after infection. **(C and F)** Clinical pathology was scored as described in the text for 18 days. Lesion scores were expressed as the mean values of 10 mice in the same group.

In order to confirm antiherpetic activity of G1-S4, we performed the viral challenge using 10^6 PFU of HSV-2 333 strain per mouse. At such a high viral challenge, we demonstrated that G1-S4 halted the inhibition of HSV-2 333 rectal infection in BALB/c mice by 70% (p<0.01 vs control) (**Fig. 37**).

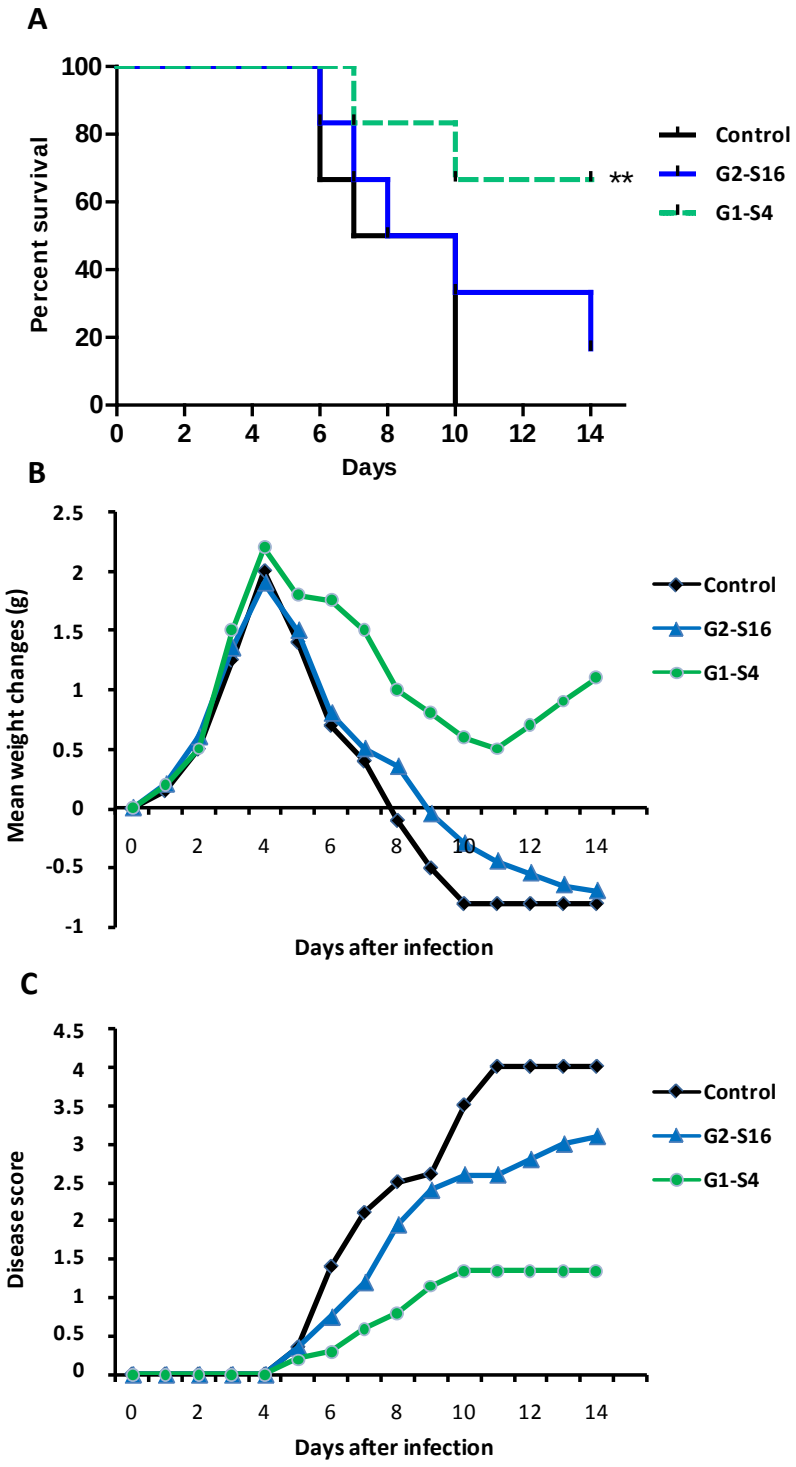

Figure 37. Polyanionic carbosilane dendrimers prevents rectal 1 log higher dose HSV-2 infection in BALB/c. BALB/c mice were rectally challenged with 10^6 PFU HSV-2 333 strain 30 min after applying the indicated gel (6 animals per group). Mice were examined daily for body weight and genital pathology over 18 days. **(A)** The percentages of infection over time, based on symptoms, are shown for each treatment group. G1-S4 was significantly protective (*: *p* vs Control) **(B)** Body weight changes were expressed as the mean values of ten animals in the same group. Each mean value was calculated by subtracting the weight at day 0 from the weight at day N after infection. **(C)** Clinical pathology was scored as described in the text for 18 days. Lesion scores were expressed as the mean values of five animals in the same group.

To improve the protection values obtained with G2-S16 against rectal HSV-2 333 strain infection and due to the good results obtained with this dendrimer in combination with TDF, we performed another rectal challenge assay to evaluate a combination of 3% G2-S16 and 1% TDF, demonstrating that this combination was able to increase the protection levels over 65% (**Fig. 36D-F**).

10. Platycodin D related assays

As previously noted, a report published in 2016 by UNAIDS estimates that there were approximately 36.9 million people living with HIV-1 in the world, of whom only 15.8 million in June 2016 were under ARV therapy. Within the HIV-infected population group, women account for more than 50% of the total, reaching in some countries, such as South Africa,values of 60% (Carter et al., 2013). According to the epidemiological distribution of the infection, it is not difficult to see that more than 80% of people infected with HIV-1 live in underdeveloped or developing countries, where access to prevention methods and ARV drugs are very limited. This fact, together with the lack of a preventive vaccine that could eradicate the disease, has generated a great interest for the development of agents for topical use with a microbicidal action. Due to this need and taking into account that globally there are more than 200 million pregnancies each year, of which approximately 40% are unintended (**Fig. 38**) (Sedgh et al., 2014), the development of a nanocompound with dual microbicidal activity and spermicide, which could prevent both HIV-1 transmission and unintended pregnancies, emerges as a promising alternative (Sedgh et al., 2014).

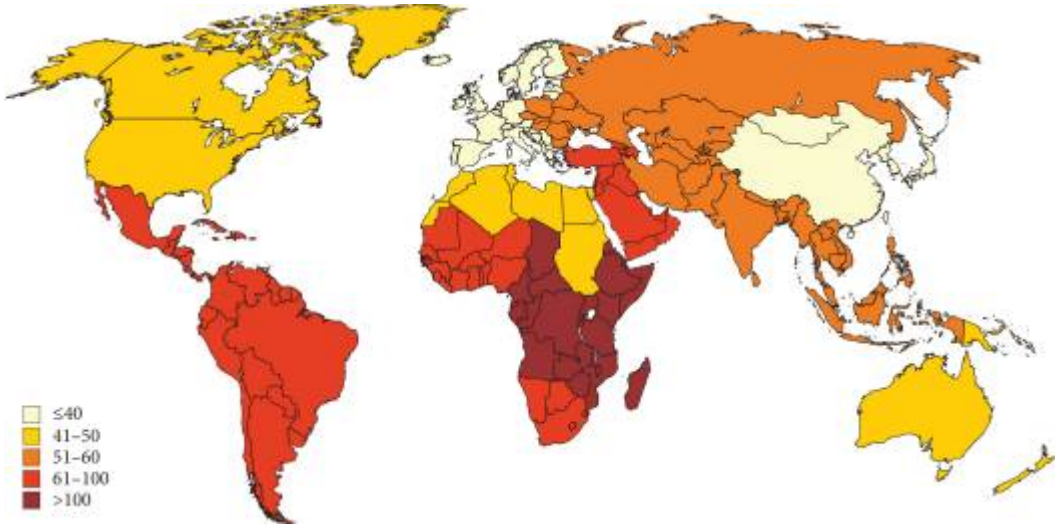

Figure. 38. Unintended pregnancies per 1,000 women aged 15–44, by subregion, 2012. Modified from (Sedgh et al., 2014).

The ultimate objective in the development of a microbicidal agent would be to achieve a compound or combination of compounds that not only reduced the number of new STIs but also had a contraceptive activity, which would be an additional advantage for those women who also wanted to avoid conception. Contraceptive pills are formulated to have a combination of estrogens and progesterone, which induces imbalance in the hypothalamic-pituitary-ovarian axis, which ultimately leads to a failure in ovulation. This type of oral contraceptive is not free of important risks and side effects such as thromboembolism, hypertension, hyperlipidemia, cardiovascular diseases or cancer of the breast and cervix (Tanphaichitr et al., 2016). In addition, continued exposure over a long period of time to these hormones has shown certain disorganization in the vaginal mucosa, which could increase susceptibility to HIV-1 infection, since vaginal mucosa is the first defense barrier against pathogens, and that HIV-1 present in the semen of an infected male could infect the woman after a sexual encounter (Haase, 2011). In this sense, a spermicide gel carries much less risk for the woman, because it is based on impeding the sperm training process. Spermicides are considered low-cost drugs, widely available and easy to acquire and administer. A compound is considered as spermicide if it has the ability to inhibit sperm motility present in the seminal fluid in 20 s (Tanphaichitr et al., 2016), although the drug is indeed considered effective whenever it acts before 120 s. The fertilization potential of a spermatozoon is based on a number of parameters such as mobility, morphology, concentration or total number of cells in the ejaculate, among others. However, sperm will only be able to fertilize an egg once it has passed through the afore mentioned process of sperm training, a series of physiological and biochemical changes that allow the sperm to attach to the egg membrane at the level of the glycoproteins present in the pellucid area and penetrate into the cytoplasm of the cell, and occurs physiologically in the reproductive tract of the woman at the level of the fallopian tubes. The effectiveness of spermatozoa to pass through the first barrier involving the cervical mucus, endocervix and cervix depends on their status as progressive mobile spermatozoa, ie their ability to advance at an average velocity greater than 25 μm/s (Vasan, 2011). The process of sperm training encompasses a series of phenomena such as the acquisition of sperm hypermotility and the loss of its disabling factor, after which the acrosomal reaction begins, which ends at the moment of contact between the inner membranes of the spermatozoid. Acrosome and oocyte plasma membrane, at which time fertilization occurs (Suarez and Pacey, 2006, Okabe, 2013). Based on this, it is logical to interest in a

spermicide administered vaginally to prevent this process of sperm training, either by acting on sperm motility in situ, acrosome reaction or by repressing the union with the pellucid zone of the ovum.

10.1. Assessment of the biosafety of polyanionic carbosilane dendrimers in combination with Platicodyn D

A cellular toxicity assay was performed to evaluate the biocompatibility of G1-S4, G2-S16, PD and their combinations in the TZM.bl cell line (**Fig. 39**). Concentrations at which compounds exceeded 80% cell viability, compared to untreated controls, were established as non-toxic concentrations. As previously demonstrated, G1-S4 and G2-S16 were non-toxic at the concentration of 10 µM. For PD the toxicity limit was set at 15 µM (**Fig. 39A**). As for the combinations of G1-S4 and G2-S16 dendrimers with PD, it was observed that G1-S4 was non-toxic in combination with PD at 15 µM, and G2-S16 was non-toxic in combination with PD at 10µM (**Fig. 39B**).

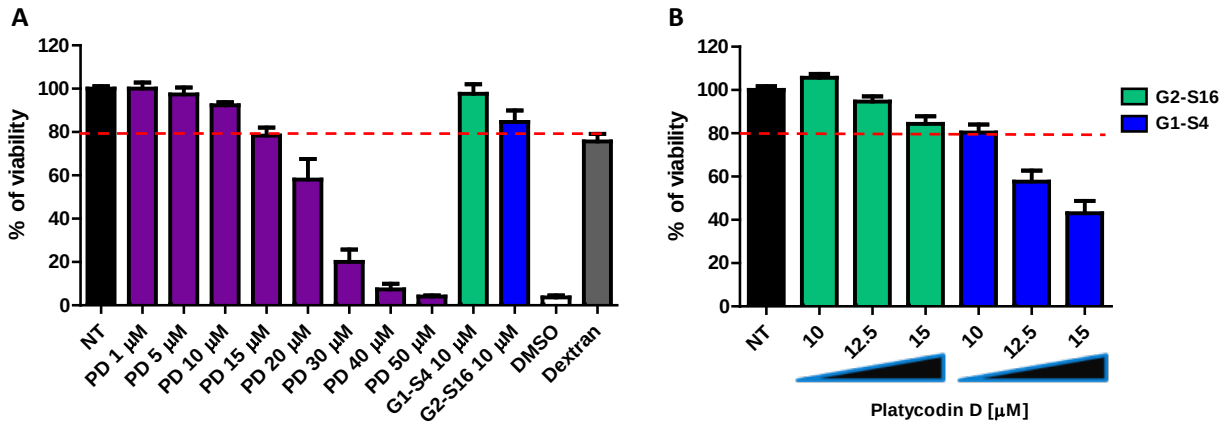

Figure 39. Biocompatibility of G1-S4, G2-S16, PD and their combinations in the cell line TZM.bl. The viability of the TZM.bl epithelial cell line was evaluated by MTT assay 48 h post-exposure to the compounds. 80% of cell viability was established as a limit of toxicity. 20 µM Dextran and 10% DMSO were used as negative and positive cell death control, respectively. The data were represented as a mean ± standard deviation (DV) of 4 different experiments.

Probably the G1-S4 combination with PD at 15 µM was non-toxic because G1-S4 is first generation dendrimer unlike the second generation dendrimer, G2-S16, whose combination with PD was non-toxic up to 10 µM. These data are in agreement with the described in the scientific literature, where it is demonstrated that to a greater generation of the polyanionic dendrimers, there is a greater toxicity of the same ones (Cena-Diez et al., 2016b).

10.2. Evaluation of the combination of polyanionic carbosilane dendrimers and PD against HIV-1 infection

G1-S4 and G2-S16 dendrimers were selected for the high antiviral activity demonstrated in *in vitro* and *in vivo* assays against several HIV-1 and HSV-2 viral isolates (Cena-Diez et al., 2016b, Sepulveda-Crespo et al., 2015b). The nanocompounds tested significantly inhibited HIV-1 infection in TZM.bl cells (**Fig. 40A**).

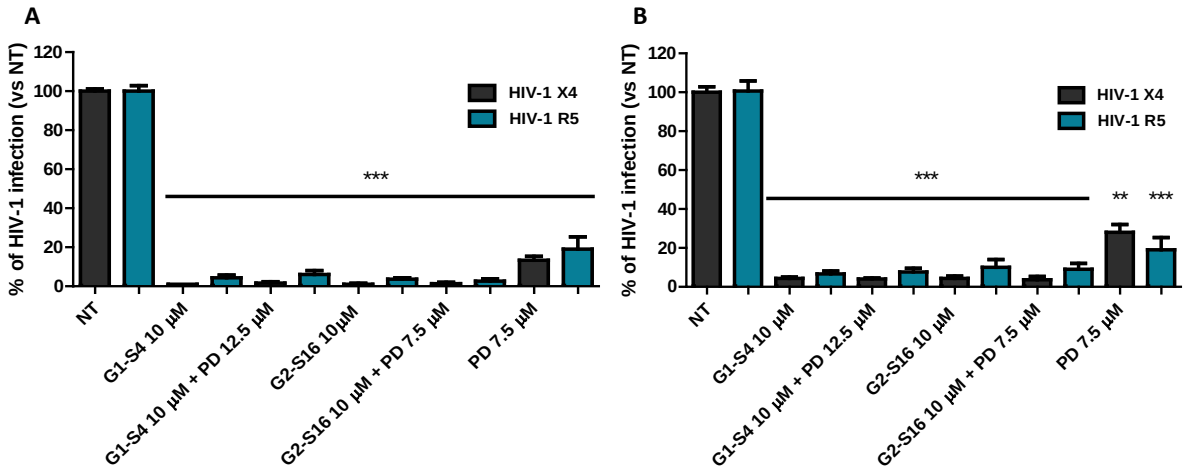

Figure 40. (A) Inhibition of HIV-1 infection in TZM.bl. The TZM.bl were pretreated for 1 h with non-toxic concentrations of the compounds and subsequently infected with HIV-1. The percentage of infection was determined after 48 h by quantification of luciferase expression levels. **(B) Inhibition of HIV-1 infection in PBMC.** The PBMC were pretreated for 1 h with non-toxic concentrations of the compounds and subsequently infected with HIV-1. After 72 h the supernatants collected from PBMC were presented on TZM.bl cells. The percentage of infection was determined after 48 h by quantification of luciferase expression levels. Data were plotted as a mean ± standard deviation of five different experiments.

When TZM.bl cells were pre-treated with the G1-S4 or G2-S16 dendrimers at 10 µM, inhibition percentages greater than 95% and 99%, respectively, were obtained versus both viral isolates. In addition, the combination of the dendrimers with PD did not modify the results obtained. It is noteworthy that PD has antiviral activity *per se*, reaching inhibition rates of 86% and 81% against R5-HIV-$1_{NL.AD8}$ and X4-HIV-$1_{NL.4.3}$ isolates, respectively. In PBMC, G1-S4, G2-S16 and PD also significantly inhibited HIV-1 infection (**Fig. 40B**). When the PBMC were pre-treated with G1-S4 or G2-S16 dendrimer at the concentration of 10 µM, the inhibitions against the X4-HIV-$1_{NL.4.3}$ isolate were greater than 98% in both cases. In contrast to the isolated HIV-$1_{NL.AD8}$ inhibition was greater than 93% with dendrimer G1-S4 and greater than 91% with dendrimer G2-S16. Again, the combination of the dendrimers with PD did not modify the results. On PBMC, PD also shows significant antiviral activity

per se over both viral isolates, reaching a percentage of inhibition greater than 85% with the isolate HIV-$1_{NL.AD8}$, and greater than 74% with the isolate X4-HIV-$1_{NL.4.3}$.

To evaluate the stage of the HIV-1 viral cycle where the PD acts, an " time of addition assay" was performed (**Fig. 41**). Only a percentage inhibition of HIV-1 infection is observed when PD is added up to 1 h post infection, which leads to the conclusion that PD would act in the early stages of the viral cycle.

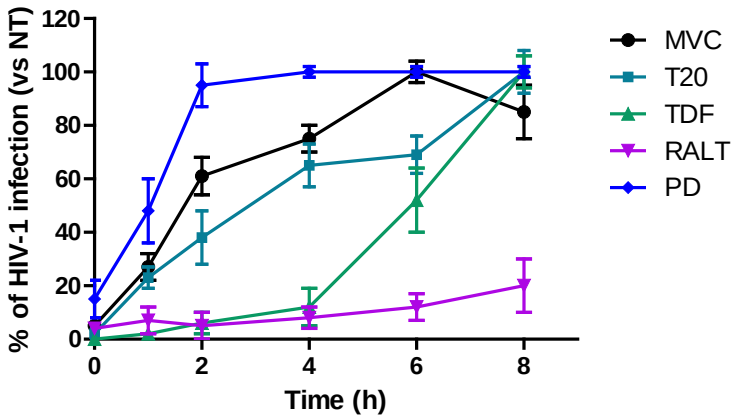

Figure 41. Time of addition assay. To determine the stage within the HIV-1 viral cycle where PD carries out its inhibitory capacity, TZM.bl cells were infected with HIV-1 and compounds were added at 0, 1, 2, 4, 6, and 8 h post-infection. MVC, T-20, TDF and RALT were used as controls of the HIV-1 infection. The percentage of viral infection was determined at 48 h by quantification of luciferase expression levels. Data were plotted as a mean ± standard deviation of three different experiments**.**

10.3. Evaluation of the effect of the combination polyanionic carbosilane dendrimers and PD in the induction of cellular proliferation in PBMC

The safety of the combination of the G1-S4 or G2-S16 dendrimers with PD was assessed by studying their ability to deregulate the proliferative activity of PBMC. The results suggest that G1-S4 and G2-S16 dendrimers do not induce cell proliferation in PBMC (**Fig. 42**). PBMC treated with 2 µg/mL PHA was used as positive control of proliferation. G2-S16 induces 81% cell proliferation compared to 100% proliferation in untreated PBMC, probably due to the toxicity range of G2-S16 when used at 10 µM. The combination of G1-S4 or G2-S16 with PD also does not significantly affect the proliferative capacity of PBMC. Only the combination of the 10 µM G1-S4 dendrimer with DP at 7.5 µM induced 127% cell proliferation compared to untreated PBMC. However, these values were not significant.

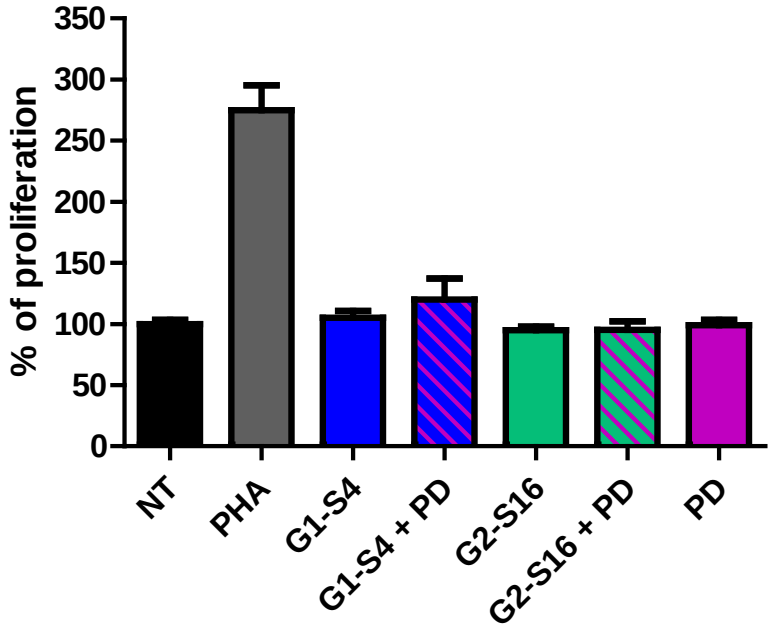

Figure 42. Cell proliferation assay in PBMC. The ability of G1-S4 or G2-S16 dendrimers to PD to induce cell proliferation in PBMC was evaluated. PBMC were treated with the compounds for 72 h. PHA 2 µg/mL was used as a positive proliferative control. The percentage of cell proliferation was determined using a Millipore® proliferation kit. Data were plotted as a mean ± standard deviation of three different experiments.

10.4. Evaluation of the spermicidal activity of the combination of the polyanionic carbosilane dendrimers and PD

To demonstrate whether PD maintains spermicidal activity in combination with G1-S4 or G2-S16 dendrimer, a sperm training experiment was performed on human spermatozoa (**Fig. 42**). Based on the training phenomenon and its ability to move, human spermatozoa can be differentiated into four different types: Type A or with rapid progressive motility (> 20 µm/s), type B or with slow progressive motility (5-20 µm/S), type C or non-progressive motility (0-5 µm/s) and type D or immotile (0 µm/s). The sperm cells type A + type B are referred to as progressive mobile spermatozoa and represent the spermatozoa that have been able to carry out the sperm training process (Vasan, 2011). Thus, a standard semen analysis that has the ability tofertilize should contain at least 50% of progressive mobile spermatozoa (Aitken et al., 1985).

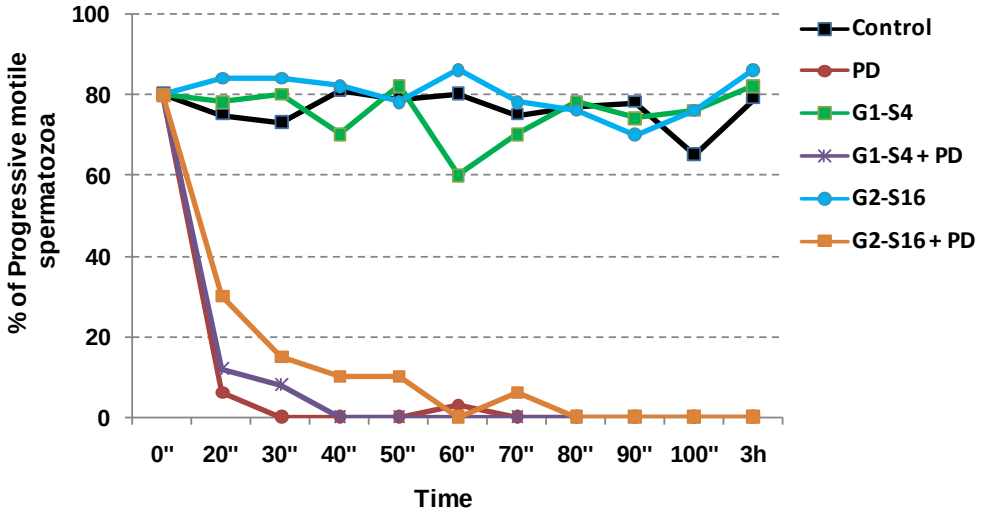

Figure 43. Sperm capacitation assay. Human sperm samples, after being processed and selected by density gradient, were treated with the dendrimer G1-S4 or G2-S16 in combination with PD. The mobile sperm count (REM) was evaluated to determine if the combination of the compounds tested affects sperm motility. The sperm motility index, which exceeds 70%, was considered optimal. Sperm from a single donor was used to perform the experiments. The data represented were obtained from a single experiment.

The results obtained show that in 20 s PD induces a significant decrease in sperm motility, reaching values close to 93% inhibition of sperm motility compared to untreated control spermatozoa. The values obtained for REM in the combination of dendrimer G1-S4 or G2-S16 with PD were also significant: the combination with PD and G1-S4 at 40 s totally reduced sperm motility. While the combination with PD and G2-S16 completely reduced sperm motility after 60 s. As already demonstrated, G1-S4 and G2-S16 dendrimers do not affect sperm motility individually (Cena-Diez et al., 2016a), because even after 100 s post-treatment the percentage of sperm motility did not fall from 70% with either of the two dendrimers. At 3 h post-treatment the results remained stable without significant variations. After 3 h PD inhibited all sperm motility, unlike dendrimers that did not affect sperm viability (**Fig. 43**).

10.5. BALB/c vaginal irritation assay in presence of PD

With the objective of knowing if the combination of the polianionic carbosilane dendrimers with PD was causing vaginal irritation to the mice, a vaginal irritation assay was performed in BALB/c mice for 7 days with daily application of the compounds. Eight female BALB/c mice of 7 weeks old with the weight of 20±3 g were purchased. G2-S16/PD or G1-S4/PD was added to 1% HEC placebo gel to a final concentration of 3% w/v of dendrimer and 0.25 mM of PD. BALB/c mice were randomized into 4 groups of 2 mice per group. Group A (control) was treated vaginally only with 30 µl of 1% HEC gel,

group B (irritation group) was treated vaginally with 4.5% N9 in PBS, group C was treated with 1% HEC gel with G2-S16/PD and group D was treated with 1% HEC gel with G1-S4/PD. The four conditions were applied intravaginally in female BALB/c mice previously anaesthetized with isoflurane. After 20 h, BALB/c mice were sacrificed and vaginas were extracted and conserved in 4% formaldehyde w/v. This histological study in BALB/c vaginal tissue showed that when mice were treated with G2-S16/PD or with G1-S4/PD combinations, after 7 days of exposureall mice had close to the same level of irritation and inflammation of their vaginal epithelium (total score = 4) as non-irritation control (**Table 9**).

Table 9. Vaginal toxicity assay of G2-16/PD or G1-S16/PD after a 7 consecutive daily applications doses.

	PBS		Control N9 (4.5%)		G2-S16/PD		G1-S4/PD	
Epithelial lesion	0	0	3	4	0	0	0	1
Inflammatory infiltrate	0	0	3	4	1	1	1	1
Vascular congestion	1	1	3	4	1	1	1	1
Edema/Fibrosis	0	0	2	2	2	2	2	1
TOTAL SCORE	**1**	**1**	**12**	**14**	**4**	**4**	**4**	**4**
Estrous cycle moment	**P**	**P**	**P-E**	**P-E**	**E**	**P**	**P**	**P**

The existence of an injury in the vaginal epithelium was evaluated in each biological sample. 0 (no change) when no injury or the observed changes were within normal range; 1 (minimum) when changes were sparse but exceeded those considered normal; 2 (light) when injuries were identifiable but with no severity; 3 (moderate) for significant injury that could increase in severity; 4 (very serious) for very serious injuries that occupy most of the analyzed tissue. These values were added up and determined the level of vaginal irritation as minimum 1-3, average 4-6, moderate 7-9 and severe >9+.

10.6. Evaluation of the combination of polyanionic carbosilane dendrimers and PD against HSV-2 *in vivo* vaginal challenge assay

To demonstrate whether G2-S16 and G1-S4 maintain anti-HSV-2 activity in combination with PD an *in vivo* vaginal challenge assay was performed. G2-S16 and G1-S4 were able to retain their antiherpetic activity in the presence of PD, being capable to halt the infection in 100% of the female mice (**Fig. 44**). When mice were exposed to a lethal dose of HSV-2, G2-S16/PD and G1-S4/PD combinations showed significant differences when compared to the control group (p< 0,001). In the control group, the weight of the mice decreased from the day 7 pi. while the disease score increased, the first signs of redness and inflammation appeared on day 5 pi., increasing the symptomatology until the moment of sacrifice between days 9 and 16 pi. No female mice treated with G2-S16/PD or G1-S4/PD showed signs of HSV-2 infection.

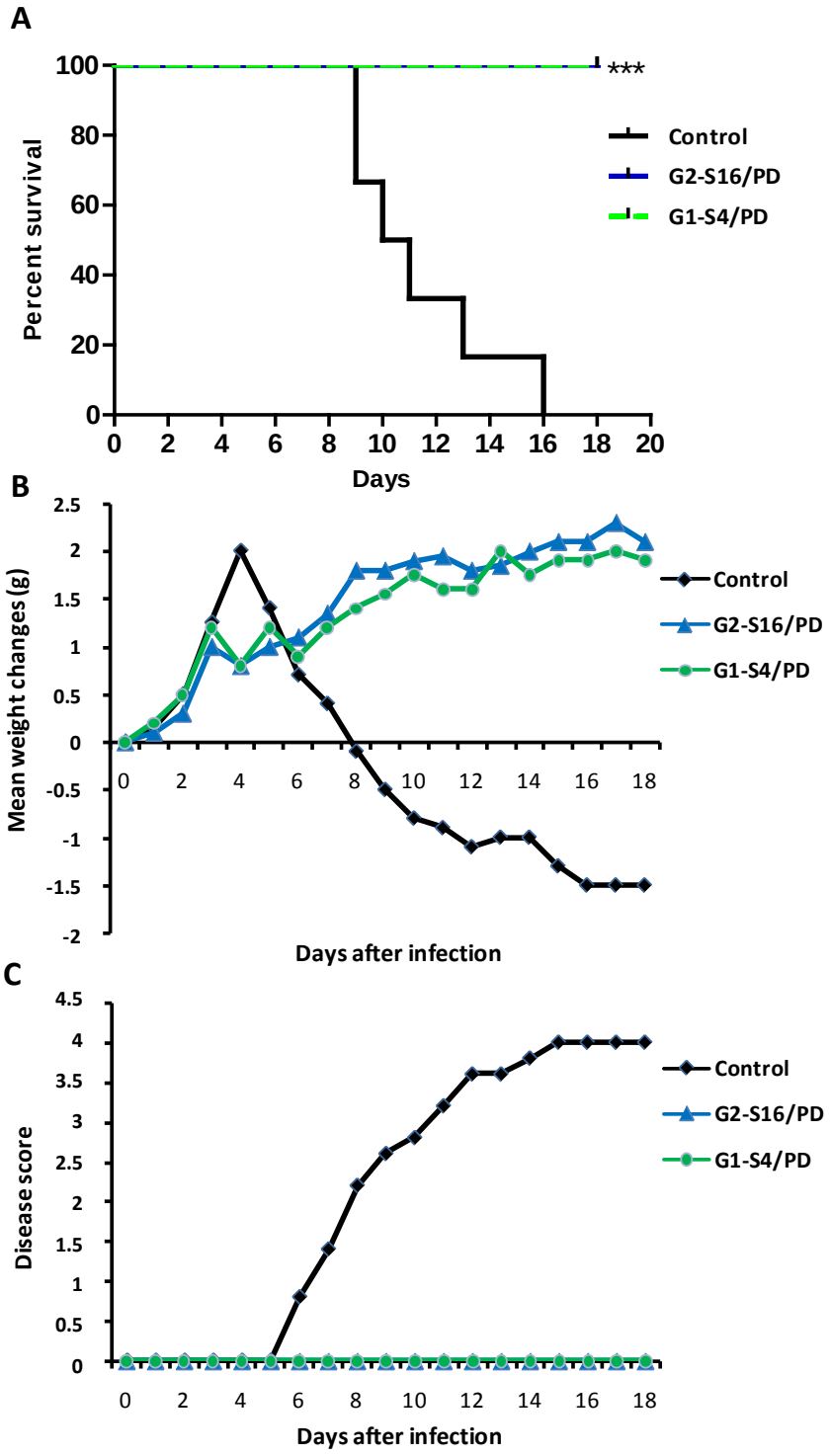

Figure 44. Polyanionic carbosilane dendrimers prevent vaginal high-dose HSV-2 infection in presence of PD. Medroxyprogesterone acetate treated BALB/c mice were vaginally challenged with 10^5 PFU HSV-2 1h after applying the indicated gel (6 mice/group). Mice were examined daily for body weight and genital pathology over 18 days. **(A)** Percentages of infection over time are shown for each treatment group. Dendrimer based gels containing 3% dendrimer and 0,25 mM PD were significantly more protective than vehicle alone (***: p<0,001 vs Placebo) **(B)** Body weight changes were expressed as the mean values of ten animals in the same group. Each mean value was calculated by subtracting the weight at day 0 from the weight at day N after infection. **(C)** Clinical pathology was scored as described in the text for 18 days. Lesion scores were expressed as the mean values of 6 mice in the same group.

11. Effect of polyanionic carbosilane dendrimers against respiratory syncytial virus infection

Through this work, we have been working with polyanionic carbosilane dendrimers as potential topical microbicides. (Briz et al., 2015, Cena-Diez et al., 2016b, Chonco et al., 2012, Sepulveda-Crespo et al., 2015b, Vacas Cordoba et al., 2013, Vacas-Cordoba et al., 2014, Vacas-Cordoba et al., 2016). These dendrimers stand out by their capacity to block the interaction between HS and HBD, resulting in inhibition of infection generated by different viruses, such as we have demonstrated in HSV-2 (Cena-Diez et al., 2016b).

This scenario makes RSV an important target for antiviral research and development and polyanionic carbosilane dendrimers stand out as promising candidates for the development of a new therapy against RSV. The aim of the present work was to screen a library of polyanionic carbosilane dendrimeric for their anti-RSV activity and to investigate the antiviral potency, the mode of action, and the biocompatibility of the best-hit compounds.

11.1. Cell viability assay

MTT toxicity assays were performed to evaluate the biocompatibility of dendrimers in A549 epithelial cells (**Fig. 45**).

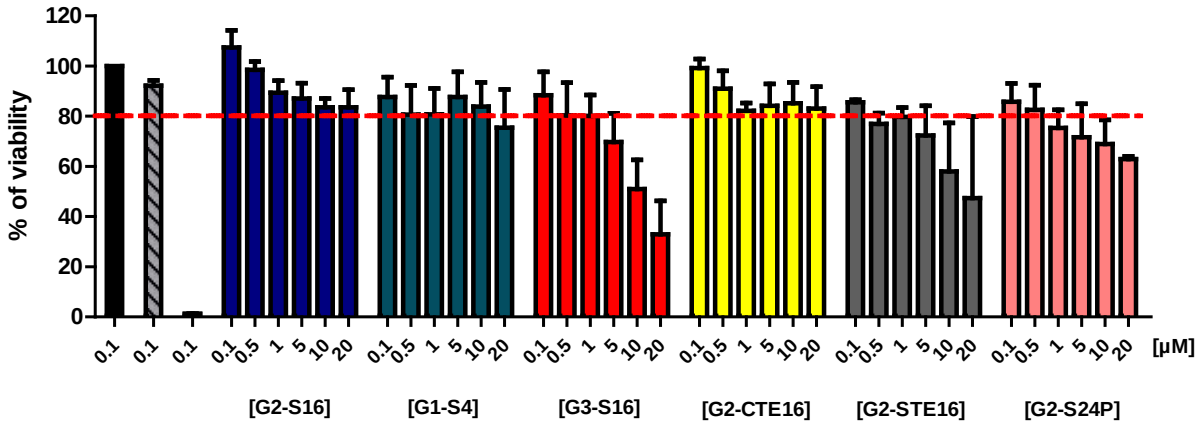

Figure 45. Biocompatibility of polyanionic carbosilane dendrimers in A549 cells. Viability of A549 cell line was evaluated by MTT assay after 24 hours of exposure to a range of dendrimer concentrations; 80% of viability was set as the limit of toxicity for all dendrimers. Dextran 20 µM and DMSO 10% were used as negative and positive control of cellular death, respectively. Data were represented as mean ± standard deviation of three independent experiments.

Dendrimers concentrations with viability >80% in comparison with non-treated control were regarded as nontoxic. G2-S16 and G1-S4 were non-toxic at 10 μM; G2-STE16 and G2-CTE16 were non-toxic at 1 μM; and G2-S24P and G3-S16 were the most toxic dendrimers, with a limit of viability of 0.5 μM.

11.2. Identificatin of polyanionic carbosilane dendrimers as RSV agents

The ability of the six compounds to inhibit RSV infection was investigated further in two cell lines commonly used in RSV studies: HEp-2 and A549.

G2-S16 at 10 μM concentration inhibited RSV infection by 99-100%; G1-S4 at 10 μM concentration inhibited RSV by 95-96%; G3-S16 at the concentration of 0.5 μM had a RSV inhibition of 94-95%; G2-STE16 at 1 μM concentration showed an inhibition against RSV of 88-89%; G2-CTE16 at 1 μM concentration showed an inhibition against RSV between 80-81%; G2-S24P at the concentration of 0.5 μM showed an inhibition against RSV between 80-81%. (**Fig. 46**).

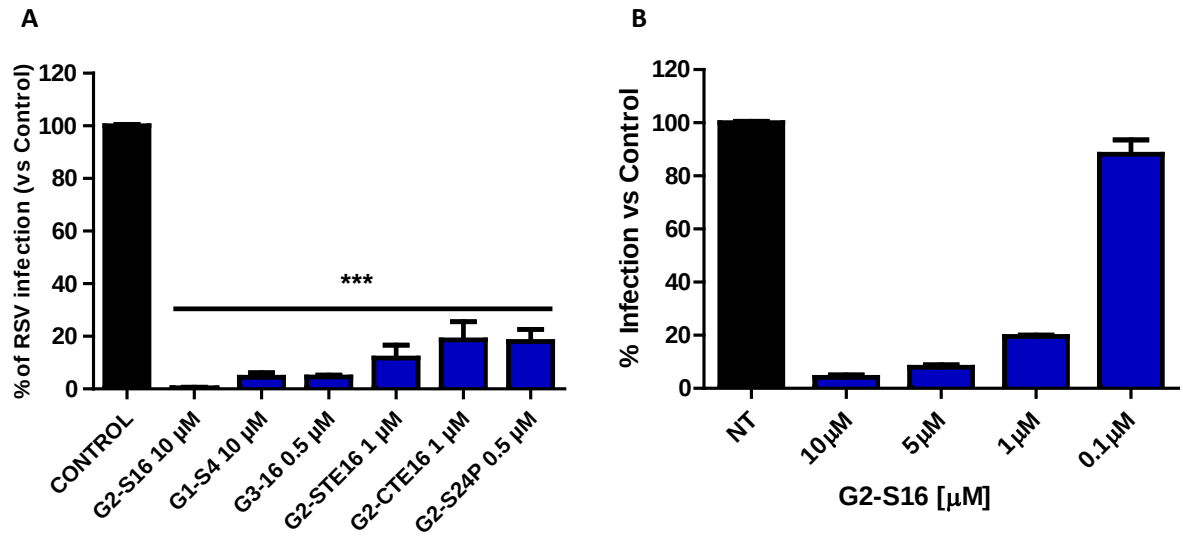

Figure 46. Primary screening of candidates inhibitory activity against RSV. A) Percentages of inhibition of the dendrimers corresponding to RSV infection on the A549 cell line, and subsequent titration of the culture infective supernatants on HEp-2 cells for 5 days. **B)** Percentages of inhibition of G2-S16 at a range of non toxic concentrations. The graph represents the relative mean of three independent experiments. Error bars corresponding to the SD inter-experiment. ***: p <0.0001 vs. Infection control. Infection control: infected A549 cells at 3 MOI. Percentages relative to infection control. Data were represented as mean ± standard deviation of three independent experiments

The data obtained showed that all dendrimers significantly halt RSV infection (p <0.001 vs control). Dendrimers G2-S16, G1-S4 and G3-S16 were selected, due to their high percentages of inhibition, for more detailed studies *in vitro*.

11.3. Polyanionic carbosilane dendrimers disrupt RSV binding to the host cell: Attachment assay

The antiviral activity of polyanionic carbosilane dendrimers is associated with the establishment of electrostatic interactions between the anionic functional peripheral groups of dendrimers and the viral envelope proteins or cell host receptors (Cena-Diez et al., 2016b, Chonco et al., 2012, Vacas Cordoba et al., 2013, Vacas-Cordoba et al., 2014). Therefore, the effect of polyanionic dendrimers in RSV binding to the host cell was studied (**Fig. 47A**).

G2-S16 dendrimer halted RSV viral particles interaction with cell host cell surface proteins in 99-100%. G1-S4 and G3-S16 dendrimers decreased the infection by 86-88%. All the data obtained were significant, with a $p< 0.0001$. No statistically significant differences were observed when comparing the results obtained with each dendrimers in the inhibition assay and the attachment assay, proving that the mechanism of action of these carbosilane polyanionic dendrimers is the inhibition of RSV infection by blocking the interaction between viral proteins and the receptors/co-receptors of the target cell.

11.4. G2-S16 provides cell protection against RSV

To evaluate whether the dendrimer activity was due to the binding of the cell surface proteins or inactivativation though binding to the viral particle, a dendrimer-cell binding assay was performed.

G2-S16 dendrimer was able to bind to the host cell receptors and decreased RSV infection in a significant manner, 83-84% ($p<0.01$). These data indicate that all inhibitory activity of the G2-S16 is due to its binding to the cell host surface (**Fig. 47B**). However, G1-S4 and G3-S16 dendrimers did not significantly reduce RSV infection. Therefore, the G1-S4 and G3-S16 anti-RSV activity was not due to dendrimer-cell interaction.

11.5. G1-S4 and G3-S16 inactivate RSV

After demonstrating that the G2-S16 dendrimer inhibits the RSV viral cycle though binding/entry level by binding to surface proteins of the target cell, the ability of the G2-S16, G1-S4 and G3-S16 dendrimers to bind to the RSV viral proteins and thereby inhibit the infection was assessed.

It was shown that the G2-S16 dendrimer was unable to inhibit RSV infection in a significant manner by its interaction with the virus (11-12%), implying that G2-S16 is not able to inhibit infection through this interaction in a meaningful way. This data is in agreement with the data observed in the previous experiments, since it had been shown that the inhibitory action of the G2-S16 dendrimer was due to

an interaction with cellular receptors. The sulfate dendrimers G1-S4 and G3-S16 significantly decreased infection by 95-98% (**Fig. 47C**), implying that their inhibition is due to this interaction with RSV. These data, coupled with those obtained in the experiment on the action of the dendrimers against the cell, show that the G1-S4 and G3-S16 dendrimers are inhibiting RSV infection at the viral entry level by a binding with RSV.

These data demonstrate that the G2-S16 dendrimer is capable of binding to cellular receptors to inhibit infection. On the other hand, G1-S4 and G3-S16 dendrimers have been shown to inhibit RSV infection by interacting with viral proteins.

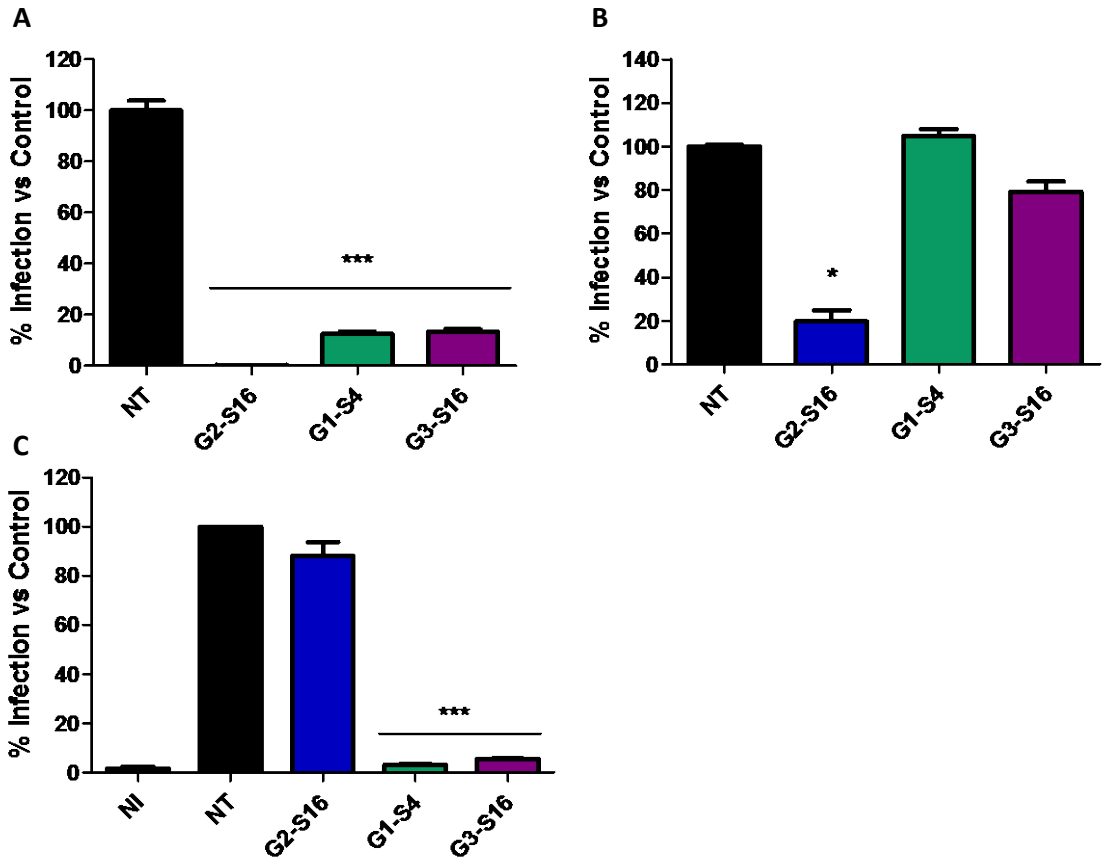

Figure 47. Mode of action of polyanionic carbosilane dendrimers against RSV infection. (**A**) Effect of anionic dendrimers on RSV binding. A549 cells were prechilled at 4 °C for 30 min and then treated with the dendrimers and infected with RSV for 1 h at 4 °C. (**B**) Binding of dendrimers to cellular surface proteins. A549 cells were pretreated with dendrimers for 1 h. After incubation, cells were washed to eliminate unbound dendrimer and then infected with RSV. The generated infectious supernatants were titrated on HEp-2. (**C**) Percentages of infection at 3 MOI of HEp-2 cells. The G2-S16, G1-S4 and G3-S16 dendrimers were preincubated with RSV for 1 h at 4 °C, after which HEp-2 cells were infected at 3 MOI for 1 h at 4 °C. Error bars corresponding to the inter-experiment SD (n = 3). ***: p <0.0001 vs. Infection control. Data were represented as mean ± standard deviation of at lest three independent experiments.

11.6. G2-S16 and G3-S16 halt RSV syncytia formation

Syncytium formation is a well-known mechanism of cell-to-cell infection that contributes significantly to virus spread in vivo. To determine whether G2-S16,G1-S4 and G3-S16 prevents cell-to-cell spread of virus after infection, a syncytium formation assay was performed on infected HEK-293T cells after 48 h. Dendrimers were not toxic at the range of concentrations evaluated on HEK-293T cell line (**Fig.48**).

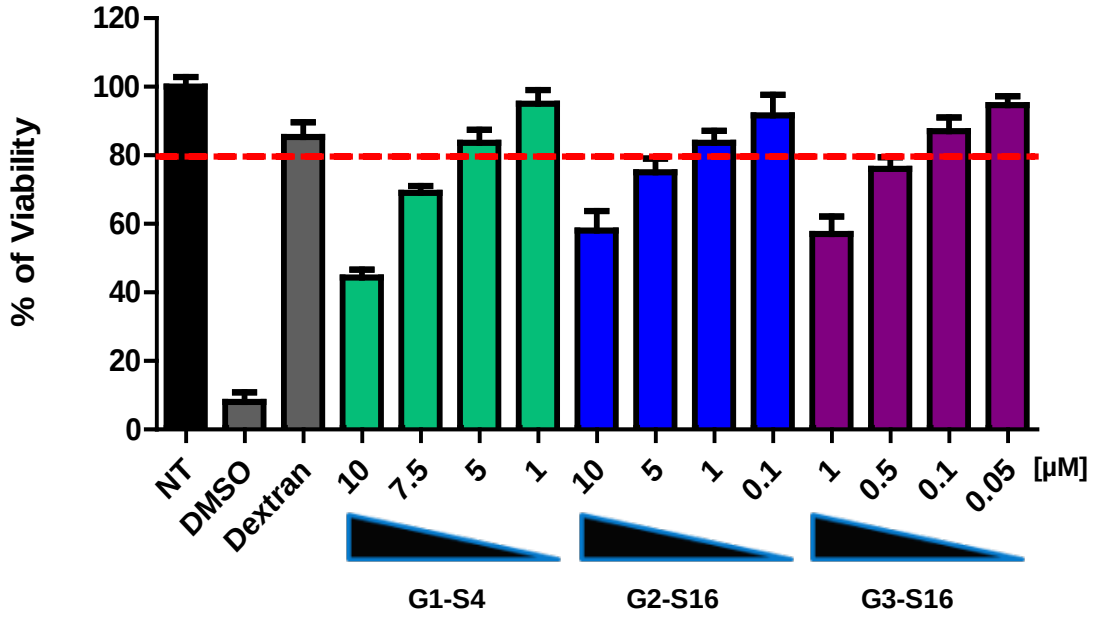

Figure 48. Biocompatibility of polyanionic carbosilane dendrimers in HEK293T cells. Viability of epithelial HEK293T cells was evaluated by MTT assay after 24 h of exposure to a range of dendrimer concentrations; 80% of viability was set as the limit of toxicity for all dendrimers. Dextran 20 μM and DMSO 10% were used as negative and positive control of cellular death, respectively. Data were represented as mean ± standard deviation of three independent experiments.

The G2-S16 dendrimer demonstrated inhibition of syncytium formation of greater than > 80% at a concentration of 5 μM. Although in the cell viability assay it was found that this concentration did not reach 80% to be considered viable, it was tested to evaluate its effectiveness since the experimental data showed that it gave values very close to the minimum percentage to be viable (75-78%); at a concentration of 1 μM inhibited syncytium formation by 79% and at a concentration of 0.5 μM inhibited syncytium formation by 62% (**Fig. 49A** and **50**). The G1-S4 dendrimer inhibited syncytium formation by 23% at a concentration of 5 μM and 20% at a concentration of 2.5 mM (**Fig. 49B** and **50**). Finally, the G3-S16 dendrimer at a concentration of 0.1 μM inhibited syncytium formation by 63% and at a concentration of 0.05 μM inhibited 60% (**Fig. 49C** and **50**).

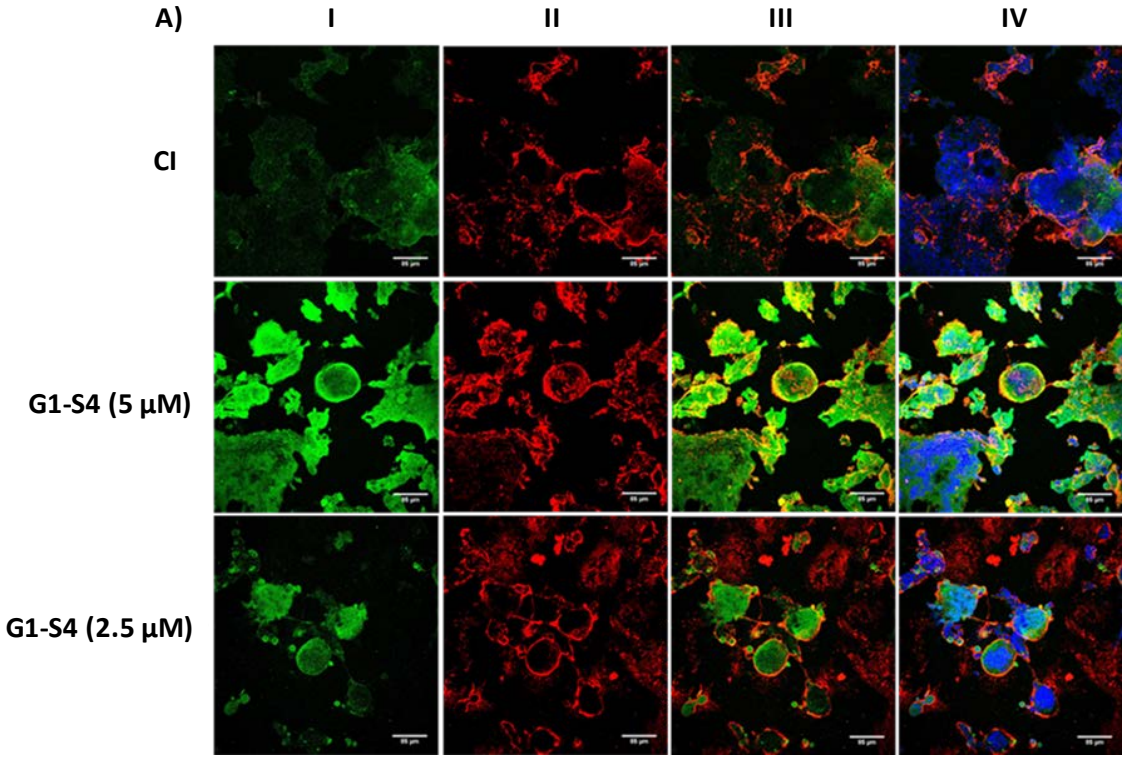
A)
I
II
III
IV
CI
G1-S4 (5 µM)
G1-S4 (2.5 µM)

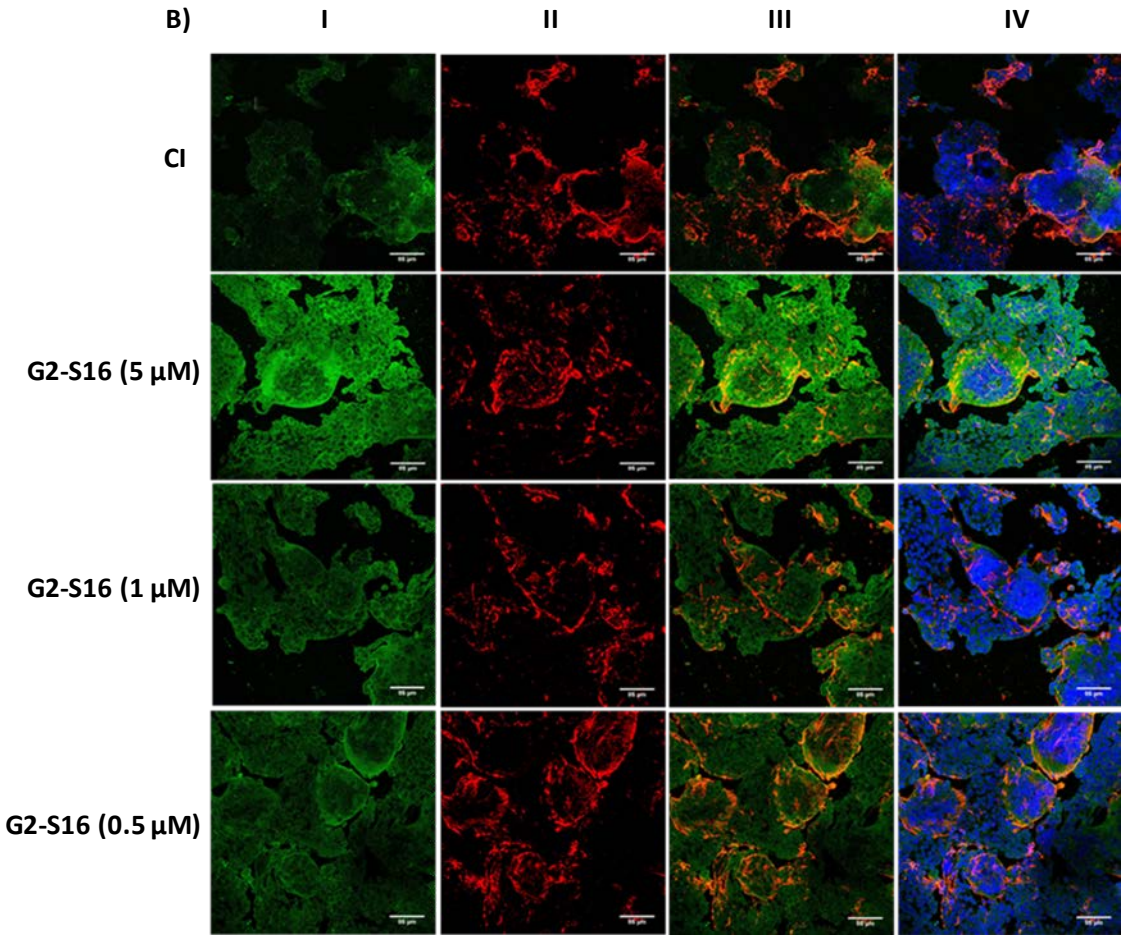
B)
I
II
III
IV
CI
G2-S16 (5 µM)
G2-S16 (1 µM)
G2-S16 (0.5 µM)

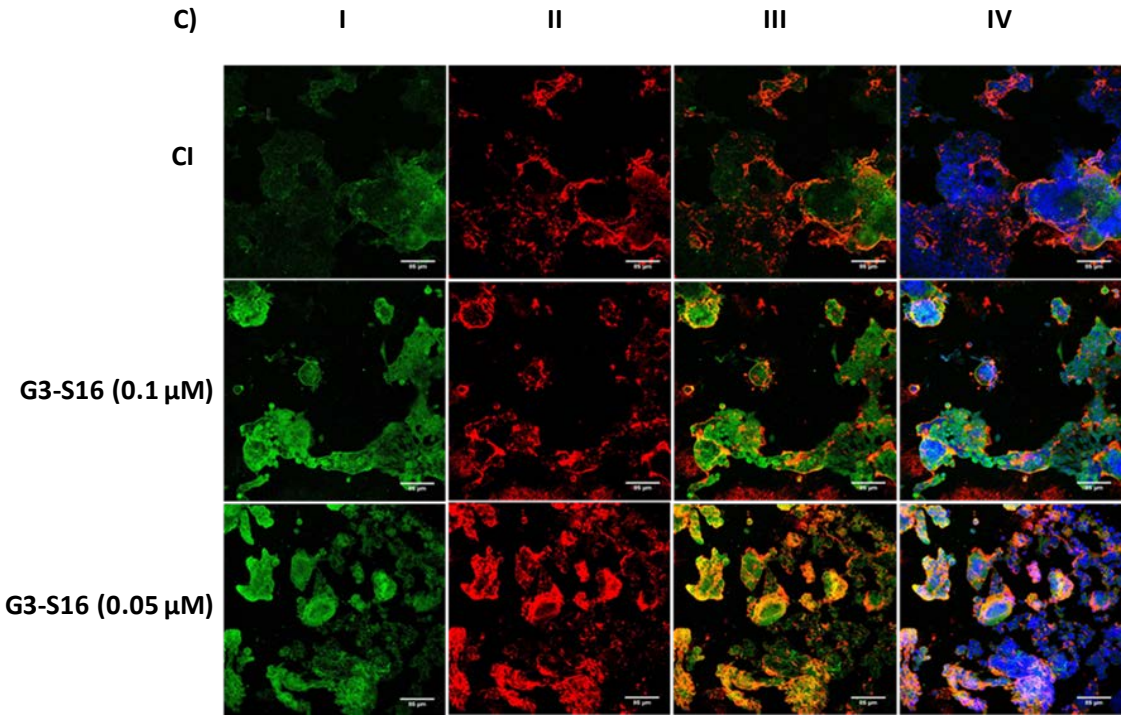

Figure 49. Confocal microscopy images of inhibition of the formation of syncytium in HEK-293T cells infected with RSV and treated with the selected dendrimers. (**A**) G1-S4, (**B**) G2-S16 and (**C**) G3-S16. Non-toxic concentrations were used (G2-S16: 1 µM, 0.5 µM and 5 µM, G3-S16: 0.1 µM and 0.05 µM; G1-S4: 5 µM and 2.5 µM). (**I**) FITC antibody is labeling the HS of cells; (**II**) anti-human RSV fusion protein antibody; (**III**) the co-location of HS and RSV; and (**IV**) represents co-localization of HS, RSV and nuclei of infected cells labelled with DAPI.

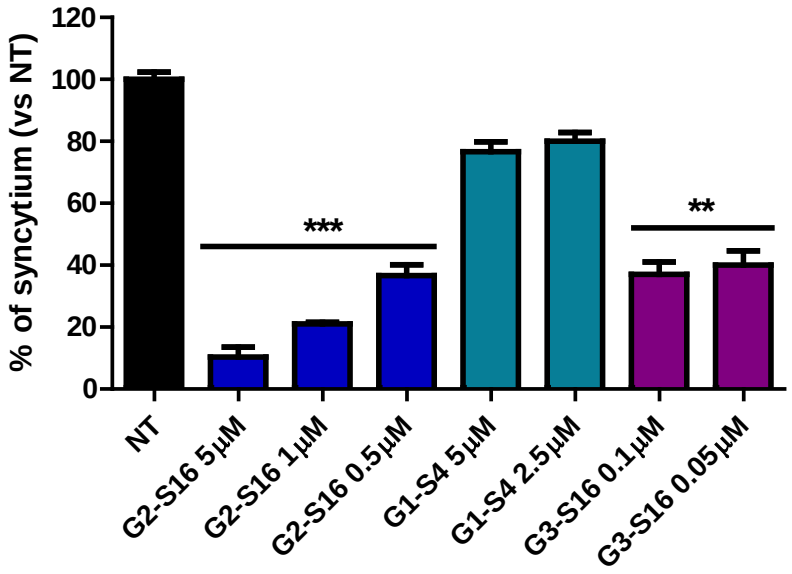

Figure 50. Graphical representation of the inhibition of syncytium formation. HEK-293T cell were treated with the three selected dendrimers in a range of non-toxic concentrations (G1-S4: 5 µM and 2.5 µM, G2-S16: 1 µM, 0.5 µM and 5 µM, G3-S16: 0.1 µM and 0.05 µM) and syncytium formation was determined with confocal microscopy. The graph represents the relative mean of three independent experiments. The error bars correspond to the SD among the experiments. *** p<0.0001 Vs. Infection control. ** p<0.01 vs. Infection control.

11.7. *In vivo* histopathological assay

Once the mechanism of action by which the polyanionic carbosilane dendrimers to inhibit RSV was determined, we evaluated the ability of G2-S16 to induce irritation and damage on the lung when administrated intranasally. It was proved that when BALB/c mice treated with G2-S16 intranasally, no damage or alteration onto the vaginal epithelium was caused at concentrations up to 500 µM. G2-S16 showed slightly toxicity on lungs (Inflamation, Vascular thrombosis & congestion and Atelectasia) at 1 mM. However, experimental data suggests that *in vivo* toxicity of G2-S16 can be due to the application method (**Table 10**).

Table 10. Lung toxicity assay.

	PBS	PBS	PBS	G2-S16 100uM	G2-S16 100uM	G2-S16 100uM	G2-S16 500uM	G2-S16 500uM	G2-S16 500uM	G2-S16 1mM	G2-S16 1mM	G2-S16 1mM
Pulmonary parenchyma												
Inflammation	0	1	2	2	2	2	2	1	3	2	2	1
Edema	0	0	0	0	0	0	0	0	0	0	0	0
Alveolar congestion	0	0	2	1	1	2	1	0	2	3	2	2
Bleeding	1	0	1	1	0	1	0	0	0	0	0	0
Vascular thrombosis & congestion	1	1	1	0	1	1	1	2	1	2	3	2
Atelectasis	1	1	2	2	2	2	2	1	2	3	2	1
Emphysema	0	0	0	0	0	0	0	0	0	0	0	0
Pleura												
Inflammatory infiltrate	0	0	0	0	0	0	0	0	0	0	0	0
Edema	0	0	0	0	0	0	0	0	0	0	0	0
Bleeding	0	0	0	0	0	0	0	0	0	1	0	0
Neovasculation	0	0	0	0	0	0	0	0	0	0	0	0
Fibrosis	0	0	0	0	0	0	0	0	0	0	0	0
Total Score	3	3	8	6	6	8	6	4	8	10	9	6

The existence of injury in pulmonary parenchyma (Inflammation, edema, alveolar congestion, bleeding and vascular thrombosis and congestion) and pleura (Inflammatory infiltrate, edema, bleeding, fibrosis and neovasculation) was evaluated in each biological sample. 0 (no change) when no injury or the observed changes were within normal range; 1 (minimum) when changes were sparse but exceeded those considered normal; 2 (light) when injuries were identifiable but with no severity; 3 (moderate) for significant injury that could increase in severity; 4 (very serious) for very serious injuries that occupy most of the analyzed tissue. These values were added up and determined the level of vaginal irritation as minimum 1-6, average 7-10, moderate 10-14 and severe 14+.

11.8. *In vivo* RSV challenge assay

Besides biocompatibility, we also assessed the antiviral activity in BalB/C mice. Intranasal administration of G2-S16 showed the ability to reduce RSV replication and infection in a significant manner. Administration of 50 µl of G2-S16 500 µM, after 48 h of exposure to a high dose of RSV, was able to abrogate RSV infection in 86% (p<0.0001 vs placebo) (**Fig. 51**). G2-S16 250 µM was able to inhibit the RSV infection in 58%.

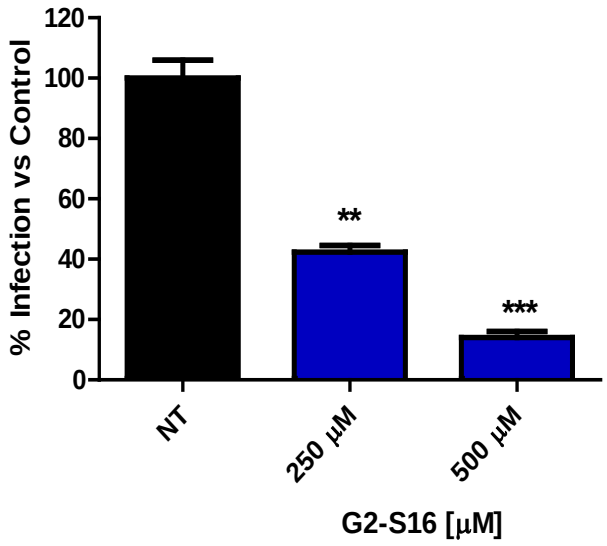

Figure 51. Evaluation of inhibitory activity of G2-S16 against RSV. Percentages of inhibition of G2-S16 corresponding to RSV infection of BALB/c mice, and subsequent titer of the lung infection HEp-2 cells for 5 days. The figure represents the relative mean of six mice. ***: $p< 0.0001$ vs. Infection control. Infection control: BALB/c mice treated with PBS. Percentages relative to infection control.

DISCUSSION

12. New candidates for the development of a topical microbicide against sexual transmitted diseases

Sexually transmitted infections are a major global cause of acute diseases, infertility, mobility and death with serious medical and psychological consequences for millions of men, women and infants. Among all the pathogens responsible for different STIs, viruses play a major role. It is estimated that several hundred million individuals worldwide are infected with viral STIs including HIV-1 and HSV-2.

HIV-1 infection stands up as one of the mayor health issues of the last decades. Despite a steady decline in new HIV-1 infections from the late 1990s to the present, yet 1.8 million people became infected in 2016. Sexual transmission is responsible for more than 80% of these new infections and continues to be one of the most difficult transmission routes to tackle. For more than twenty-five years, the idea of developing new strategies to prevent HIV-1 infection, especially in women, such as the use of topical vaginal microbicides has been present. Several investigations have focused on the study of dendrimers as non-specific microbicides and the first positive results were obtained in clinical trials in humans. This was the case of SPL7013, a polynomic dendrimer functionalized with 32 terminal naphthalenesulfon groups that reached cinical trials Phase II (Telwatte et al., 2011, Cohen et al., 2011). However, the development of this negatively-charged dendrimer as a microbicide was concluded just recently due to adverse events (McGowan et al., 2011).

After numerous unsuccessful research and clinical trials on topical microbicides (Grant et al., 2008, Vanpouille et al., 2012, Fichorova et al., 2001, McCormack et al., 2010), it has been found that *in vivo* ineffectiveness of these topical microbicides was not only due to the lack of adherence, but also due to the induction of inflammation and cytotoxic effect. Even more important, Zirafi et al. have shown that semen reduces the sensitive of HIV-1 of different compounds that were considered for microbicides development due to their potent *in vitro* activity but failed to prevent HIV-1 transmission in individuals (Zirafi et al., 2014). Amyloid fibrils of the semen have been called SEVI. The SEVI showed to capture HIV-1 virions promoting their adhesion to the target cells, increasing the ability of HIV-1 to infect human cells, regardless of the cell type (Kim et al., 2010, Roan et al., 2011).

The objective of this work was to evaluate the ability of several polyanionic carbosilane dendrimers with high inhibitory profile against HIV-1 infection in the presence of semen as well as their biocompatibility *in vivo*.

Reports indicate that exposure of HIV-1 particles to a concentration of 10% semen increases infectivity up to 10-fold because amyloid seminal fibrils can bind to HIV-1 virions and efficiently enhance and accelerate their attachment to the target cells (Arnold et al., 2012, Neurath et al., 2006, Usmani et al., 2014, Roan et al., 2011, Zirafi et al., 2014) shortening the exposure time of virions to microbicide entry inhibitors that act outside of the cell, impeding accessibility to the viral membrane and glycoproteins. ARVs that act intracellularly are inhibitors of RT, PR or IN. In contrast, MVC binds to the cellular CCR5 co-receptor (Tan et al., 2013a), occupying all CCR5 receptors on the cell membrane, and it inhibits viral entry independently of the presence of semen.

Polyanionic carbosilane dendrimers have multifactorial and non-specific capacity and act as virucidal agents that inhibit viral entry, provide a barrier to infection for a long time and block the spread of HIV-1 from cell-to-cell (Chonco et al., 2012, Sanchez-Rodriguez et al., 2015, Vacas Cordoba et al., 2013). Because semen is the major vector for the global spread of HIV-1 infections, we performed inhibition experiments with the G2-STE16, G2-S16 and G3-S16 dendrimers, as well as their combinations with TDF and/or MVC, up to a maximum non-toxic concentration of 20 µM in the presence of amyloid fibrils in semen against the R5-HIV-$1_{NL(AD8)}$ laboratory strain and the T/F pCH058 and pTHRO R5-HIV-1 founder virus strains. In spite of a steep increase in the IC_{50} between 25- and 869-fold against all viral isolates (**Table 3**) because the infectivity was enhanced by the presence of semen, we clearly showed that G2-STE16, G2-S16 and G3-S16 retained an inhibitory effect on HIV-1 infection at non-toxic concentrations in the TZM.bl cells and PBMC (**Fig. 15, 16 and 20**). Unlike polyanions, the polyanionic dendrimers decreased the rates of HIV-1 infection not only by neutralization of the negative charges of virus but also by competitive binding to viral targets (the gp120 complex) and to cellular targets (the CD4 receptor in areas relevant to CD4/gp120 and CXCR4 or CCR5/gp120 interactions). The antiviral activity of their sulfonate end-groups was not modified by semen components, by the alkaline pH of semen (Neurath et al., 2006, Lackman-Smith et al., 2008, Tan et al., 2013b, Keller et al., 2010, Herold et al., 2011, Patel et al., 2007) or by competitive binding to the viral envelope proteins (Platt et al., 1998). This provides a reasonable explanation for the abrogation of the antiviral activity of polyanionic compounds by semen (Telwatte et al., 2011), whereas the dendrimers retained their anti-HIV-1 ability at non-toxic concentrations when exposed to semen (**Fig. 15, 16** and **20**).

In addition, when the dendrimers were combined with ARV drugs, they demonstrated high protection against HIV-1 infection in presence of amyloid seminal fibrils as evidenced by low IC_{50} increases of 2-

to 8-fold at lower doses of the compounds (Table 3). The enhanced function of the polyanionic dendrimers in combination with TDF compared with MVC in presence of SEVI (**Fig. 18, 19** and **21**) in various cell lines could have occurred because MVC is an entry inhibitor and TDF acts as an RT inhibitor, thus action at different levels cause a synergism which counters the enhancement of HIV-1 infectivity by the sperm. Due to the fact that the virions are attached and concentrated onto the cell surface by the amyloid fibrils (Mondor et al., 1998, Yolamanova et al., 2013), the dendrimers could block the CCR5 receptors, and TDF could limit intracellular viral enzyme production during cell-to-cell transmission, causing a decrease in the amount of drug required for the effective inhibition of HIV-1 replication in presence of semen.

G2-S16 dendrimer was selected among those polyanionic carbosilane dendrimers capable of retaining its inhibitory effect at nontoxic concentrations against HIV-1 which infectivity has been enhanced by the presence of amyloid fibrils of semen to exhaustive evaluate its biocompatibility *in vivo.*

Transmission of HIV-1 through the mucosal epithelium plays a critical role in the onset of systemic HIV-1 infection and the development of AIDS. Adult cervical and foreskin epithelia serve as an entry site for the sexual transmission of HIV-1 (Carias et al., 2013, Ganor et al., 2010, Prodger and Kaul, 2017). Therefore, the activity of the dendrimers should be limited to these regions.

For that, the G2-S16 dendrimer needed to be labelled with FITC or another probe but it could not be done with this dendrimer, because the functionalization of the G2-S16 with sulfonate terminal groups is achieved by a Michael type addition reaction of sodium vinyl sulfonate over carbosilane dendrimers, this reaction requiring very high temperatures (above 100 °C) and longer reaction times, which makes the introduction of fluorescein impossible. However, labelling an anionic carbosilane dendrimer with fluorescein was achieved with a similar G2-STE16 dendrimer functionalized by thiol– ene addition reactions (Cena-Diez et al., 2016b, Chonco et al., 2012, Sepulveda-Crespo et al., 2015c). In this case, the soft reaction conditions provided during the functionalization lead to the simultaneous introduction of terminal sulfonate units and one amino group (–NH2) in the periphery of the carbosilane dendrimer, by the sequential addition of two different thiols over allyl terminated carbosilane dendrimer (**Fig. 13**).

The G2-STE16-FITC dendrimer's ability to penetrate vaginal epithelium in BALB/c mice was evaluated by detecting the bioluminescence in the vagina and in the whole animal by using a IVIS Lumina Image System and confocal microscopy. The ability of the G2-ST16-FITC dendrimer to be retained

exclusively in the vaginal tissue was even observed (**Fig. 22**), 20 h after intravaginal application. G2-ST16-FITC biodistribution, when applied intravaginally, is limited to the vaginal tissue, which is ideal because of the ability of the dendrimer to halt the viral infection in the early stages of the viral cycle, binding/attachment steps. Confocal microscopy showed that G2-STE16 was penetrating the non-sterile areas of the mouse female reproductive tract after 20 h (**Fig. 23**). The hypothesis was that the ability of G2-STE16-FITC to cross the vagina, ectocervix and fornix epithelium after 20 h of exposure, and not to cross the endocervix epithelium was because of the irritation caused by the labelled dendrimer. In previous studies, it was shown that histopathological examination did not induce vaginal irritation, inflammation, lesions or damage in the vaginal mucosa after vaginal administration of G2-S16 dendrimer at different concentrations, even when repeatedly treated with high doses in rabbits, 15 female CD1 (ICR) mice (Arnaiz et al., 2012, Vacas Cordoba et al., 2013) and female BALB/c mice (Briz et al., 2015, Sepulveda-Crespo et al., 2015c). Although these findings confirm the *in vivo* safety of this G2-S16 dendrimer for topical application the next step demonstrated, using a new experiment (**Table 4** and **5**) , that the potential microbicide candidate, G2-S16 dendrimer, was not toxic to the vaginal epithelium in the nonsterile part of the female reproductive tract (Briz et al., 2015, Chonco et al., 2012, Sepulveda-Crespo et al., 2015c, Vacas Cordoba et al., 2013). The hypothesis was that the ability of G2-STE16-FITC to cross the vagina, ectocervix and fornix epithelium after 20 h of exposure but not the endocervix epithelium was because of the irritation caused by the labelled dendrimer. This was confirmed by the ability of G2-STE16-FITC and G2-STE16 dendrimer itself to cause vaginal damage and irritation was found in BALB/c mice for 20 h with a single dose of both dendrimers, creating the same conditions of exposure as in the previous experiments (**Table 4**). In addition, it was shown that when BALB/c mice were treated with G2-S16 for seven consecutive days, no damage or alteration of the vaginal epithelium was observed, indicating that this dendrimer is safe for the development of a topical microbicide against HIV-1 infection (**Table 5**).

The EpiVaginal™ (VEC-100) ectocervical tissue model was used to evaluate the safety of the G2-S16 for vaginal application. The EpiVaginal™ *in vitro* test is gradually replacing the traditional *in vivo* models to study vaginal irritation because of its higher reliability and reproducibility. The data obtained in this research revealed that G2-S16 is a safe dendrimer preparation for vaginal application to control viral transmission (**Fig. 24**).

Finally, although rodents are the standard animal models for evaluating toxic drugs, the zebrafish embryo is emerging as an important tool for toxicity testing and for the opportunity to carry out fast reproducible tests (Olivares et al., 2016, Strahle et al., 2012). The zebrafish genome has approximately 70% homology with the human genome. The small size, rapid external development, optical transparency, a requirement for less space and husbandry care, and easy manipulation are a few of the added advantages that are in its favour (Howe et al., 2013, Lammer et al., 2009, Lawrence, 2011). A wide range of substances, which exhibit different modes of action, such as solubility, volatility and hydrophobicity, have been successfully, studied using this test. The embryonic MDT, the LC_{50} and teratogenicity as well as LOEC of the G2-S16 dendrimer at 48 and 96 hpf were studied and were all >100 mg L−1. It was shown that no significant differences were found in mortality, sublethal or teratogenic effects when the embryos were treated with 100 mg L−1 of G2- S16 when compared with the negative control (**Table 6**). In conclusion, MDT at 48 and 96 hpf were all >100 mg/L which gives one more favourable result for the good tolerance of this dendrimer *in vivo*, increasing the chances of its success in clinical trials with humans. These findings emphasize the potential of zebrafish embryos for use in the study of the toxic effects of dendrimers. It could also act as a model for the screening of other related nanoparticles for toxicity.

Although the emphasis has been on preventing HIV-1, protection from other STIs is desirable in terms of avoiding diseases and associated consequences. Importantly, many STIs may increase vulnerability to HIV-1 infection (e.g., genital herpes infection facilitates the transmission of HIV-1) (Freeman et al., 2006). Genital herpes is the STIs with the highest global prevalence and appears frequently associated with other infections (Cusini and Ghislanzoni, 2001). Consistent with this, polyanionic carbosilane dendrimers could be great candidates for the development of microbicide with dual activity against HIV-1 and HSV-2 sexual infections.

We performed a screening of eight selected polyanionic dendrimers that previously demonstrated anti-HIV-1 activity *in vitro* and *in vivo* to select proper candidates for the development of a topical microbicide against HSV-2 infection. Plaque reduction assay showed that G1-S4, G2-S16, and G3-S16 have strong antiviral activity against HSV-2 *in vitro* by inhibiting HSV-2 binding and internalization into the Vero cells. Time of addition assay showed strong inhibition of HSV-2 infection when dendrimers were added 1 h after HSV-2 infection, indicating that dendrimers act at the early phases of

the HSV-2 life cycle (**Fig. 28**). The fact that G2-S16 is able to keep its inhibitory effect close to 50% 8 h post infection suggests that it acts both at the early and late stages of the HSV-2 life cycle.

HSV-2 gB plays an important role in HSV-2 entry by binding to cell-surface HS (Akhtar and Shukla, 2009). G1-S4 and G3-S16 have sulfate groups on their surface, which leads to the hypothesis that these dendrimers could bind to HSV-2 gB and achieve their inhibitory effect. Viral inactivation assay showed that functionalized dendrimers with sulfate could bind directly on viral proteins on the surface of HSV-2 particles and block and inactivate HSV-2 infectivity. However, G2-S16, a sulfonate dendrimer, carried out its inhibitory effect by binding to cellular surface molecules of the host cells. Hence, it is possible that various polyanionic dendrimers exhibit different binding specificities. Athough; these dendrimers are generally considered non-specific. This difference is due to the fact that the variability in the number of charged groups, the size, the structure of the polyanion, or the type of functional groups involved.

Molecular modeling showed that G1-S4 and G2-S16 were able to bind the gB protein in all selected binding sites including suggested binding area for gH-gL. Better results were achieved with G1-S4 than G2-S16 except the binding site on the top of the gB. Therefore, both dendrimers can successfully block the viral fusion machinery. However, G1-S4 and G2-S16 differ in reaching the key binding sites. The smaller, more flexible, and faster moving dendrimer G1-S4 is better suited to reach worse accessible binding sites than G2-S16. If we focus on the proposed gH–gL binding area, G2-S16 could have problem to reach position A, B of HSV-2 gB and G1-S4 could reach at least the edge of A, B area (case E) and disturb gH–gL/gB binding process. G1-S4, unlike G2-S16, could penetrate inside the gB trimer in its more open prefusion state and block the right fusion state of the gB trimer. Another interesting result which favours dendrimer G1-S4 in the context of interference with gB/gH-gL interaction is significantly higher affinity of dendrimer G2-S16 in position F comparing to the most “gB/gH-gL” relevant positions A, B which is not the case for dendrimer G1-S4. In other words, unlike dendrimer G1-S4, for G2-S16 dendrimer is significantly more preferable position F comparing to A, B. Ability of G1-S4 and G2-S16 to bind in position F and to the missing N-terminus part (**Fig. 30** and **31**) can influence the interaction of gB with its eventual cell receptor and cell glycosaminoglycans. However, experimental results with G2-S16 suggest that this effect has small impact on the HSV-2 fusion machinery. Dendrimer binding on the top of HSV-2 gB (mainly position F, eventually beginning part of N-terminus) could somewhat decrease the probability that the more important place on this

protein (eg, gB/gH–gL binding area) will be achieved by another dendrimer in the solution due to the electrostatic repulsion (**Fig. 31**).

This electrostatic repulsion will be more significant in the case of G2-S16 which has four times higher charge than G1-S4. Interestingly enough, the fact that G2-S16 exhibited only small inhibition effect when previously mixed and incubated with HSV-2 suggests that successful blocking of the gB/receptor binding can prevent HSV-2 fusion, but preferred precise binding site position and/or the insufficient affinity of G2-S16 to the N-terminal cationic part can be the reason for the less efficient blocking effect of G2-S16 in comparison with G1-S4. These molecular modeling observations would explain the *in vitro* results obtained in this Thesis. G1-S4 binds directly to the virus particle hindering HSV-2 fusion through gB with host cell, while G2-S16 binds to cell-surface receptors. Then, the affinity of binding site may depend on the target cells in different epitheliums decreasing its effectiveness antiviral. The hypothesis that G1-S4 and G2-S16 dendrimers work in a different manner opens up the gate to alternative strategies such as the combination of the dendrimers not only with antiviral, but also with various non-specific nanocompounds acting at different stages of the HSV-2 life cycle. This strategy has proven to be effective against other viruses, such as HIV-1 or HCV (Sepulveda-Crespo et al., 2014, Xiao et al., 2015).

In addition, G1-S4, G2-S16 and G3-S16 have shown an additive or synergistic profile when combined with ACV or TDF. The obtained synergy can be due to the fact that the dendrimers and ACV or TDF act at different steps in the viral cycle. We have demonstrated that dendrimers act at the attachment and entry step, whereas ACV plays a role at replication level and TDF inhibits HSV-2 DNA polymerase (**Fig. 34** and **Table 8**) (Andrei et al., 2011).

Microbicides are applied directly to the genital tract or rectum before intercourse to protect against STIs. However, the activity of vaginal microbicides can be altered by the physiological characteristics of the vagina. Consequently, we studied the anti-HSV-2 activity of these candidates at various pHs and we proved that the vaginal pH exercised no significant influence on the antiherpetic activity of the dendrimers (**Fig. 27**).

HSV-2 vaginal and rectal challenge results reached *in vivo* are promising; G2-S16 has shown 100% protection against vaginal HSV-2 infection and G1-S4 has shown 90% of protection against vaginal HSV-2 infection and 90% against rectal HSV-2 infection (**Fig. 35, 36** and **37**). The high inhibitory

capacity of G1-S4 against HSV-2, equally to vaginal or rectal, could be due in large part to its ability to perform its function by direct binding to the particle virus, regardless of the environment in which it is found. The great morphological and structural difference between the vaginal and rectal epithelium could be the cause between different inhibitory activities shown with G2-S16, even more considering that this dendrimer attaches to proteins on the surface epithelial cells to carry out their antiherpetic activity. The multilayered epithelium of the vagina could offer a structural advantage over the simple columnar epithelium and stratified squamous epithelium of the rectum (Tanaka et al., 2012).

G1-S4 and G2-S16 are ideal antivirals because they play a major role in a multifunctional manner and are effective at non-cytotoxic concentrations easily achievable in BALB/c. G1-S4 acts directly on the HSV-2, inactivating it. Interestingly, G2-S16 provides protection due to its ability to bind to the host cell rather than to the viral particles. This has been showed previously for HIV-1 prevention, in which G2-S16 binds to the CD4-receptor and HIV-1 CCR5/CXCR4 co-receptors of the cells, in addition to binds to the gp120 of HIV-1 (Chonco et al., 2012). With these results, we can speculate on the existence of a second mechanism of action that can enable G2-S16 to maintain the 50% of its antiherpetic effect when it is applied 8 h later on exposure to HSV-2 333, suggesting that G2-S16 also exerts its inhibition at one different level than the virus cell attachment. This mechanism should be linked with later stage of the HSV-2 333 lifecycle.

Although the transmission of STIs stands out as the greatest problem of unprotected sex, it is also needed to take into account the possibility of unintended pregnancies. Annually there are about 200 million pregnancies, of which 40% are unintended. Therefore, a topical vaginal compound with dual activity as microbicide and contraceptive, which could prevent both the transmission of HIV-1 and HSV-2 as well as unintended pregnancies, emerges as a promising alternative. Throughout this work, it was evaluated the potential of combining the dendrimer G1-S4 or G2-S16 with the spermicide PD, in order to know its possible development as microbicidal gels of topical use for the prevention of sexual transmission of STIs and unintended pregnancies.

It is of great importance that all the properties already demonstrated for the polyanionic carbosilane dendrimers, and in particular for G2-S16 and G1-S4, were not modified in the presence of PD and *vice versa*.

In vitro HIV-1 inhibition experiments with G1-S4 or G2-S16 dendrimer and in combination with PD in the TZM.bl cell line and PBMC show that the percentage of inhibition in both viral R5-HIV- $1_{NL.AD8}$ or X4-HIV-$1_{NL.4.3}$ is practically the same compared with results obtained in the absence of PD (**Fig. 40**). On TZM.bl cells, in both presence and absence of PD, the percentage of inhibition is greater than 95% and 99% when the cells are pre-treated with G1-S4 or G2-S16 dendrimer. Similarly, the presence of PD does not modify the inhibition rates in PBMC. Differences in inhibition rates with both viral isolates used were not significant, although a higher percentage of inhibition was observed in the TZM.bl cell line and in the PBMC compared to the X4-HIV-$1_{NL.4.3}$ isolate. Several theories have been proposed as a possible explanation: polyanionic carbosilane dendrimers act as antiviral nanocompounds because they bind to the V3 region of the HIV-1 gp120. In the case of X4-HIV-$1_{NL.4.3}$ isolates, the V3 region of gp120 is more exposed at the viral surface. Thus, the availability of positive charges with which the dendrimers can interact is greater than in the case of the R5-HIV-$1_{NL.AD8}$ isolate, which use CCR5 as co-receptor and whose V3 region appears to have a more internal arrangement in the virus membrane (**Fig. 40**).

It was also shown that the combination of G1-S4 or G2-S16 with PD does not induce significant PBMC proliferation (**Fig. 42**). This property is of great relevance to develop a topical microbicide because an increase in the proliferation of PBMC by the combination of G1-S4 or G2-S16 with PD would favour PBMC recruitment, alter the profile of cytokine secretion, and there would be an increase in HIV-1 infection due to the fact that the CD4+ T lymphocytes are one of the main target cells of the HIV-1. PD is a plant-derived spermicide that induces its contraceptive action by disrupting the sperm plasma membrane (Lu et al., 2013). One of the hypotheses that could justify the antiviral activity *perse* presented by PD, which was studied by carrying out a time of addition assay, is that its saponin-like nature could act by disrupting the HIV-1 envelope (**Fig. 41**). This result would justify its performance on the early stages of the HIV-1 cycle.

A histopathological experiment was also performed on BALB/c mice, where it is shown that the daily administration for 7 days of a single dose of 3% gel of the polyanionic carbosilane dendrimer G1-S4 or G2-S16 in combination with the 0.25 mM of PD does not generate alteration of epithelial cells, or inflammation, or damage to the vaginal mucosa of BALB/c mice (**Table 9**). Although, it had previously been shown that the administration of one, two or seven doses of 3% gel of G2-S16 or G1-S14 in BALB/c mice did not cause any irritation or alteration on the epithelial barrier of the urogenital tract or

the vaginal mucosa (Cena-Diez et al., 2017), this experiment consolidates the use of the combination of PD as a biocompatible and safe potential spermicida in the genital tract.

Following *in vitro* HIV-1 assays and *in vivo* toxicity studies, we proceeded to evaluate whether the antiherpetic ability of the dendrimers remained intact in the presence of PD. As can be seen in **Fig. 44**, both dendrimers, G1-S4 and G2-S16, are capable of 100% halting of the vaginal transmission of HSV-2 after prophylactic application in combination with PD.

Moreover, on samples of human spermatozoa, it has been shown that the combination of PD at the concentration in which the compound produced its maximum spermicidal effect, 0.25 mM; together with the dendrimer G1-S4 or G2-S16, was able to induce a total decrease in sperm motility in less than 40 and 60 s, respectively. The maximum spermicidal effect of PD occurs at 20 s (**Fig. 43**). After copulation, the spermatozoa may take minutes to reach the vaginal canal, and about 10 min if they travel at an average velocity of approximately 25 μm/s, traversing the uterine cavity (Vasan, 2011, Suarez and Pacey, 2006). Although, it seems clear that the presence of the polyanionic carbosilane dendrimers somewhat retard the spermicidal action of saponin, it remains effective over a relatively short period of time. For this reason, 60 s are sufficient to consider the spermicidal action of the combination of the two dendrimers analyzed and PD to be completely effective.

13. Polyanionic carbosilane dendrimers against RSV infection

The RSV is the leading viral cause of respiratory morbidity and mortality in infants and young children worldwide (Lozano et al., 2012, Nair et al., 2010). The RSV is the major causal agent of bronchiolitis and diseases related to of the low respiratory track and it is estimated that 90% of children under 2 years of age have suffered some type of infection caused by this type of virus (Kutsaya et al., 2016) and 2% of the annual hospitalizations of children under 5 years are related to RSV (Pitzer et al., 2015). Despite the existence of drugs used in severe cases of RSV infection or as prophylaxis in high-risk patients, such as Palivizumab (Feltes et al., 2003), the fact that there is no effective drug to deal with RSV shows the need of the development of a new treatment effective against this virus.

In order to identify alternative molecules that provide significant improvements over existing therapies, a suitable target in the viral cycle must be identified. The HS stands out as such alternative. Many viruses use HSPGs as co-receptors or major receptors to infect the target cell. At the molecular level,

sulfate groups with negative charges of HSPG interact with the positive charges of the amino acids present in the HBD belonging to the RSV glycoprotein G. In addition, HSPGs ligand is known to be stable and long-lasting, suggesting that an HSPG-masking drug may retain its inhibitory effect for a prolonged period of time (Rusnati and Presta, 1996, Rusnati et al., 1993). This binding is potential target for the development of novel antiviral drugs based on molecules that are capable of slowing down or disrupting such as binding. In previous studies, the use of polyanionic heparin antagonist molecules capable of binding to RSV has been addressed as possible inhibitors of RSV infection (Donalisio et al., 2012).

It has been shown that polyanionic carbosilane dendrimers have been shown to have high antiviral activity against HIV-1, HIV-2 and HSV-2 (Briz et al., 2015, Cena-Diez et al., 2016b, Chonco et al., 2012). In this work, a series of carbosilane polyanionic dendrimers with different characteristics have been studied against RSV infection. The antiviral action of several dendrimers has been confirmed and their mechanism of action against RSV has been shown.

The evaluation of polianionic carbosilane dendrimers (G2-S16, G1-S4, G3-S16, G2-CTE16, G2-STE16 and G2-S24P) ability to inhibit RSV infection *in vitro* has shown that all of they are capable of halting the infection in a significant manner at their maximum non-toxic concentrations (**Fig. 46**). G2-S16, G1-S4 and G3-S16 dendrimers showed inhibitory values over 95%. Therefore, they were selected for further *in vitro* evaluation.

To date, it has been shown that G2-S16 or G1-S4 exert their capacity to block the interaction between HS and HBD, resulting in inhibition of infections generated by different viruses, such as HSV-2 (Cena-Diez et al., 2016b, Sepulveda-Crespo et al., 2015b, Vacas Cordoba et al., 2013, Vacas-Cordoba et al., 2014). RSV shares with these viruses the ability to bind heparin and the requirement for interaction with HSPGs on the target cell proteins for infection, to carry out the infection, either in their initial union or the fusion of viral membrane with the cell. The binding of the afore mentioned viruses to heparin and HSPGs depends on the presence of HBDs in their surface proteins. Therefore, we evaluated the capacity of the dendrimers to disrupt the initial interaction between the viral particle and their target cells (Rusnati et al., 2009).

The evaluation of the mechanism of action of the dendrimers showed that they were preventing the binding of the viral particles to the target cells (**Fig. 47A**). Also, as stated in the introduction, RSV

surface glicoproteins play an important role in RSV entry by binding to cell-surface HS (Bourgeois et al., 1998, Escribano-Romero et al., 2004, Feldman et al., 2000, Feldman et al., 1999, Harris and Werling, 2003, Karger et al., 2001, Krusat and Streckert, 1997, Martinez and Melero, 2000). G1-S4 and G3-S16 have sulfate groups on their surface, which lead to the hypothesis that these dendrimers could bind to RSV gG and gF and achieve their inhibitory effect. Viral inactivation assay showed that functionalized dendrimers with sulfate could bind directly on viral proteins on the surface of RSV particles and block and inactivate RSV infectivity (**Fig. 47B**). However, G2-S16, a sulfonate dendrimer, proved to carry out its inhibitory effect by binding to cellular surface molecules of host cell (**Fig. 47C**). Hence, it is possible that various polyanionic dendrimers show different binding specificities, although these dendrimers are generally considered nonspecific. This difference is due to the variability in the number of charged groups, the size, the structure of the polyanion, or the type of functional groups involved.

These data suggest that depending on the dendrimer characteristics, their mechanism of action changes. This result agrees with previously published data, where it was shown that the G2-S16 dendrimer also acts to protect the infection of the target cells against HSV-2. Therefore, it can be speculated that this dendrimer can act as a heparin analog, binding to HSPG receptors, masking HBD, competing with RSV and protecting cells from infection.

The G2-S16 was able to halt RSV infection in a significant manner through binding to host cell surface proteins and G1-S4 and G3-S16 did so by binding to the viral particles. However, we evaluated their ability to disturb syncytia formation by RSV. Syncytium formation is a well-known mechanism of cell-to-cell infection that contributes significantly to virus spread *in vivo*. In addition to the ability to halt RSV infection *in vitro*, the ability of G1-S16, G2-S16 and G3-S16 to abrogate syncytium formation as well as syncytium size in HEK-293T cell line was shown (**Fig. 49 and 50**). Concentrations of G2-S16 10 times lower than those needed to completely halt RSV infection were found to be high enough to inhibit RSV syncytium formation by 80%. The RSV infection inhibition by G2-S16 is concentration dependant reaching values of 95% at 5 µM (**Fig. 49A**). On the other hand, G1-S4 and G3-S16 were able to halt syncytium formation in 20% and 60%, respectively. This suggest that dendrimers targeting RSV virion are less likely to halt the syncytium formation than these targeting cellular receptors.

With regard to the potential administration of polianionic carbosilane dendrimers as a treatment against RSV *in vivo*, we assessed their biocompatibility on BALB/C mice. The results demonstrate that G2-S16 500 µM administrated intranasally is well tolerated by the mice, and no significant signs of damage were observed in the pulmonary parenchyma or the pleura (**Table 10**). Besides biocompatibility, we also assessed the antiviral activity of G2-S16 in BALB/c. It was shown that when mice infected with RSV were treated, four days later the viral yield decreased in 86% (**Fig. 51).**

Summing up, we have shown the efficacy of G2-S16 against RSV infection, as well as the mechanism of action by which it carries out its inhibitory action and its *in vivo* biocompatibility and inhibition *in vitro* and *in vivo*. All this gives an intrinsic value to G2-S16 to be formulated as an aerosol and to evaluate it in studies in greater depth both *in vivo* and in clinical trials against RSV infection. This treatment would alleviate the serious effects of pathologies generated by RSV in children under 5 years of age.

CONCLUSIONS

14. CONCLUSIONS

I. Polyanionic carbosilane dendrimers G2-S16, G2-ST16 and G3-S16 prevent *in vitro* HIV-1 infection in the presence of SEVI when applied alone, or in combination with TDF or MVC, in the concentration ranks studied, always under maximum non-toxic concentrations.

II. The evaluation of toxicity of G2-S16 dendrimer *in vivo* showed that vaginal application of G2-S16 3% w/v limits its distribution to the female vaginal tract, specifically to the non-sterile part. In addition, its vaginal application for 7 consecutive days was non-toxic.

III. G2-S16 dendrimer is non-toxic for *in vivo* application in BALB/c mice and zebrafish. It is also non-toxic in *ex-vivo* human artificial tissue (Epivaginal tissue) according to the MTT results at the studied concentrations.

IV. G1-S4, G2-S16 and G3-S16 have proved their ability to inhibit HSV-2 infection *in vitro*. These dendrimers inhibit the viral infection at the first steps of HSV-2 life-cycle: binding/entry-mediated events. G1-S4 and G3-S16 bind directly to the virus, inactivating it; whereas G2-S16 adheres to the host cell surface proteins. Molecular modeling of G1-S4 and G2-S16 with HSV-2 gB showed that G1-S4 binds better in general to selected binding sites on gB surface than G2-S16 and it is better suited to reach less accessible binding sites. In addition, G1-S4, G2-S16 and G3-S16 showed synergistic or additive effect in combination with ACV or TDF.

V. G1-S4 and G2-S16 dendrimers prevent HSV-2 infection *in vivo* in BALB/c mice. G1-S4 and G2-S16 showed 100% and 90% inhibition of HSV-2 after a vaginal challenge, respectively. In the case of anal exposure, G1-S4 inhibits 90% of the infection, whereas G2-S16 needs to be combined with TDF to exert significative inhibitory profile.

VI. Combination of carboxylane polyanionic dendrimers, G1-S4 and G2-S16, with Platicodin D showed that PD does not affect the antiviral activity of the dendrimers, and the dendrimers do not affect to the spermicide activity of PD. It was shown that combination of

PD with the polyanionic carbosilane dendrimers has a spermicide effect over human semen in less than 30 seconds.

VII. The efficacy of polyanionic carbosilane dendrimers G1-S4, G2-S16 and G3-S16 to stop RSV replication *in vitro* has been demonstrated. G1-S4 and G3-S16 bind directly to the virus, inactivating it, whereas G2-S16 adheres to the host cell surface proteins. G2-S16 dendrimer proved not to be toxic when applied intranasally to BALB/c mice and halted RSV infection by 80% at 500 µM.

CONCLUSIONES

I. Los dendrímeros polianiónicos carbosilanos G2-S16, G2-STE16 y G3-S16 previenen la infección por el VIH-1 en presencia de SEVI al aplicarse de forma independiente o en combinación con TDF o MCV, en el rango de concentraciones estudiadas y siempre dentro de las concentraciones máximas no tóxicas.

II. La evaluación de la toxicidad del dendrimero G2-S16 *in vivo* demostró que la aplicación vaginal del 3% (p/v) de G2-S16 limita su distribución al tracto genital femenino, concretamente a la parte no estéril. Además, cuando se aplicó el dendrímero a nivel vaginal durante 7 días consecutivos no mostró toxicidad.

III. El dendrímero G2-S16 no mostró toxicidad cuando se aplicó *in vivo* en ratones BALB/c y en pez cebra. Tampoco mostró toxicidad a 500 µM en tejido humano artificial *ex vivo*, tejido EpiVaginal, evaluado mediante un ensayo MTT.

IV. Se estudió la capacidad de los dendrímeros G1-S4, G2-S16 y G3-S16 para inhibir la infección por el VHS-2 *in vitro.* Estos dendrímeros inhiben la infección del VHS-2 en las primeras etapas del ciclo viral: unión-entrada. G1-S4 y G3-16 se unen directamente al VHS-2, inactivándolo; sin embargo, el G2-S16 se une a las proteínas de la superficie de la célula diana. El estudio de modelaje molecular de G1-S4 y G2-S16 con la gB del VHS-2 mostró que G1-S4 se une, generalmente, de manera más eficiente a los sitios de unión seleccionados en la superficie de la gB que el G2-S16 y, está mejor adaptado para llegar a los sitios de unión con peor accesibilidad. Además, G1-S4, G2-S16 y G3-S16 presentan un perfil sinérgico o aditivo en combinación de ACV o TDF.

V. G1-S4 y G2-S16 previenen la infección por el VHS-2 *in vivo* en ratones BALB/c. G1-S4 y G2-S16 mostraron un 90% y 100% de inhibición de VHS-2, respectivamente, tras una infección vaginal. A nivel rectal, G1-S4 inhibió la infección del VHS-2 un 90%, mientras que el G2-S16 necesitó de la combinación con TDF para obtener valores significativos de inhibición.

VI. La combinación de los dendrímeros polianiónicos carbosilanos, G1-S4 y G2-S16, con PD mostró que el PD no afecta a la actividad antiviral de los dendrímeros ni los dendrímeros afectan a la actividad espermicida de PD. Se demostró que la combinación del PD con G1-S4 y G2-S16 tiene un efecto espermicida sobre el semen humano en menos de 30 segundos.

VII. Se ha demostrado la eficacia de los dendrímeros polianiónicos carbosilanos G1-S4, G2-S16 y G3-S16 para frenar la replicación del RSV *in vitro*. G1-S4 y G3-S16 se unen al virus, inactivándolo; mientras que el G2-S16 se une a las proteínas de la superficie de la célula diana. G2-S16 demostró no ser tóxico cuando se aplicó de manera intranasal en ratones BALB/c inhibiendo el 80% de la infección del RSV a una concentración de 500 µM.

REFERENCES

15. REFERENCE

ABDOOL KARIM, S. S., RICHARDSON, B. A., RAMJEE, G., HOFFMAN, I. F., CHIRENJE, Z. M., TAHA, T., KAPINA, M., MASLANKOWSKI, L., COLETTI, A., PROFY, A., MOENCH, T. R., PIWOWAR-MANNING, E., MASSE, B., HILLIER, S. L. & SOTO-TORRES, L. 2011. Safety and effectiveness of BufferGel and 0.5% PRO2000 gel for the prevention of HIV infection in women. *AIDS,* 25**,** 957-66.

AKHTAR, J. & SHUKLA, D. 2009. Viral entry mechanisms: cellular and viral mediators of herpes simplex virus entry. *FEBS J,* 276**,** 7228-36.

ANDREI, G., LISCO, A., VANPOUILLE, C., INTROINI, A., BALESTRA, E., VAN DEN OORD, J., CIHLAR, T., PERNO, C. F., SNOECK, R., MARGOLIS, L. & BALZARINI, J. 2011. Topical tenofovir, a microbicide effective against HIV, inhibits herpes simplex virus-2 replication. *Cell Host Microbe,* 10**,** 379-89.

ARII, J., UEMA, M., MORIMOTO, T., SAGARA, H., AKASHI, H., ONO, E., ARASE, H. & KAWAGUCHI, Y. 2009. Entry of herpes simplex virus 1 and other alphaherpesviruses via the paired immunoglobulin-like type 2 receptor alpha. *J Virol,* 83**,** 4520-7.

ARNAIZ, E., DOUCEDE, L. I., GARCIA-GALLEGO, S., URBIOLA, K., GOMEZ, R., TROS DE ILARDUYA, C. & DE LA MATA, F. J. 2012. Synthesis of cationic carbosilane dendrimers via click chemistry and their use as effective carriers for DNA transfection into cancerous cells. *Mol Pharm,* 9**,** 433-47.

ARNOLD, F., SCHNELL, J., ZIRAFI, O., STURZEL, C., MEIER, C., WEIL, T., STANDKER, L., FORSSMANN, W. G., ROAN, N. R., GREENE, W. C., KIRCHHOFF, F. & MUNCH, J. 2012. Naturally occurring fragments from two distinct regions of the prostatic acid phosphatase form amyloidogenic enhancers of HIV infection. *J Virol,* 86**,** 1244-9.

AUGUST, A., GLENN, G. M., KPAMEGAN, E., HICKMAN, S. P., JANI, D., LU, H., THOMAS, D. N., WEN, J., PIEDRA, P. A. & FRIES, L. F. 2017. A Phase 2 randomized, observer-blind, placebo-controlled, dose-ranging trial of aluminum-adjuvanted respiratory syncytial virus F particle vaccine formulations in healthy women of childbearing age. *Vaccine,* 35**,** 3749-3759.

AVITABILE, E., FORGHIERI, C. & CAMPADELLI-FIUME, G. 2009. Cross talk among the glycoproteins involved in herpes simplex virus entry and fusion: the interaction between gB and gH/gL does not necessarily require gD. *J Virol,* 83**,** 10752-60.

BAKER, N. A., SEPT, D., JOSEPH, S., HOLST, M. J. & MCCAMMON, J. A. 2001. Electrostatics of nanosystems: Application to microtubules and the ribosome. *Proceedings of the National Academy of Sciences of the United States of America,* 98**,** 10037-10041.

BALDWIN, J., SHUKLA, D. & TIWARI, V. 2013. Members of 3-O-Sulfotransferases (3-OST) Family: A Valuable Tool from Zebrafish to Humans for Understanding Herpes Simplex Virus Entry. *Open Virol J,* 7**,** 5-11.

BARAM-PINTO, D., SHUKLA, S., RICHMAN, M., GEDANKEN, A., RAHIMIPOUR, S. & SARID, R. 2012. Surface-modified protein nanospheres as potential antiviral agents. *Chem Commun (Camb),* 48**,** 8359-61.

BARRE-SINOUSSI, F., CHERMANN, J. C., REY, F., NUGEYRE, M. T., CHAMARET, S., GRUEST, J., DAUGUET, C., AXLER-BLIN, C., VEZINET-BRUN, F., ROUZIOUX, C., ROZENBAUM, W. & MONTAGNIER, L. 1983. Isolation of a T-lymphotropic retrovirus from a patient at risk for acquired immune deficiency syndrome (AIDS). *Science,* 220**,** 868-71.

BARRE-SINOUSSI, F., ROSS, A. L. & DELFRAISSY, J. F. 2013. Past, present and future: 30 years of HIV research. *Nat Rev Microbiol,* 11**,** 877-83.

BASHA, S. H., TALLURI, D. & RAMINNI, N. P. 2013. Computational repositioning of ethno medicine elucidated gB-gH-gL complex as novel anti herpes drug target. *Bmc Complementary and Alternative Medicine,* 13.

BAYLY, C. I., CIEPLAK, P., CORNELL, W. D. & KOLLMAN, P. A. 1993. A WELL-BEHAVED ELECTROSTATIC POTENTIAL BASED METHOD USING CHARGE RESTRAINTS FOR DERIVING ATOMIC CHARGES - THE RESP MODEL. *Journal of Physical Chemistry,* 97**,** 10269-10280.

BELANGER, S. E., RAWLINGS, J. M. & CARR, G. J. 2013. Use of fish embryo toxicity tests for the prediction of acute fish toxicity to chemicals. *Environ Toxicol Chem,* 32**,** 1768-83.

BERKLEY, J. A., MUNYWOKI, P., NGAMA, M., KAZUNGU, S., ABWAO, J., BETT, A., LASSAUNIERE, R., KRESFELDER, T., CANE, P. A., VENTER, M., SCOTT, J. A. & NOKES, D. J. 2010. Viral etiology of severe pneumonia among Kenyan infants and children. *JAMA,* 303**,** 2051-7.

BERNSTEIN, D. I., STANBERRY, L. R., SACKS, S., AYISI, N. K., GONG, Y. H., IRELAND, J., MUMPER, R. J., HOLAN, G., MATTHEWS, B., MCCARTHY, T. & BOURNE, N. 2003. Evaluations of unformulated and formulated dendrimer-based microbicide candidates in mouse and guinea pig models of genital herpes. *Antimicrob Agents Chemother,* 47**,** 3784-8.

BLISH, C. A., MCCLELLAND, R. S., RICHARDSON, B. A., JAOKO, W., MANDALIYA, K., BAETEN, J. M. & OVERBAUGH, J. 2012. Genital Inflammation Predicts HIV-1 Shedding Independent of Plasma Viral Load and Systemic Inflammation. *J Acquir Immune Defic Syndr,* 61**,** 436-40.

BOURGEOIS, C., BOUR, J. B., LIDHOLT, K., GAUTHRAY, C. & POTHIER, P. 1998. Heparin-like structures on respiratory syncytial virus are involved in its infectivity in vitro. *J Virol,* 72**,** 7221-7.

BOWMAN, M. C., BALLARD, T. E., ACKERSON, C. J., FELDHEIM, D. L., MARGOLIS, D. M. & MELANDER, C. 2008. Inhibition of HIV fusion with multivalent gold nanoparticles. *J Am Chem Soc,* 130**,** 6896-7.

BOYOGLU-BARNUM, S., TODD, S. O., MENG, J., BARNUM, T. R., CHIRKOVA, T., HAYNES, L. M., JADHAO, S. J., TRIPP, R. A., OOMENS, A. G., MOORE, M. L. & ANDERSON, L. J. 2017. Mutating the CX3C Motif in the G Protein Should Make a Live Respiratory Syncytial Virus Vaccine Safer and More Effective. *J Virol,* 91.

BRANDENBURG, A. H., VAN BEEK, R., MOLL, H. A., OSTERHAUS, A. D. & CLAAS, E. C. 2000. G protein variation in respiratory syncytial virus group A does not correlate with clinical severity. *J Clin Microbiol,* 38**,** 3849-52.

BRIZ, V., SEPULVEDA-CRESPO, D., DINIZ, A. R., BORREGO, P., RODES, B., DE LA MATA, F. J., GOMEZ, R., TAVEIRA, N. & MUNOZ-FERNANDEZ, M. A. 2015. Development of water-soluble polyanionic carbosilane dendrimers as novel and highly potent topical anti-HIV-2 microbicides. *Nanoscale,* 7**,** 14669-83.

BUCHBINDER, S. P., KATZ, M. H., HESSOL, N. A., O'MALLEY, P. M. & HOLMBERG, S. D. 1994. Long-term HIV-1 infection without immunologic progression. *AIDS,* 8**,** 1123-8.

BUKRINSKY, M. I. & HAFFAR, O. K. 1998. HIV-1 nuclear import: matrix protein is back on center stage, this time together with Vpr. *Mol Med,* 4**,** 138-43.

BURROWS, F. S., CARLOS, L. M., BENZIMRA, M., MARRIOTT, D. J., HAVRYK, A. P., PLIT, M. L., MALOUF, M. A. & GLANVILLE, A. R. 2015. Oral ribavirin for respiratory syncytial virus infection after lung transplantation: Efficacy and cost-efficiency. *J Heart Lung Transplant,* 34**,** 958-62.

BUSQUET, F., NAGEL, R., VON LANDENBERG, F., MUELLER, S. O., HUEBLER, N. & BROSCHARD, T. H. 2008. Development of a new screening assay to identify proteratogenic substances using zebrafish danio rerio embryo combined with an exogenous mammalian metabolic activation system (mDarT). *Toxicol Sci,* 104**,** 177-88.

CALLE, A., UGRINOVA, I., EPSTEIN, A. L., BOUVET, P., DIAZ, J. J. & GRECO, A. 2008. Nucleolin is required for an efficient herpes simplex virus type 1 infection. *J Virol,* 82**,** 4762-73.

CARIAS, A. M., MCCOOMBE, S., MCRAVEN, M., ANDERSON, M., GALLOWAY, N., VANDERGRIFT, N., FOUGHT, A. J., LURAIN, J., DUPLANTIS, M., VEAZEY, R. S. & HOPE, T. J. 2013. Defining the interaction of HIV-1 with the mucosal barriers of the female reproductive tract. *J Virol,* 87**,** 11388-400.

CARON, J., REDDY, L. H., LEPETRE-MOUELHI, S., WACK, S., CLAYETTE, P., ROGEZ-KREUZ, C., YOUSFI, R., COUVREUR, P. & DESMAELE, D. 2010. Squalenoyl nucleoside monophosphate nanoassemblies: new prodrug strategy for the delivery of nucleotide analogues. *Bioorg Med Chem Lett,* 20**,** 2761-4.

CARTER, A. J., BOURGEOIS, S., O'BRIEN, N., ABELSOHN, K., THARAO, W., GREENE, S., MARGOLESE, S., KAIDA, A., SANCHEZ, M., PALMER, A. K., CESCON, A., DE POKOMANDY, A. & LOUTFY, M. R.

2013. Women-specific HIV/AIDS services: identifying and defining the components of holistic service delivery for women living with HIV/AIDS. *J Int AIDS Soc,* 16**,** 17433.

CENA-DIEZ, R., GARCIA-BRONCANO, P., DE LA MATA, F. J., GOMEZ, R. & MUNOZ-FERNANDEZ, M. A. 2016a. Efficacy of HIV antiviral polyanionic carbosilane dendrimer G2-S16 in the presence of semen. *Int J Nanomedicine,* 11**,** 2443-50.

CENA-DIEZ, R., GARCIA-BRONCANO, P., JAVIER DE LA MATA, F., GOMEZ, R., RESINO, S. & MUNOZ-FERNANDEZ, M. 2017. G2-S16 dendrimer as a candidate for a microbicide to prevent HIV-1 infection in women. *Nanoscale,* 9**,** 9732-9742.

CENA-DIEZ, R., VACAS-CORDOBA, E., GARCIA-BRONCANO, P., DE LA MATA, F. J., GOMEZ, R., MALY, M. & MUNOZ-FERNANDEZ, M. A. 2016b. Prevention of vaginal and rectal herpes simplex virus type 2 transmission in mice: mechanism of antiviral action. *Int J Nanomedicine,* 11**,** 2147-62.

CLARK, S. J., SAAG, M. S., DECKER, W. D., CAMPBELL-HILL, S., ROBERSON, J. L., VELDKAMP, P. J., KAPPES, J. C., HAHN, B. H. & SHAW, G. M. 1991. High titers of cytopathic virus in plasma of patients with symptomatic primary HIV-1 infection. *N Engl J Med,* 324**,** 954-60.

CLEMENT, C., TIWARI, V., SCANLAN, P. M., VALYI-NAGY, T., YUE, B. Y. & SHUKLA, D. 2006. A novel role for phagocytosis-like uptake in herpes simplex virus entry. *J Cell Biol,* 174**,** 1009-21.

COHEN, C. R., BROWN, J., MOSCICKI, A. B., BUKUSI, E. A., PAULL, J. R., PRICE, C. F. & SHIBOSKI, S. 2011. A phase I randomized placebo controlled trial of the safety of 3% SPL7013 Gel (VivaGel(R)) in healthy young women administered twice daily for 14 days. *PLoS One,* 6**,** e16258.

COLLINS, P. L. & MELERO, J. A. 2011. Progress in understanding and controlling respiratory syncytial virus: still crazy after all these years. *Virus Res,* 162**,** 80-99.

COOPER, R. S. & HELDWEIN, E. E. 2015. Herpesvirus gB: A Finely Tuned Fusion Machine. *Viruses,* 7**,** 6552-69.

COPELAND, A. M., NEWCOMB, W. W. & BROWN, J. C. 2009. Herpes simplex virus replication: roles of viral proteins and nucleoporins in capsid-nucleus attachment. *J Virol,* 83**,** 1660-8.

CORTINI, R. & WILKIE, N. M. 1978. Physical maps for HSV type 2 DNA with five restriction endonucleases. *J Gen Virol,* 39**,** 259-80.

CUSINI, M. & GHISLANZONI, M. 2001. The importance of diagnosing genital herpes. *J Antimicrob Chemother,* 47 Suppl T1**,** 9-16.

CUTLER, B. & JUSTMAN, J. 2008. Vaginal microbicides and the prevention of HIV transmission. *Lancet Infect Dis,* 8**,** 685-97.

CHANG, D. D. & SHARP, P. A. 1990. Messenger RNA transport and HIV rev regulation. *Science,* 249**,** 614-5.

CHIAPPETTA, D. A., FACORRO, G., DE CELIS, E. R. & SOSNIK, A. 2011. Synergistic encapsulation of the anti-HIV agent efavirenz within mixed poloxamine/poloxamer polymeric micelles. *Nanomedicine,* 7**,** 624-37.

CHOE, H., FARZAN, M., SUN, Y., SULLIVAN, N., ROLLINS, B., PONATH, P. D., WU, L., MACKAY, C. R., LAROSA, G., NEWMAN, W., GERARD, N., GERARD, C. & SODROSKI, J. 1996. The beta-chemokine receptors CCR3 and CCR5 facilitate infection by primary HIV-1 isolates. *Cell,* 85**,** 1135-48.

CHONCO, L., PION, M., VACAS, E., RASINES, B., MALY, M., SERRAMIA, M. J., LOPEZ-FERNANDEZ, L., DE LA MATA, J., ALVAREZ, S., GOMEZ, R. & MUNOZ-FERNANDEZ, M. A. 2012. Carbosilane dendrimer nanotechnology outlines of the broad HIV blocker profile. *J Control Release,* 161**,** 949-58.

CHOW, J. W., CHICELLA, M. F., CHRISTENSEN, A. M., MONEYMAKER, C. S., HARRINGTON, J. & DICE, J. E. 2017. Improving Palivizumab Compliance rough a Pharmacist-Managed RSV Prevention Clinic. *J Pediatr Pharmacol Ther,* 22**,** 338-343.

D.A. CASE, V., BABIN, J. T., BERRYMAN, R. M., BETZ, Q., CAI, D. S., CERUTTI, T. E., CHEATHAM, I., T.A , DARDEN, R. E., DUKE, H., GOHLKE, A. W., GOETZ, S., GUSAROV, N., HOMEYER, P., JANOWSKI, J., KAUS, I., KOLOSSVÁRY, A., KOVALENKO, T. S., LEE, S., LEGRAND, T., LUCHKO, R., LUO, B., MADEJ, K. M., MERZ, F., PAESANI, D. R., ROE, A., ROITBERG, C., SAGUI, R., SALOMON-FERRER,

G., SEABRA, C. L., SIMMERLING, W., SMITH, J., SWAILS, R. C., WALKER, J., WANG, R. M., WOLF, X. W. & KOLLMAN, P. A. 2014. AMBER 14, University of California, San Francisco. .

DAAR, E. S., MOUDGIL, T., MEYER, R. D. & HO, D. D. 1991. Transient high levels of viremia in patients with primary human immunodeficiency virus type 1 infection. *N Engl J Med,* 324**,** 961-4.

DALGLEISH, A. G., BEVERLEY, P. C., CLAPHAM, P. R., CRAWFORD, D. H., GREAVES, M. F. & WEISS, R. A. 1984. The CD4 (T4) antigen is an essential component of the receptor for the AIDS retrovirus. *Nature,* 312**,** 763-7.

DAVISON, A. J. & WILKIE, N. M. 1981. Nucleotide sequences of the joint between the L and S segments of herpes simplex virus types 1 and 2. *J Gen Virol,* 55**,** 315-31.

DEVINCENZO, J. P. 2004. Natural infection of infants with respiratory syncytial virus subgroups A and B: a study of frequency, disease severity, and viral load. *Pediatr Res,* 56**,** 914-7.

DICKENS, L. E., COLLINS, P. L. & WERTZ, G. W. 1984. Transcriptional mapping of human respiratory syncytial virus. *J Virol,* 52**,** 364-9.

DONALISIO, M., RUSNATI, M., CAGNO, V., CIVRA, A., BUGATTI, A., GIULIANI, A., PIRRI, G., VOLANTE, M., PAPOTTI, M., LANDOLFO, S. & LEMBO, D. 2012. Inhibition of human respiratory syncytial virus infectivity by a dendrimeric heparan sulfate-binding peptide. *Antimicrob Agents Chemother,* 56**,** 5278-88.

DRAGIC, T., LITWIN, V., ALLAWAY, G. P., MARTIN, S. R., HUANG, Y., NAGASHIMA, K. A., CAYANAN, C., MADDON, P. J., KOUP, R. A., MOORE, J. P. & PAXTON, W. A. 1996. HIV-1 entry into CD4+ cells is mediated by the chemokine receptor CC-CKR-5. *Nature,* 381**,** 667-73.

DRAIN, P. K., SMITH, J. S., HUGHES, J. P., HALPERIN, D. T. & HOLMES, K. K. 2004. Correlates of national HIV seroprevalence: an ecologic analysis of 122 developing countries. *J Acquir Immune Defic Syndr,* 35**,** 407-20.

DUPRADEAU, F. Y., PIGACHE, A., ZAFFRAN, T., SAVINEAU, C., LELONG, R., GRIVEL, N., LELONG, D., ROSANSKI, W. & CIEPLAK, P. 2010. The R.ED. tools: advances in RESP and ESP charge derivation and force field library building. *Physical Chemistry Chemical Physics,* 12**,** 7821-7839.

DUTTA, T., AGASHE, H. B., GARG, M., BALAKRISHNAN, P., KABRA, M. & JAIN, N. K. 2007. Poly (propyleneimine) dendrimer based nanocontainers for targeting of efavirenz to human monocytes/macrophages in vitro. *J Drug Target,* 15**,** 89-98.

EMERMAN, M. & MALIM, M. H. 1998. HIV-1 regulatory/accessory genes: keys to unraveling viral and host cell biology. *Science,* 280**,** 1880-4.

ESCRIBANO-ROMERO, E., RAWLING, J., GARCIA-BARRENO, B. & MELERO, J. A. 2004. The soluble form of human respiratory syncytial virus attachment protein differs from the membrane-bound form in its oligomeric state but is still capable of binding to cell surface proteoglycans. *J Virol,* 78**,** 3524-32.

FARRELL, M. J., MARGOLIS, T. P., GOMES, W. A. & FELDMAN, L. T. 1994. Effect of the transcription start region of the herpes simplex virus type 1 latency-associated transcript promoter on expression of productively infected neurons in vivo. *J Virol,* 68**,** 5337-43.

FELDMAN, S. A., AUDET, S. & BEELER, J. A. 2000. The fusion glycoprotein of human respiratory syncytial virus facilitates virus attachment and infectivity via an interaction with cellular heparan sulfate. *J Virol,* 74**,** 6442-7.

FELDMAN, S. A., HENDRY, R. M. & BEELER, J. A. 1999. Identification of a linear heparin binding domain for human respiratory syncytial virus attachment glycoprotein G. *J Virol,* 73**,** 6610-7.

FELTES, T. F., CABALKA, A. K., MEISSNER, H. C., PIAZZA, F. M., CARLIN, D. A., TOP, F. H., JR., CONNOR, E. M. & SONDHEIMER, H. M. 2003. Palivizumab prophylaxis reduces hospitalization due to respiratory syncytial virus in young children with hemodynamically significant congenital heart disease. *J Pediatr,* 143**,** 532-40.

FENG, Y., BRODER, C. C., KENNEDY, P. E. & BERGER, E. A. 1996. HIV-1 entry cofactor: functional cDNA cloning of a seven-transmembrane, G protein-coupled receptor. *Science,* 272**,** 872-7.

FICHOROVA, R. N., TUCKER, L. D. & ANDERSON, D. J. 2001. The molecular basis of nonoxynol-9-induced vaginal inflammation and its possible relevance to human immunodeficiency virus type 1 transmission. *J Infect Dis,* 184**,** 418-28.

FLEMING, D. T., MCQUILLAN, G. M., JOHNSON, R. E., NAHMIAS, A. J., ARAL, S. O., LEE, F. K. & ST LOUIS, M. E. 1997. Herpes simplex virus type 2 in the United States, 1976 to 1994. *N Engl J Med,* 337**,** 1105-11.

FREEMAN, E. E., WEISS, H. A., GLYNN, J. R., CROSS, P. L., WHITWORTH, J. A. & HAYES, R. J. 2006. Herpes simplex virus 2 infection increases HIV acquisition in men and women: systematic review and meta-analysis of longitudinal studies. *AIDS,* 20**,** 73-83.

FUJIMOTO, Y., TOMIOKA, Y., OZAKI, K., TAKEDA, K., SUYAMA, H., YAMAMOTO, S., TAKAKUWA, H., MORIMATSU, M., UEDE, T. & ONO, E. 2017. Comparison of the antiviral potential among soluble forms of herpes simplex virus type-2 glycoprotein D receptors, herpes virus entry mediator A, nectin-1 and nectin-2, in transgenic mice. *J Gen Virol,* 98**,** 1815-1822.

GABIZON, A., CATANE, R., UZIELY, B., KAUFMAN, B., SAFRA, T., COHEN, R., MARTIN, F., HUANG, A. & BARENHOLZ, Y. 1994. Prolonged circulation time and enhanced accumulation in malignant exudates of doxorubicin encapsulated in polyethylene-glycol coated liposomes. *Cancer Res,* 54**,** 987-92.

GAGLIARDI, M. 2017. Biomimetic and bioinspired nanoparticles for targeted drug delivery. *Ther Deliv,* 8**,** 289-299.

GALLO, P., PICCINNO, M., PAGNI, S. & TAVOLATO, B. 1988. Interleukin-2 levels in serum and cerebrospinal fluid of multiple sclerosis patients. *Ann Neurol,* 24**,** 795-7.

GANOR, Y., ZHOU, Z., TUDOR, D., SCHMITT, A., VACHER-LAVENU, M. C., GIBAULT, L., THIOUNN, N., TOMASINI, J., WOLF, J. P. & BOMSEL, M. 2010. Within 1 h, HIV-1 uses viral synapses to enter efficiently the inner, but not outer, foreskin mucosa and engages Langerhans-T cell conjugates. *Mucosal Immunol,* 3**,** 506-22.

GARCIA-MERINO, I., DE LAS CUEVAS, N., JIMENEZ, J. L., GALLEGO, J., GOMEZ, C., PRIETO, C., SERRAMIA, M. J., LORENTE, R. & MUNOZ-FERNANDEZ, M. A. 2009. The Spanish HIV BioBank: a model of cooperative HIV research. *Retrovirology,* 6**,** 27.

GAYNOR, R. 1992. Cellular transcription factors involved in the regulation of HIV-1 gene expression. *AIDS,* 6**,** 347-63.

GILJOHANN, D. A., SEFEROS, D. S., DANIEL, W. L., MASSICH, M. D., PATEL, P. C. & MIRKIN, C. A. 2010. Gold nanoparticles for biology and medicine. *Angew Chem Int Ed Engl,* 49**,** 3280-94.

GOLDBERG, M., LANGER, R. & JIA, X. 2007. Nanostructured materials for applications in drug delivery and tissue engineering. *J Biomater Sci Polym Ed,* 18**,** 241-68.

GOLDSTEIN, E., GREENE, S. K., OLSON, D. R., HANAGE, W. P. & LIPSITCH, M. 2015. Estimating the hospitalization burden associated with influenza and respiratory syncytial virus in New York City, 2003-2011. *Influenza Other Respir Viruses,* 9**,** 225-33.

GONZALEZ-SANZ, R., MATA, M., BERMEJO-MARTIN, J., ALVAREZ, A., CORTIJO, J., MELERO, J. A. & MARTINEZ, I. 2016. ISG15 Is Upregulated in Respiratory Syncytial Virus Infection and Reduces Virus Growth through Protein ISGylation. *J Virol,* 90**,** 3428-38.

GONZALEZ, M. E. 2017. The HIV-1 Vpr Protein: A Multifaceted Target for Therapeutic Intervention. *Int J Mol Sci,* 18.

GOTZ, A. W., WILLIAMSON, M. J., XU, D., POOLE, D., LE GRAND, S. & WALKER, R. C. 2012. Routine Microsecond Molecular Dynamics Simulations with AMBER on GPUs. 1. Generalized Born. *Journal of Chemical Theory and Computation,* 8**,** 1542-1555.

GRANT, R. M., HAMER, D., HOPE, T., JOHNSTON, R., LANGE, J., LEDERMAN, M. M., LIEBERMAN, J., MILLER, C. J., MOORE, J. P., MOSIER, D. E., RICHMAN, D. D., SCHOOLEY, R. T., SPRINGER, M. S., VEAZEY, R. S. & WAINBERG, M. A. 2008. Whither or wither microbicides? *Science,* 321**,** 532-4.

GUPTA, R., WARREN, T. & WALD, A. 2007. Genital herpes. *Lancet,* 370**,** 2127-37.

HAASE, A. T. 2011. Early events in sexual transmission of HIV and SIV and opportunities for interventions. *Annu Rev Med,* 62**,** 127-39.

HALL, C. B., WEINBERG, G. A., IWANE, M. K., BLUMKIN, A. K., EDWARDS, K. M., STAAT, M. A., AUINGER, P., GRIFFIN, M. R., POEHLING, K. A., ERDMAN, D., GRIJALVA, C. G., ZHU, Y. & SZILAGYI, P. 2009. The burden of respiratory syncytial virus infection in young children. *N Engl J Med,* 360**,** 588-98.

HARRIS, J. & WERLING, D. 2003. Binding and entry of respiratory syncytial virus into host cells and initiation of the innate immune response. *Cell Microbiol,* 5**,** 671-80.

HASSAN, S. T. S., SUDOMOVA, M. & MASARCIKOVA, R. 2017. [Herpes simplex virus infection: an overview of the problem, pharmacologic therapy and dietary measures]. *Ceska Slov Farm,* 66**,** 95-102.

HAWKINS, G. D., CRAMER, C. J. & TRUHLAR, D. G. 1996. Parametrized models of aqueous free energies of solvation based on pairwise descreening of solute atomic charges from a dielectric medium. *Journal of Physical Chemistry,* 100**,** 19824-19839.

HELDWEIN, E. E. 2016. gH/gL supercomplexes at early stages of herpesvirus entry. *Curr Opin Virol,* 18**,** 1-8.

HEROLD, B. C., MESQUITA, P. M., MADAN, R. P. & KELLER, M. J. 2011. Female genital tract secretions and semen impact the development of microbicides for the prevention of HIV and other sexually transmitted infections. *Am J Reprod Immunol,* 65**,** 325-33.

HIRSH, S., HINDIYEH, M., KOLET, L., REGEV, L., SHERBANY, H., YAARY, K., MENDELSON, E. & MANDELBOIM, M. 2014. Epidemiological changes of respiratory syncytial virus (RSV) infections in Israel. *PLoS One,* 9**,** e90515.

HOGAN, A. B., CAMPBELL, P. T., BLYTH, C. C., LIM, F. J., FATHIMA, P., DAVIS, S., MOORE, H. C. & GLASS, K. 2017. Potential impact of a maternal vaccine for RSV: A mathematical modelling study. *Vaccine,* 35**,** 6172-6179.

HOWE, K., CLARK, M. D., TORROJA, C. F., TORRANCE, J., BERTHELOT, C., MUFFATO, M., COLLINS, J. E., HUMPHRAY, S., MCLAREN, K., MATTHEWS, L., MCLAREN, S., SEALY, I., CACCAMO, M., CHURCHER, C., SCOTT, C., BARRETT, J. C., KOCH, R., RAUCH, G. J., WHITE, S., CHOW, W., KILIAN, B., QUINTAIS, L. T., GUERRA-ASSUNCAO, J. A., ZHOU, Y., GU, Y., YEN, J., VOGEL, J. H., EYRE, T., REDMOND, S., BANERJEE, R., CHI, J., FU, B., LANGLEY, E., MAGUIRE, S. F., LAIRD, G. K., LLOYD, D., KENYON, E., DONALDSON, S., SEHRA, H., ALMEIDA-KING, J., LOVELAND, J., TREVANION, S., JONES, M., QUAIL, M., WILLEY, D., HUNT, A., BURTON, J., SIMS, S., MCLAY, K., PLUMB, B., DAVIS, J., CLEE, C., OLIVER, K., CLARK, R., RIDDLE, C., ELLIOT, D., THREADGOLD, G., HARDEN, G., WARE, D., BEGUM, S., MORTIMORE, B., KERRY, G., HEATH, P., PHILLIMORE, B., TRACEY, A., CORBY, N., DUNN, M., JOHNSON, C., WOOD, J., CLARK, S., PELAN, S., GRIFFITHS, G., SMITH, M., GLITHERO, R., HOWDEN, P., BARKER, N., LLOYD, C., STEVENS, C., HARLEY, J., HOLT, K., PANAGIOTIDIS, G., LOVELL, J., BEASLEY, H., HENDERSON, C., GORDON, D., AUGER, K., WRIGHT, D., COLLINS, J., RAISEN, C., DYER, L., LEUNG, K., ROBERTSON, L., AMBRIDGE, K., LEONGAMORNLERT, D., MCGUIRE, S., GILDERTHORP, R., GRIFFITHS, C., MANTHRAVADI, D., NICHOL, S., BARKER, G., et al. 2013. The zebrafish reference genome sequence and its relationship to the human genome. *Nature,* 496**,** 498-503.

HU, K., HE, S., XIAO, J., LI, M., LUO, S., ZHANG, M. & HU, Q. 2017. Interaction between herpesvirus entry mediator and HSV-2 glycoproteins mediates HIV-1 entry of HSV-2-infected epithelial cells. *J Gen Virol,* 98**,** 2351-2361.

HUSKENS, D., VERMEIRE, K., PROFY, A. T. & SCHOLS, D. 2009. The candidate sulfonated microbicide, PRO 2000, has potential multiple mechanisms of action against HIV-1. *Antiviral Res,* 84**,** 38-47.

JOHNSTON, C., KOELLE, D. M. & WALD, A. 2014. Current status and prospects for development of an HSV vaccine. *Vaccine,* 32**,** 1553-60.

JOHNSTON, C., SARACINO, M., KUNTZ, S., MAGARET, A., SELKE, S., HUANG, M. L., SCHIFFER, J. T., KOELLE, D. M., COREY, L. & WALD, A. 2012. Standard-dose and high-dose daily antiviral therapy for short episodes of genital HSV-2 reactivation: three randomised, open-label, cross-over trials. *Lancet,* 379**,** 641-7.

JORGENSEN, W. L., CHANDRASEKHAR, J., MADURA, J. D., IMPEY, R. W. & KLEIN, M. L. 1983. COMPARISON OF SIMPLE POTENTIAL FUNCTIONS FOR SIMULATING LIQUID WATER. *Journal of Chemical Physics,* 79**,** 926-935.

KAESTLE, C. E., HALPERN, C. T., MILLER, W. C. & FORD, C. A. 2005. Young age at first sexual intercourse and sexually transmitted infections in adolescents and young adults. *Am J Epidemiol,* 161**,** 774-80.

KARGER, A., SCHMIDT, U. & BUCHHOLZ, U. J. 2001. Recombinant bovine respiratory syncytial virus with deletions of the G or SH genes: G and F proteins bind heparin. *J Gen Virol,* 82**,** 631-40.

KAUVAR, L. M., HARCOURT, J. L., HAYNES, L. M. & TRIPP, R. A. 2010. Therapeutic targeting of respiratory syncytial virus G-protein. *Immunotherapy,* 2**,** 655-61.

KELLER, M. J., MESQUITA, P. M., TORRES, N. M., CHO, S., SHUST, G., MADAN, R. P., COHEN, H. W., PETRIE, J., FORD, T., SOTO-TORRES, L., PROFY, A. T. & HEROLD, B. C. 2010. Postcoital bioavailability and antiviral activity of 0.5% PRO 2000 gel: implications for future microbicide clinical trials. *PLoS One,* 5**,** e8781.

KIM, K. A., YOLAMANOVA, M., ZIRAFI, O., ROAN, N. R., STAENDKER, L., FORSSMANN, W. G., BURGENER, A., DEJUCQ-RAINSFORD, N., HAHN, B. H., SHAW, G. M., GREENE, W. C., KIRCHHOFF, F. & MUNCH, J. 2010. Semen-mediated enhancement of HIV infection is donor-dependent and correlates with the levels of SEVI. *Retrovirology,* 7**,** 55.

KLAJNERT, B. & BRYSZEWSKA, M. 2001. Dendrimers: properties and applications. *Acta Biochim Pol,* 48**,** 199-208.

KLATZMANN, D., CHAMPAGNE, E., CHAMARET, S., GRUEST, J., GUETARD, D., HERCEND, T., GLUCKMAN, J. C. & MONTAGNIER, L. 1984. T-lymphocyte T4 molecule behaves as the receptor for human retrovirus LAV. *Nature,* 312**,** 767-8.

KNOBEL, M., BUSSER, F. J., RICO-RICO, A., KRAMER, N. I., HERMENS, J. L., HAFNER, C., TANNEBERGER, K., SCHIRMER, K. & SCHOLZ, S. 2012. Predicting adult fish acute lethality with the zebrafish embryo: relevance of test duration, endpoints, compound properties, and exposure concentration analysis. *Environ Sci Technol,* 46**,** 9690-700.

KOSZ-VNENCHAK, M., JACOBSON, J., COEN, D. M. & KNIPE, D. M. 1993. Evidence for a novel regulatory pathway for herpes simplex virus gene expression in trigeminal ganglion neurons. *J Virol,* 67**,** 5383-93.

KRUSAT, T. & STRECKERT, H. J. 1997. Heparin-dependent attachment of respiratory syncytial virus (RSV) to host cells. *Arch Virol,* 142**,** 1247-54.

KUMAR, A., MA, H., ZHANG, X., HUANG, K., JIN, S., LIU, J., WEI, T., CAO, W., ZOU, G. & LIANG, X. J. 2012. Gold nanoparticles functionalized with therapeutic and targeted peptides for cancer treatment. *Biomaterials,* 33**,** 1180-9.

KUTSAYA, A., TEROS-JAAKKOLA, T., KAKKOLA, L., TOIVONEN, L., PELTOLA, V., WARIS, M. & JULKUNEN, I. 2016. Prospective clinical and serological follow-up in early childhood reveals a high rate of subclinical RSV infection and a relatively high reinfection rate within the first 3 years of life. *Epidemiol Infect,* 144**,** 1622-33.

LACKMAN-SMITH, C., OSTERLING, C., LUCKENBAUGH, K., MANKOWSKI, M., SNYDER, B., LEWIS, G., PAULL, J., PROFY, A., PTAK, R. G., BUCKHEIT, R. W., JR., WATSON, K. M., CUMMINS, J. E., JR. & SANDERS-BEER, B. E. 2008. Development of a comprehensive human immunodeficiency virus type 1 screening algorithm for discovery and preclinical testing of topical microbicides. *Antimicrob Agents Chemother,* 52**,** 1768-81.

LAMMER, E., CARR, G. J., WENDLER, K., RAWLINGS, J. M., BELANGER, S. E. & BRAUNBECK, T. 2009. Is the fish embryo toxicity test (FET) with the zebrafish (Danio rerio) a potential alternative for the fish acute toxicity test? *Comp Biochem Physiol C Toxicol Pharmacol,* 149**,** 196-209.

LAWRENCE, C. 2011. Advances in zebrafish husbandry and management. *Methods Cell Biol,* 104**,** 429-51.

LAZNIEWSKA, J., MILOWSKA, K. & GABRYELAK, T. 2012. Dendrimers--revolutionary drugs for infectious diseases. *Wiley Interdiscip Rev Nanomed Nanobiotechnol,* 4**,** 469-91.

LE, T., WRIGHT, E. J., SMITH, D. M., HE, W., CATANO, G., OKULICZ, J. F., YOUNG, J. A., CLARK, R. A., RICHMAN, D. D., LITTLE, S. J. & AHUJA, S. K. 2013. Enhanced CD4+ T-cell recovery with earlier HIV-1 antiretroviral therapy. *N Engl J Med,* 368**,** 218-30.

LIFLAND, A. W., JUNG, J., ALONAS, E., ZURLA, C., CROWE, J. E., JR. & SANTANGELO, P. J. 2012. Human respiratory syncytial virus nucleoprotein and inclusion bodies antagonize the innate immune response mediated by MDA5 and MAVS. *J Virol,* 86**,** 8245-58.

LIFSON, A. R., BUCHBINDER, S. P., SHEPPARD, H. W., MAWLE, A. C., WILBER, J. C., STANLEY, M., HART, C. E., HESSOL, N. A. & HOLMBERG, S. D. 1991. Long-term human immunodeficiency virus infection in asymptomatic homosexual and bisexual men with normal CD4+ lymphocyte counts: immunologic and virologic characteristics. *J Infect Dis,* 163**,** 959-65.

LII, J. H. & ALLINGER, N. L. 1991. THE MM3 FORCE-FIELD FOR AMIDES, POLYPEPTIDES AND PROTEINS. *Journal of Computational Chemistry,* 12**,** 186-199.

LINDQUIST, M. E., MAINOU, B. A., DERMODY, T. S. & CROWE, J. E., JR. 2011. Activation of protein kinase R is required for induction of stress granules by respiratory syncytial virus but dispensable for viral replication. *Virology,* 413**,** 103-10.

LOOKER, K. J., ELMES, J. A. R., GOTTLIEB, S. L., SCHIFFER, J. T., VICKERMAN, P., TURNER, K. M. E. & BOILY, M. C. 2017. Effect of HSV-2 infection on subsequent HIV acquisition: an updated systematic review and meta-analysis. *Lancet Infect Dis*.

LOOKER, K. J. & GARNETT, G. P. 2005. A systematic review of the epidemiology and interaction of herpes simplex virus types 1 and 2. *Sex Transm Infect,* 81**,** 103-7.

LOOKER, K. J., MAGARET, A. S., TURNER, K. M., VICKERMAN, P., GOTTLIEB, S. L. & NEWMAN, L. M. 2015. Global estimates of prevalent and incident herpes simplex virus type 2 infections in 2012. *PLoS One,* 10**,** e114989.

LOZANO, R., NAGHAVI, M., FOREMAN, K., LIM, S., SHIBUYA, K., ABOYANS, V., ABRAHAM, J., ADAIR, T., AGGARWAL, R., AHN, S. Y., ALVARADO, M., ANDERSON, H. R., ANDERSON, L. M., ANDREWS, K. G., ATKINSON, C., BADDOUR, L. M., BARKER-COLLO, S., BARTELS, D. H., BELL, M. L., BENJAMIN, E. J., BENNETT, D., BHALLA, K., BIKBOV, B., BIN ABDULHAK, A., BIRBECK, G., BLYTH, F., BOLLIGER, I., BOUFOUS, S., BUCELLO, C., BURCH, M., BURNEY, P., CARAPETIS, J., CHEN, H., CHOU, D., CHUGH, S. S., COFFENG, L. E., COLAN, S. D., COLQUHOUN, S., COLSON, K. E., CONDON, J., CONNOR, M. D., COOPER, L. T., CORRIERE, M., CORTINOVIS, M., DE VACCARO, K. C., COUSER, W., COWIE, B. C., CRIQUI, M. H., CROSS, M., DABHADKAR, K. C., DAHODWALA, N., DE LEO, D., DEGENHARDT, L., DELOSSANTOS, A., DENENBERG, J., DES JARLAIS, D. C., DHARMARATNE, S. D., DORSEY, E. R., DRISCOLL, T., DUBER, H., EBEL, B., ERWIN, P. J., ESPINDOLA, P., EZZATI, M., FEIGIN, V., FLAXMAN, A. D., FOROUZANFAR, M. H., FOWKES, F. G., FRANKLIN, R., FRANSEN, M., FREEMAN, M. K., GABRIEL, S. E., GAKIDOU, E., GASPARI, F., GILLUM, R. F., GONZALEZ-MEDINA, D., HALASA, Y. A., HARING, D., HARRISON, J. E., HAVMOELLER, R., HAY, R. J., HOEN, B., HOTEZ, P. J., HOY, D., JACOBSEN, K. H., JAMES, S. L., JASRASARIA, R., JAYARAMAN, S., JOHNS, N., KARTHIKEYAN, G., KASSEBAUM, N., KEREN, A., KHOO, J. P., KNOWLTON, L. M., KOBUSINGYE, O., KORANTENG, A., KRISHNAMURTHI, R., LIPNICK, M., LIPSHULTZ, S. E., OHNO, S. L., et al. 2012. Global and regional mortality from 235 causes of death for 20 age groups in 1990 and 2010: a systematic analysis for the Global Burden of Disease Study 2010. *Lancet,* 380**,** 2095-128.

LU, Z., WANG, L., ZHOU, R., QIU, Y., YANG, L., ZHANG, C., CAI, M., MI, M. & XU, H. 2013. Evaluation of the spermicidal and contraceptive activity of Platycodin D, a Saponin from Platycodon grandiflorum. *PLoS One,* 8**,** e82068.

MA, N., MA, C., DENG, Y., WANG, T. & HE, N. 2013. Advances in applications of dendritic compounds. *J Nanosci Nanotechnol,* 13**,** 33-9.

MALLIPEDDI, R. & ROHAN, L. C. 2010. Progress in antiretroviral drug delivery using nanotechnology. *Int J Nanomedicine,* 5**,** 533-47.

MARCHI, S., TROMBETTA, C. M., GASPARINI, R., TEMPERTON, N. & MONTOMOLI, E. 2017. Epidemiology of herpes simplex virus type 1 and 2 in Italy: a seroprevalence study from 2000 to 2014. *J Prev Med Hyg,* 58**,** E27-E33.

MARTINEZ, I., DOPAZO, J. & MELERO, J. A. 1997. Antigenic structure of the human respiratory syncytial virus G glycoprotein and relevance of hypermutation events for the generation of antigenic variants. *J Gen Virol,* 78 (Pt 10)**,** 2419-29.

MARTINEZ, I., LOMBARDIA, L., GARCIA-BARRENO, B., DOMINGUEZ, O. & MELERO, J. A. 2007. Distinct gene subsets are induced at different time points after human respiratory syncytial virus infection of A549 cells. *J Gen Virol,* 88**,** 570-81.

MARTINEZ, I. & MELERO, J. A. 2000. Binding of human respiratory syncytial virus to cells: implication of sulfated cell surface proteoglycans. *J Gen Virol,* 81**,** 2715-22.

MAURER, U. E., ZEEV-BEN-MORDEHAI, T., PANDURANGAN, A. P., CAIRNS, T. M., HANNAH, B. P., WHITBECK, J. C., EISENBERG, R. J., COHEN, G. H., TOPF, M., HUISKONEN, J. T. & GRUNEWALD, K. 2013. The Structure of Herpesvirus Fusion Glycoprotein B-Bilayer Complex Reveals the Protein-Membrane and Lateral Protein-Protein Interaction. *Structure,* 21**,** 1396-1405.

MBIGUINO, A. & MENEZES, J. 1991. Purification of human respiratory syncytial virus: superiority of sucrose gradient over percoll, renografin, and metrizamide gradients. *J Virol Methods,* 31**,** 161-70.

MCCORMACK, S., RAMJEE, G., KAMALI, A., REES, H., CROOK, A. M., GAFOS, M., JENTSCH, U., POOL, R., CHISEMBELE, M., KAPIGA, S., MUTEMWA, R., VALLELY, A., PALANEE, T., SOOKRAJH, Y., LACEY, C. J., DARBYSHIRE, J., GROSSKURTH, H., PROFY, A., NUNN, A., HAYES, R. & WEBER, J. 2010. PRO2000 vaginal gel for prevention of HIV-1 infection (Microbicides Development Programme 301): a phase 3, randomised, double-blind, parallel-group trial. *Lancet,* 376**,** 1329-37.

MCGEOCH, D. J., RIXON, F. J. & DAVISON, A. J. 2006. Topics in herpesvirus genomics and evolution. *Virus Res,* 117**,** 90-104.

MCGOWAN, I., GOMEZ, K., BRUDER, K., FEBO, I., CHEN, B. A., RICHARDSON, B. A., HUSNIK, M., LIVANT, E., PRICE, C. & JACOBSON, C. 2011. Phase 1 randomized trial of the vaginal safety and acceptability of SPL7013 gel (VivaGel) in sexually active young women (MTN-004). *AIDS,* 25**,** 1057-64.

MCNEIL, S. E. 2011. Unique benefits of nanotechnology to drug delivery and diagnostics. *Methods Mol Biol,* 697**,** 3-8.

MEISSNER, H. C., WELLIVER, R. C., CHARTRAND, S. A., LAW, B. J., WEISMAN, L. E., DORKIN, H. L. & RODRIGUEZ, W. J. 1999. Immunoprophylaxis with palivizumab, a humanized respiratory syncytial virus monoclonal antibody, for prevention of respiratory syncytial virus infection in high risk infants: a consensus opinion. *Pediatr Infect Dis J,* 18**,** 223-31.

MILLER, B. R., MCGEE, T. D., SWAILS, J. M., HOMEYER, N., GOHLKE, H. & ROITBERG, A. E. 2012. MMPBSA.py: An Efficient Program for End-State Free Energy Calculations. *Journal of Chemical Theory and Computation,* 8**,** 3314-3321.

MITTERREITER, J. G., TITULAER, M. J., VAN NIEROP, G. P., VAN KAMPEN, J. J., ARON, G. I., OSTERHAUS, A. D., VERJANS, G. M. & OUWENDIJK, W. J. 2016. Prevalence of Intrathecal Acyclovir Resistant Virus in Herpes Simplex Encephalitis Patients. *PLoS One,* 11**,** e0155531.

MOHAN, P., SCHOLS, D., BABA, M. & DE CLERCQ, E. 1992. Sulfonic acid polymers as a new class of human immunodeficiency virus inhibitors. *Antiviral Res,* 18**,** 139-50.

MONDOR, I., UGOLINI, S. & SATTENTAU, Q. J. 1998. Human immunodeficiency virus type 1 attachment to HeLa CD4 cells is CD4 independent and gp120 dependent and requires cell surface heparans. *J Virol,* 72**,** 3623-34.

MORA-HUERTAS, C. E., FESSI, H. & ELAISSARI, A. 2010. Polymer-based nanocapsules for drug delivery. *Int J Pharm,* 385**,** 113-42.

MOSCICKI, A. B., KAUL, R., MA, Y., SCOTT, M. E., DAUD, II, BUKUSI, E. A., SHIBOSKI, S., REBBAPRAGADA, A., HUIBNER, S. & COHEN, C. R. 2012. Measurement of mucosal biomarkers in a phase 1 trial of intravaginal 3% StarPharma LTD 7013 gel (VivaGel) to assess expanded safety. *J Acquir Immune Defic Syndr,* 59**,** 134-40.

MUESING, M. A., SMITH, D. H., CABRADILLA, C. D., BENTON, C. V., LASKY, L. A. & CAPON, D. J. 1985. Nucleic acid structure and expression of the human AIDS/lymphadenopathy retrovirus. *Nature,* 313**,** 450-8.

MUTHU, M. S. & SINGH, S. 2009. Targeted nanomedicines: effective treatment modalities for cancer, AIDS and brain disorders. *Nanomedicine (Lond),* 4**,** 105-18.

NAIR, H., NOKES, D. J., GESSNER, B. D., DHERANI, M., MADHI, S. A., SINGLETON, R. J., O'BRIEN, K. L., ROCA, A., WRIGHT, P. F., BRUCE, N., CHANDRAN, A., THEODORATOU, E., SUTANTO, A., SEDYANINGSIH, E. R., NGAMA, M., MUNYWOKI, P. K., KARTASASMITA, C., SIMOES, E. A., RUDAN, I., WEBER, M. W. & CAMPBELL, H. 2010. Global burden of acute lower respiratory infections due to respiratory syncytial virus in young children: a systematic review and meta-analysis. *Lancet,* 375**,** 1545-55.

NEURATH, A. R., STRICK, N. & LI, Y. Y. 2006. Role of seminal plasma in the anti-HIV-1 activity of candidate microbicides. *BMC Infect Dis,* 6**,** 150.

NGUYEN, H., ROE, D. R. & SIMMERLING, C. 2013. Improved Generalized Born Solvent Model Parameters for Protein Simulations. *Journal of Chemical Theory and Computation,* 9**,** 2020-2034.

NICOLA, A. V. & STRAUS, S. E. 2004. Cellular and viral requirements for rapid endocytic entry of herpes simplex virus. *J Virol,* 78**,** 7508-17.

OKABE, M. 2013. The cell biology of mammalian fertilization. *Development,* 140**,** 4471-9.

OLIVARES, C. I., FIELD, J. A., SIMONICH, M., TANGUAY, R. L. & SIERRA-ALVAREZ, R. 2016. Arsenic (III, V), indium (III), and gallium (III) toxicity to zebrafish embryos using a high-throughput multi-endpoint in vivo developmental and behavioral assay. *Chemosphere,* 148**,** 361-8.

OMORI, R. & ABU-RADDAD, L. J. 2017. Sexual network drivers of HIV and herpes simplex virus type 2 transmission. *AIDS,* 31**,** 1721-1732.

PARBOOSING, R., MAGUIRE, G. E., GOVENDER, P. & KRUGER, H. G. 2012. Nanotechnology and the treatment of HIV infection. *Viruses,* 4**,** 488-520.

PARR, M. B., KEPPLE, L., MCDERMOTT, M. R., DREW, M. D., BOZZOLA, J. J. & PARR, E. L. 1994. A mouse model for studies of mucosal immunity to vaginal infection by herpes simplex virus type 2. *Lab Invest,* 70**,** 369-80.

PATEL, S., HAZRATI, E., CHESHENKO, N., GALEN, B., YANG, H., GUZMAN, E., WANG, R., HEROLD, B. C. & KELLER, M. J. 2007. Seminal plasma reduces the effectiveness of topical polyanionic microbicides. *J Infect Dis,* 196**,** 1394-402.

PAZ-BAILEY, G., RAMASWAMY, M., HAWKES, S. J. & GERETTI, A. M. 2007. Herpes simplex virus type 2: epidemiology and management options in developing countries. *Sex Transm Infect,* 83**,** 16-22.

PERELSON, A. S., NEUMANN, A. U., MARKOWITZ, M., LEONARD, J. M. & HO, D. D. 1996. HIV-1 dynamics in vivo: virion clearance rate, infected cell life-span, and viral generation time. *Science,* 271**,** 1582-6.

PERRI, M. J. & WEBER, S. H. 2014. Web-Based Job Submission Interface for the GAMESS Computational Chemistry Program. *Journal of Chemical Education,* 91**,** 2206-2208.

PETERMANN, P., THIER, K., RAHN, E., RIXON, F. J., BLOCH, W., OZCELIK, S., KRUMMENACHER, C., BARRON, M. J., DIXON, M. J., SCHEU, S., PFEFFER, K. & KNEBEL-MORSDORF, D. 2015. Entry mechanisms of herpes simplex virus 1 into murine epidermis: involvement of nectin-1 and herpesvirus entry mediator as cellular receptors. *J Virol,* 89**,** 262-74.

PETROS, R. A. & DESIMONE, J. M. 2010. Strategies in the design of nanoparticles for therapeutic applications. *Nat Rev Drug Discov,* 9**,** 615-27.

PETTERSEN, E. F., GODDARD, T. D., HUANG, C. C., COUCH, G. S., GREENBLATT, D. M., MENG, E. C. & FERRIN, T. E. 2004. UCSF chimera - A visualization system for exploratory research and analysis. *Journal of Computational Chemistry,* 25**,** 1605-1612.

PETTIFOR, A. E., VAN DER STRATEN, A., DUNBAR, M. S., SHIBOSKI, S. C. & PADIAN, N. S. 2004. Early age of first sex: a risk factor for HIV infection among women in Zimbabwe. *AIDS,* 18**,** 1435-42.

PICKERING, J. M., WHITWORTH, J. A., HUGHES, P., KASSE, M., MORGAN, D., MAYANJA, B., VAN DER PAAL, L. & MAYAUD, P. 2005. Aetiology of sexually transmitted infections and response to syndromic treatment in southwest Uganda. *Sex Transm Infect,* 81**,** 488-93.

PINNINTI, S. G. & KIMBERLIN, D. W. 2013. Maternal and neonatal herpes simplex virus infections. *Am J Perinatol,* 30**,** 113-9.

PITZER, V. E., VIBOUD, C., ALONSO, W. J., WILCOX, T., METCALF, C. J., STEINER, C. A., HAYNES, A. K. & GRENFELL, B. T. 2015. Environmental drivers of the spatiotemporal dynamics of respiratory syncytial virus in the United States. *PLoS Pathog,* 11**,** e1004591.

PLATT, E. J., WEHRLY, K., KUHMANN, S. E., CHESEBRO, B. & KABAT, D. 1998. Effects of CCR5 and CD4 cell surface concentrations on infections by macrophagetropic isolates of human immunodeficiency virus type 1. *J Virol,* 72**,** 2855-64.

POETS, C. F. 1998. When do infants need additional inspired oxygen? A review of the current literature. *Pediatr Pulmonol,* 26**,** 424-8.

PRICE, C. F., TYSSEN, D., SONZA, S., DAVIE, A., EVANS, S., LEWIS, G. R., XIA, S., SPELMAN, T., HODSMAN, P., MOENCH, T. R., HUMBERSTONE, A., PAULL, J. R. & TACHEDJIAN, G. 2011. SPL7013 Gel (VivaGel(R)) retains potent HIV-1 and HSV-2 inhibitory activity following vaginal administration in humans. *PLoS One,* 6**,** e24095.

PRODGER, J. L. & KAUL, R. 2017. The biology of how circumcision reduces HIV susceptibility: broader implications for the prevention field. *AIDS Res Ther,* 14**,** 49.

RADTKE, K., KIENEKE, D., WOLFSTEIN, A., MICHAEL, K., STEFFEN, W., SCHOLZ, T., KARGER, A. & SODEIK, B. 2010. Plus- and minus-end directed microtubule motors bind simultaneously to herpes simplex virus capsids using different inner tegument structures. *PLoS Pathog,* 6**,** e1000991.

RALSTON, S. L., LIEBERTHAL, A. S., MEISSNER, H. C., ALVERSON, B. K., BALEY, J. E., GADOMSKI, A. M., JOHNSON, D. W., LIGHT, M. J., MARAQA, N. F., MENDONCA, E. A., PHELAN, K. J., ZORC, J. J., STANKO-LOPP, D., BROWN, M. A., NATHANSON, I., ROSENBLUM, E., SAYLES, S., 3RD & HERNANDEZ-CANCIO, S. 2014. Clinical practice guideline: the diagnosis, management, and prevention of bronchiolitis. *Pediatrics,* 134**,** e1474-502.

REIS, J. & SHAMAN, J. 2016. Retrospective Parameter Estimation and Forecast of Respiratory Syncytial Virus in the United States. *PLoS Comput Biol,* 12**,** e1005133.

REJINOLD, N. S., MUTHUNARAYANAN, M., CHENNAZHI, K. P., NAIR, S. V. & JAYAKUMAR, R. 2011. Curcumin loaded fibrinogen nanoparticles for cancer drug delivery. *J Biomed Nanotechnol,* 7**,** 521-34.

RINCHEVAL, V., LELEK, M., GAULT, E., BOUILLIER, C., SITTERLIN, D., BLOUQUIT-LAYE, S., GALLOUX, M., ZIMMER, C., ELEOUET, J. F. & RAMEIX-WELTI, M. A. 2017. Functional organization of cytoplasmic inclusion bodies in cells infected by respiratory syncytial virus. *Nat Commun,* 8**,** 563.

ROAN, N. R., MULLER, J. A., LIU, H., CHU, S., ARNOLD, F., STURZEL, C. M., WALTHER, P., DONG, M., WITKOWSKA, H. E., KIRCHHOFF, F., MUNCH, J. & GREENE, W. C. 2011. Peptides released by physiological cleavage of semen coagulum proteins form amyloids that enhance HIV infection. *Cell Host Microbe,* 10**,** 541-50.

ROBERTS, S. S., MILLER, R. K., JONES, J. K., LINDSAY, K. L., GREENE, M. F., MADDREY, W. C., WILLIAMS, I. T., LIU, J. & SPIEGEL, R. J. 2010. The Ribavirin Pregnancy Registry: Findings after 5 years of enrollment, 2003-2009. *Birth Defects Res A Clin Mol Teratol,* 88**,** 551-9.

ROIZMAN, B. 1979. The structure and isomerization of herpes simplex virus genomes. *Cell,* 16**,** 481-94.

RUSCONI, S., MOONIS, M., MERRILL, D. P., PALLAI, P. V., NEIDHARDT, E. A., SINGH, S. K., WILLIS, K. J., OSBURNE, M. S., PROFY, A. T., JENSON, J. C. & HIRSCH, M. S. 1996. Naphthalene sulfonate polymers with CD4-blocking and anti-human immunodeficiency virus type 1 activities. *Antimicrob Agents Chemother,* 40**,** 234-6.

RUSNATI, M. & PRESTA, M. 1996. Interaction of angiogenic basic fibroblast growth factor with endothelial cell heparan sulfate proteoglycans. Biological implications in neovascularization. *Int J Clin Lab Res,* 26**,** 15-23.

RUSNATI, M., URBINATI, C. & PRESTA, M. 1993. Internalization of basic fibroblast growth factor (bFGF) in cultured endothelial cells: role of the low affinity heparin-like bFGF receptors. *J Cell Physiol,* 154**,** 152-61.

RUSNATI, M., VICENZI, E., DONALISIO, M., ORESTE, P., LANDOLFO, S. & LEMBO, D. 2009. Sulfated K5 Escherichia coli polysaccharide derivatives: A novel class of candidate antiviral microbicides. *Pharmacol Ther,* 123**,** 310-22.

RYCKAERT, J. P., CICCOTTI, G. & BERENDSEN, H. J. C. 1977. NUMERICAL-INTEGRATION OF CARTESIAN EQUATIONS OF MOTION OF A SYSTEM WITH CONSTRAINTS - MOLECULAR-DYNAMICS OF N-ALKANES. *Journal of Computational Physics,* 23**,** 327-341.

SAMARAS, N., CHEVALLEY, T., SAMARAS, D. & GOLD, G. 2010. Older patients in the emergency department: a review. *Ann Emerg Med,* 56**,** 261-9.

SANCHEZ-LUNA, M., BURGOS-POL, R., OYAGUEZ, I., FIGUERAS-ALOY, J., SANCHEZ-SOLIS, M., MARTINON-TORRES, F. & CARBONELL-ESTRANY, X. 2017. Cost-utility analysis of Palivizumab for Respiratory Syncytial Virus infection prophylaxis in preterm infants: update based on the clinical evidence in Spain. *BMC Infect Dis,* 17**,** 687.

SANCHEZ-RODRIGUEZ, J., VACAS-CORDOBA, E., GOMEZ, R., DE LA MATA, F. J. & MUNOZ-FERNANDEZ, M. A. 2015. Nanotech-derived topical microbicides for HIV prevention: the road to clinical development. *Antiviral Res,* 113**,** 33-48.

SANTOS-MARTINEZ, M. J., RAHME, K., CORBALAN, J. J., FAULKNER, C., HOLMES, J. D., TAJBER, L., MEDINA, C. & RADOMSKI, M. W. 2014. Pegylation increases platelet biocompatibility of gold nanoparticles. *J Biomed Nanotechnol,* 10**,** 1004-15.

SANVICENS, N. & MARCO, M. P. 2008. Multifunctional nanoparticles--properties and prospects for their use in human medicine. *Trends Biotechnol,* 26**,** 425-33.

SCORDI-BELLO, I. A., MOSOIAN, A., HE, C., CHEN, Y., CHENG, Y., JARVIS, G. A., KELLER, M. J., HOGARTY, K., WALLER, D. P., PROFY, A. T., HEROLD, B. C. & KLOTMAN, M. E. 2005. Candidate sulfonated and sulfated topical microbicides: comparison of anti-human immunodeficiency virus activities and mechanisms of action. *Antimicrob Agents Chemother,* 49**,** 3607-15.

SCHIFFER, J. T. & COREY, L. 2013. Rapid host immune response and viral dynamics in herpes simplex virus-2 infection. *Nat Med,* 19**,** 280-90.

SCHMIDT, M. W., BALDRIDGE, K. K., BOATZ, J. A., ELBERT, S. T., GORDON, M. S., JENSEN, J. H., KOSEKI, S., MATSUNAGA, N., NGUYEN, K. A., SU, S. J., WINDUS, T. L., DUPUIS, M. & MONTGOMERY, J. A. 1993. GENERAL ATOMIC AND MOLECULAR ELECTRONIC-STRUCTURE SYSTEM. *Journal of Computational Chemistry,* 14**,** 1347-1363.

SCHUTZ, C. A., JUILLERAT-JEANNERET, L., MUELLER, H., LYNCH, I. & RIEDIKER, M. 2013. Therapeutic nanoparticles in clinics and under clinical evaluation. *Nanomedicine (Lond),* 8**,** 449-67.

SEDGH, G., SINGH, S. & HUSSAIN, R. 2014. Intended and unintended pregnancies worldwide in 2012 and recent trends. *Stud Fam Plann,* 45**,** 301-14.

SEPULVEDA-CRESPO, D., CENA-DIEZ, R., JIMENEZ, J. L. & ANGELES MUNOZ-FERNANDEZ, M. 2017. Mechanistic Studies of Viral Entry: An Overview of Dendrimer-Based Microbicides As Entry Inhibitors Against Both HIV and HSV-2 Overlapped Infections. *Med Res Rev,* 37**,** 149-179.

SEPULVEDA-CRESPO, D., GOMEZ, R., DE LA MATA, F. J., JIMENEZ, J. L. & MUNOZ-FERNANDEZ, M. A. 2015a. Polyanionic carbosilane dendrimer-conjugated antiviral drugs as efficient microbicides: Recent trends and developments in HIV treatment/therapy. *Nanomedicine,* 11**,** 1481-98.

SEPULVEDA-CRESPO, D., LORENTE, R., LEAL, M., GOMEZ, R., DE LA MATA, F. J., JIMENEZ, J. L. & MUNOZ-FERNANDEZ, M. A. 2014. Synergistic activity profile of carbosilane dendrimer G2-STE16 in combination with other dendrimers and antiretrovirals as topical anti-HIV-1 microbicide. *Nanomedicine,* 10**,** 609-18.

SEPULVEDA-CRESPO, D., SANCHEZ-RODRIGUEZ, J., SERRAMIA, M. J., GOMEZ, R., DE LA MATA, F. J., JIMENEZ, J. L. & MUNOZ-FERNANDEZ, M. A. 2015b. Triple combination of carbosilane dendrimers, tenofovir and maraviroc as potential microbicide to prevent HIV-1 sexual transmission. *Nanomedicine (Lond),* 10**,** 899-914.

SEPULVEDA-CRESPO, D., SERRAMIA, M. J., TAGER, A. M., VRBANAC, V., GOMEZ, R., DE LA MATA, F. J., JIMENEZ, J. L. & MUNOZ-FERNANDEZ, M. A. 2015c. Prevention vaginally of HIV-1 transmission in humanized BLT mice and mode of antiviral action of polyanionic carbosilane dendrimer G2-S16. *Nanomedicine,* 11**,** 1299-308.

SIMPSON-HOLLEY, M., COLGROVE, R. C., NALEPA, G., HARPER, J. W. & KNIPE, D. M. 2005. Identification and functional evaluation of cellular and viral factors involved in the alteration of nuclear architecture during herpes simplex virus 1 infection. *J Virol,* 79**,** 12840-51.

SMITH, R. J., HOGAN, A. B. & MERCER, G. N. 2017. Unexpected Infection Spikes in a Model of Respiratory Syncytial Virus Vaccination. *Vaccines (Basel),* 5.

SODEIK, B., EBERSOLD, M. W. & HELENIUS, A. 1997. Microtubule-mediated transport of incoming herpes simplex virus 1 capsids to the nucleus. *J Cell Biol,* 136**,** 1007-21.

SOPER, A., JUAREZ-FERNANDEZ, G., ASO, H., MORIWAKI, M., YAMADA, E., NAKANO, Y., KOYANAGI, Y. & SATO, K. 2017. Various plus unique: Viral protein U as a plurifunctional protein for HIV-1 replication. *Exp Biol Med (Maywood),* 242**,** 850-858.

SPEAR, P. G. 2004. Herpes simplex virus: receptors and ligands for cell entry. *Cell Microbiol,* 6**,** 401-10.

STANBERRY, L. R., CUNNINGHAM, A. L., MINDEL, A., SCOTT, L. L., SPRUANCE, S. L., AOKI, F. Y. & LACEY, C. J. 2000. Prospects for control of herpes simplex virus disease through immunization. *Clin Infect Dis,* 30**,** 549-66.

STRAHLE, U., SCHOLZ, S., GEISLER, R., GREINER, P., HOLLERT, H., RASTEGAR, S., SCHUMACHER, A., SELDERSLAGHS, I., WEISS, C., WITTERS, H. & BRAUNBECK, T. 2012. Zebrafish embryos as an alternative to animal experiments--a commentary on the definition of the onset of protected life stages in animal welfare regulations. *Reprod Toxicol,* 33**,** 128-32.

SUAREZ, S. S. & PACEY, A. A. 2006. Sperm transport in the female reproductive tract. *Hum Reprod Update,* 12**,** 23-37.

SVENSON, S. & TOMALIA, D. A. 2005. Dendrimers in biomedical applications--reflections on the field. *Adv Drug Deliv Rev,* 57**,** 2106-29.

TAN, Q., ZHU, Y., LI, J., CHEN, Z., HAN, G. W., KUFAREVA, I., LI, T., MA, L., FENALTI, G., ZHANG, W., XIE, X., YANG, H., JIANG, H., CHEREZOV, V., LIU, H., STEVENS, R. C., ZHAO, Q. & WU, B. 2013a. Structure of the CCR5 chemokine receptor-HIV entry inhibitor maraviroc complex. *Science,* 341**,** 1387-90.

TAN, S., LU, L., LI, L., LIU, J., OKSOV, Y., LU, H., JIANG, S. & LIU, S. 2013b. Polyanionic candidate microbicides accelerate the formation of semen-derived amyloid fibrils to enhance HIV-1 infection. *PLoS One,* 8**,** e59777.

TANAKA, E., NOGUCHI, T., NAGAI, K., AKASHI, Y., KAWAHARA, K. & SHIMADA, T. 2012. Morphology of the epithelium of the lower rectum and the anal canal in the adult human. *Med Mol Morphol,* 45**,** 72-9.

TANPHAICHITR, N., SRAKAEW, N., ALONZI, R., KIATTIBURUT, W., KONGMANAS, K., ZHI, R., LI, W., BAKER, M., WANG, G. & HICKLING, D. 2016. Potential Use of Antimicrobial Peptides as Vaginal Spermicides/Microbicides. *Pharmaceuticals (Basel),* 9.

TAYLOR, G., WYLD, S., VALARCHER, J. F., GUZMAN, E., THOM, M., WIDDISON, S. & BUCHHOLZ, U. J. 2014. Recombinant bovine respiratory syncytial virus with deletion of the SH gene induces increased apoptosis and pro-inflammatory cytokines in vitro, and is attenuated and induces protective immunity in calves. *J Gen Virol,* 95**,** 1244-54.

TELWATTE, S., MOORE, K., JOHNSON, A., TYSSEN, D., STERJOVSKI, J., ALDUNATE, M., GORRY, P. R., RAMSLAND, P. A., LEWIS, G. R., PAULL, J. R., SONZA, S. & TACHEDJIAN, G. 2011. Virucidal activity of the dendrimer microbicide SPL7013 against HIV-1. *Antiviral Res,* 90**,** 195-9.

THELLMAN, N. M. & TRIEZENBERG, S. J. 2017. Herpes Simplex Virus Establishment, Maintenance, and Reactivation: In Vitro Modeling of Latency. *Pathogens,* 6.

TINDALL, B. & COOPER, D. A. 1991. Primary HIV infection: host responses and intervention strategies. *AIDS,* 5**,** 1-14.

TIWARI, V., TARBUTTON, M. S. & SHUKLA, D. 2015. Diversity of heparan sulfate and HSV entry: basic understanding and treatment strategies. *Molecules,* 20**,** 2707-27.

TOMALIA, D. A. & KHANNA, S. N. 2016. A Systematic Framework and Nanoperiodic Concept for Unifying Nanoscience: Hard/Soft Nanoelements, Superatoms, Meta-Atoms, New Emerging Properties, Periodic Property Patterns, and Predictive Mendeleev-like Nanoperiodic Tables. *Chem Rev,* 116**,** 2705-74.

UNAIDS 2016. Report on the global AIDS epidemic/2016. http://aidsinfo.unaids.org/.

USMANI, S. M., ZIRAFI, O., MULLER, J. A., SANDI-MONROY, N. L., YADAV, J. K., MEIER, C., WEIL, T., ROAN, N. R., GREENE, W. C., WALTHER, P., NILSSON, K. P., HAMMARSTROM, P., WETZEL, R., PILCHER, C. D., GAGSTEIGER, F., FANDRICH, M., KIRCHHOFF, F. & MUNCH, J. 2014. Direct visualization of HIV-enhancing endogenous amyloid fibrils in human semen. *Nat Commun,* 5**,** 3508.

VACAS-CORDOBA, E., GALAN, M., DE LA MATA, F. J., GOMEZ, R., PION, M. & MUNOZ-FERNANDEZ, M. A. 2014. Enhanced activity of carbosilane dendrimers against HIV when combined with reverse transcriptase inhibitor drugs: searching for more potent microbicides. *Int J Nanomedicine,* 9**,** 3591-600.

VACAS-CORDOBA, E., MALY, M., DE LA MATA, F. J., GOMEZ, R., PION, M. & MUNOZ-FERNANDEZ, M. A. 2016. Antiviral mechanism of polyanionic carbosilane dendrimers against HIV-1. *Int J Nanomedicine,* 11**,** 1281-94.

VACAS CORDOBA, E., ARNAIZ, E., RELLOSO, M., SANCHEZ-TORRES, C., GARCIA, F., PEREZ-ALVAREZ, L., GOMEZ, R., DE LA MATA, F. J., PION, M. & MUNOZ-FERNANDEZ, M. A. 2013. Development of sulphated and naphthylsulphonated carbosilane dendrimers as topical microbicides to prevent HIV-1 sexual transmission. *AIDS,* 27**,** 1219-29.

VALYI-NAGY, T., DESHMANE, S. L., SPIVACK, J. G., STEINER, I., ACE, C. I., PRESTON, C. M. & FRASER, N. W. 1991. Investigation of herpes simplex virus type 1 (HSV-1) gene expression and DNA synthesis during the establishment of latent infection by an HSV-1 mutant, in1814, that does not replicate in mouse trigeminal ganglia. *J Gen Virol,* 72 (Pt 3)**,** 641-9.

VAN DAMME, L., GOVINDEN, R., MIREMBE, F. M., GUEDOU, F., SOLOMON, S., BECKER, M. L., PRADEEP, B. S., KRISHNAN, A. K., ALARY, M., PANDE, B., RAMJEE, G., DEESE, J., CRUCITTI, T. & TAYLOR, D. 2008. Lack of effectiveness of cellulose sulfate gel for the prevention of vaginal HIV transmission. *N Engl J Med,* 359**,** 463-72.

VANPOUILLE, C., ARAKELYAN, A. & MARGOLIS, L. 2012. Microbicides: still a long road to success. *Trends Microbiol,* 20**,** 369-75.

VASAN, S. S. 2011. Semen analysis and sperm function tests: How much to test? *Indian J Urol,* 27**,** 41-8.

WALD, A. & ASHLEY-MORROW, R. 2002. Serological testing for herpes simplex virus (HSV)-1 and HSV-2 infection. *Clin Infect Dis,* 35**,** S173-82.

WALSH, P. & ROTHENBERG, S. J. 2015. American Academy of Pediatrics 2014 bronchiolitis guidelines: bonfire of the evidence. *West J Emerg Med,* 16**,** 85-8.

WANG, D., PHAN, S., DISTEFANO, D. J., CITRON, M. P., CALLAHAN, C. L., INDRAWATI, L., DUBEY, S. A., HEIDECKER, G. J., GOVINDARAJAN, D., LIANG, X., HE, B. & ESPESETH, A. S. 2017. A Single-Dose Recombinant Parainfluenza Virus 5-Vectored Vaccine Expressing Respiratory Syncytial Virus (RSV) F or G Protein Protected Cotton Rats and African Green Monkeys from RSV Challenge. *J Virol,* 91.

WANG, J. M., WOLF, R. M., CALDWELL, J. W., KOLLMAN, P. A. & CASE, D. A. 2005. Development and testing of a general amber force field (vol 25, pg 1157, 2004). *Journal of Computational Chemistry,* 26**,** 114-114.

WEISSHAAR, M., COX, R. & PLEMPER, R. K. 2015. Blocking Respiratory Syncytial Virus Entry: A Story with Twists. *DNA Cell Biol,* 34**,** 505-10.

WHITESIDES, G. M. 2003. The 'right' size in nanobiotechnology. *Nat Biotechnol,* 21**,** 1161-5.

WU, H., PFARR, D. S., LOSONSKY, G. A. & KIENER, P. A. 2008. Immunoprophylaxis of RSV infection: advancing from RSV-IGIV to palivizumab and motavizumab. *Curr Top Microbiol Immunol,* 317**,** 103-23.

WU, J. T., YANG, G. W., QI, C. H., ZHOU, L., HU, J. G. & WANG, M. S. 2016. ANTI-INFLAMMATORY ACTIVITY OF PLATYCODIN D ON ALCOHOL-INDUCED FATTY LIVER RATS VIA TLR4-MYD88-NF-kappaB SIGNAL PATH. *Afr J Tradit Complement Altern Med,* 13**,** 176-183.

WU, X. W. & BROOKS, B. R. 2003. Self-guided Langevin dynamics simulation method. *Chemical Physics Letters,* 381**,** 512-518.

WU, X. W., VANDEN-EIJNDEN, E. & BROOKS, B. R. 2014. Generalization of the self-guided Langevin dynamic simulation method. *Abstracts of Papers of the American Chemical Society,* 248.

XIAO, F., FOFANA, I., THUMANN, C., MAILLY, L., ALLES, R., ROBINET, E., MEYER, N., SCHAEFFER, M., HABERSETZER, F., DOFFOEL, M., LEYSSEN, P., NEYTS, J., ZEISEL, M. B. & BAUMERT, T. F. 2015. Synergy of entry inhibitors with direct-acting antivirals uncovers novel combinations for prevention and treatment of hepatitis C. *Gut,* 64**,** 483-94.

YOLAMANOVA, M., MEIER, C., SHAYTAN, A. K., VAS, V., BERTONCINI, C. W., ARNOLD, F., ZIRAFI, O., USMANI, S. M., MULLER, J. A., SAUTER, D., GOFFINET, C., PALESCH, D., WALTHER, P., ROAN, N. R., GEIGER, H., LUNOV, O., SIMMET, T., BOHNE, J., SCHREZENMEIER, H., SCHWARZ, K., STANDKER, L., FORSSMANN, W. G., SALVATELLA, X., KHALATUR, P. G., KHOKHLOV, A. R., KNOWLES, T. P., WEIL, T., KIRCHHOFF, F. & MUNCH, J. 2013. Peptide nanofibrils boost retroviral gene transfer and provide a rapid means for concentrating viruses. *Nat Nanotechnol,* 8**,** 130-6.

ZACK, J. A., ARRIGO, S. J., WEITSMAN, S. R., GO, A. S., HAISLIP, A. & CHEN, I. S. 1990. HIV-1 entry into quiescent primary lymphocytes: molecular analysis reveals a labile, latent viral structure. *Cell,* 61**,** 213-22.

ZARE-ZARDINI, H., FESAHAT, F., ANBARI, F., HALVAEI, I. & EBRAHIMI, L. 2016. Assessment of spermicidal activity of the antimicrobial peptide sarcotoxin Pd: A potent contraceptive agent. *Eur J Contracept Reprod Health Care,* 21**,** 15-21.

ZHANG, Z., ZHAO, M., ZHENG, W. & LIU, Y. 2017. Platycodin D, a triterpenoid saponin from Platycodon grandiflorum, suppresses the growth and invasion of human oral squamous cell carcinoma cells via the NF-kappaB pathway. *J Biochem Mol Toxicol,* 31.

ZHONG, Y., WANG, J., WANG, Y. & WU, B. 2012. Preparation and evaluation of liposome-encapsulated codrug LMX. *Int J Pharm,* 438**,** 240-8.

ZHU, C. G. & ZHANG, L. S. 2017. [Effect of platycodin D on radiosensitivity of human hepatoma cell line and related mechanisms of action]. *Zhonghua Gan Zang Bing Za Zhi,* 25**,** 458-462.

ZIRAFI, O., KIM, K. A., ROAN, N. R., KLUGE, S. F., MULLER, J. A., JIANG, S., MAYER, B., GREENE, W. C., KIRCHHOFF, F. & MUNCH, J. 2014. Semen enhances HIV infectivity and impairs the antiviral efficacy of microbicides. *Sci Transl Med,* 6**,** 262ra157.

PUBLICATIONS

LIST OF PUBLICATIONS

Publications that are part of this thesis:

- **Ceña-Diez R**, Rodriguez-Izquierdo I, Rodriguez R, Martinez Gonzalez I, Muñoz-Fernández MA. G2-S16 dendrimer as a potential RSV Therapy: *in vitro* and *in vivo*. (Manuscript in preparation).
- **Ceña-Diez R**, Muñoz-Fernández MA. Potential use of the combination of polyanionic carbosilane dendrimers with Platycodin D as vaginal spermicides/microbicides. (Manuscript in preparation).
- Guerrero- Beltran C, **Ceña-Diez R**, Sepulveda Crespo D, de la Mata J, Gomez R, Leal M, Muñoz-Fernández MA*, Jimenez JL*. Carbosilane dendrons with fatty acids at the core as new potential microbicide against HSV-2/HIV-1 co-infection. Nanoscale 2017. IF: 7,367 (Manuscript Acepted). **Second authorship**.
- **Ceña-Diez R**, García-Broncano P, Javier de la Mata F, Gómez R, Resino S, Muñoz-Fernández MA. G2-S16 dendrimer as a candidate for a microbicide to prevent HIV-1 infection in women. Nanoscale. 2017 Jul 13;9(27):9732-9742. IF: 7,367.
- García-Broncano P*, **Ceña-Diez R***, de la Mata FJ, Gómez R, Resino S, Muñoz-Fernández MA. Efficacy of carbosilane dendrimers with an antiretroviral combination against HIV-1 in the presence of semen-derived enhancer of viral infection.Eur J Pharmacol. 2017 Sep 15;811:155-163. IF: 2,896. **First authorship (Co-authors)**
- Sepúlveda-Crespo D, **Ceña-Díez R**, Jiménez JL, Muñoz-Fernández MA. Mechanistic studies of viral entry: an overview of dendrimer-based microbicides as entry inhibitors against both HIV and HSV-2 Overlapped Infections. Med Res Rev. 2017 Jan;37(1):149-179. Review. IF: 8,763. **Second authorship**.
- **Ceña-Diez R**, Sepúlveda-Crespo D, Maly M, Muñoz-Fernández MA. Dendrimeric based microbicides against sexual transmitted infections associated to heparan sulfate. RSC Adv., 2016,6, 46755-46764. IF: 3,108.
- **Ceña-Diez R***, García-Broncano P*, de la Mata FJ, Gómez R, Muñoz-Fernández MÁ. Efficacy of HIV antiviral polyanionic carbosilane dendrimer G2-S16 in the presence of semen. Int J Nanomedicine. 2016 May 30;11:2443-50. IF: 5,034.

- **Ceña-Diez R*,** Vacas-Córdoba E*, García-Broncano P, de la Mata FJ, Gómez R, Maly M, Muñoz-Fernández MÁ. Prevention of vaginal and rectal herpes simplex virus type 2 transmission in mice: mechanism of antiviral action. Int J Nanomedicine. 2016 May 19;11:2147-62. IF: 5,034.

*** Co-authors**

Patent that is part of this thesis:

- Inventores (p.o. de firma): Francisco J. de la Mata de la Mata; Rafael Gómez Ramírez; Javier Sánchez-Nieves; Gabriel Mencía Berlinches; Jesús Cano Sierra; Jose Luis Copa Patiño; Juan Soliveri de Carranza; Jorge Pérez Serrano; Mercedes Valiente Martínez, Carlos Emilio Gutiérrez Ulloa; MA Muñoz Fernández; Jose Luis Jiménez Fuentes; Carlos Guerrero Beltrán; Daniel Sepúlveda Crespo: **Rafael Ceña Diez**.

Título: "Dendrones carbosilano funcionalizados con ácidos grasos: formación de micelas y usos".

N. de solicitud: P-201600726

País de prioridad: España

Fecha de prioridad: 02/09/2016

Entidad titular: Universidad de Alcalá de Henares y la Fundación de Investigación del Hospital General Universitario Gregorio Marañón